



Review on Black Carbon (BC) and Polycyclic Aromatic Hydrocarbons (PAHs) emission reductions induced by PM emission abatement techniques

TFTEI background informal technical document
December 2020

Prepared by Citepa (TFTEI Techno-Scientific Secretariat)
Bertrand Bessagnet and Nadine Allemand

Review on Black Carbon (BC) and Polycyclic Aromatic Hydrocarbons (PAHs) emission reductions induced by PM emission abatement techniques

December 2020

For more information

TFTEI Techno-Scientific Secretariat

Nadine Allemand (head of the TFTEI techno-scientific secretariat)

Bertrand Bessagnet

Citepa

42 Rue de Paradis

75010 Paris

bertrand.bessagnet@citepa.org

nadine.allemand@citepa.org

Acknowledgments:

Isaline Fraboulet (INERIS)

Cécile Raventos (INERIS)

Outline

Outline.....	3
Index of Tables.....	5
Index of Figures	7
List of main abbreviations and acronyms	12
Executive summary	15
1 Introduction	21
2 Legal framework	22
2.1 The Gothenburg Protocol	22
2.2 The EU legal framework	24
2.3 Air pollution and climate change: a grey area of international environmental law?	26
3 Scientific Background	27
3.1 Black carbon and Elemental Carbon	27
3.2 Brown Carbon	28
3.3 Polycyclic Aromatic Hydrocarbons (PAHs)	31
3.4 The concept of “Condensables”	32
3.5 Ultrafine Particles.....	40
3.6 Overview of BC/PAH/PM _{2.5} emissions in the EMEP countries	42
3.7 Co-benefits of Air Quality and Climate Change mitigation through BC emission reductions	45
4 Mitigation measures for PM emissions and its impact on BC and PAH emissions.....	50
4.1 Small combustion appliances in the residential sector.....	50
4.1.1 General overview of measures to abate PM and BC emissions.....	50
4.1.2 Performances of modern appliances compared to traditional ones under real uses	55
4.1.3 Impact of combustion conditions on PM and BC emissions	59
4.1.4 Innovative solutions to reduce PM.....	69
4.1.5 Impact of wood type and quality on emissions	72
4.1.6 Electrostatic precipitators (ESP)	79
4.1.7 Catalyst combustors	81
4.1.8 Other techniques or operating conditions for larger combustion plants	84
4.1.9 Key conclusions	89
4.2 Road transport	91
4.2.1 Aftertreatment systems.....	91
4.2.2 Carbonaceous composition of exhaust	93

4.2.3	Impact of After-treatment systems on particulate matter emissions	95
4.2.4	The increasing role of gasoline vehicle on particle emissions (mass and number) 102	
4.2.5	Impact of renewable fuels on emissions.....	107
4.2.6	Impact of real driving conditions	109
4.2.7	Brake and tyre emissions.....	110
4.2.8	Post Euro 6 regulations	112
4.2.9	Key conclusions	114
4.3	Gas Flaring	116
4.3.1	Definition and use of Gas Flaring	116
4.3.2	Emissions flaring activities	117
4.3.3	BC Gas Flaring emissions factors	120
4.3.4	Measures to reduce flare emissions.....	123
4.3.5	Gas flaring reduction technologies.....	124
4.3.6	Steam assisted flares.....	126
4.3.7	Other Optimized Combustion systems – Advanced Flare Design.....	128
4.3.8	Multiple tips for soot reduction.....	130
4.3.9	Modelling approaches	131
4.3.10	Key conclusions	133
5	Conclusions	135
6	Bibliography.....	136

Index of Tables

Table 1: Recommended limit values for dust emissions released from new solid fuel combustion installations with a rated thermal input < 500 kWth to be used with product standards (Note: O ₂ reference content: 13%.)	23
Table 2: Euro 6 emission limits for passenger cars and light-commercial vehicles, table from (Rodríguez et al., 2019).....	25
Table 3: Volatility classes of volatile organic compounds (Donahue et al., 2012; Murphy et al., 2014). † VOC or NMVOC is not given as an explicit abbreviation here since they are superset, e.g., typically IVOC and some SVOC.	34
Table 4: Summary of the experiments and conditions in the chamber before lights-on (after a homogenization and stabilization period). MCE stands for modified combustion efficiency and THC is total hydrocarbon (Bertrand et al., 2018).....	39
Table 5: Sectoral emissions of particulate matter in 2010, ECLIPSE V5a, Gg year ⁻¹ (Klimont et al., 2017). (a) Values are middle-of-the-range estimates based on the ranges reported in (Stettler et al., 2013; Yim et al., 2015), and based on global fuel consumption and ranges of emission factors from (Kinsey, 2009). (b) GFED3.1 without agricultural waste burning that is included based on GAINS estimates in category “Agriculture”; PM10 value based on TPM (total particulate matter); PM1 not available in GFED – here assumed equal to PM2.5. Report to (Randerson et al., 2017) for the last GFED version.	42
Table 6: Main 10 emitting sectors in EU28 for Black Carbon.....	43
Table 7: Typical PM emission factors for various appliance types for wood combustion indicated as solid particles sampled on hot filters (not including condensable organic compounds) in real-life operation today (left), and achievable best-practice PM emission levels under ideal conditions (right). *only if operated at full load, which cannot be guaranteed for space heating. From (Nussbaumer, 2010a).....	50
Table 8: Mean performance and emissions metrics for a three stone fire (TSF) and the modular 431 stove (MOD), and the percent change of each metric from TSF to MOD from (Caubel et al., 2018).....	70
Table 9: Used fuel types of one-fuel type users from (Wöhler et al., 2016).....	72
Table 10: Emission factors in mg MJ ⁻¹ from traditional appliances (fireplace <i>versus</i> woodstove) from (Querol et al., 2016) with the following references: [1] (Gonçalves et al., 2011), [2] (Martins, 2012), [3] (Duarte, 2011), [4] (Vicente, 2013). <i>Note: Calorific value 18.5 MJ kg⁻¹</i>	73
Table 11: Emission factors in mg MJ ⁻¹ for ecolabelled wood stoves (Fernandes et al., 2011) 74	74
Table 12: Emission factors in mg MJ ⁻¹ for pellet stoves (Querol et al., 2016)	74
Table 13: Mean emission factors (EFs) and concentrations of some carbonaceous gaseous and particulate species from regular combustion experiments (modern masonry heater: beech, birch and spruce; pellet boiler: softwood pellets) and combustion experiments with slow ignition (modern masonry heater: spruce* and birch*). Entries of b.l.q. refer to EFs below the limit of quantification (Czech et al., 2018). IP: Indeno(1,2,3-cd)fluoranthene, BaP: Benzo(a)pyrene.	75
Table 14: Contents and percentae of the C forms in the emitted fly ash from (Koniczyński et al., 2017) – ND stands for “no data”. *CFB as for circulating fluidized bed boiler	78

Table 15: PM2.5 emission factors, split of PM in elemental (BC) and organic mass (OM) from (Ntziachristos and Samarras, 2019). <i>Notes: The values originate from available data in the literature and engineering estimates of the effects of specific technologies (catalysts, DPFs, etc.) on emissions. The estimates are also based on the assumption that low-sulphur fuels (< 50 ppm t. S) are used. Hence, the contribution of sulphate to PM emissions is generally low. In cases where advanced aftertreatment is used (such as catalysed DPFs), then EC and OM does not add up to 100 %. The remaining fraction is assumed to be ash, nitrates, sulphates, water and ammonium salts.** L-categories are Mopeds and Motorbikes.....</i>	94
Table 16: Emission factors ranges for vehicles from two-whelled to light heavy duty vehicles according to the Tier 2 methodology (Ntziachristos and Boulter, 2019).....	110
Table 17: Summary of recommendations for post-Euro 6 standards by (Rodríguez et al., 2019). Bold characters highlith relevant statements for particulate matter emissions.	114
Table 18: Comparison of flaring emissions in Africa by (Doumbia et al., 2019), ECLIPSEv5a, EDGARv4.2 in 2005. For (Doumbia et al., 2019), a range of emissions using lowest and highest EFs is provided. The unit is in kiloton (kt yr ⁻¹).	119
Table 19: Emission factors for source category “1.B.2.c Venting and Flaring” (Plejdrup et al., 2019). * Tier2 and **Tier1	122
Table 20: Summary of the properties of flare types by (Fawole et al., 2016).....	127
Table 21: Comparaision of soot emissions after (Wang et al., 2016)	132

Index of Figures

- Figure 1: Mean hot NO_x emission factors of gasoline (left) and diesel (right) passenger cars and light commercial vehicles as a function of model year. Whiskers represent the 95% confidence interval over the mean. Added are the type approval limit values for Euro 1 to Euro 5 passenger cars over the homologation test cycle in force in the respective year (Chen and Borken-Kleefeld, 2014) 25
- Figure 2: Major chemical component composition of PM_{2.5} collected during winter campaigns in London (North Kensington), Beijing and Delhi. (Online version in colour) (Laskin et al., 2015)..... 27
- Figure 3: Optical and thermochemical classification of atmospheric carbonaceous particulate matter. BrC material is an ensemble of light-absorbing (colored) organic compounds with a variety of molecular structures and molecule-specific optical properties. (Reprinted with permission from (Pöschl, 2005). Copyright 2005 Wiley-VCH Verlag GmbH & Co.) (Laskin et al., 2015)..... 29
- Figure 4: Soot formation pathway from (Frenklach and Wang, 1991; Omidvarborna et al., 2015; Pang et al., 2013)..... 32
- Figure 5: Schematic description of emission ageing in the atmosphere 35
- Figure 6: Normalized Organic Aerosol Emission factor as a function of organic aerosol loading for a diesel motor exhaust at 300 K (Robinson et al., 2007)..... 36
- Figure 7: Synoptic description of the carbonaceous species from graphitic Carbon (EC) to the NMVOCs 37
- Figure 8: Comparison of PM sampling with PM in the ambient from (Nussbaumer, 2010a). SP: Filter (Method a) resulting in solid particles SP (total suspended particles TSP). SPC: Filter + Impinger (Method b) resulting in solid particles and condensables SPC. DT: Dilution Tunnel (Method c) with typical dilution ratio (DR) in the order of 10 resulting in a PM measurement including SPC and most or all C. DT is identical or slightly smaller than SPC + C due to potentially incomplete condensation, depending on dilution ratio and sampling temperature (since dilution reduces not only the temperature but also the partial pressure of contaminants). DS: Dilution Sampling with high dilution ratio (DR > 100). PM₁₀: Total Particulate Matter < 10 microns in the ambient including SP and SOA. SOA: Secondary organic aerosols, consisting of condensables C at ambient and SOA formed by secondary reactions such as photochemical oxidation. *SO₂ and other soluble gaseous compounds in the flue gas may be dissolved in the impingers. **In case of determination of TOC in impingers, the mass of O, H, N, S and other elements contained in the organic condensables needs to be accounted for separately. ***Organic compounds that are liquid or solid at partial pressure in the flue gas and ambient temperature but volatile at sampling due to reduced partial pressure by dilution and temperature above ambient. 38
- Figure 9: Comparison of the surface area of particles with different diameters. The diagram assumes that all particles in each category are perfect spheres, have the same density, and are present in an equal amount of mass. The mass, particle number, and surface area of coarse particles are all arbitrarily designated as 1. Other numbers are relative to the coarse particle. The large surface area and ability to enter circulation are the two most significant characteristics of ultrafine particles that make them more toxic than other larger particles (Kwon et al., 2020)..... 41

Figure 10: EU28 official emissions in kt or t/year (Gg or Mg) for BC, PM2.5 and PAH (as the sum of benzo(a)pyrene, benzo(b)fluoranthene, benzo(k)fluoranthene and indeno(1,2,3-cd)pyrene) in 2018 for the main emitting NFR sectors (refer to Table 6). Sectors are ordered in decreasing magnitude for BC emissions computed from the EMEP database (EMEP/CEIP, 2020).....	43
Figure 11: ratio BC/PM2.5 for EU28 official emissions in 2018 computed from the EMEP database (EMEP/CEIP, 2020)	44
Figure 12: Potential versus effort for single forcer mitigation from (Samset et al., 2020)	46
Figure 13: Emission reductions from the policy scenarios. 2018 legislation includes all controls that have been decided by 2018 according (Amann et al., 2020)	47
Figure 14: Finnish 2010 emission (Mt CO ₂ equivalents) as a pulse emission weighted by various global metrics described in (Kupiainen et al., 2019). CO ₂ is separated out and the net impact of the non-CO ₂ is given by the star.	48
Figure 15: Boxplot summary of all data points (number given between brackets) for each type of wood combustion appliance. *category containing outliers above 1000 mg/MJ from (Tytgat et al., 2017)	57
Figure 16: A visual summary of (Lai et al., 2019) findings.....	58
Figure 17: Comparison of PM2.5 and ultrafine particle emission factors from residential combustion. When burning three different coals, the same stove was used. Error bar represents standard deviations among repeated experiments. Bit, Ant, and SC mean bituminous, anthracite and semi-coke coals, respectively (Wang et al., 2020)	59
Figure 18: Visual summary of the effect of combustion on organic pollutant emissions (Bhattu et al., 2019).....	61
Figure 19: Combustion phase-specific “averaged EFs” (g kg ⁻¹ of wood) of gas (CH ₄ , CO, NO and NMVOCs) and particle (eBC) phase compounds for device 1-7 of all investigated conditions (1: Pellet boiler, 2:Logwood Boiler, 3: Industrial Wood Chip Moving Grate Boiler, 4: Pellet stove, 5: Single-stage Combustion Logwood Stove, 6: Two-stage Combustion Logwood Stove, 7: Two-stage Combustion Logwood Stove) from (Bhattu et al., 2019).....	62
Figure 20: Average wood stove particulate emissions at nominal and high burn rates in mg and mg/MJ for the three combustion phases and the full cycle. Error bars represent range of observations (n = 2) (Eriksson et al., 2014)	63
Figure 21: Evolution of refractory BC and PAH emissions during a combustion cycle from (Nielsen et al., 2017)	64
Figure 22: Full cycle emission factors of OA, rBC, PAH and m/z 60 for nominal (NB), high (HB), and very high (VHB) burn rate in mg/kg _{batch fuel} , where kg _{batch fuel} refers to the dry weight of the whole batch. The results are based on 7, 6 and 3 cycles, respectively. The contributions to the full cycle emissions are given for the three phases: fuel addition, intermediate, and burn out. Error bars represent the variation of the full cycles and are given as the standard error of the mean (Nielsen et al., 2017)	65
Figure 23: UFP species emission factors (mg kg _{fuel} ⁻¹). (PF: pellet stove – fir pellets PB: pellet stove – beech pellets; WF: wood stove – fir firewood; WB: wood stove – beech firewood) (Ozgen et al., 2017)	68
Figure 24: Primary and secondary aerosol emission factors of carbonaceous aerosol calculated for three types of stove (averaged over the replicates). The emission factors for the	

secondary emissions were determined at OH exposure = 5×10^6 molecules cm^{-3} hour. The top panels illustrate the variability within the results. On graph (a), the box encompasses the minimum and maximum values of POA and BC EF normalized to that of the average. The average value is indicated in the bolted line in the middle of the box. The actual value is noted on top. On graph (b) the box encompasses the minimum and maximum OA enhancement ratio (dark green). Stove A is a wood stove from before 2002, stove B is a wood stove from 2010, and stove C is an automated pellet stove from 2010 – from (Bertrand et al., 2017). 69

Figure 25: Wood stove and the retrofitting interventions: A – Wood stove as sold in the market (WSref); B – Wood stove with annular chimney (WSMC1); C – Combustion chamber of the wood stove with component of secondary air-inlets (18 nozzles) (WSMC2) (Carvalho et al., 2018)..... 71

Figure 26: Monthly frequency of heater usage from (Wöhler et al., 2016)- : firewood stoves (FWS), tiled stoves (TIS), cookers (COK) and other firewood operated room heaters (oFH) 72

Figure 27: Box and whisker plots showing the total OH-PAH emissions ($\text{mg}/\text{MJ}_{\text{fuel}}$) from NB (Nominal Burn) and HB (High Burn) samples for different wood types (the bottom and the top of the box plot are the first and the third quartiles, the band is the second quartile (the median), the ends of the whisker are the minimum and maximum of all the data and the black square represent the average) (Avagyan et al., 2016)..... 75

Figure 28: Emission factors of PAHs measured from SPE/PTFE (Teflon/Solid Phase Extraction) where (G) and (A) represent gas- and aerosol-phase samples, respectively, excluding naphthalene as well as naphthalenes with C1 and C2 substituents (Stewart et al., 2020)..... 77

Figure 29: Efficiencies in % of ESP as a function of particle size compared to other secondary techniques inspired from (Ghafghazi et al., 2011) 79

Figure 30: Concentration of particulate EC, OC, and unknown material. In. = Upstream ESP. Out. = Downstream ESP (Bäfvér et al., 2012) 80

Figure 31: Comparison of the measured particle size distributions at all three biomass fired power plants equipped with ESP (ESP: ElectroStatic Precipitator) from (Mertens et al., 2020)..... 81

Figure 32: Result of combustion tests. Ceramic Foam Element (CFE), Catalytic Ceramic Foam Element (CCFE), Honeycomb Catalyst (HC), DYI and DYII are dummy devices (Wöhler et al., 2017)..... 82

Figure 33: The average particle mass size distributions from combustions with (CAT) and without (NCAT) the catalytic combustor measured with a Dekati low pressure impactor (DLPI). Number of parallel samples in NCAT is four and in CAT is three (Hukkanen et al., 2012)..... 83

Figure 34: . Proportions of different PAH compounds in the total concentration of 14 PAHs (Kaivosoja et al., 2012) 84

Figure 35: Fabric filter testing facility presented in (Brandelet et al., 2020)..... 85

Figure 36: Schematic diagram of the three stages of the (biomass) reburning process by (Oluwoye et al., 2020)..... 86

Figure 37: Schematic of non-TES (Thermal Energy Storage) and TES systems from (Wang et al., 2019)..... 87

- Figure 38: (a) Evolution of the individual PAH emission factors with the pre-treatment (total emission factors of the three phases (solid, condensed and gas); (b) number of cycle distributions of total PAH emissions (data expressed in $\mu\text{g} \cdot \text{kg}_{\text{dw}}^{-1}$); and (c) number of cycle distributions of total PAH emissions expressed into toxic equivalent (data expressed in μg eq. Benzo[a]Pyrene $\cdot \text{kg}_{\text{dw}}^{-1}$) – From (Schmidt et al., 2018)..... 88
- Figure 39: KBA emission limits values. Limit values for passenger cars (upper left). Detailed view of EURO 3 to 6 norm for passenger cars (upper right). Limit values for commercial vehicles (lower right). Market penetration of new emission limit levels for passenger cars (Fiebig et al., 2014) 96
- Figure 40: Schematic overview of DPF efficiency from (Guan et al., 2015). (a) Vehicle emission proposal for EURO 6 (Piock et al., 2011); (b) Comparison of particulate number and particulate mass emissions for gasoline and diesel engines (Whitaker et al., 2011); (c) Data set in PN-PM space for European light-duty vehicles (* Diesel only, ** Diesel and Direct Injection Spark Ignition only) (Braisher et al., 2010); and (d) NEDC PN emissions and filtration efficiency of GPF (Richter et al., 2012), Samples evaluated in NEDC on 2.0 L GTDI vehicle and high dynamic engine bench: reference) Reference system; systeme 1) test system with uncoated GPF in underbody position, systeme 2) test system with coated GPF in underbody position, system 3) test system with zoned close coupled TWC and coated GPF in underbody position. 97
- Figure 41: BC/PN and BC/PM10 correlations for gasoline (a and b) and Diesel vehicles (c and d). BC: black carbon; PN: particle number; PM10: particle mass with particle diameter below $10 \mu\text{m}$ - From (Louis et al., 2016b) 98
- Figure 42: (Left) Comparison between the PAH emission factors (EF) for Diesel vehicles (red bar) and the findings of (Polo Rehn, 2013) (blue bar) and (Pillot et al., 2006) (green bar). Comparison between the aldehyde emission factors (EF) for gasoline vehicles (middle) and Diesel vehicles (right) (red bar) and the findings of (Polo Rehn, 2013) (blue bar) and (Caplain et al., 2006) (green bar). From (Louis et al., 2016b). 99
- Figure 43: Emission factors for three diesel (D1, D3 and D4) and four gasoline (GDI1, GDI3, PFI4, GDI5) vehicles Euro5: BC EFs are expressed in mg km^{-1} , while for organics, PAHS, sulfate, ammonium and nitrate the values are expressed in $\mu\text{g km}^{-1}$. Two cycles ARTEMIS and WLTC are studied. Gasoline cars are shown with solid bars and diesel cars with pattern bars. The error bars correspond to $\pm 1\sigma$ standard deviation (Kostenidou et al., 2020) ... 100
- Figure 44: Impact of legislation on PM emissions including SOA formation from (Drozd et al., 2019). Vehicles are classified by their emissions certification standard. The test fleet included: one Tier 0 vehicle (T0), one low emission vehicle (LEV I), two Tier 2 low emission vehicles (LEV II) vehicles, five ultralow emission vehicles (ULEV), five superultra-low emission vehicles (SULEV), and six partial-zero emission vehicles (PZEV). Because the PZEV and SULEV vehicles have the same tailpipe emission standards, results from these are combined and termed SULEV. 101
- Figure 45: Emission factors from in-use vehicles of POA, SOA and BC in $\text{g kg}_{\text{fuel}}^{-1}$. SOA produced after 5hrs aging. After (Chirico et al., 2010). 102
- Figure 46: The number of different types of particles in the emissions from the GDI vehicle under the different running states by the burning per unit of fuel, including cold-start, hot-start, hot stabilized, idle, and acceleration states. Data presented as mean \pm standard deviation, $N=3$ from (Xing et al., 2020)..... 103
- Figure 47: (A) Chemical composition of diesel fuel, gasoline, and evaporative gasoline emissions, with (B) SOA yield of each emission profile shown as a sum of SOA

contributions; both are shown as a function of compound class and carbon number. Partitioning of oxidation products is calculated at an organic aerosol concentration of $10 \mu\text{g m}^{-3}$ after ~ 6 h of photochemical aging. Note: “branched cycloalkanes” refers to those with more than a single linear alkyl substituent (Gentner et al., 2017)..... 104

Figure 48: Cumulated and weighted genotoxic potential of GDI- and diesel vehicle exhausts (ng TEQ m^{-3}) in the cold (upper), hot WLTC (middle) and the Start / Stop Coasting (SSC) (lower diagram. Mean values (\pm standard deviation) of the GDI fleet ($n = 7$) and the bench mark diesel vehicle with DPF are highlighted in grey and red. A zoom of the SSC data is also given (bottom) from (Muñoz et al., 2018) 105

Figure 49: (a) Results of BC emission of EURO 3, 5, and 6 on five different NIER modes. (b) BC Emission from EURO 3 on CVS-75 mode, and EURO 4, 5, and 6 on NEDC mode as presented in (Park et al., 2020)..... 106

Figure 50: Primary and fresh exhaust emission factors (mg/km) for BC (a) and BrC (b) during the NEDC and WLTC with different fuels (MY diesel, EN950, Indian diesel). Emission factors were calculated from the AE33 data (880 nm for BC and 370 nm for BrC). Note that cs and hs refer to the cold start and hot start cycles, respectively from (Pirjola et al., 2019) in supplementary material. 108

Figure 51: BC against simultaneous PM1 from 5 and 13% graphite brake material with correlated linear regression from (Lyu and Olofsson, 2020) 111

Figure 52: Schematic flow diagram of an overall elevated flare stack system in an industrial plant..... 117

Figure 53: Upstream Gas Flaring 2019 - million cubic meters for flaring - $\text{mln m}^3 \text{ yr}^{-1}$ (GGFR, 2016)..... 118

Figure 54: Top 30 Flaring countries by the World Bank (GGFR, 2016)..... 118

Figure 55: Size modes of PM as determined by SMPS (scanning mobility particle sizer) are depicted as a function of DRE (Destruction Removal Efficiency from 60 to 100%) for steam and air assisted flares. Propene/TNG is 80% propene 20% Tulsa Natural Gas, and Propane/TNG is 80% propane 20% Tulsa Natural Gas. SMPS scanned from 15 to 500 nm mobility diameters in all cases. 121

Figure 56: Mean and 95% confidence interval of measured BC yields on a mass-per-volume basis shown as a function of volumetric higher heating value (Conrad and Johnson, 2017) 122

Figure 57: The global map of the mean values of $\text{EF}_{\text{flare,BC}}$ for various gas flaring regions by (Huang and Fu, 2016). A histogram of $\text{EF}_{\text{flare,BC}}$ is shown inside the bottom left corner of the figure. Abbreviations of some regions are defined as: USA—United States of America; CONUS—Conterminous United States; UK—United Kingdom of Great Britain and Northern Ireland; DR Congo—Congo (Democratic Republic of the); UAE—United Arab Emirates..... 123

Figure 58: Emission indices of a natural gas flame with air or steam coflow. Data includes error bars for the propagation of measurement uncertainties in calculating emission indices and mass flow rates for the methodologies described in (Ahsan et al., 2019)..... 128

Figure 59: Upper view of the flare with multiple tips (left: $n=4$ left, right: $n=6$) 130

Figure 60: Soot yield at diferent branches and diameters from (Mostafayi and Rashidi, 2020) 131

List of main abbreviations and acronyms

AC	Arctic Council
ACAP	Arctic Contaminants Action Program
AGP	Amended Gothenburg Protocol
AMS	Aerosol Mass Spectrometer
APG	Associated Petroleum Gas
AQ	Air Quality
ARTEMIS	Assessment and Reliability of Transport Emission Models and Inventory Systems
BaP	Benzo(a)pyrene
BAT	Best Available Technology
BB	Biomass Burning
BC	Black Carbon
BrC	Brown Carbon
BREF	Best Available Technologies Reference document
BTEX	Benzene, Toluene, Ethylbenzene, Xylenes
CC	Climate Change
CDPF	Catalyzed Diesel Particulate Filter
CE	Combustion Efficiency
CEN	Comité Européen de Normalisation - European Committee for Standardization <i>in english</i>
CEIP	Centre on Emission Inventories and Projections
CFD	Computational Fluid Dynamic
CLRTAP	Convention on Long-Range Transboundary Air Pollution
CO	Carbon monoxide
CO ₂	Carbon dioxide
DI	Diesel
DOC	Diesel Oxidation Catalyst
DPF	Diesel Particulate Filter
DRF	Direct Radiative Forcing
DT	Dilution Tunnel
EB	Executive Body
eBC	Equivalent BC
EC	European Commission or Elemental Carbon
ECE	Economic Commission for Europe
EECCA	Eastern Europe, Caucasus and Central Asia
EEA	European Environmental Agency

EF	Emission Factor
EGR	Exhaust Gas Recirculation
ELV	Emission Limit Values
EMEP	European Monitoring and Evaluation Programme
ESP	Electrostatic Precipitator
EU	European Union
FP	Fine Particle
GAINS	Greenhouse Gas-Air pollution Interactions and Synergies (IIASA model)
GDI	Gasoline Direct Injection
GF	Gas Flaring
GFED	Global Fire Emissions Database
GHG	Greenhouse Gases
GPF	Gasoline Particle Filter
HC	Hydrocarbons
HDV	High Duty Vehicle
HVO	Hydrotreated vegetable oil
IP	Indeno(1,2,3-cd)fluoranthene
IVOC	Intermediary Volatility Organic Compounds
IR	InfraRed
ISP	Incipient Smoke Point
LCV	Light Commercial Vehicle
LDV	Light Duty Vehicle
LLE	Loss of Life Expectancy
LNG	Liquefied Natural Gas
LPG	Liquefied Petroleum Gas
LRTAP	Long-range Transboundary Air Pollution
MCE	Modified Combustion Efficiency
MPI	Multi-Point-Injection
m/z	Mass/Charge ratio
NDC	Nationally Determined Contributions
NEDC	New European Driving Cycle
NFR	Nomenclature For Reporting
NH ₃	Ammonia
NMVOC	Non Methane Volatile Organic Compounds
NO _x	Nitrogen Oxides
NP	Nanoparticles
OC	Organic Carbon

OGC	Organic Gas Carbon
OM	Organic Matter
OOA	Oxidized organic aerosol
O ₃	Ozone
PAH	Polycyclic Aromatic Hydrocarbons
PAM	Potential Aerosol Mass
PC	Passenger Car
PCDD/F	Polychlorinated dibenzo-p-dioxin and dibenzofuran
PFI	Port Fuel Injection
PM	Particulate Matter
PM _x	Particulate Matter for particle diameter below x μm (x=0.1, 1, 2.5, 10)
POA	Primary Organic Aerosols
POP	Persistent Organic Pollutant
PUF	Polyurethane foam
rBC	Refractory BC
RWC	Residential Wood Combustion
SCR	Selective Catalyst Reduction
SDG	Sustainable Development Goal
SLCP	Short-Lived Climate Pollutants
SNAP	Selected Nomenclature for Air Pollution
SOA	Secondary Organic Aerosol
SO _x	Sulphur Oxides
SVOC	Semi-Volatile Organic Compounds
TFTEI	Task Force on Techno-Economic Issues
THC	Total HC
TSP	Total Suspended Particles
TWC	Three Way Catalyst
UFP	Ultrafine particle
UN	United Nations
UNECE	United Nations Economic Commission for Europe
UNFCCC	United Nations Framework Convention on Climate Change
UV	UltraViolet
VOC	Volatile Organic Compounds
WHO	World Health Organization
WMO	World Meteorological Organization
WLTC	Worldwide harmonized Light vehicles Test Cycles
ZRF	Zero Routine Flaring

Executive summary

Black carbon (BC) is a component of Particulate Matter (PM) with short term health impact and an active substance enhancing global warming due to its capacity to absorb sun radiations. Polycyclic Aromatic Hydrocarbons (PAHs) are a large group of organic compounds with multiple fused aromatic rings presenting health impacts. The heaviest ones are in solid form, those with a small number of rings may be volatile and present in gaseous form in the atmosphere. PM presents a large spectrum of components such as dust, BC, organic compounds, sulphates, nitrates, ammonium, etc... These different components may have a warming or cooling effect in the atmosphere.

To mitigate health risks and climate change, proper knowledge regarding the physical and chemical properties of particulate pollutants and particularly carbonaceous species along with their fate, transport and transformation through the environment is consequently required. Fossil fuel consumption both in stationary and mobile sources, biomass burning (BB) and industrial emissions are the key sources of BC and associated PAHs into the atmosphere. As BC has a short life span, it may be easy to overcome the environmental burden by cutting up or controlling its emissions.

Secondary processes in the atmosphere are also a large source of PM. Recently (Daellenbach et al., 2020) showed that the oxidative potential concentration is associated mostly with anthropogenic sources, in particular with fine-mode secondary organic aerosols largely from residential biomass burning and coarse-mode metals from vehicular non-exhaust emissions.

Reduction of emissions of BC and PAHs is linked to the reduction of PM emissions. This report provides an overview of BC, PAH and also Ultrafine Particles (UFP) emissions and the effect of PM emission reduction measures on these species emissions. The investigation has been extended when possible to the whole spectrum of carbonaceous species like secondary organic aerosols (SOA) and brown carbon (BrC) which have an impact on the radiative budget and the PM mass. Three target sectors have been considered, two of them, small combustion sources, and road transport because they are the major sources of BC, and Gas Flaring (GF) because this activity is an important source of pollutants for both air quality and climate impact in the Arctic regions.

This document completes the Guidance document on prioritising the measures (ECE,2020) by providing in depth analysis of capacities of techniques to really reduce BC and PAHs. It will serve the review of ELVs (Emission Limit Values) of annex X of the AGP (amended Gothenburg Protocol) to be carried out in 2021.

Residential wood burning remains a major issue, and many efforts still need to be made to reduce emissions of PM and BC. Advanced or eco-labelled stoves and boilers enable PM and BC emission reduction. The quality and the type of wood is also important and dry wood is usually recommended. Good practices are also essential (Code of Good Practices developed by (TFTEI, 2019)). Many policy interventions have led to effective PM and BC emission reduction in the household sector. However, if BC emissions is likely to be reduced, particle number is questioning during the dilution of emissions. The decrease of available mass for condensation and lower temperature can increase nucleation processes and then increase the number of particles.

The determination of PM Emission Factors with more reliable standards is a critical issue. Methods should inform on the filterable and **condensable fractions of particles** to better know real PM emissions from small wood appliances and develop emission inventories more relevant

for the modelling community who use these data to help the development strategies for policy makers to both curb air pollution and adverse climate impacts.

With the shift to more stringent regulations applied to road vehicles, PM emissions and all particulate species including BC at the exhaust pipe are likely to decrease. Therefore, **tyre and brake emissions are turning dominant** sources and they are also a source of BC even if these particles are mainly in the coarse mode (diameter > 2.5 µm). Ultrafine particles can also be emitted by brake uses. The choice of pad material is the main technical way to decrease emissions even some suction devices could be used to remove most particles from brakes.

At least 90% of particulate carbonaceous species in the gas flare flue gas is made of black carbon. **Steam-assist Flares** are clearly **the most efficient** in terms of soot emission reductions. However high pressure-assisted flares can be an efficient technique if water is not available on site. New models based on neural networks (advanced statistical methods) could help to better assist the flaring operations to better control soot formation.

To better tackle Climate Change and Air Quality not only through the BC emission reduction, the emissions of Brown Carbon (BrC) are also important. BrC is a light-absorbing particulate matter mainly co-emitted by biomass burning or produced later during the plume dilution. So far, this species is not very well identified, and there are uncertainties in the radiative properties assigned to this species in climate models.

Key conclusions

Small scale combustion

- Exposure to outdoor and indoor air pollution is known to affect respiratory and cardiovascular health, and a recent study also shows its effects on cognitive function. Open fireplaces, traditional stoves and cookers as a source of indoor and outdoor air pollution, can be the origin of environmental inequities (gender, age) particularly in developing countries. There is a clear advantage to tackle residential wood combustion to both reduce health effects (and associated costs) and rapidly have a benefit on climate even if the impact is weak compare to other GHG.
- BC emissions from *residential combustion* is by far the largest contributor at the global scale. In EU27+UK, BC from *stationary combustion* emissions is 3 times higher than BC from the *passenger car* emissions in 2018. These emissions are mostly due to biomass burning and particularly wood burning.
- BC concentrations in waste gases are usually determined by thermo optical methods and certainly account for a fraction of organics. OM is usually derived from OC measurements issued from thermal methods.
- PM emitted by biomass burning from small combustion appliances are mainly composed of carbonaceous compounds (Elemental Carbon (EC) and Organic Matter (OM)). Most of particles are fine particles with diameter below 2.5 µm. A secondary production of particles is identified during the dilution of the plume and later in ambient conditions.
- Birch, Spruce and Pine often exhibit the highest emission factors of PM, BC and PAHs. Raw fir is a strong emitter of PAHs. Wood Oak emits the lowest BC. Burning wet wood is not recommended as presented in the Code of good practices for wood burning and small combustion installations (TFTEI, 2019), however some studies showed higher

PM1, PAH and BC emissions using very dry wood (11%) compared to wet wood (18%) while the particulate number (PN) is lower for dry wood.

- The use of modern stoves implementing advanced methods to limit the emission of pollutants like catalytic combustors, wood pellets and masonry stoves enables to reach the emission standards as defined in the EU by latest eco-design standards. The ban of not eco-labelled wood stove seems the most beneficial in some recent studies. However, the use of catalytic combustor can increase the emissions of PCDD/F due to the effect of the catalyst. Organic gases are also largely reduced with modern wood stoves which involve a potential positive effect to reduce the secondary organic aerosol (SOA) potential formation.
- Automatic fuel feeding and improvement of air staging combustion clearly improve the combustion efficiency. Low cost strategies of retrofit air injection on traditional stoves can reduce PM and BC emissions. High burn rates should be avoided as they are associated to higher pollutant emissions.
- Wood pellet stoves have 2 to 3 times lower PM, EC and PAH emissions than wood logs in advanced wood stoves. However, their efficiency to reduce particle number is not as high as expected.
- Electrostatic Precipitator would be a good strategy to reduce particles. Efficiency exceeding more than 99% are commonly obtained in combustion plants, however in practice this technology is not suitable for residence appliances. The efficiency of ESPs to reduce nanoparticles is not clear yet. Under favourable combustion conditions, after the ESP during the cooling of the flue gas, organic matter can appear due to condensable species.
- Additional strategies like Thermal Energy Storage can help to optimize the heating cycle from the start-up and the shutdown. Start-up is a critical phase with high emissions of pollutants.
- The formation of solid particulate matters is highly sensitive to secondary air distance and uniformity of air distribution in the secondary air modules. Air staging can be optimized to reduce air pollutant emissions. However, air staging strategy in combination to reburning in order to reduce NOx can produce nitro-PAH known to have a high carcinogenic potential.
- From (TFTEI, 2019), the following list of new technologies were identified and can be recommended. New advanced stoves equipped with improved air control, reflective materials and two combustion chambers; New smart stoves with automated control of air supply and combustion, thermostatic control, Wi-Fi-connected to collect and send combustion data to the manufacturer for better service; New advanced masonry stoves, operating at high efficiencies and low emissions; New advanced pellet boilers: fully automated boilers (electronic control of air supply, lambda sensors), condensing boilers, using standardised pellets; Wood carburettor boilers using log wood or chip wood; Heat accumulating equipment with heat accumulating reducing stop/start frequencies and operation at partial load, which generates higher emissions than operation at full load; Other: flue gas recirculation, reverse combustion, gasifier.
- Currently, test procedures for delivering labels are not able to characterise real conditions of use of domestic appliances. New normalised test procedures would be useful to better account for real utilisations of small-scale combustion appliances (starting phases, closing phases).

- Harmonized methods to determine the emission concentrations of PM and BC would be necessary. For PM, methods accounting for condensables like dilution tunnels are existing.

Road Traffic

Diesel particulate filters (DPFs) have been widely used in the motor vehicle industry for decades and found to be cost-effective, including in their reduction of pre-mature deaths and other health problems. In parallel, as PM and BC emissions have decreased with very efficient aftertreatment systems, the PM emissions portion from tires and brakes is continuously increasing. From the recent literature review the following statements can be drawn.

- PM produced by combustion emitted at the exhaust pipe are mostly fine particles below 2.5 μm and are mainly composed of carbonaceous species.
- PM, BC, PN (particle number), and PAH emissions are effectively reduced using tailpipe aftertreatment systems as Diesel Particulate Matter (DPF) or Gasoline Particulate Matter (GPF). Decreases from 90 to 100% are commonly observed for most particulate pollutants.
- As an order of magnitude of PM_{2.5} emission factors, changes from Conventional to Euro VI for Heavy Duty Vehicles (HDV) from 333-491 to 0.5-1.3 mg km⁻¹ can be observed. The fraction of BC in PM ranges from 10 to 20% in Euro VI HDV vehicles.
- Since emission factors of solid particles have decreased by at least 2 orders of magnitude, the counter part is an increase of the part of the OM due to the dilution and cooling effects producing mainly organic condensable species.
- However, the cooling and dilution effects in the exhaust plumes produce less and less absolute emissions of condensables with the implementation of successive Euro legislations. Aftertreatment systems reduce the intermediate volatility organic compounds (IVOC) emissions but there are still several gaps in the knowledge of these compounds and their chemical transformation after emissions and in ambient conditions.
- With the decrease of PM emissions, gasoline vehicles even recent, can now produce more particles. The use of GPF for gasoline is a key technology to reduce PN and PM emissions. However, a study has reported larger genotoxic PAH emissions from gasoline vehicles (mainly Gasoline Direct Injection vehicles) even equipped with DPF compared to diesel equipped with DPF (2 orders of magnitude higher).
- Recent research findings show that different after-treatment technologies have an important effect on the level and the chemical composition of the emitted particles, and highlight the importance of the particle filter device conditions and their regular checking to maintain the best performances.
- For non-equipped diesel vehicles, the use of biofuels can reduce BC emissions by 30% and could be an option to achieve sooner the legal air quality thresholds.
- Even if brake, tire and road wear emit mainly coarse particles, a non-negligible fine fraction of PM is emitted. The TSP emissions per km are larger than current Euro 6/VI emissions and a similar fraction of BC is observed either in exhaust and non-exhaust PM emissions. Brakes also produce ultrafine particles, metals and PAHs, the temperature greatly affect the PM emissions. BC emissions from brakes are very correlated to PM₁ emissions.

- There is no widely used after-treatment system to control brake, tire and road wear emissions. The type of materials, and the behaviour of the driver is often cited as a key to reduce emissions. Some companies have developed brake particles collection system that would reduce by 80% to 90 % respectively the brake mass and number emissions.
- PM resuspension from the road are also significant. This emission is responsible for a large fraction of total road traffic emissions. It depends on meteorology (wind, temperature, humidity, precipitation) and the site climatology (land use in the vicinity).

Gas Flaring (GF)

- Black carbon emissions from the oil & gas industry by Gas Flares is an important source and particularly in areas surrounding the Arctic zone as they affect the radiative budget and enhance snow melting. Russia, USA, Africa and some Middle East countries are among the largest emitting countries.
- Usually, at least 90% of carbonaceous species in the Gas Flare flue gas is made of Black Carbon.
- Emission factors from GF are uncertain since the combustion conditions can vary and can be not monitored enough. The emission factors (EF) can vary over several order of magnitude generally in the range 0.2 to 2.27 g m⁻³.
- Emission inventories deriving from these EF are therefore uncertain and often gap filled or assessed by Satellite observations.
- Routine flaring from a lack of gas utilisation sources is the most important and largest source of BC emissions from flaring, however, intermittent flaring and continuous flaring for operational reasons can also be significant sources.

An overview of the potential routes to reduce BC emissions from gas flaring can be broken down into several type of options.

- Using associated gas for on-site application or export (Power, heat, gas generation) is a natural solution to reduce BC and other flaring emissions by avoiding the flue gas emission. Associated gas utilization virtually eliminates BC emissions, however, flaring and low gas utilization rates are often common during the first years of production in new fields because decisions on gas infrastructure construction are often made only after production starts. In addition, even when it is economically interesting to utilize Associated Petroleum Gas (APG), there will typically be some degree of flaring for safety or other operational reasons. Finally, in some cases, no gas recovery solution will be available or considered feasible.
- Under these conditions, other options to minimize BC emissions exist: extraction of heavy components from the flared gas stream.
- A flare with multiple tips seems a good example showing good performances on BC emission reductions.
- Steam-assist flares are clearly the most efficient in terms of suppressing soot formation. However high pressure-assisted flares can be an efficient technique if water is not available on site. Steams assisted flares show less emission of very small particles (below 50 nm) compared to air steam assisted flares.

- The optimization of flare design and combustion conditions is an option thanks to the use of Computational Fluid Dynamic (CFD) model. Model and control systems can be used to monitor the flue gas characteristics and control the input data.
- New models based on Artificial Intelligence techniques can be used to set optimized input parameters to lower emission flaring and therefore reduce BC emissions.

1 Introduction

Ambient air pollution is one of the main global health risks, causing significant excess mortality and Loss of Life Expectancy (LLE), especially through cardiovascular diseases. It causes an LLE that rivals that of tobacco smoking. The global mean LLE from air pollution strongly exceeds that by violence (all forms together), *i.e.* by an order of magnitude (LLE being 2.9 and 0.3 years, respectively) according (Lelieveld et al., 2020) based on the calculation of exposure to Ozone and PM_{2.5}. The ambition to reduce emissions, improve air quality and reduce the impacts on public health and the environment on one hand, and questions of cost, technical feasibility and societal acceptability on the other hand as described in (Monks and Williams, 2020) is a key issue.

The Convention on Long-range Transboundary Air Pollution (LRTAP) of the UNECE (United Nation Economic Commission for Europe) signed in 1983 is the first international instrument aiming at reducing air pollutant emissions and decrease its impacts on health and ecosystems. Several Protocols were implemented and the latest one, the Protocol to abate Acidification, Eutrophication and Ground level Ozone or Gothenburg Protocol amended in 2012, entered into force on 7 October 2019. Pursuant to its article 10, the Protocol is under review following a Decision of the Executive Body (EB) in December 2019. The review process should be finalised in December 2022.

The Task Force on Techno-economic Issues (TFTEI) has been tasked of a certain number of activities to help the process of review.

According to the Decision 2018/7 (ECE, 2018a) of the EB of the CRTAP (thirty-eighth session (ECE, 2019), Geneva, 10–14 December 2018), the revised mandate of the Task Force on Techno-economic Issues (TFTEI), the Task Force will continue among other tasks, to:

- i. Investigate co-benefits and trade-offs between emission abatement technologies and policies under consideration to address air pollution, climate change and biodiversity;
- ii. Carry out the tasks specified for it in the biennial workplans approved by the Executive Body and report thereon to the Working Group on Strategies and Review, while keeping the Working Group on Effects and the Steering Body to the Cooperative Programme for Monitoring and Evaluation of the Long-range Transmission of Air Pollutants in Europe, apprised of its activities;
- iii. Carry out other tasks requested by the Executive Body for the Convention on Long-range Transboundary Air Pollution or by the Working Group on Strategies and Review, subject to availability of adequate financial and human resources;

The biennial workplan (2020-2021) for the implementation of the Convention aims at translating the vision and strategic priorities, set out in the long-term strategy for the Convention (2020–2030 and beyond (ECE, 2018b) into a list of activities to be carried out by the respective bodies under the Convention in accordance with their revised mandates, as adopted by the Executive Body at its thirty-eight and thirty-ninth sessions. The workplan also contains additional activities of the task forces and centres, not mentioned in the mandates, which are decided by the EB, from time to time, as needed. The following report was to be addressed:

Development of guidance in relation to prioritizing reductions of particulate matter in its sources that are also significant sources of black carbon

It has been prepared by TFIAM with the support of TFTEI (ECE, 2020).

This document prepared by TFTEI is a review of recent findings on the impact on PM emission reduction on Black Carbon (BC) and Polycyclic Aromatic Hydrocarbons (PAH) emission reductions for key activity sectors. The investigation has been extended when possible to the whole spectrum of carbonaceous species like secondary organic aerosols (SOA) and brown carbon (BrC) which have an impact on the radiative budget and the PM mass.

This document completes the guidance document on prioritising the measures (ECE,2020) by providing in depth analysis of capacities of techniques to really reduce BC and PAHs. It will serve the review of ELVs (Emission Limit Values) of annex X of the AGP (amended Gothenburg Protocol) to be carried out in 2021.

Moreover, this report fulfils the conclusions of the Long Term Strategy (ECE, 2018b), such as:

- (a) Continuing to use the best available science and to further develop the multi-pollutant, multi-effect approach;
- (b) Striving for an integrated approach to environmental policymaking that includes ground-level ozone-nitrogen-climate-biodiversity interaction; integrated nitrogen management, including its impact on health; the climate change co-benefits of air pollution policies and measures; and the impact of climate policies on air pollution.

2 Legal framework

2.1 The Gothenburg Protocol

On 4 May 2012, during the thirtieth session of the EB (30 April–4 May 2012), the Parties to the Convention on Long range Transboundary Air Pollution adopted the decisions to amend the Gothenburg Protocol and its annexes (ECE, 2013) as follows:

- Decision 2012/1 on amendment of annex I to the Protocol;
- Decision 2012/2 on amendment of the text of and annexes II to IX to the Protocol and the addition of new annexes X and XI;

The objective of the present Protocol is to control and reduce emissions of sulphur, nitrogen oxides, ammonia, volatile organic compounds and particulate matter that are caused by anthropogenic activities and are likely to cause adverse effects on human health and the environment, natural ecosystems, materials, crops and the climate in the short and long term, due to acidification, eutrophication, particulate matter or ground-level ozone as a result of long-range transboundary atmospheric transport, and to ensure, as far as possible, that in the long term and in a stepwise approach, taking into account advances in scientific knowledge, atmospheric depositions or concentrations do not exceed the ceilings over target regions as defined in Annex I of the Amended Gothenburg Protocol (AGP).

National reduction commitments for the PM emissions are defined for PM_{2.5} (particles with diameter below 2.5 µm). Black carbon (BC) is a major constituent of PM while Polycyclic Aromatic Hydrocarbons (PAHs) are trace elements with potential carcinogenic effect. While PAHs are not cited in the AGP, Black Carbon is largely evoked without binding decisions but with recommendations on the monitoring of this substance in the ambient air and at the emission. It is also encouraged to take synergic measures reducing both PM and BC to both (i) curb climate change effects and (ii) improve air quality. Some PAHs are covered by the amended Aarhus Protocol on Persistent Organic Pollutants (ECE, 2010). In Annex X of the

AGP, emission limit values (ELVs) of particulate matter from stationary sources are provided, applying to Parties other than Canada and the United States of America. In this annex, ELVs are defined for “dust” expressed as mg m⁻³, assuming standard conditions for temperature and pressure for dry gas (volume at 273.15 K, 101.3 kPa). “dust” and “total suspended particulate matter” (TSP) means the mass of particles, of any shape, structure or density, dispersed in the gas phase at the sampling point conditions which may be collected by filtration under specified conditions after representative sampling of the gas to be analysed, and which remain upstream of the filter and on the filter after drying under specified conditions.

For combustion installations with a rated thermal input < 50 MWth, only recommended ELVs are provided as follows:

Emissions from new residential combustion stoves and boilers with a rated thermal input < 500 kWth can be reduced by the application of:

- *Product standards as described in CEN standards (e.g., EN 303–5) and equivalent product standards in the United States and Canada. Countries applying such product standards may define additional national requirements considering, in particular, the contribution of **emissions of condensable organic** compounds to the formation of ambient PM; or*
- *Ecolabels specifying performance criteria that are typically stricter than the minimum efficiency requirements of the EN product standards or national regulations.*

For instance, Table 1 extracted from annex X of the AGP reports ELVs for very small combustion installation particularly in use by households.

Table 1: Recommended limit values for dust emissions released from new solid fuel combustion installations with a rated thermal input < 500 kWth to be used with product standards (Note: O₂ reference content: 13%.)

	Dust (mg m⁻³)
<i>Open/closed fireplaces and stoves using wood</i>	75
<i>Log wood boilers (with heat storage tank)</i>	40
<i>Pellet stoves and boilers</i>	50
<i>Stoves and boilers using solid fuels than wood</i>	50
<i>Automatic combustion installations</i>	50

Emissions from existing residential combustion stoves and boilers can be reduced by the following primary measures:

- *Public information and awareness-raising programmes regarding:*
 - i) *The proper operation of stoves and boilers;*
 - ii) *The use of untreated wood only;*
 - iii) *The correct seasoning of wood for moisture content.*
 - *Establishing a programme to promote the replacement of the oldest existing boilers and stoves by modern appliances; or*
 - *Establishing an obligation to exchange or retrofit old appliances*

2.2 The EU legal framework

The National Emission Directive (EU, 2016) is the general framework which transposes the AGP obligation at the EU level defining for instance the national emission reductions for the main pollutants among a long list of measures to combat air pollution.

As reminded by (ALPINE SPACE, 2019), solid fuel combustion in households represents about 2.6% of total energy consumption in the EU but contributes more than 46% to total emissions of fine particulate matter. The Ecodesign Directive (EC, 2009; ETC/ACM, 2016) is a framework Directive: it does not set binding requirements on products by itself, but through implementing measures adopted on a case by case basis for each product group. The list of product groups to be addressed through implementing measures is established in the so-called periodic Working Plan. The Directive compiles a list of Ecodesign Measures for specific types of the Energy Use Products directive, which in the case of residential heating are included in the Commission Regulation on solid fuels local space heaters (EC, 2015a) and on boilers (EC, 2015b), implementing Directive (EC, 2009) of the European Parliament and of the Council with regard to Ecodesign requirements for space heaters and combination heaters (EC, 2009). It is then stated in (EC, 2015a) that :

“Particulate matter (PM) shall not exceed the declared value by more than 20 mg m^{-3} at 13 % O_2 for open fronted solid fuel local space heaters, closed fronted solid fuel local space heaters using solid fuel other than compressed wood in the form of pellets and cookers and 10 mg m^{-3} at 13 % O_2 for closed fronted solid fuel local space heaters using compressed wood in the form of pellets when measured according to the method described in Annex III, point 4(a)(i)(1) or by more than 1 g kg^{-1} when measured according to the method described in Annex III, point 4(a)(i)(2) or by more than $0,8 \text{ g kg}^{-1}$ when measured according to the method described in Annex III, point 4(a)(i)(3);”

The limit values defined in the Ecodesign directive is more ambitious compared to the requirements of the AGP. A recent study in Denmark shows that there are large net welfare gains from most types of regulation of existing installations, but the largest gains result from imposing a differentiated tax or a general ban on non-ecolabeled stoves (Bjørner et al., 2019).

(Savolahti et al., 2014) studied the impact of the EcoDesign directive in Finland. This study estimated the impacts of such legislation to the Finnish appliance stock and for reducing national RWC emissions by the year 2030. EcoDesign will only affect new appliances placed on the market and due to the long lifetime of commonly used stoves in Finland, there is a notable lag between the legislation entering into force and achieving visible results in emission reduction. In a studied baseline scenario, the implementation of EcoDesign from the start of 2022 will produce 6% reductions to PM_{2.5} emissions and 4% reductions to black carbon emissions in 2030. Although it is a step in the right direction, it takes a long time for the legislation to have notable effects on emissions, and, according to the authors, it also doesn't address the single most important appliance type in Finland – sauna stoves. This study means that additional measures are needed to reduce emissions in this sector depending on the country habits.

For the road transport which still emit a large amount of PM (Eastwood, 2008), the so-called EURO regulations are the legal framework in EU to fix ELVs for all type of vehicles. As summarized for passenger cars and light commercial vehicles, the limit values for the last EURO 6 (EC, 2007) regulation provides ELVs for PM in mg/km but also for particle numbers (PN) in #/km.

Black carbon emissions are among the core regulatory policy issues in all three industries, and they have not yet been adequately addressed by policymakers (Brewer, 2019).

Table 2: Euro 6 emission limits for passenger cars and light-commercial vehicles, table from (Rodríguez et al., 2019)

	LDVs, LCVs Class 1 ^(a)		LCVs Class 2		LCVs Class 3	
	Gasoline ^(b)	Diesel ^(c)	Gasoline	Diesel	Gasoline	Diesel
NMHC*	68	-	90	-	108	-
THC*	100	-	130	-	160	-
NO _x *	60	80	75	105	82	125
THC+NO _x *	-	170	-	195	-	215
CO*	1000	500	1810	630	2270	740
PM*	4.5 ^(d)	4.5 ^(d)	4.5 ^(d)	4.5	4.5 ^(d)	4.5
PN**	6×10 ^{11(d)}	6×10 ^{11(d)}	6×10 ^{11(d)}	6×10 ¹¹	6×10 ^{11(d)}	6×10 ¹¹

Notes: (a) Classes 1 through 3 are weight classes. (b) Gasoline is used as a proxy term for positive ignition (PI) engines. (c) Diesel is used as a proxy term for compression ignition (CI) engines. (d) Applicable to direct injection engines. * unit in mg km⁻¹, ** unit in # km⁻¹.

The way emissions are calculated largely depends on the relevance of the driving cycle used for emission calculations as it was described in (Chen and Borcken-Kleefeld, 2014) for NO_x emissions some years before the “Dieselgate” scandal (Archer, 2016). For diesel vehicles, there was a clear divergence on real emissions and homologation limits values (Figure 1).

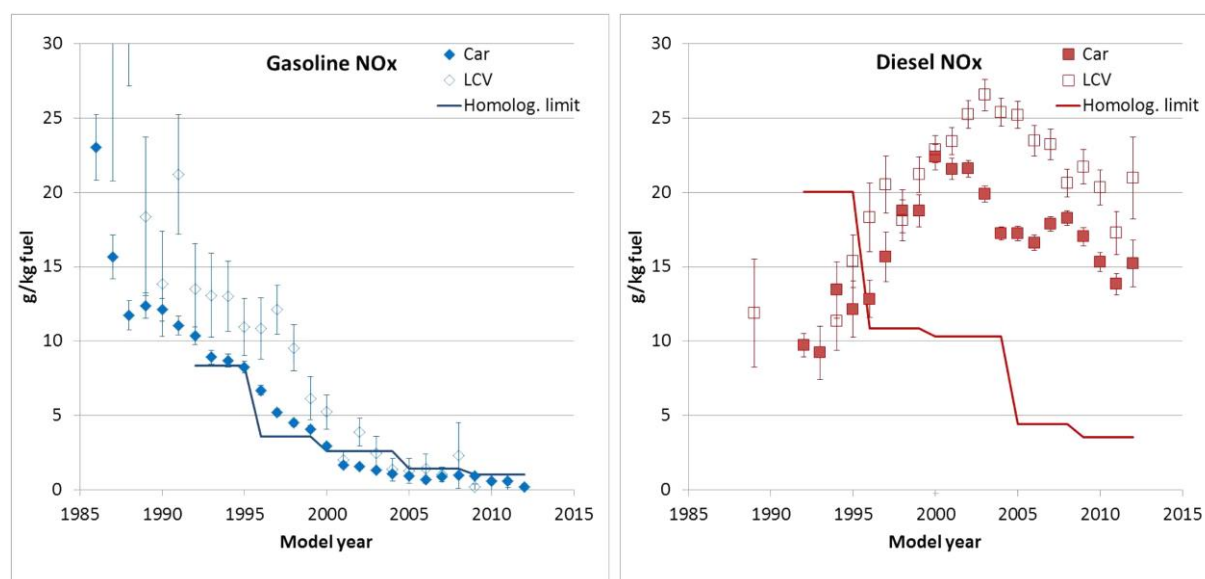


Figure 1: Mean hot NO_x emission factors of gasoline (left) and diesel (right) passenger cars and light commercial vehicles as a function of model year. Whiskers represent the 95% confidence interval over the mean. Added are the type approval limit values for Euro 1 to Euro 5 passenger cars over the homologation test cycle in force in the respective year (Chen and Borcken-Kleefeld, 2014)

2.3 Air pollution and climate change: a grey area of international environmental law?

(Yamineva and Romppanen, 2017) highlighted the “grey area” where the links between Air pollution and Climate stand. There are numerous links between air pollution and climate change policies, but these are poorly integrated into international law and there is little acknowledgement of potential synergies. Recently, greater attention has been paid to SLCPs (Short-Lived Climate Pollutants), some of which contribute to both air pollution and global warming (BC and CH₄ as example). Reducing emissions of black carbon and methane is particularly important where SLCPs are concerned, but international law does not yet provide clear answers as to how such emissions are to be regulated. Methane emissions have traditionally been covered by the UN climate change regime and are part of national reports. The Kyoto Protocol includes methane in its basket of six greenhouse gases; however, the geographical reach of its mitigation actions is limited. The Paris Agreement, which requires all countries to contribute to climate mitigation, does not specify which greenhouse gases it covers. It is based on a bottom-up approach to mitigation where individual countries define the action they will take and report on it through nationally determined contributions (NDCs), in which potentially any greenhouse gas or substance can be included. In fact, in their intended NDCs many countries included methane, several mentioned SLCPs and some countries such as Mexico and Chile specifically mentioned black carbon. At the same time, the dominant focus of the UN climate change regime has been on reducing carbon dioxide emissions while less attention has been given to methane, and black carbon (considered as an aerosol and not as a greenhouse gas) has hardly been discussed at all.

Black carbon emissions are most comprehensively covered in the Northern hemisphere. Through its 2012 amendments, the Gothenburg Protocol to the CLRTAP includes emissions reduction targets for fine PM, of which black carbon is a component. Although the BC component is not specified, Parties are encouraged in implementing measures to achieve their national targets for particulate matter, to give priority, to the extent they consider appropriate, to emission reduction measures which also significantly reduce BC to provide benefits for human health and the environment and to help mitigation of near-term climate change (article 2.2) and to report on their current BC emissions and projections. The AGP came into force in October 2019, 7th.

In addition, action on BC (and methane) has been taken by the Arctic Council through the adoption of the Framework for Action on Enhanced Black Carbon and Methane Emission Reductions and, more recently, of a first collective regional goal for reducing black carbon emissions. The outputs of the Arctic Council are not legally binding. In sum, there is a clear gap in the regulation of black carbon emissions, as no legal frameworks of global reach are currently in place to cover this pollutant.

3 Scientific Background

For the best understanding of the report, definitions and a scientific background from a recent literature review are provided in this section.

3.1 Black carbon and Elemental Carbon

Airborne particulate matter (PM) is a pollutant of concern not only because of its adverse effects on human health but because of its ability to reduce visibility and soil buildings and materials. It can be regarded as a suite of pollutants since PM covers a very wide range of particle sizes and also has a diverse chemical composition. Historically, much of the PM arose from coal burning and was measured as black smoke. However, in the second half of the twentieth century in developed countries, there was a reduction in black smoke emissions from coal burning and PM steadily became dominated by carbonaceous particles from road traffic exhaust and the secondary pollutants, ammonium salts and secondary organic carbon. This is exemplified by the composition of fine particles (referred to as PM_{2.5}) as measured in London, Delhi and Beijing (Figure 2). Steadily, as control strategies have addressed the more tractable sources of emissions, so sources previously regarded as unconventional have emerged and have been seen to make a significant contribution to airborne PM concentrations. Among these are non-exhaust particles from road traffic, cooking aerosol and wood smoke. The particle size distribution of airborne PM is hugely diverse, ranging from newly formed particles of a few nanometres in diameter through to particles of tens of micrometres in diameter. There has been a great deal of interest in ultrafine (nano) particles because of suspicions of enhanced toxicity, and as traffic emissions decrease as a source, so regional nucleation processes have become much bigger relative contributors to particle number, but not mass (Harrison, 2020).

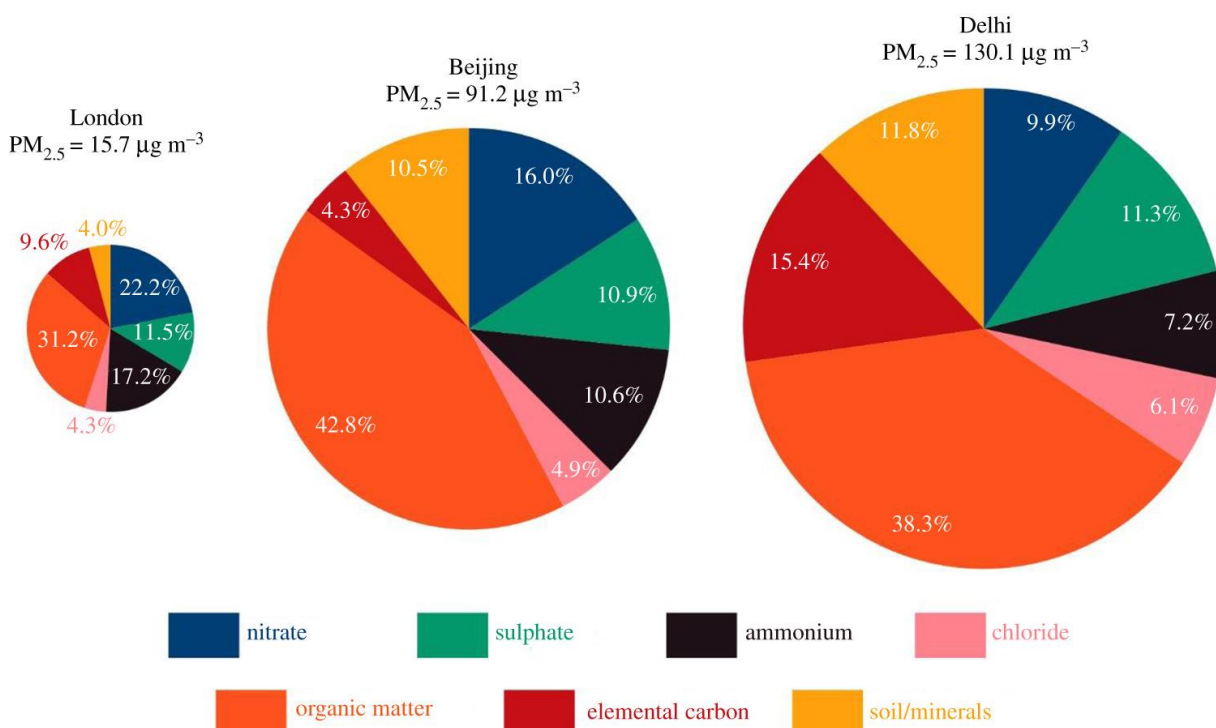


Figure 2: Major chemical component composition of PM_{2.5} collected during winter campaigns in London (North Kensington), Beijing and Delhi. (Online version in colour) (Laskin et al., 2015)

Carbonaceous constituents like BC or Elemental carbon (EC) depending on the sampling measurement method (respectively using pure or thermo-optical method and pure thermal method), and Organic Carbon (OC) are major compounds of PM whatever the location in the

world. BC is a generic term that describes a range of carbonaceous substances from partly charred plant residues to highly graphitized (*i.e.*, highly ordered molecular carbon structures as found in graphite) soot that are generated as products of incomplete combustion. There is no universally accepted chemical definition of the term “black carbon”, and it is oftentimes referred to as soot, graphitic carbon, and/or elemental carbon. Some definitions proposed for black carbon have focused on its chemical and/or physical properties (*e.g.*, its light-absorbing properties), while others are operationally based and reflect the results of measurement and estimation approaches (Chow et al., 2018; Long et al., 2013) and reference therein).

BC and OC have antagonist effects on the radiative budget of Earth (Laskin et al., 2015). **Organic aerosol** can be characterized as “white” because they efficiently **scatter visible radiation**. However, a significant and highly variable fraction of **carbonaceous and organic aerosols absorbs radiations**. The best-known type of light-absorbing carbonaceous aerosol is BC, which represents soot-like particulates generated by fossil fuel combustion and biomass burning. BC absorbs solar radiation over a broad spectral range, from ultraviolet (UV) all the way into infrared (IR). The effects of BC are especially significant in areas that rely on burning biomass and coal. Most OC compounds absorb IR and UV radiation strongly but are relatively transparent to visible (vis, 400–700 nm) and near-IR (700–2500 nm) wavelengths. However, certain types of OC absorb radiation efficiently in the near-UV (300–400 nm) and vis ranges. A new term, “brown carbon” (BrC), has emerged in recent scientific literature to describe this type of aerosol, characterized by an absorption spectrum that smoothly increases from the vis to UV wavelengths. In addition to their direct effects on vis radiation, both BC and BrC immersed in cloud droplets absorb light and facilitate water evaporation and cloud dispersion, an additional indirect effect that counteracts the cooling effect of cloud droplet nucleation by aerosols.

In the literature, two other notions are mentioned as discussed in (Lack et al., 2014). (i) **Equivalent black carbon (eBC)**: A number of commercial instruments that measure the absorption coefficient of absorbing particles derive a mass concentration of “BC” using a conversion constant referred to as a mass absorption coefficient (MAC). In order to clarify that what is being measured may not be 100 % BC, it is sometimes recommended to use of eBC when reporting the carbon mass derived from the absorption coefficient. (ii) **Refractory black carbon (rBC)**: The carbon mass derived from laser induced incandescence (LII) is referred to as refractory black carbon since it is derived by measuring the thermal emission of the carbon component of the particle that absorbs the laser energy.

“**Soot carbon**” or “Soot” particles is also used as a terminology (Petzold et al., 2013). It contains carbon with the morphological and chemical properties typical of soot particles from fossil fuel combustion. Soot carbon particles are formed from agglomerates of spherules composed of graphite-like microcrystallites. They consist almost exclusively of carbon, with minor amounts of hydrogen and oxygen. Note that this definition excludes any organic species that might be present as a coating on the spherules.

3.2 Brown Carbon

Figure 3 taken from (Laskin et al., 2015) shows a range of atmospheric carbonaceous compounds subdivided into operationally defined classes on the basis of the most common methods of bulk particulate matter (PM) analysis. At the top of the chart, BC compounds have the lowest volatility and strongest light-absorption properties. While BC is inherently complex, its basic chemical structure and optical properties are reasonably well-known. In BC, carbon atoms are organized in two-dimensional honeycomb graphitic layers stacked together

perpendicular to the planes of the layers. A large number of electrons delocalized along the extended network of graphitic layers defines the strong broadband absorption properties of the BC material with only weak (λ^{-1}) spectral dependence of the absorption coefficient. The bottom of the chart corresponds to volatile organic compounds with characteristic absorption in the UV spectral range. These organic species are highly relevant to atmospheric photochemical processes, but they have nearly no direct implications for radiative forcing determined by the absorption of visible radiation. Between the two extremes of the chart, there is a broad range of moderately volatile (refractory) organic compounds with different and poorly characterized molecular structures. Among them, a subset corresponds to coloured compounds with optical properties relevant to the BrC material. In contrast to BC, the light-absorption coefficient of BrC has strong wavelength dependence with absorption increasing sharply from the vis to the UV range. The complexity of light-absorbing organic compounds and variations in their relative concentrations make it difficult to characterize the molecular composition and determine which types of molecules or molecular aggregates dictate the optical properties of BrC. One goal of this review is to assess the current state of knowledge regarding the molecular structures of these BrC compounds on the basis of analysis of recent field and laboratory measurements.

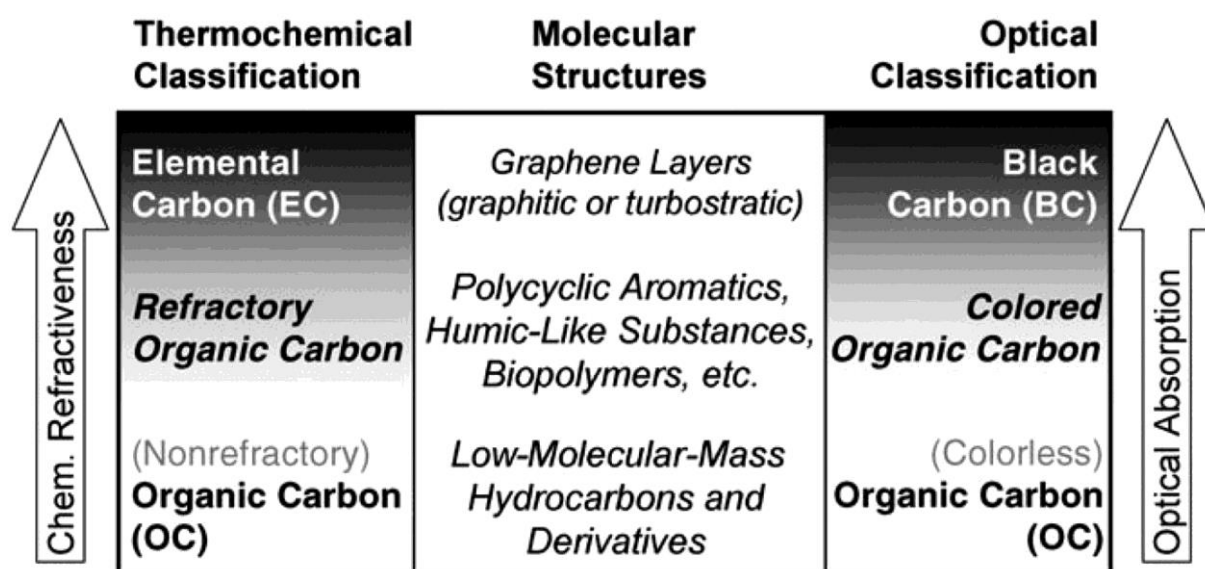


Figure 3: Optical and thermochemical classification of atmospheric carbonaceous particulate matter. BrC material is an ensemble of light-absorbing (colored) organic compounds with a variety of molecular structures and molecule-specific optical properties. (Reprinted with permission from (Pöschl, 2005). Copyright 2005 Wiley-VCH Verlag GmbH & Co.) (Laskin et al., 2015)

There is limited understanding of how particle optical properties – especially the contributions of black carbon (BC) and brown carbon (BrC) – evolve with photochemical aging of smoke. (Cappa et al., 2020) analyse the evolution of the optical properties and chemical composition of particles produced from combustion of a wide variety of biomass fuels, largely from the western United States. The smoke is photochemically aged in a reaction chamber over atmospheric-equivalent timescales ranging from 0.25 to 8 days. In the USA, in a rural environment, (Washenfelder et al., 2015) found that the majority of brown carbon aerosol mass was associated with biomass burning, with smaller contributions from biogenically derived secondary organic aerosol.

There is a key challenge on BrC. As a result of the uncertainty surrounding the sources and properties of BrC, and its tendency to be coemitted and mixed with BC, these aerosols are not well represented in atmospheric chemistry and climate models. Inclusion of BrC in the

population of organic carbon (OC) aerosols changes the net effect of OC from scattering to close to zero, especially in areas with heavy biomass burning (McNeill, 2017). In a recent study for China, (Sun et al., 2020) corroborates the dominant role of BrC in total biomass burning absorption. Therefore, BrC is not optional but indispensable when considering the climate energy budget, particularly for biomass burning emissions (contained and open).

(Xie et al., 2017) measured the light absorption of methanol-extractable OC derived from biomass burning (BB) and gasoline vehicle emissions, which exhibited strong wavelength dependence with \AA *absorption* (light absorption coefficient at a given wavelength) values much higher than 2. The OC generated during BB under high temperature or flaming combustion shows strong light absorption; the biomass fuel type may also play a role in the light-absorbing properties of OC generated from BB. However, how biomass fuel type affects the light absorption of OC from BB is uncertain and merits further investigations. Gasoline vehicles tend to emit stronger light-absorbing OC in winter than in summer. Compared to BB, the light absorption of OC from gasoline vehicle emissions was of the same magnitude but weaker, suggesting the importance of gasoline vehicle emissions as a BrC source in urban regions. Non-extractable OC accounted for a substantial part (~25%) of the total OC from gasoline vehicle emissions, and further study to measure its potential light-absorbing properties is warranted. Definitively, treating organic aerosol as **non-absorbing particles would underestimate the radiative effect of organic aerosols**, especially in urban areas where motor vehicle emissions are a substantial fraction of the aerosol. BrC from residential wood burning has also been found to be a major source of carbonaceous compounds in France in wintertime (Y. Zhang et al., 2020).

Lensing and Photobleaching are two important processes involving BrC in the radiative budget of Earth (Yan et al., 2018). The **lensing** effect induces a radiative effect in the atmosphere depending on the type of material coated. The radiative forcing of an internal mixture of BC and BrC is larger than the radiative forcing of an internal mixture of BC and non-light-absorbing OC when the absorption wavelength varies from 365 to 470 nm. Thus, the lensing effect induced by the internal of mixing BC and BrC cannot be ignored and should be included in global climate models. **Photobleaching** induces significant changes in the absorptive properties of BrC aerosols, which further influence radiative forcing of the atmosphere. Secondary BrC can be produced during the aging of BrC, which undergoes rapid photobleaching (Wong et al., 2017; Zhao et al., 2015). Recently (A. Zhang et al., 2020) in a modelling of the global radiative effect of Brown Carbon showed a potentially larger heating source in the Tropical Free Troposphere than Black Carbon.

However, taking into account the BrC in climate models can lead to counterintuitive effects as depicted by (Sumlin et al., 2017). Indeed BrC aerosol contributes to positive forcing (warming) over bright terrain throughout the atmospheric aging time scales investigated in (Sumlin et al., 2017). However, with increased atmospheric residence time from 0 to 4.5 PED (PAM Equivalent Day with PAM for Potential Aerosol Mass reactor), the integrated Direct Radiative Forcing (DRF) efficiency decreases by approximately 27%, from 40.4 ± 1.7 to 29.4 ± 2.8 W m⁻². The PED is the time in days to reach the maximum aerosol mass produced in the PAM reactor. A corresponding decrease in DRF efficiency over ground is ~5%, from -4.0 ± 0.0 to -4.3 ± 0.1 W m⁻² for particle aging from fresh to 4.5 PED. Although approximately half of the solar spectrum's energy is distributed between 400 and 700 nm, 375–532 nm forcing represents a significant warming potential over arctic terrain, providing additional momentum for climate imbalance. However, the change in optical properties at longer aging time scales imply that model-based estimates of warming due to **BrC light absorption could be overestimated**.

Given the ubiquity of smouldering boreal peat fires, this study highlights the importance of including atmospheric processing effects of these aerosols to refine climate models and satellite retrieval algorithms.

3.3 Polycyclic Aromatic Hydrocarbons (PAHs)

PAHs co-emitted with BC during incomplete combustion are believed to be blocked in the BC matrix and trapped in micro porous structure of BC, due to the high affinity of PAHs for flat aromatic surface (Ali et al., 2020). PAHs are colourless, white, or pale to yellow organic compounds. Several routes are involved in its addition to the environment and are often found as a mixture. It is a group of several hundreds of chemically related compounds with different structures, toxicity, and persistence soot. These compounds are comprised of numerous individual compounds having at least two condensed rings. PAHs are characterized by their multiple aromatic rings with different organic constituents, aromatic rings number and functional groups attached to these rings. PAHs are divided into two categories based upon their molecular weight, those with less than four rings are termed as low molecular weight compounds, while those having more than four or more rings are high molecular weight compounds.

Understanding the association between BC and PAHs is critical in order to find out their negative effects, transport and fate throughout the environment. BC is considered to be purely ubiquitous in the atmosphere and have a strong sportive power for organic pollutants such as persistent organic pollutants (POPs) and PAHs. It has been revealed that the distribution of PAHs in different environmental sections is dependent upon BC distribution due to the strong sorption ability of BC for PAHs (Cornelissen et al., 2005).

PAH are fully involved in the formation of soot particles (Figure 4) although, the early stages of soot formation, namely inception and growth, are highly debated and central to many ongoing studies in combustion research. The combustion process of fuel starts with the decomposition reactions of the fuel molecules, *i.e.*, pyrolysis and oxidation, and subsequent recombination and cyclization reactions lead to the formation of polycyclic aromatic hydrocarbons (PAHs). Recent results (Commodo et al., 2019) conduce to the understanding of soot formation by providing a framework of molecules that are decisively contributing to this process, and thereby deepen the knowledge of its underlying chemistry at the molecular level. In the long run, this information could eventually help to improve technologies relying on fuel combustion to prevent the emergence of harmful by-products.

Four PAH are particularly targeted in the legislation: benzo(a)pyrene, benzo(b)fluoranthene, benzo(k)fluoranthene and Indeno(1,2,3-cd)pyrene (Aarhus Protocol on POPs). Benzo(a)pyrene and naphthalene contributed the most to the PAH carcinogenic potency of biomass-burning emissions according (Samburova et al., 2016).

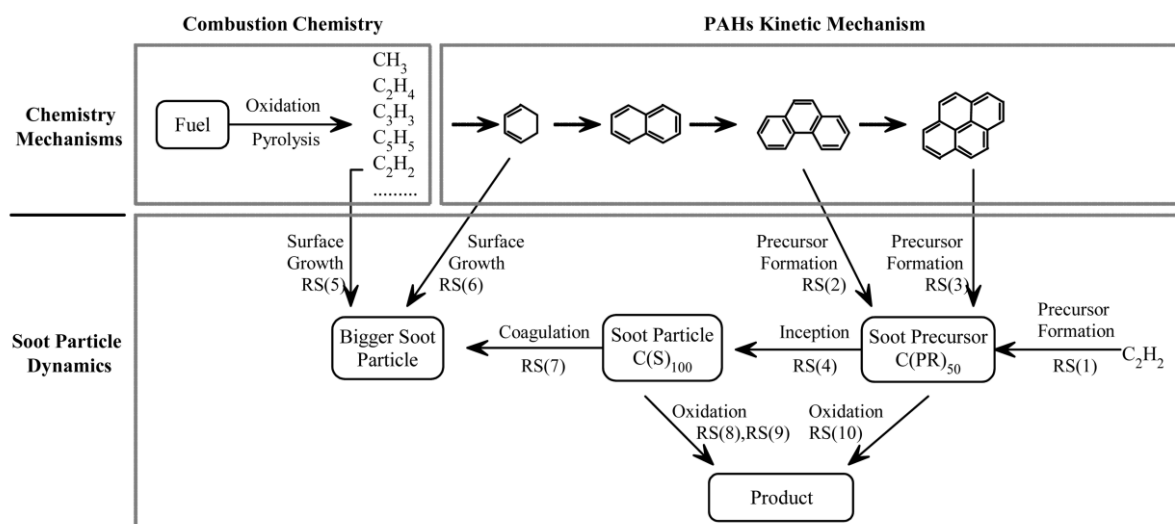


Figure 4: Soot formation pathway from (Frenklach and Wang, 1991; Omidvarborna et al., 2015; Pang et al., 2013)

3.4 The concept of “Condensables”

Condensable PM (CPM) is a branch of condensable particles under the temperature of the exhaust gas outlet (Feng et al., 2018). As reminded by (Evans, 2019), EPA’s specific definition of CPM is:

“Material that is vapor phase at stack conditions, but condenses and/or reacts upon cooling and dilution in the ambient air to form solid or liquid PM immediately after discharge from the stack. Note that all condensable PM is assumed to be in the PM_{2.5} size fraction.”

CPM is gaseous at the pre-discharge flue temperature, but it immediately enters the particulate state after releasing into the atmosphere. CPM is formed by the “vaporization–condensation” mechanism. This mechanism includes two types of particle formation processes: “homogeneous nucleation” and “heterogeneous condensation”. CPM belongs to PM_{2.5}, and it is harmful to the environment and human body. CPM test methods can be divided into two categories: impinger cooling method and dilution cooling method. In many activity sectors, analyses of CPM composition reveals that CPM is dominated by inorganic components due to the presence of sulphur in the fuel (Yang et al., 2018, 2015, 2014). The organic components mainly consist of alkanes, esters, and other complex organic compounds (*e.g.* PAHs). The inorganic components of CPM may contribute significantly to the water-soluble ions in the atmospheric PM_{2.5}. The concept of “condensables” is of major importance to understand the role of carbonaceous species from the emissions (High temperature and low dilution) to the ambient conditions (cooler temperature and high dilution). A specific action has been jointly organized to define new and common practices to handle condensables in emissions for modelling activities (Simpson, 2020).

Primary Organic Aerosols (POA) have been traditionally assumed to be non-volatile and unreactive in atmospheric aerosol models. Although these assumptions are still used by the great majority of chemical transport models, it has been shown that in many cases, such assumptions are not correct (Donahue et al., 2009). Most measurements of ambient Organic Aerosol concentrations displayed significant negative (particle evaporation after collection on

the filter) and/or positive artefacts/biases (vapour adsorption on the filter), providing strong hints about the semi-volatile nature of organic aerosols (Turpin et al., 2000).

For more than twenty years, dilution samplers have been used to measure POA emission factors. The use of these samplers was motivated by the semi-volatile character of primary emissions. Although some primary emissions are clearly semi-volatile, models generally treat them as non-volatile. The implicit assumption is that the partitioning measured using a dilution sampler is representative over the full range of atmospheric conditions simulated by the model, and that the semi-volatile primary mass is a small fraction of the total POA.

According to the volatility, POA should be viewed in the broad sense as a continuum of organic species from light VOCs to solid soot. We can consider seven categories sorted by decreasing volatility:

- i. Methane (the lighter VOC)
- ii. Non methanic VOC (NMVOC) usually molecules up to 12 carbons but higher HC could also be included
- iii. Organic compounds of intermediate volatility (IVOC)
- iv. Semi volatile organic compound (SVOC) which can be split in SVOC and LVOC (Low volatile organic compounds)
- v. Non-volatile Organic aerosol or extremely low volatile organic compounds (ELVOC)
- vi. Elemental carbon or black carbon, it contains some atoms of hydrogen but it is mainly composed of carbon. This species is usually not defined as an organic species.

Categories (i) and (ii) can be always considered in the gas phase regardless of the dilution ratio and temperature. The definition of a volatile organic compound varies from country to country. Even within a country, there are often differences. A general scientific definition of VOC is an organic compound that evaporates or vaporizes under ambient conditions. These gases are emitted from various materials. From a legal point of view the definition of VOC can be different, in the National Emission Ceiling directive: *volatile organic compounds' and 'VOC' mean all organic compounds arising from human activities, other than methane, which are capable of producing photochemical oxidants by reactions with nitrogen oxides in the presence of sunlight.*

Categories (iii) and (iv) are partitioned between the gas and particle phases depending on the temperature and dilution ratios. The notion of IVOC is questionable and will be addressed further in this report. These compounds, which have saturation concentrations between 10^3 and $10^6 \mu\text{g m}^{-3}$, are termed intermediate volatility organic compounds (IVOCs) by Donahue *et al.* (2009). The heaviest SVOC are carboxylic acid, long alkane chains. The IVOC category could overlap with the VOC since the definition is not clear. Recently (Stewart et al., 2020) has analysed and determined emission factors for IVOC for different type of domestic fuels including wood.

Categories (v) and (vi) can be considered only in the particle phase. This phase is composed of heavy hydrocarbons and organic species.

Species in categories (ii) to (iv) can react in the atmosphere and produce aerosol particles, the products of these reaction fall in categories (iv) to (v) by increasing their molar mass mainly due to the addition of oxygen atoms.

(Donahue et al., 2012; Murphy et al., 2014) have proposed a breakdown in volatility classes based on saturation concentration (Table 3).

Table 3: Volatility classes of volatile organic compounds (Donahue et al., 2012; Murphy et al., 2014). † VOC or NMVOC is not given as an explicit abbreviation here since they are superset, e.g., typically IVOC and some SVOC.

Description	Abbrev.	Saturation concentration range ($\mu\text{g m}^{-3}$) at 298K	State in the atmosphere
Extremely-low volatility	ELVOC	$< 3.2 \times 10^{-4}$	Particle
Low volatility	LVOC	$3.2 \times 10^{-4} - 3.2 \times 10^{-1}$	Mainly particle
Semi-volatile	SVOC	$3.2 \times 10^{-1} - 3.2 \times 10^2$	PM and/or vapour phase
Intermediate-volatility	IVOC	$3.2 \times 10^2 - 3.2 \times 10^6$	Vapour phase, readily oxidised to SVOC
Volatile [†]	-	$> 3.2 \times 10^6$	Vapour phase

Therefore, organic condensables are species belonging to categories ELVOC to SVOC primary and secondary (as SOA - secondary Organic Aerosol) in origins. Regarding SOA from wood burning (Akherati et al., 2020) demonstrates the necessity of accounting for oxygenated aromatics from biomass burning emissions and their SOA formation in chemical mechanisms.

In a real atmosphere, the evolution of emissions can be described as in Figure 5. In the first centimetres and meters, freshly emitted primary organic species tend to evaporate due to strong dilution, while temperature cooling tends to maintain or condense them in the particle phase. However, the dilution process is much more efficient than the temperature decrease and generally the resulting process tends to evaporate the primary condensed species. At the same time, reactions can occur very quickly in the emission plume thanks to the dilution with fresh air loaded with oxidants.

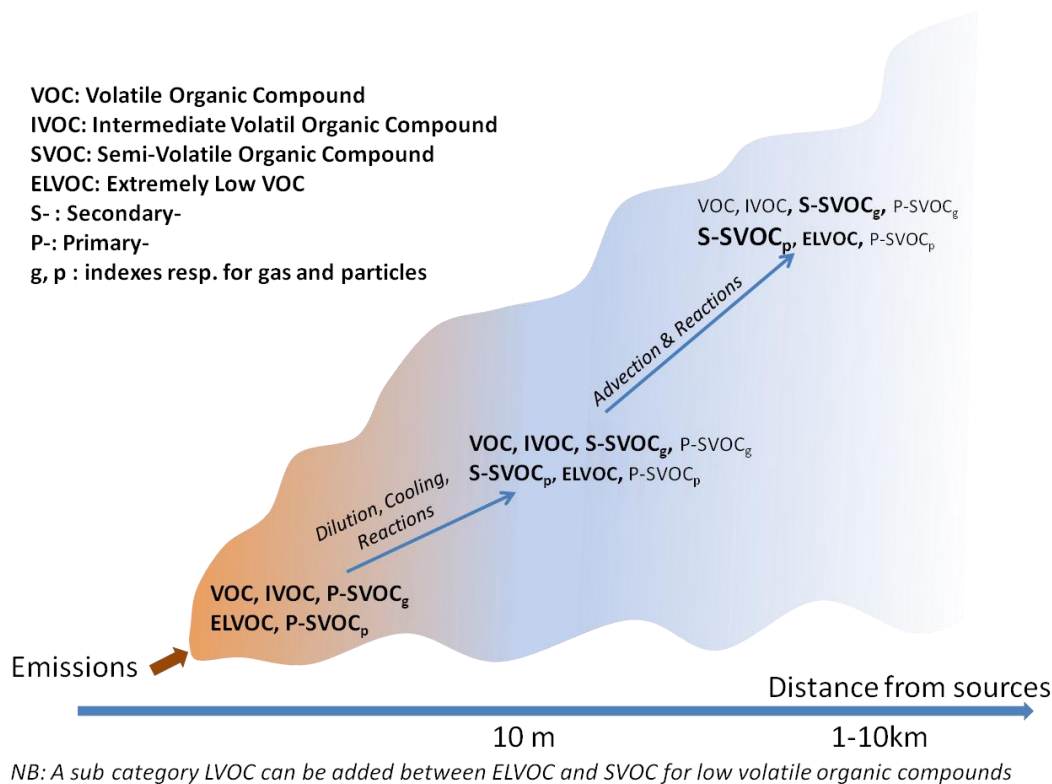


Figure 5: Schematic description of emission ageing in the atmosphere

The IVOC terminology has been introduced to gather compounds that were too coarse to be captured by the VOC measurement and too volatile to be captured by a particle filter with a PUF sampling (Robinson et al., 2007). However, IVOC can be measured by denuder (Schauer et al., 1999). These IVOCs can be viewed as gas-phase SVOC that were not captured by the particle filter. (Schauer et al., 1999) used indeed the term “gas-phase SVOC” for the same compound. There is therefore no clear distinction between SVOC and IVOC. Moreover, the amount of SVOC captured by the particle filter is a function of some experimental conditions (temperature and organic aerosol loading), which means that the split between SVOC and IVOC would depend on those conditions. Figure 6 illustrates the dependence of the particle-phase SVOC on gas+particle SVOC ratio (or SVOC/(SVOC+IVOC) ratio) on the organic mass loading. Based on this figure, emissions of particles are dependent on experimental conditions and a part of SVOC emissions could be missing from inventory emissions. **If dilution curves are known, they can be used by modellers to estimate SVOC/POA ratio for an emission factor by using temperature and organic mass loading.**

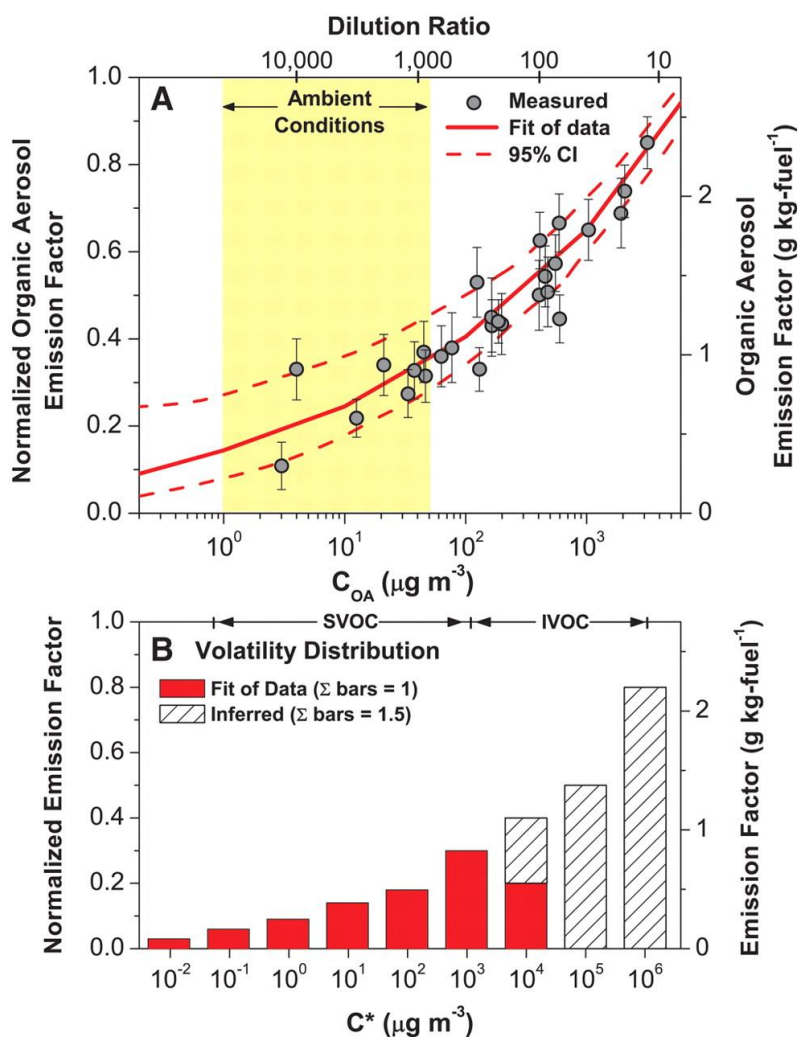


Figure 6: Normalized Organic Aerosol Emission factor as a function of organic aerosol loading for a diesel motor exhaust at 300 K (Robinson et al., 2007)

Based on the assumption that “gas-phase SVOC” or IVOC are missing from inventory emissions, (Robinson et al., 2007) introduced an IVOC/POA ratio or gas-phase SVOC/particle-phase SVOC ratio to take into account those missing emissions. In their paper, they report a ratio of 2.8 for emissions from a catalyst-equipped, gasoline-powered car and 1.5 for medium-duty diesel engine emissions based respectively on (Schauer et al., 2002, 1999) and chose to use the 1.5 value. This ratio of 1.5 is used to account for IVOC species by most modelling team working in this field (Bergström et al., 2012; Chen et al., 2019; Couvidat et al., 2018a, 2018b; Denier van der Gon et al., 2015; Hodzic et al., 2010; Koo et al., 2014; Tsimpidi et al., 2010; Zhang et al., 2013): (Ots et al., 2016) proposed to scale IVOC emissions on VOC based on field campaigns perform in a urban station in London.

Those results reported in the Schauer’s publications (Schauer et al., 2002, 1999) are representative of late 90s American diesel vehicle and are therefore difficult to extrapolate to a recent fleet of European passenger cars. However, using measurements on French passenger vehicles, (Kim et al., 2016) estimated that this factor of 1.5 may be well suited for passenger cars in France. However, **this factor 1.5 is certainly inappropriate as a presentation of the whole current vehicle fleet.** It is interesting to note that the EMEP/EEA air pollutant emission inventory guidebook only constraint reported emission factor to be measured on a filter at less than 52°C. Reported emission factors could gather emission factors at cold, ambient and hot

temperatures and therefore could gather emission factors having various gas-phase SVOC/particle-phase SVOC ratio.

Moreover, with the implementation of particle filters on diesel passenger cars, the amount of organic aerosols emitted has decreased strongly and therefore, based on Figure 6, the fraction of SVOC in the gas phase is expected to strongly increase due to the decrease of the organic aerosol loading in the dilution sampler.

Brown carbon could be a part of the low volatile organic compounds which could be directly emitted or produced during the dilution process or formed later in ambient conditions (Figure 7) as discussed in (Kampf et al., 2016) for nitrogen SOA. The “grey zone” corresponds to a list of compounds which could be not captured by a sampling technique or we could affect to volatile or non-volatile species. The evolution of relative ratios between the mass concentrations of non-refractory organic species and black carbon is interesting. It varied between fuel types and displayed an inverse correlation with the modified combustion efficiency (MCE) of the burns (Fortner et al., 2018), and a positive correlation with aging.

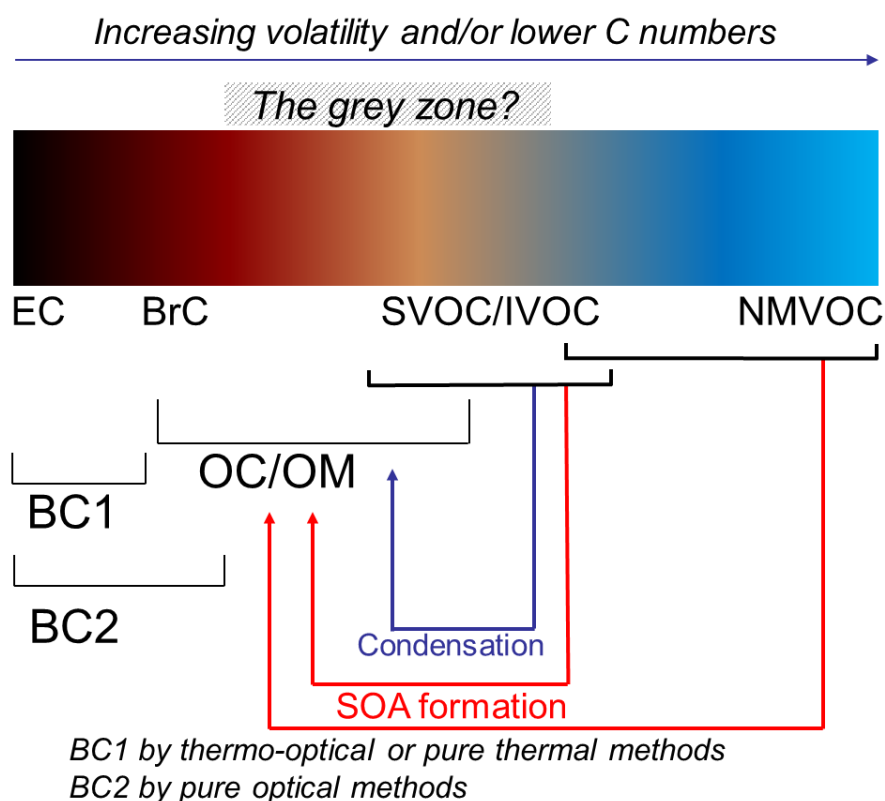


Figure 7: Synoptic description of the carbonaceous species from graphitic Carbon (EC) to the NMVOCs

Depending on the aim of the measurement, different sampling strategies are commonly used for product testing and health studies, they are presented in (Nussbaumer, 2010a) and clearly show the impact of the method used to estimate the PM EF and the way of how condensables can affect the measurement (Table 10 and Figure 8). The effects of physical phenomena was illustrated by (Habib and Kumar, 2016) who have developed a portable dilution system for aerosol measurement from stationary and mobile combustion sources. PM_{2.5} emission factors for wood combustion in gasifier cookstove showed mild decrease (13%) with increasing dilution ratio from 75:1 to 108:1 mg km⁻¹. However, a considerable decrease of 37% (221–139 mg km⁻¹) was observed for Light Duty Diesel Vehicle with increase in dilution ratio from 39:1

to 144:1. Similar decrease in particulate organic carbon emission rates were observed indicating scarcity of sorptive organics, and insufficient residence time for condensation limited the particle formation from vapor phase organic compounds at high dilution ratios.

One important finding by (Giechaskiel, 2020) also illustrate the importance of the configuration of the dilution sampler was very important (*i.e.*, open or closed transfer tube to the dilution tunnel; both allowed in the current regulation) for a Euro 4 motorcycle. More representative of the actual particulate emissions of the motorcycle ($3 \times 10^{11} \# \text{ km}^{-1}$) were found for the “open” method. The closed configuration resulted in lower solid particle emissions due to agglomeration (30%), but most importantly very high total particle emissions (*i.e.*, including volatiles) (more than one order of magnitude) due to desorption of deposited material in the transfer tube to the dilution tunnel during high-speed driving. Thus, mixing directly at the tailpipe (*e.g.*, open configuration or mixing tee) should be preferred for motorcycle measurements.

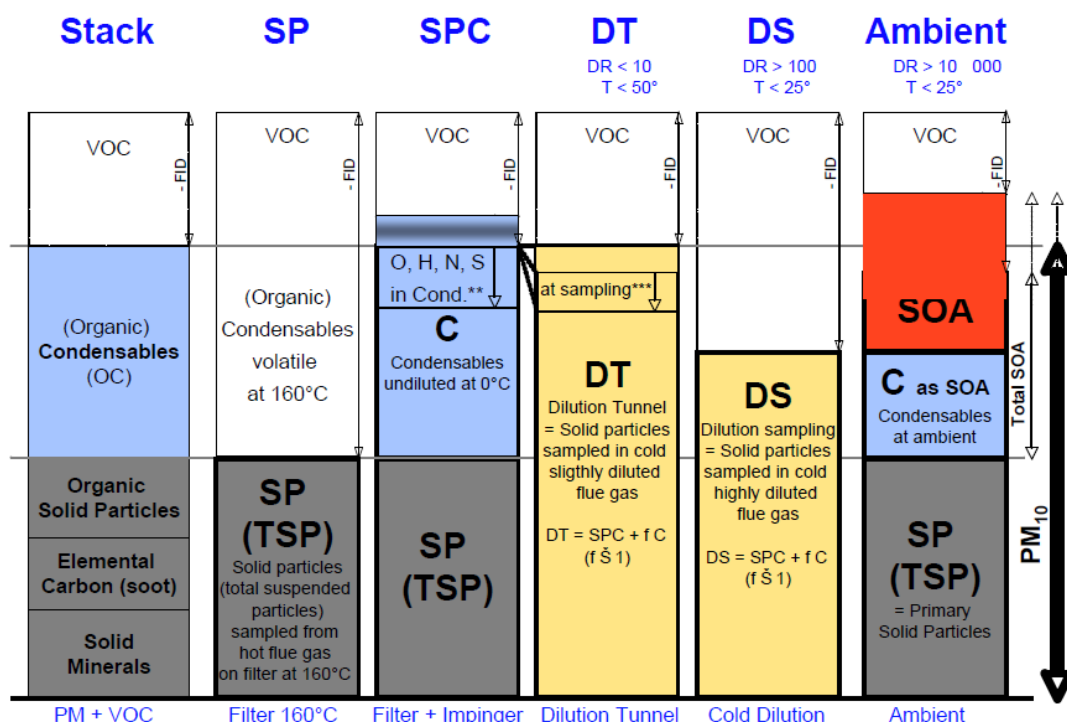


Figure 8: Comparison of PM sampling with PM in the ambient from (Nussbaumer, 2010a). SP: Filter (Method a) resulting in solid particles SP (total suspended particles TSP). SPC: Filter + Impinger (Method b) resulting in solid particles and condensables SPC. DT: Dilution Tunnel (Method c) with typical dilution ratio (DR) in the order of 10 resulting in a PM measurement including SPC and most or all C. DT is identical or slightly smaller than SPC + C due to potentially incomplete condensation, depending on dilution ratio and sampling temperature (since dilution reduces not only the temperature but also the partial pressure of contaminants). DS: Dilution Sampling with high dilution ratio (DR > 100). PM₁₀: Total Particulate Matter < 10 microns in the ambient including SP and SOA. SOA: Secondary organic aerosols, consisting of condensables C at ambient and SOA formed by secondary reactions such as photochemical oxidation. *SO₂ and other soluble gaseous compounds in the flue gas may be dissolved in the impingers. **In case of determination of TOC in impingers, the mass of O, H, N, S and other elements contained in the organic condensables needs to be accounted for separately. *Organic compounds that are liquid or solid at partial pressure in the flue gas and ambient temperature but volatile at sampling due to reduced partial pressure by dilution and temperature above ambient.**

The issue of condensable is critical to calculate the emission factors of PM. Recently, a scientific project suggested EN-PME test method as temporary test method for particles (similar to heat filter technique) from wood heating (Kausch et al., 2020). This method is now suggested

as test method for EN16510 and there is an ongoing verification project to validate this test method. The direct comparison of the EN-PME sampling method and NS3058 (based on dilution tunnel) in parallel from the current experimental campaign showed that emissions from the NS measurements are 11 times higher with 108 mg MJ⁻¹ compared to EN-PME test with 14 mg MJ⁻¹. The differences range between 2 until 60 times and is largely due to condensables.

To illustrate the complexity of the phenomena just after emissions, (Bertrand et al., 2018) use a thermal desorption aerosol gas chromatograph coupled to an aerosol mass spectrometer (TAG-AMS) connected to an atmospheric chamber. The setup serves the quantitative study of the impact of combustion conditions and atmospheric aging on the chemical fingerprint at the molecular level of biomass burning organic aerosol. Table 4 presents the results of these investigations involving three type of stoves. The secondary production of organic aerosols OA is the largest for log wood stoves resulting from a more or less fast oxidation of a fraction of primary organic aerosol. These results are in line with (Zhou et al., 2018) which shows that aged EF_{ROS} (emission factor of reactive oxygen species) under bad combustion conditions were ~ 2–80 times higher than under optimum combustion conditions. Also, (Kodros et al., 2020) show that fresh emissions from biomass burning exposed to NO₂ and O₃ (precursors to the NO₃ radical) rapidly form OOA (Oxidized organic aerosol) in the laboratory **over a few hours and without any sunlight**.

Table 4: Summary of the experiments and conditions in the chamber before lights-on (after a homogenization and stabilization period). MCE stands for modified combustion efficiency and THC is total hydrocarbon (Bertrand et al., 2018)

Stove	Exp n°	MCE	N° of TAG-AMS	*eBC µg m ⁻³	*POA µg m ⁻³	**OA µg m ⁻³	*NOx ppb	THC/NOx ppb ppb ⁻¹	Cresol/NOx ppb ppb ⁻¹
<i>Stove A (Beech as logs)</i>	1	0.85	6	17	122	495	98	31.5	1.1 × 10 ⁻¹
	2	0.84	7	12	177	785	252	26.9	1.1 × 10 ⁻¹
	3	0.83	7	6	71	388	90	38.5	1.2 × 10 ⁻¹
	4	0.91	8	5	10	72	128	7.7	2.7 × 10 ⁻²
<i>Stove B (Beech as logs)</i>	5	0.80	7	5	41	143	50	47.2	1.2 × 10 ⁻¹
	6	0.87	7	13	38	202	119	18.1	5.0 × 10 ⁻²
	7	0.82	6	6	45	289	114	24.3	7.2 × 10 ⁻²
	8	0.90	7	4	9	53	80	19.6	4.5 × 10 ⁻²
<i>Stove C (Softwood pellets)</i>	9	0.97	5	107	10	19	161	5.2	1.2 × 10 ⁻³
	10	0.97	6	130	10	19	205	5.8	4.7 × 10 ⁻⁴
	11	0.97	5	144	10	22	228	5.9	3.5 × 10 ⁻⁴

Notes: * Values retrieved just before light on, ** Values retrieved as integrated OH exposure = 5 × 10⁶ molecules cm⁻³ h

As discussed in (Vicente and Alves, 2018), the compilation of emission factors presented in the next sections derived from fresh smoke sampled at the source that had usually cooled to ambient temperature, but undergone minimal photochemical aging. Rather few studies have been focused on the post emission processing and, thus, data for testing or constraining the chemical mechanism in smoke photochemistry models are very limited. Photochemical oxidation produced substantial new OA. Only a small fraction of this new OA can be explained using

state-of-the-art secondary organic aerosol models and the measured decay of traditional SOA precursors. The application of models that explicitly track the partitioning and aging of low-volatility organics, including water-soluble species, should be compared to measurements with a suite of instruments in chambers. This kind of models have been used as in (Kim et al., 2016). To relate elapsed times and measured concentrations of OC, the condensation of SVOC between the gas and particle phases is simulated with a dynamic aerosol model. The simulation results presented in (Kim et al., 2016) allow to understand the relation between elapsed times and concentrations in the gas and particle phases. They indicate that the characteristic times to reach thermodynamic equilibrium between gas and particle phases may be as long as 8 min. Therefore, if the elapsed time is less than this characteristic time to reach equilibrium, gas-phase SVOC are not at equilibrium with the particle phase and a larger fraction of emitted SVOC will be in the gas phase than estimated by equilibrium theory, leading to **an underestimation of emitted OC if only the particle phase is considered or if the gas-phase SVOC** are estimated by equilibrium theory.

3.5 Ultrafine Particles

Ultrafine particles (UFPs) are aerosols with an aerodynamic diameter of 0.1 μm (100 nm) or less. There is a growing concern in the public health community about the contribution of UFPs to human health. Despite their modest mass and size, they dominate in terms of the number of particles in the ambient air. A particular concern about UFPs is their ability to reach the most distal lung regions (alveoli) and circumvent primary airway defenses. Moreover, UFPs have a high surface area and a capacity to adsorb a substantial amount of toxic organic compounds. Harmful systemic health effects of PM₁₀ or PM_{2.5} are often attributable to the UFP fraction. Combustion sources are the main sources of UFPs (Corsini et al., 2019; Kwon et al., 2020).


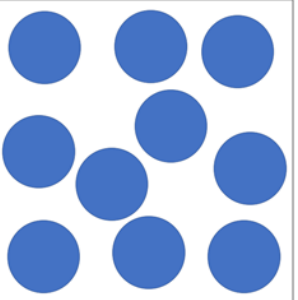
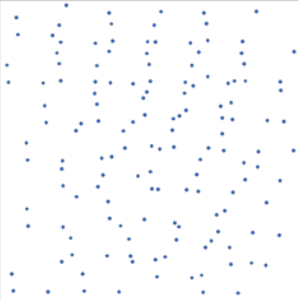
	10 μm (Coarse)	2.5 μm (Fine)	0.1 μm (Ultrafine)
			
Total mass	1	1	1
Particle number	1	64	1,000,000
Surface area per particle	1	0.0625	0.0001
Total surface area per mass	1	4	100
	<ul style="list-style-type: none"> • Filtered in proximal airway • May irritate skin, mucosa 	<ul style="list-style-type: none"> • Reaches peripheral airway • Cannot enter systemic circulation 	<ul style="list-style-type: none"> • Higher adsorbed toxic material on surface • May enter systemic circulation

Figure 9: Comparison of the surface area of particles with different diameters. The diagram assumes that all particles in each category are perfect spheres, have the same density, and are present in an equal amount of mass. The mass, particle number, and surface area of coarse particles are all arbitrarily designated as 1. Other numbers are relative to the coarse particle. The large surface area and ability to enter circulation are the two most significant characteristics of ultrafine particles that make them more toxic than other larger particles (Kwon et al., 2020)

When inhaled, UFPs can pass through the respiratory tract with high efficiency down to the alveoli due to their small size. A small fraction of UFPs penetrate the alveolar–capillary barrier and can thus be distributed throughout the body via the circulatory system. Because of this property of UFPs, extrapulmonary diseases related to PM exposure may be particularly attributable to UFPs. Furthermore, UFPs are thought to be more threatening than larger PM due to their higher specific surface area (total exposed surface area per unit of mass). Large surface area and high surface reactivity enable UFPs to adsorb, for a given mass of PM, greater quantities of hazardous metals, and organic compounds that can generate oxidative stress Figure 9.

At the exhaust pipe of a vehicle or in a plume of a heating system, UFPs can quickly evolve and/or disappear through deposition, condensation and coagulation processes, particularly for the smallest UFPs. In clean environment the nucleation of inorganic (Sulfate, nitrate, ammonium) and organic compounds can be a secondary source of UFPs (Bessagnet and Rosset, 2001; Kulmala et al., 2014). The size of 80 – 100 nm is the lower limit of the particles range where particles have the highest time of residence usually between 0.1 μm and 1 μm . In this range of particles, the deposition processes are known to be the less efficient.

3.6 Overview of BC/PAH/PM2.5 emissions in the EMEP countries

At the global scale, PM emissions are mainly driven by biomass burning emissions as depicted in (Klimont et al., 2017) with a large contribution of residential combustion and wildfire emissions (Table 5).

Table 5: Sectoral emissions of particulate matter in 2010, ECLIPSE V5a, Gg year⁻¹ (Klimont et al., 2017). (a) Values are middle-of-the-range estimates based on the ranges reported in (Stettler et al., 2013; Yim et al., 2015), and based on global fuel consumption and ranges of emission factors from (Kinsey, 2009). (b) GFED3.1 without agricultural waste burning that is included based on GAINS estimates in category “Agriculture”; PM10 value based on TPM (total particulate matter); PM1 not available in GFED – here assumed equal to PM2.5. Report to (Randerson et al., 2017) for the last GFED version.

	PM10	PM2.5	PM1	BC	OC	OM
<i>Agriculture</i>	6555	3848	2883	337	1313	2364
<i>Residential combustion</i>	23078	21857	20742	4163	8852	15329
<i>Industrial processes</i>	12162	8340	4135	462	633	823
<i>Large Scale combustion</i>	11561	6420	3812	136	164	248
<i>Oil and gas, mining</i>	1706	571	412	226	93	120
<i>Transport - road</i>	3339	2925	2524	1349	1116	1451
<i>Transport – non road</i>	861	823	795	363	217	283
<i>Waste</i>	1388	1272	876	97	751	977
<i>International shipping</i>	1856	1758	1612	120	398	517
<i>International aviation^(a)</i>	30	30	28	10	10	13
<i>Global anthropogenic</i>	62537	47843	37819	7264	13548	22125
<i>Forest and savannah fires^(b)</i>	48207	33014	33014	2268	19489	31363
<i>Global total</i>	110 744	80858	70834	9532	33037	53489

In the EU28, the main emitting sector by far is the **residential sector**, followed by **road transport** and open burning of waste (Figure 10). The lowest ratio BC/PM2.5 is also for the residential combustion sectors (Figure 11). This ratio of 10% corresponds to the ratio proposed in EEA guidebook (Kuenen and Trozi, 2019) and (Klimont et al., 2017) for the combustion of solid fuels. This low ratio refers to previous works of (Alves et al., 2011; Fernandes et al., 2011; Gonçalves et al., 2011) and is based on Emission Factors measurement method which accounts for condensables. For solid biomass like wood, the corresponding EF is 74 g GJ⁻¹. To be more specific it is written in the EEA guidebook: “*Since the condensable component is not expected to include any BC, in case a filterable only approach is used an EF of 10% * 740 = 74 g/GJ can be assumed for BC*”. Therefore, one can expect an underestimation of BC EF if the measurement method does not account for condensables. (Raventos and INERIS, 2018) highlighted that BC should be calculated over the TSP since BC has been found in coarse particles of industrial installations and this could lead to an underestimation.

Table 6: Main 10 emitting sectors in EU28 for Black Carbon

Code	Name
1A4bi	Residential: stationary
1A3bi	Road transport: passenger car
5C2	Open burning of waste
11B	Forest fires (natural wildfires)
1A3di(i)	International maritime shipping
1A4cii	Agriculture/Forestry/Fishing: Off-road vehicles and other machinery
1A3bii	Road transport: Light duty vehicles
1A3biii	Road transport: Heavy duty vehicles and buses
1A2gviii	Stationary combustion in manufacturing industries and construction: IIR
1A2gvii	Stationary combustion in manufacturing industries and construction: Other

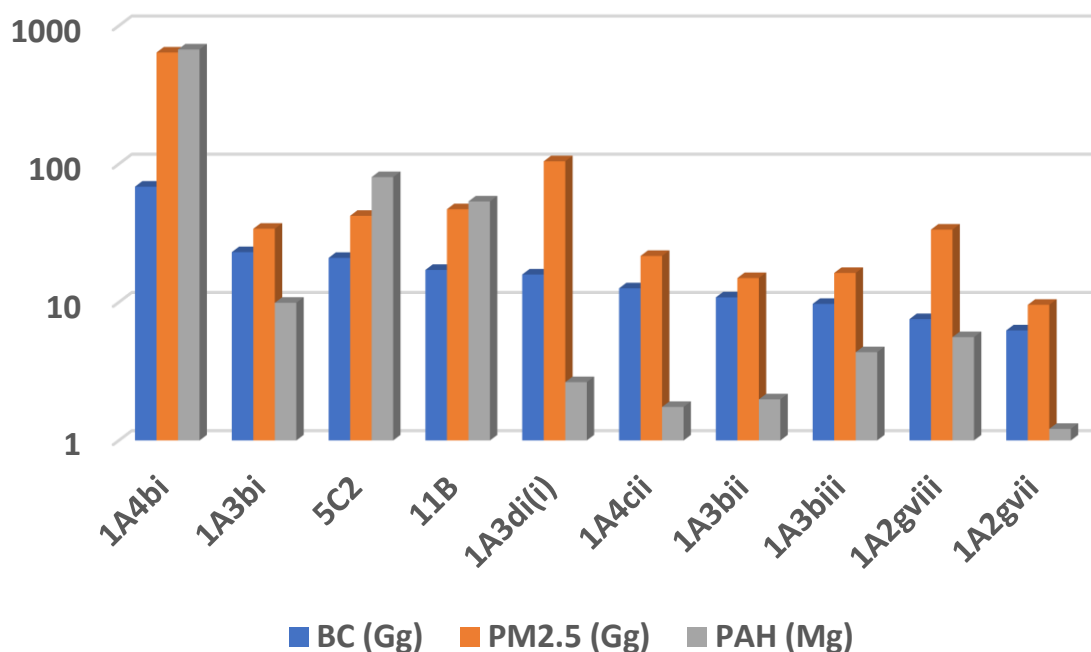


Figure 10: EU28 official emissions in kt or t/year (Gg or Mg) for BC, PM2.5 and PAH (as the sum of benzo(a)pyrene, benzo(b)fluoranthene, benzo(k)fluoranthene and indeno(1,2,3-cd)pyrene) in 2018 for the main emitting NFR sectors (refer to Table 6). Sectors are ordered in decreasing magnitude for BC emissions computed from the EMEP database (EMEP/CEIP, 2020).

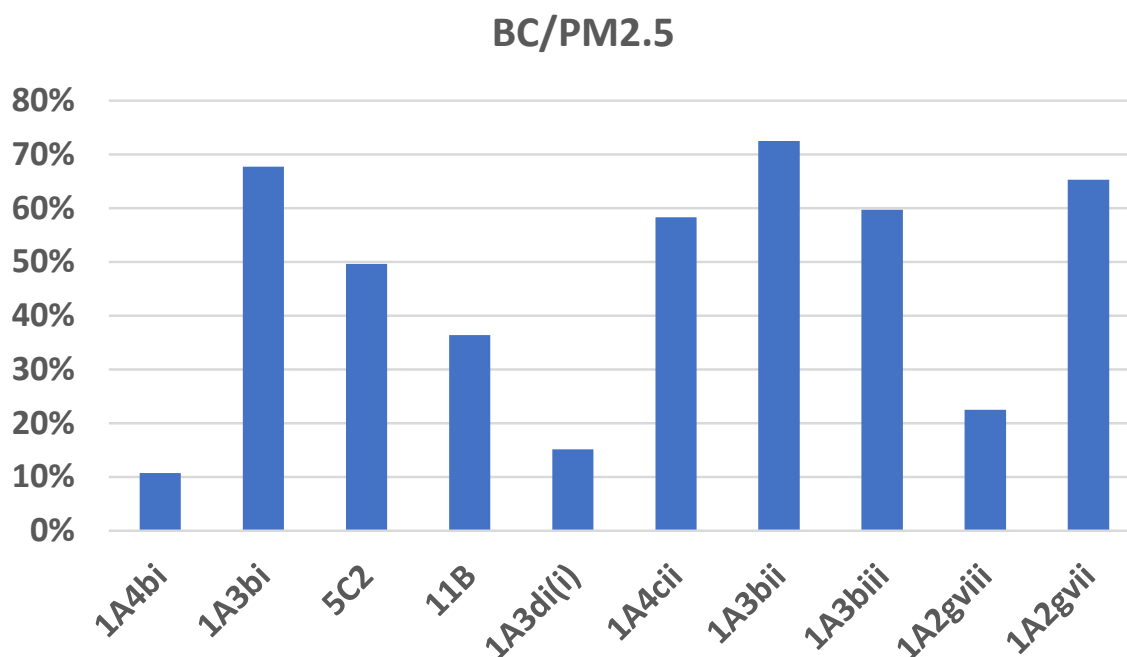


Figure 11: ratio BC/PM2.5 for EU28 official emissions in 2018 computed from the EMEP database (EMEP/CEIP, 2020)

Gas Flaring is another important sector in oil and gas industry. It has a strong impact on climate in Arctic areas due to emissions from the LRTAP countries that is why it has been targeted in this report. In addition to major global oil reservoirs, such as those in the Middle East and United States, huge amounts of untapped oil lie in Arctic regions (Cho et al., 2019). Gas flaring is a conventional method for disposing of gaseous and liquid hydrocarbons through combustion at oil/gas production and processing sites due to a lack of pipelines and other gas transportation infrastructure, as well as for protection against the dangers of over-pressurizing industrial plant equipment (Huang and Fu, 2016). Despite continual BC emissions near the Arctic Ocean via gas flaring, the climatic impact of BC related to gas flaring remains uncertain. (Cho et al., 2019) present simulations of potential gas flaring using an earth system model with comprehensive aerosol physics to show that increases in BC from gas flaring can potentially explain a significant fraction of Arctic warming. BC emissions from gas flaring over high latitudes contribute to locally confined warming over the source region, especially during the Arctic spring through BC-induced local albedo reduction. This local warming invokes remote and temporally lagging sea-ice melting feedback processes over the Arctic Ocean during winter. Their findings imply that a regional change in anthropogenic aerosol forcing is capable of changing Arctic temperatures in regions far from the aerosol source via time-lagged, sea-ice-related Arctic physical processes. They suggest that both energy consumption and production processes can increase Arctic warming. In their studies they used two emission inventories. The BC emissions in Arctic regions north of 60°N were 19 Gg yr⁻¹ in the reference inventory (Lamarque et al., 2010) and 80 Gg yr⁻¹ in an updated inventory with gap filling with satellite imagery. Recently, the ECLIPSE (evaluating the climate and air quality impacts of short-lived pollutants) emission inventory has considered gas-flaring-related BC emissions (Stohl et al., 2013).

This document prepared by TFTEI covers road transport (all types of vehicles), residential small appliances burning solid fuels, stationary combustion plants using solid fuels and flares. BC emissions from shipping are covered in the recent TFTEI report “Background informal

technical document on maritime shipping emissions, reduction techniques and determination of their costs” of December 2020.

The Guidance Document on the Reduction of Emissions from Agriculture Residue Burning prepared by TFTEI is in progress and will be available in early 2021.

3.7 Co-benefits of Air Quality and Climate Change mitigation through BC emission reductions

A recent contribution to the review of the Gothenburg Protocol, on prioritizing the actions to reduce PM and BC emissions (ECE, 2020) underline that BC emission factors still are uncertain, and future research might come to change their results slightly. According to current legislation, PM_{2.5} and BC emission reductions through **absolute co-benefit technologies** decrease with 73% and 79% between 2020 and 2030 in a region with the EU27, Norway, Switzerland and the United Kingdom. In the EECCA region, these figures are 36% and 64% respectively and in the non EU-Balkan + Turkey region of 39% and 73% respectively. In the EU, again, it is the introduction of new installations (including pellet stoves) to control emissions from household stoves and boilers that are inducing largest emission reductions. The improved engine exhaust technologies in diesel-fuelled vehicles and machinery are also important in this category. Relative co-benefit technologies contribute with 2% of the emission reduction for both PM_{2.5} and BC and are engine exhaust technologies in diesel engines and high-grade coal in stoves. The most important trade-off technology for this period is newer installations in household fireplaces. On top of current legislation, there are still several clean technologies that could be utilised more to reduce emissions further by 2030. The remaining absolute co-benefit technologies constitute 59% and 87% of the PM_{2.5} and BC emission reduction potential. In this category, emissions from wood fuels used in household stoves and boilers can be reduced more through increased introduction of newer installations and pellets stoves. Ensuring a 100% effectiveness of bans on open burning, using briquette stoves and newer installations in households using coal stoves, and installation of kitchen filters to reduce emissions from coking/BBQ are other technologies in this category. Technologies with relative co-benefits have relatively small potential, whilst technologies to reduce PM_{2.5} emissions from industrial processes, fireplaces, and from biomass combustion in industrial furnaces are the most important trade-off technologies.

To improve the communication and start developing a common understanding on BC there is a clear need to develop simple metrics for BC, and establishing a “**BC Footprint**” concept as proposed by (Timonen et al., 2019) could be a first step. BC Footprint would allow the comparison of different BC emission sources and levels of atmospheric BC concentrations, and would enable more efficient communication regarding the climate, health, and air quality impacts of BC. Analogous to CO₂, it would be an efficient tool for BC emission mitigation and impact assessment and would support the development of new BC emission mitigation technologies and emission reduction policies.

Figure 12 from (Samset et al., 2020) shows the mitigation potential of a single emission component plotted versus the effort it requires to achieve emergence of a mitigation signal *i.e.* which component can give the most bang for the buck. This figure quantifies the latter as the total amount of mass that is mitigated (emissions avoided) at time-of-emergence. This gives a first order indication of the amount of effort required to implement our idealized mitigation scenarios. The figure correlates surface temperature change in 2100 with the cumulative mitigated mass (in megatons; see the sidebar for the precise units). The size of the symbols scales with the time of emergence, with large symbols showing earlier emergence times. This

analysis confirms that for mitigation to **be rapidly effective** at reducing the rate of global warming, targeting **BC emissions** (where they are not co-emitted *e.g.* with SO₂) would be efficient—however, with a **low final payoff**. However, in recent studies like (Takemura and Suzuki, 2019), it has been shown that the decline in surface air temperatures with **reduced BC emissions is weaker than would be expected from the magnitude** of its instantaneous radiative forcing at the top of the atmosphere.

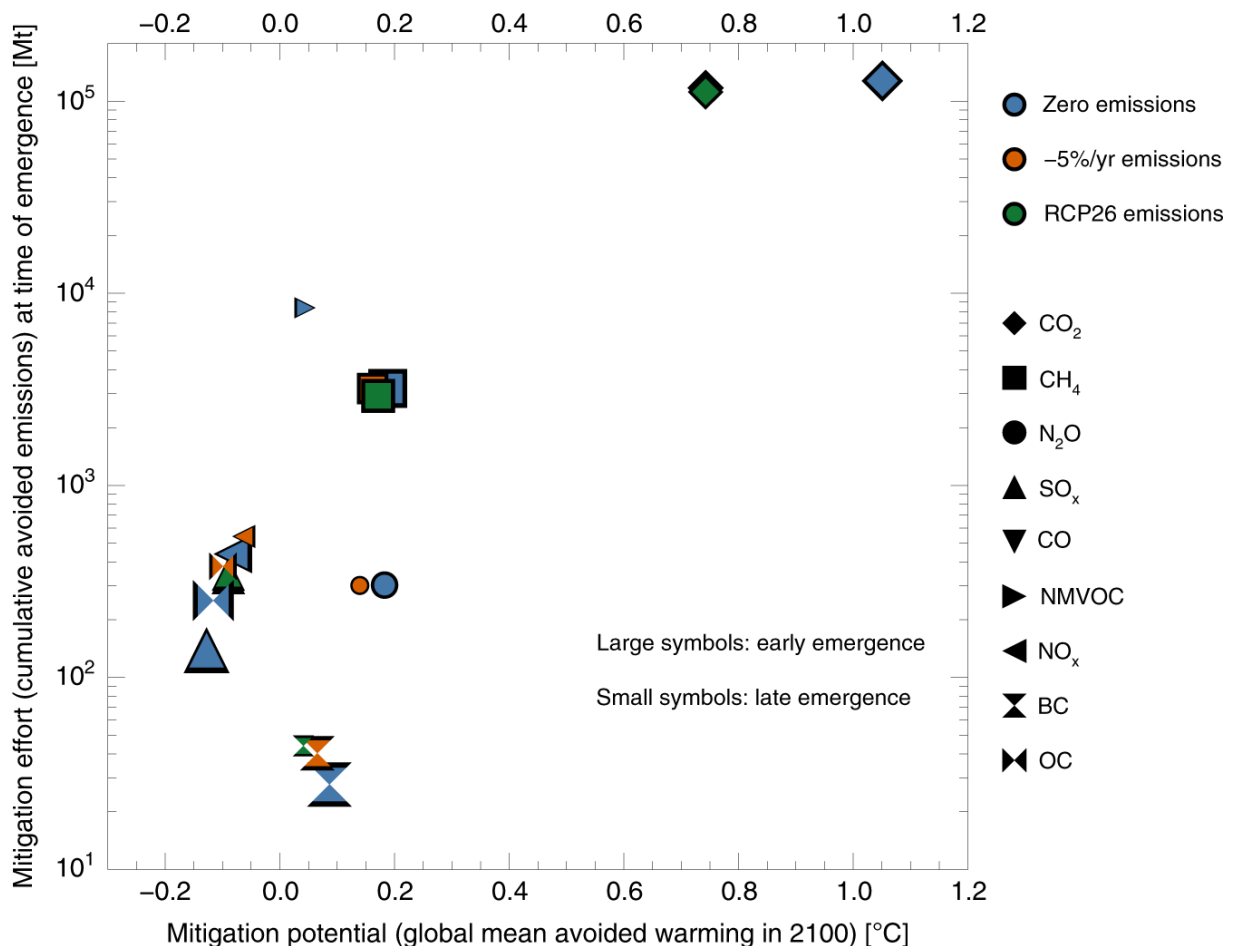


Figure 12: Potential versus effort for single forcer mitigation from (Samset et al., 2020)

To explore the conceivable range of future air quality and, in particular, of population exposure to PM_{2.5} which has been associated with the most harmful health impacts, (Amann et al., 2020) develop a series of alternative emission scenarios up to 2040 at the global level. Building on a widely accepted economic growth path with its structural economic changes, these scenarios combine different assumptions on the key policy areas that have been identified as critical for air pollution trends in the past, i.e. (a) energy/climate policy, (b) agricultural policies and (c) dedicated pollution control policies. A Clean Air scenario explores the theoretical potential of achieving clean air worldwide through a combination of further ambitious policy interventions in four areas, i.e. (i) traditional air pollution policies, (ii) energy and climate policies, (iii) agricultural policies and (iv) food policies. In particular, the scenario assumes full implementation of the best emission control technologies that are currently available on the market and, with a visionary perspective, policies and measures. As described by (Amann et al., 2020), in addition to improved human health (SDG 3—Improve human health and wellbeing), particularly in urban areas (SDG 11—Sustainable cities and communities), a clean air scenario would deliver a host of **co-benefits** in other policy areas through several pathways. For mitigating climate change (SDG 13—climate action), some of the measures will not only

reduce emissions of PM2.5 precursors but will simultaneously reduce emissions that contribute to temperature increase. In particular, CO₂ emissions of the Clean Air scenario will be about 40% lower than in the reference case in 2040, CH₄ 33%, and **black carbon** by 90% (Figure 13).

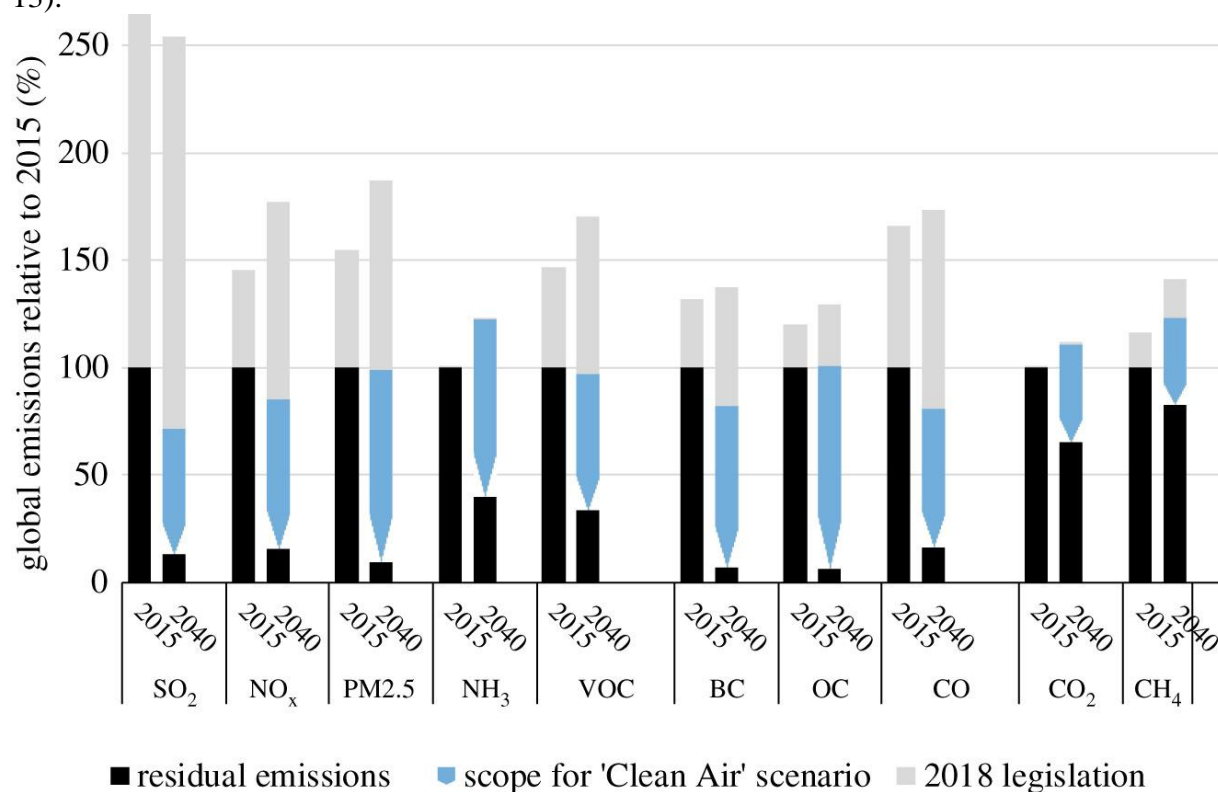


Figure 13: Emission reductions from the policy scenarios. 2018 legislation includes all controls that have been decided by 2018 according (Amann et al., 2020)

A recent study (Harmsen et al., 2020) contributed with an integrated assessment model-based scenario analysis of BC-focused mitigation strategies aimed at maximizing air quality and climate benefits. The impacts of these policy strategies have been examined under different socioeconomic conditions, climate ambitions, and BC mitigation strategies. The study finds that measures targeting BC emissions (including reduction of co-emitted organic carbon, sulphur dioxide, and nitrogen dioxides) result in significant decline in premature mortality due to ambient air pollution, in the order of 4 to 12 million avoided deaths between 2015 and 2030. Under certain circumstances, BC mitigation can also reduce climate change, *i.e.*, mainly by lowering BC emissions in the residential sector and in high BC emission scenarios. Still, the effect of BC mitigation on global mean temperature is found to be modest at best (with a maximum short-term GMT decrease of 0.02 °C in 2030) and could even lead to warming (with a maximum increase of 0.05 °C in case of a health-focused strategy, where all aerosols are strongly reduced). At the same time, strong climate policy would improve air quality (the opposite relation) through reduced fossil fuel use, leading to an estimated 2 to 5 million avoided deaths in the period up to 2030. By combining both air quality and climate goals, net health benefits can be maximized.

(Miller and Jin, 2019) estimate the projected tons of BC emissions avoided under recently adopted policies and the potential to further reduce BC emissions by accelerating the global implementation of soot-free standards for vehicles, engines and fuels. It also evaluates the implications for global temperature pathways and societal costs that include climate and health damages. The authors estimate that currently adopted policies will reduce global on-road diesel

black carbon emissions to 40% below 2010 levels by 2030. They show projected global diesel BC emissions for five policy scenarios in comparison with a 75% reduction in global diesel BC emissions from 2010 to 2030, corresponding to the level of BC reduction targeted by the CCAC Scientific Advisory Panel (Shindell et al., 2017). Policies that have been adopted or implemented since 2015 are projected to avoid 2 million tons of diesel BC emissions cumulatively from 2015 to 2030, equivalent to a 16% reduction in cumulative emissions compared with a baseline without these policies. More than 70% of these BC reductions are attributable to soot-free standards in China and India. Nevertheless, currently adopted policies are still insufficient to achieve a 75% reduction in global diesel BC emissions from 2010 to 2030.

In Finland, climate impact of Finnish air pollutants and greenhouse gases using multiple emission metrics have been investigated (Kupiainen et al., 2019). This study assesses the climate impact of Finnish air pollutants and greenhouse gas emissions from 2000 to 2010, as well as future emissions until 2030 (Figure 14). The pollutants included are SO₂, NO_x, NH₃, non-methane volatile organic compound (NMVOC), black carbon (BC), organic carbon (OC), CO, CO₂, CH₄ and N₂O, and their study is the first one for Finland to include all of them in one coherent dataset. These pollutants have different atmospheric lifetimes and influence the climate differently; hence, they look at different climate metrics and time horizons. The study uses the global warming potential (GWP), the global temperature change potential (GTP) and the regional temperature change potential (RTP) with different timescales for estimating the climate impacts by species and sectors globally and in the Arctic. They compare the climate impacts of emissions occurring in winter and summer. This assessment is an example of how the climate impact of emissions from small countries and sources can be estimated, as it is challenging to use climate models to study the climate effect of national policies in a multi-pollutant situation. Their methods are applicable to other countries and regions and present a practical tool to analyse the climate impacts in multiple dimensions, such as assessing different sectors and mitigation measures. While their study focuses on short-lived climate forcers, they found that the CO₂ emissions have the most significant climate impact, and the significance increases over longer time horizons. In the short term, **emissions of especially CH₄ and BC played an important role as well**. The warming impact of BC emissions is enhanced during winter.

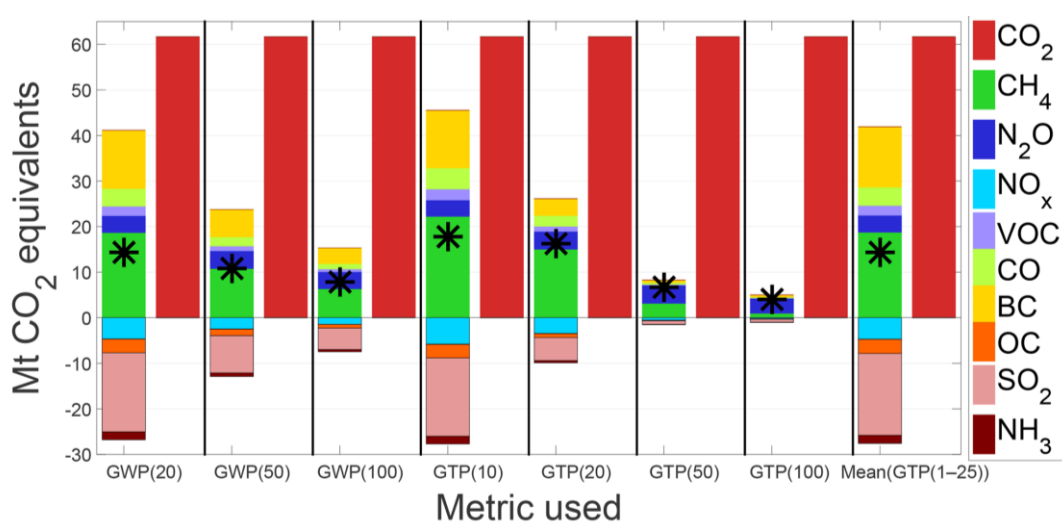


Figure 14: Finnish 2010 emission (Mt CO₂ equivalents) as a pulse emission weighted by various global metrics described in (Kupiainen et al., 2019). CO₂ is separated out and the net impact of the non-CO₂ is given by the star.

In Denmark, based on a modelling study, (Bjørner et al., 2019) found that there are large net welfare gains from most types of regulation of existing installations, but the largest gains result from imposing a differentiated tax or a general ban on non-ecolabeled stoves. **The gains mainly derive from the regulation of wood-burning stoves** located in urban areas. Thus, supplementing the existing regulation of new installations, with regulation of existing installations would result in a significant welfare improvement in Denmark. They find it likely that this would also be welfare improving in many other parts of Europe and North America where regulations are currently primarily aimed at new installations.

Over Swedish cities, (Segersson et al., 2017) found the major part of the premature deaths is in their assessment related to local emissions, with road traffic and residential wood combustion having the largest impact. Among the local sources, RWC and road traffic cause the most premature deaths. Using PM_{2.5} as an indicator attributes most deaths to RWC, while using BC puts more weight on road traffic exhaust. It is also concluded that fine traffic related particles (<2.5 µm) are likely a more important cause of mortality associated with long-term exposure than the coarser wear related fraction (2.5–10 µm). The health impact from RWC, together with the uncertainties related to this category, indicates a clear need for improvement of the emission inventories. Considering that the health impact of RWC in parts of Europe may be comparable to that of road traffic, the same level of detail in the description of emissions should be aimed for. This is far from the case today, with few cities having inventories of heating appliances. Also, to allow quantification of uncertainties in the source attribution, more monitoring data in areas dominated by RWC would be needed. A major finding is that using relative risk factors representing within-city comparisons or **using BC as an indicator for PM** from local combustion sources, the local sources of PM cause more premature deaths as compared to Long Range Transport. When risk assessments are instead based on the total PM₁₀ or PM_{2.5} concentrations, and using corresponding relative risk factors based on “between-city” comparisons, LRT is normally attributed a larger impact and there is an evident risk of underestimating the impact of local sources. The results emphasize the importance to resolve within-city gradients in the concentration field when assessing population exposure and raise more concern to reduce local PM and BC emissions in Swedish cities.

Exposure to **outdoor and indoor air pollution** is known to affect respiratory and cardiovascular health, and a recent study (Maher et al., 2021) also show its effects on cognitive function. Concentrations and magnetite content of airborne particulate matter (PM) in the indoor environment arising from burning peat, wood or coal in residential open fires. Highest indoor PM_{2.5} concentrations (60 µg m⁻³ *i.e.* 2.4 times the WHO-recommended 24-h mean) occurred when peat was burned, followed by burning of coal (30 µg m⁻³) and wood (17 µg m⁻³). Conversely, highest concentrations of coarser PM (PM_{10-2.5}) were associated with coal burning (20 µg m⁻³), with lower concentrations emitted during burning of wood (10 µg m⁻³) and peat (8 µg m⁻³). They found a negative association between open fire usage and cognitive function as measured by widely-used cognitive tests such as word recall and verbal fluency tests. The negative association was largest and statistically strongest among women, a finding explained by the greater exposure of women to open fires in the home because they spent more time at home than men. Their findings were also robust to stratifying the sample between old and young, rich and poor, and urban and rural areas.

4 Mitigation measures for PM emissions and its impact on BC and PAH emissions

In the following sections, a general overview of technologies to reduce emissions of particulate matter, focussing on BC and Organic Matter (OM) as PAH. Although ultrafine particles (UFP) are not in the main scope of this report an analysis of trade-off or co-benefits on these species are reported from the literature and described because these species are linked to BC emissions. A recent literature review is proposed to illuminate the role of technologies to abate emissions of particulate species.

In **section 4.1**, the small combustion appliances in the residential sector are addressed with some inputs from studies addressing larger installations which provide additional information extrapolatable in a certain extent to the technologies applied to small scale devices.

In **section 4.2**, the road traffic sector is covered. The role of usual after-treatment systems to reduce BC, OM and (UFP) will be emphasized. The role of tyre and brake abrasion is also addressed.

Section 4.3 is devoted to the gas flaring activity which is of major importance particularly in the Arctic regions both for health and climate issues. BC emissions is the main carbonaceous particulate emissions emitted by flaring with very uncertain emission factors.

4.1 Small combustion appliances in the residential sector

4.1.1 General overview of measures to abate PM and BC emissions

A wide range of emission factors is reported in (Nussbaumer, 2010a) for residential wood combustion in practice in those times (Table 7), while emission factors of medium and large scale applications mainly depend on particle removal equipment, related to national or local emission limit values. Compared to real-life emission factors, far lower emission levels are achievable for correctly operated 2010 modern combustion devices.

Table 7: Typical PM emission factors for various appliance types for wood combustion indicated as solid particles sampled on hot filters (not including condensable organic compounds) in real-life operation today (left), and achievable best-practice PM emission levels under ideal conditions (right). *only if operated at full load, which cannot be guaranteed for space heating. From (Nussbaumer, 2010a)

Appliance type	Typical PM emission factors today (mg MJ ⁻¹)	Achievable PM emission levels (mg MJ ⁻¹)
Open fireplaces	50 to > 1000	50 - 100
Wood stoves & closed inset appliances	20 to > 1000	15 - 25
Log wood boilers without heat storage tank	20* to > 1000	Not recommended
Log wood boilers with heat storage tank	20 to > 100	10 - 20
Pellet stoves & boilers	10 - 50	10 - 20
Automatic wood combustion plants		
With cyclone	50 - 300	50 - 100
With simple ESP	25 - 50	15 - 35
With advanced ESP	5 - 15	5 - 15
With fabric filter	< 5	<5

A host of new technologies allows significant reductions of PM_{2.5} emissions, especially from biomass combustion (Amann et al., 2018). These innovative **small scale combustion technologies** represent current best available technology, and their commercial availability has been triggered by stringent national emission regulations for small combustion facilities in some countries. The following examples are provided by (Amann et al., 2018):

- Wood chip boilers with low emissions (7 to 60 kWth): a wood carburettor using updraft gasification with activated charcoal filter effect and an enhanced fuel suction technology enable ultra-low PM emissions of 0.9 mg m^{-3} at 13% O₂ (at full load on test bench).
- Pellet boilers with low emissions (8 to 35 kWth): an underfeed pellet combustion with integrated particulate separation using cyclone effect are used. The PM emissions are 0.9 mg m^{-3} at 13% O₂ (full load on test bench).
- Pellet boilers with low emissions and integrated electricity generation (Micro-CHP) (3 to 18 kWth): it is a condensing pellet boiler with up to 107 % thermal efficiency with efficient combustion control, adjustable boiler temperature (28 °C to 85 °C) and possibility to upgrade with Stirling engine for power generation and combination with solar thermal collectors and photovoltaics. PM emission obtained are 12 mg m^{-3} at 13% O₂ (at full load on test bench).
- Pellet boilers with low emissions and integrated heat pumps (10 to 16 kWth): this product combines the use of pellets, ambient heat and electricity production. A software adjusts the system to the most economical or efficient operational mode, depending on the home owners preferences. PM concentration obtained is 17 mg m^{-3} at 13% O₂ (at full load on test bench).
- Log wood boilers with low emissions and integrated heat pumps (10 to 30 kW): a wood carburettor boiler with rotating combustion chamber and heat pump hybrid system is used which can be combined with photovoltaics. PM emissions are 17 mg m^{-3} at 13% O₂ (at full load on test bench).
- Log wood stoves with low emissions and high energy efficiency (8 to 10 kWth): it is a log wood stove with two combustion chambers, high energy efficiency with up to 93 %. The PM emissions are 20 mg m^{-3} at 13% O₂ (at full load on test bench).

From (TFTEI, 2019), the following list of new technologies were identified. New advanced stoves equipped with improved air control, reflective materials and two combustion chambers; New smart stoves with automated control of air supply and combustion, thermostatic control, Wi-Fi-connected to collect and send combustion data to the manufacturer for better service; New advanced masonry stoves, operating at high efficiencies and low emissions; New advanced pellet boilers: fully automated boilers (electronic control of air supply, lambda sensors), condensing boilers, using standardized pellets; Wood carburettor boilers using log wood or chip wood; Heat accumulating equipment with heat accumulating reducing stop/start frequencies and operation at partial load, which generates higher emissions than operation at full load; Other: flue gas recirculation, reverse combustion, gasifier.

As reported in (ETC/ACM, 2016), in relation to small combustion installations, primary measures of emission reduction include technological activities for reducing primary emissions from incomplete combustion, such as TSP, PM, CO, NMVOC, PAH, PCDD/F as well as heavy metals and SO₂, and NO_x.

The quality of fuels is also of major importance, such as actions for preventing or reducing emissions reported by (Kubica et al., 2007):

For coal:

- pre-cleaning, pre-treatment of raw coals and improvement of their quality to reduce the fine subfraction that achieves the reduction of ash content and sulphur content as well as chlorine and mercury;

- modification of the fuels granulation by means of compactification processes, *e.g.* briquetting, pelletizing, selection of grain size in relation to heating appliances requirements (stove, boilers) and supervision of its distribution;
- replacing of coal by upgraded solid derived fuel, biomass, oil, gas. For example, thermal upgrading of raw coal will reduce the fuel's volatile content (typically from around 35% to around 9%) to produce "smokeless" fuels as briquettes or as coke (the volatile contents are ranged about 2%);
- regulating coal quality,

for wood:

- avoiding the combustion of recycled wood (frequently treated with chemicals), in order to reduce emissions of SO₂ and metals, among others;
- application of combustion;
- homogenization and stabilization of the moisture contents in the fuel, especially in the case of solid biofuels;

Secondary measures can be applied to small combustion installations to remove emissions, in particular of PM but are more rarely applied to small domestic appliances. Simultaneously, emissions of pollutants attached to the PM, such as heavy metals, PAHs and PCDD/F are also reduced. For particulate matter the following options can be considered in larger combustion plants (ETC/ACM, 2016; Kubica et al., 2007):

- cyclone separators: to achieve high effectiveness of 94-99%, units with multiple cyclones (cyclone batteries) are applied, and multi-cyclones for increased gas flow rates;
- electrostatic precipitators with an efficiency between 99,5% to 99,9%) or fabric filters (with efficiency about 99,9%).

Wood combustion appliances, stoves in particular, can be equipped with a catalyst. When flue gas passes through the catalytic combustor, smoke that otherwise would leave the chimney as dirty, wasted fuel is recirculated and burnt. The catalyst decreases emissions caused by incomplete combustion by reducing the temperature that smoke catches fire at so that it can safely burn while still inside the stove. The catalytic converter is a cellular or honeycomb heat ceramic monolith covered with a very small amount of platinum, rhodium, or combination of these. It is usually placed inside the flue gas channel beyond the main combustion chamber. How efficient a catalyst is in reducing emissions depends on the catalyst material and on its construction (active surface, the conditions of flue gases flow inside converter, temperature, flow pattern, residence time, type of pollutants, etc.). The operation of a catalytic stove is a little more complicated compared to a non-catalytic one because they have a lever-operated catalyst bypass damper which is opened for starting and loading and the stove has to be burned hot before the catalyst is engaged. This means that these stoves are most efficient for full load unlike to the non-catalytic stove. Further, the catalytic element degrades over time and must be replaced; its durability is largely in the hands of the stove user. However, due to the greater fuel capacity and efficiency, the fuel load lasts longer. A key issue with regard to emissions and secondary measures are the emissions of condensable compounds, which form particulate pollutants shortly after emission. Condensable compounds are complex to address from an emission reduction point of view. They should be included in emissions inventories in order to more accurately represent the particle emissions from stoves. Secondary measures with reference to NO_x and SO₂ are not applied for small combustion installations due to technical and economical restrictions (Kubica et al., 2007).

(TFTEI, 2019) proposes a list of good practices for small combustion appliances to reduce emissions of PM and BC. In order to reduce environmental impact and to improve energy efficiency, careful consideration should be given to the type, size and installation requirements of the heating device. When choosing a new heating system for a house, alternative heating systems other than wood boilers and stoves and with less emissions and higher efficiencies should be considered; this includes heat pumps, photovoltaics, solar boilers and connection to a local heating network. If a wood-heating installation is chosen, the following practices are recommended in the document:

- (a) Choose a heating installation that uses best available techniques to reduce emissions and increase efficiency. Emissions from automated heating installations, with automatic control of air supply, feed and ignition, and, consequently, decreased influence of user and wind speed, are considerably lower than those from manually operated heating devices;
- (b) Choose a heating installation that matches the size of the space to be heated and that is adjusted to its function (primary or additional heating source). The heat demand should be calculated based on the volume of the room(s) to be heated, with due consideration of heat dispersion, degree of insulation of the building and outdoor temperature. A heating installation that is too large for the room will overheat the space quickly and will have to be operated with slow, smouldering fires much of the time to avoid overheating the room, resulting in high emissions and low efficiency. An undersized heating installation can be damaged by frequent over-firing to keep up with heat demand. Heating installations of the correct size will use less firewood;
- (c) Choose a certified heating installation or one bearing a high energy efficiency label or eco-label, if possible. Certification or labelling guarantees the appropriate quality of the heating installation and compliance with safety regulations and/or minimum efficiency and emission requirements;
- (d) Choose a heating installation according to available indoor or outdoor firewood (logs, pellets, chips) storage capacity;
- (e) Avoid installing an open fireplace. Heating with an open fireplace is inefficient and results in significant emissions; poor indoor air quality can cause a fire if burning material leaps out;
- (f) Ask for a user manual when purchasing a heating installation. The user manual should be easy to read and to use and should contain all necessary information specific to the heating installation, especially regarding its proper use;
- (g) Foresee that the combustion air for the heating installation is extracted from outside the house, through proper piping. This ensures safer operation and reduces heat loss. Requirements concerning insulation, airtightness and ventilation of energy-efficient buildings should be taken into account for the management of air intake for the heating installation;
- (h) Use licensed/qualified technicians for the installation of the heating device;
- (i) Ensure that the flue gas channels and chimney are well placed. The chimney must extend above the ridge of the roof and adjoining buildings. The diameter of the flue gas channels must be adjusted to the heating installation in order to avoid a bad chimney draft and the risk of a chimney fire. Have the flue gas channels and the chimney installed by a specialized technician. Corners in the flue gas channel and horizontal lines should be avoided;
- (j) Use state-of-the-art technologies to ensure good discharge conditions for exhaust gases.

Successful policy interventions that have led to effective reductions of air pollutant emissions in the household sector include (i) awareness campaigns, informal platforms, qualification of focus groups, product declaration, (ii) and expert advice at the site, (iii) subsidies for thorough

building renovation, for the switch to other fuels or the upgrade to new facilities, (iv) a ban of the use of solid fuels, as well as (v) measures in combination to fight energy poverty (Amann et al., 2018). In addition, integration of smart flue gas abatement technologies with other technologies is emerging.

The Arctic Council has recognized the climate and health benefits of reducing short-lived climate forcers, and has therefore encouraged work to reduce black carbon (BC) emissions in the Arctic (ACAP, 2015, 2014). Arctic is a key region and observatory to analyse relevant measures to both combat Climate Change and Air Pollution. The AC has developed a set of recommendations (more policy oriented than technically oriented) to reduce BC emissions from residential heating. Some of these recommendations are provided hereafter:

- **Establish emission limits for new and resold stoves**, if such standards do not exist, or more stringent emission limits, if existing standards can be improved. As a prerequisite, this mitigation action would require a study of an agreement on a suitable emission measurement protocol that would form the basis for establishing the standard.
- **Introduce voluntary black carbon emission testing and ecolabelling by interested producers** to drive further product design and reward innovation by producers.
- **Introduce legal instruments** that would enable local authorities to implement bans on wood burning in certain areas where many people are affected by poor air quality. Burn bans in certain areas at certain times can help to improve local air quality and health.
- **Establish national or regional change-out programmes**: to promote the replacement of older wood-burning stoves with low-emission wood stove appliances.
- **Introduce regular stove inspections combined with maintenance**: to reduce emissions from aging clean-burning stoves.
- **Introduce regular end-user information campaigns**: to educate households operating wood-burning stoves and boilers on their correct use and climate and health benefits.
- **Establish fuel wood guidelines or information campaigns**: to reduce particle emissions through increased fuel homogeneity.
- **Advocate the development and use of stoves with improved combustion efficiency or increased heat storage capabilities**: to influence the choice of residential wood combustion technology and development.
- **Support transition from wood stoves to pellet stoves**: to replace wood fuel with cleaner fuel.
- **Develop uniform BC measurement methods and emission limits**. The Arctic countries that are members of the European Union could encourage EU member countries to reach a consensus on a BC measurement protocol and wood stove emission limits to reduce particulate and black carbon emissions from wood-burning stoves and boilers.
- **Establish uniform BC reporting guidelines**. A common framework for BC inventories would be of great use when comparing BC emission inventories across nations, and across scenarios in various countries. The updated CLRTAP Gothenburg Protocol is a natural arena for such work. The AC countries could be active promoters, make joint statements and work actively with the LRTAP secretariat and specialized groups to help develop uniform BC reporting guidelines.
- **Create a regional toolbox for developing national action plans or equivalent measures**. The Arctic countries could share information and experiences with regard to the development of national action plans whose primary or secondary aim is to reduce black carbon emissions from residential wood combustion. Such mitigation plans and actions should consider emissions, impacts, mitigation instruments and measures, and their cost-effectiveness.

- **Facilitate information sharing.** A lot of work is underway to reduce PM/BC emissions from residential wood combustion, and knowledge is constantly evolving. Examples include task forces under the Arctic Council, projects under the Nordic Council, reporting requirements under the Convention on Long Range Transboundary Air Pollution and directives from the EU. ACAP is in a position to gather this knowledge on a pan-Arctic level and facilitate capacity-building by making the information more easily available.
- **Encourage shared research efforts to close knowledge gaps.** BC inventories and reduction strategies have to overcome knowledge gaps and inherent uncertainties. The number of knowledge gaps could be reduced more efficiently by joint research at a regional level. The Arctic region hosts substantial research capacity and many BC-relevant research projects are on-going or planned. It would be interesting to explore the potential for even more structured cooperation and development. This could be done through common research programmes and/or demonstration projects under ACAP or other coordinated projects.
- **Run demonstration projects.** To verify the effect of mitigation instruments and measures.

4.1.2 Performances of modern appliances compared to traditional ones under real uses

From the Figure 15 from (Tytgat et al., 2017), it becomes clear that PM emissions vary significantly within and between different types of appliances. In general, more recent devices with newer technology show lower PM emissions compared to the older devices, which are more on the left in the graph. It is important to note that in this study, the majority of the collected data originates from tests in laboratory, either following standard test procedures or simulating real life operation. Most tested stoves are several years old, making it difficult to estimate emissions from stoves with most recent technology incorporated.

In addition to the overview of the available wood combustion devices presented in (Tytgat et al., 2017), an overview is also included of technologies that can result in a reduction of the emissions. Two strategies exist to achieve the latter.

- First, it can be done by means of source control, in which especially stove design and air flow prove to be crucial elements. Source control measures typically aim to achieve optimal combustion at real operation conditions. This effect is particularly visible in the reduced emission rates of more recent stoves, which contain these types of measures. It is this effect that is visible.
- Secondly, end-of-pipe solutions can also result in reduced emissions. A widely used and commercially available technology is electrostatic precipitation. This technology is based on the collection of PM on an electrode. In practice, this appears to reduce part of the emissions, but the achieved reduction is highly dependent on the circumstances and the used stove. A second end-of pipe solution is the incorporation of a catalyst inside the combustion chamber or inside the chimney. This is mainly effective for the reduction of CO and organic substances and is less suitable for PM. Fluctuating efficiencies are reported and in some cases, there is a risk of forming harmful by-products. Correct use and maintenance of such systems is therefore important.

An important conclusion from (Tytgat et al., 2017) is that a considerable knowledge gap exists on several subjects. First, there is a limited amount of data collected under real-life conditions. Additionally, the interpretation and comparison of emissions in literature and in legislation appear to be difficult because of the difference in the use of units. In literature, emissions are

based on energy input to allow comparisons between different types of stoves. The legislation on the other hand, relies on emissions per volume of air. The latter is highly stove specific and often not known, which makes a comparison between different stoves very difficult.

Another aspect with a lot of ambiguity is the formation of secondary organic aerosols (SOA). The formation of this fraction of particulate matter occurs when the exhaust gases exit the chimney and end up in the atmosphere. Under the influence of various external factors, the organic components present in the exhaust gases will react. Consequently, a new fraction of particulate matter is formed. The concentration of SOA emissions can be of the same order of magnitude as the concentration of primary PM during the combustion process. The precise mechanism of SOA formation is very complex and dependent on various factors, making the quantification of this fraction in real life very difficult. Since SOA are formed after leaving the chimney, most tests do not measure the SOA fraction which could result in a significant underestimation of real-life PM emissions.

Several aspects play a role in this variation, *e.g.* used technology, test method and operational conditions. The latter is mainly focused on the behaviour of the user of a wood combustion device. Elements such as the type of wood used, the degree of humidity, the fire lighting procedure etc. all have a direct influence on emissions from residential wood combustion. In the standard tests, the experimental conditions are based on the most optimal conditions while in reality a lot of the conditions are far from ideal, resulting in large differences between lab and real-life tests.

An important problem with estimating real-life emissions is that consistent information of typical or average real user behaviour is lacking. As a result, assumptions currently made in scientific literature on (pseudo) real life emissions can prove to be completely different. A better understanding of these aspects is still required. This can be done by performing surveys with real-life users in order to gain knowledge about their operation of a stove. Another problem is that a small fraction of real users (*e.g.* people burning wet, contaminated wood in old stoves) could have a relatively high contribution to the total emissions. Therefore, good knowledge of best, average and worst-case scenarios and their occurrence is essential to estimate the total real-life emissions.

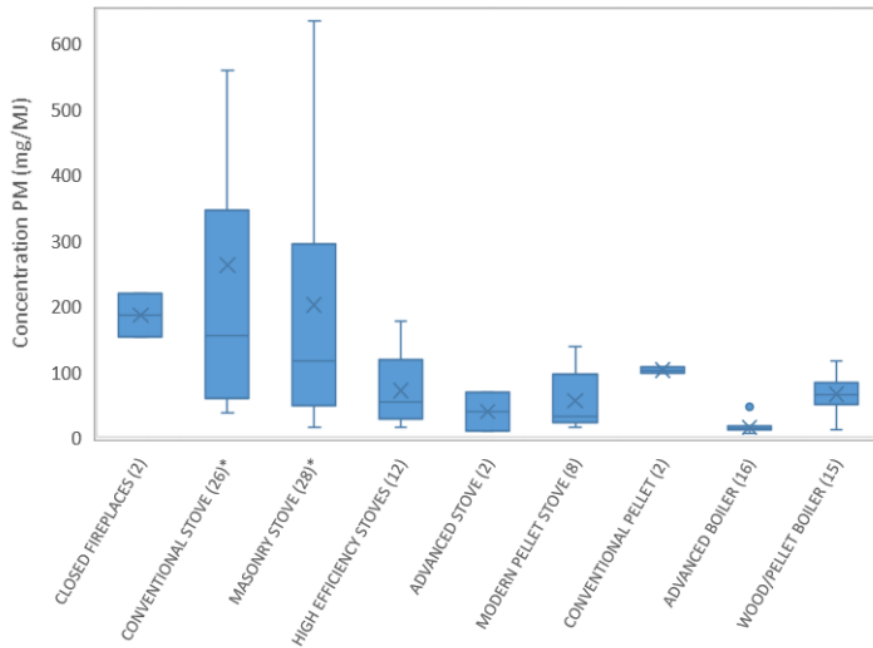


Figure 15: Boxplot summary of all data points (number given between brackets) for each type of wood combustion appliance. *category containing outliers above 1000 mg/MJ from (Tytgat et al., 2017)

Chemical composition of PM is affected by numerous combustion parameters (Figure 16), but is often not considered in energy transitions, despite varying toxicity among chemical components. (Lai et al., 2019) analysed PM_{2.5} emissions from combustion of solid fuels (coal, wood, and straw; whole and pelletized) in a variety of stoves (cookstoves and heating stoves; traditional and semi-gasifier, including forced versus natural draft and fixed versus reciprocating grate). To assess the effects of fuel and stove type on PM_{2.5} composition, they measured elemental carbon (EC), organic carbon (OC), water-soluble OC, water-soluble inorganic ions (*e.g.* SO₄, Cl, Kp), and organic molecular markers. PM_{2.5} emissions from traditional stoves were mostly carbonaceous: 76-90% organic matter (OM), 5-6% EC, and less than 2% inorganic ions. In contrast, semi-gasifier stoves emitted more inorganic PM_{2.5}: on average, ions comprised 65%, 9% was OM, and 4% was EC. Within the semi-gasifier cookstoves, forced-draft cookstove emissions had lower OM (1-3%) and higher ion concentrations (84-88%) than the natural-draft cookstove (5-14% OM, 30-83% ions). Across a range of different fuels and stoves, **stove types would influence emitted PM composition more than fuel type, underscoring the impact of combustion conditions on PM chemical composition.**

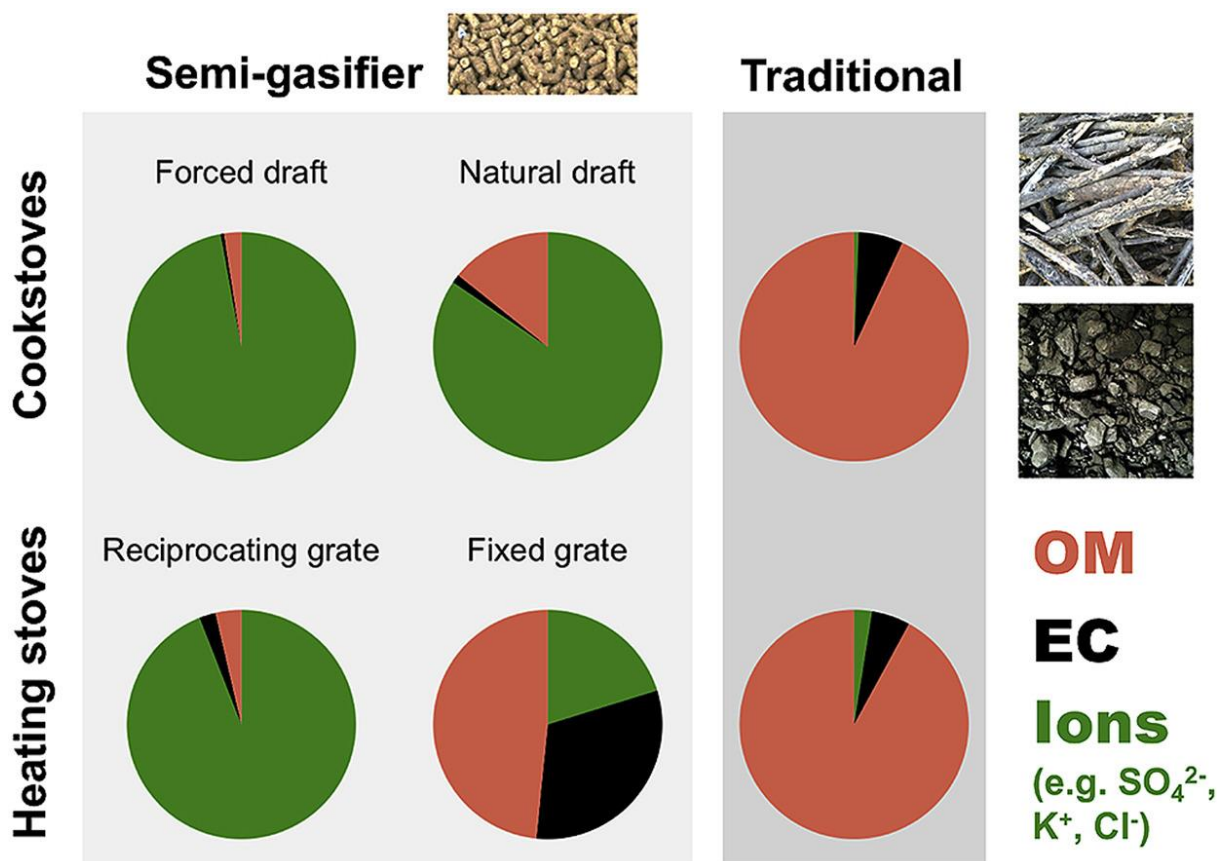


Figure 16: A visual summary of (Lai et al., 2019) findings

The experience of new boilers in the industry can also inspire the technologies to apply for smaller scale combustion systems as described in (Oberberger et al., 2017). To satisfy the market demand for fuel-flexible low-emission biomass combustion systems, a new approach based on an **updraft gasifier directly coupled with a multi-stage gas burner** and a boiler has been developed. In the gasifier, semi-volatile ash forming elements (*i.e.* mainly potassium - K) are released in the hot charcoal combustion zone and are precipitated again in the upper regions of the fuel bed. Therefore, an almost particle free product gas can be achieved which can then be efficiently combusted at low excess air ratios in the subsequent multi-stage burner. In this paper, the principle of ash embedding in the gasifier is described with a special focus on the K chemistry. Combining this approach with appropriate **fuel bed cooling measures**, the new technology can be applied for a wide spectrum of biomass fuels reaching from conventional wood fuels over short rotation coppice to agricultural fuels/residues such as miscanthus and olive stones. Test runs performed at a lab-scale testing plant confirmed this high fuel flexibility and the possibility to operate this system at almost zero CO and OGC emissions as well as **dust emissions of less than 5 mg MJ_{NCV}⁻¹**.

Impact of PM reduction strategies on ultrafine particles

(Wang et al., 2020) explored ultrafine particle emissions during residential combustion under both laboratory-controlled and real-world rural household conditions (Figure 17). Significant ultrafine particle emissions (*i.e.* with emission factors between 2×10^{15} to 2×10^{16} particles per kg of fuel) are found for both coal and biomass. High emissions of particle mass concentration often occur at the beginning of the combustion (*i.e.* the first 30 min after fire start) while high emissions of particle number concentration occur in a later combustion period (60–150 min).

Ultrafine particles account for over 90% of the emitted total particle number concentration from 3 nm to 10 μm. These emissions elevate ultrafine particle number concentrations by more than a decade in indoor environment under which household residents are directly exposed. In addition, they show that there is notable inconsistency between reducing PM_{2.5} mass-based emissions and reducing ultrafine particle number-based emissions among various control strategies that were proposed for reducing pollution from residential combustion. Both “cleaner” fuels and stoves that are designed to reduce PM_{2.5} emissions are found to be not necessarily effective in reducing ultrafine particle emissions, even increase their emissions in some cases. These findings indicate that the overlook of ultrafine particle emissions from residential solid fuel combustion can lead to potential health risk to household residents, especially to those vulnerable ones (*e.g.*, the elderly and children) who are more sensitive to indoor air pollution. More attentions are needed on ultrafine particle pollution and its potential health risk in comparison to using the PM mass concentration index alone.

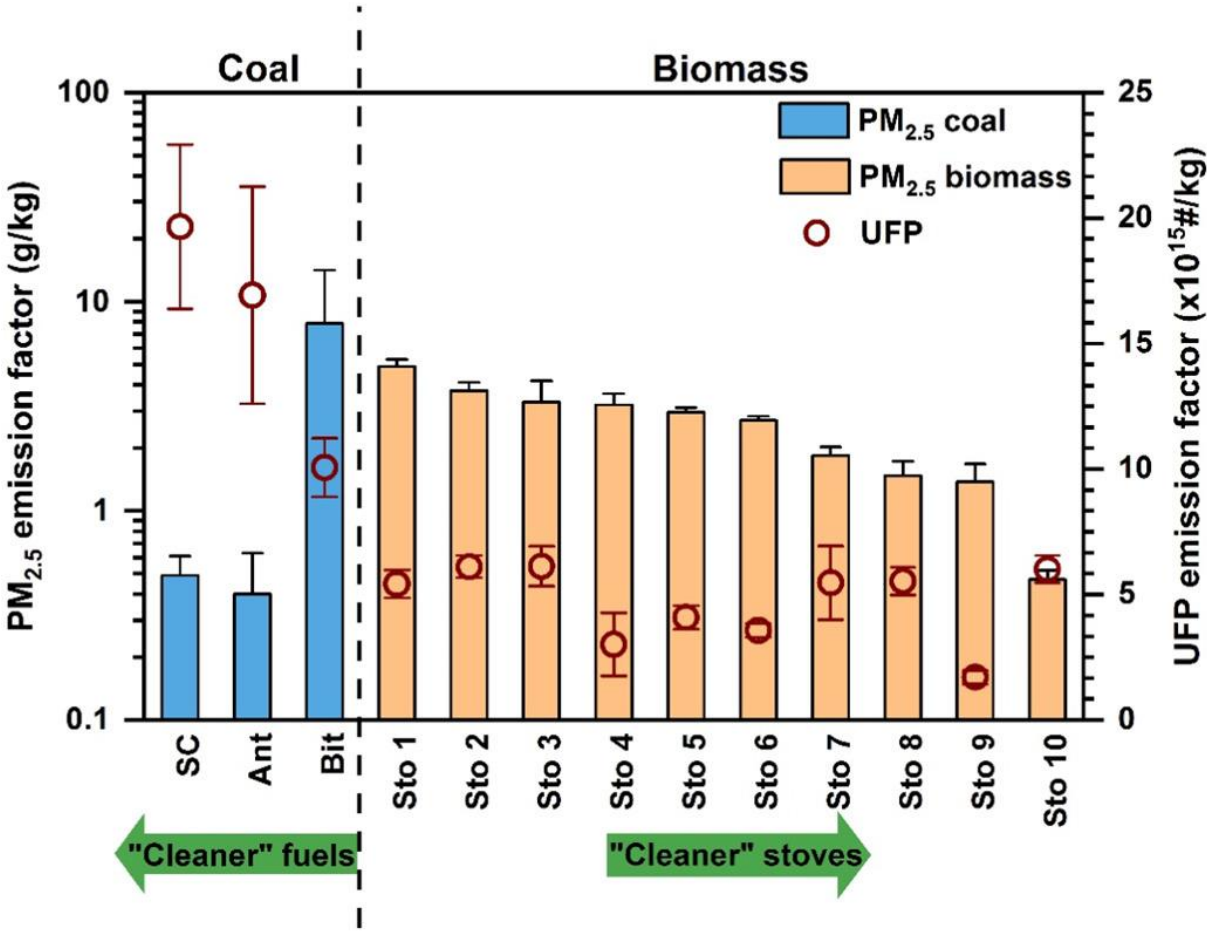


Figure 17: Comparison of PM_{2.5} and ultrafine particle emission factors from residential combustion. When burning three different coals, the same stove was used. Error bar represents standard deviations among repeated experiments. Bit, Ant, and SC mean bituminous, anthracite and semi-coke coals, respectively (Wang et al., 2020)

4.1.3 Impact of combustion conditions on PM and BC emissions

As explain in (TFTEI, 2019), poor combustion results in reduced energy efficiency and higher emissions of air pollutants, especially of fine particulate matter, and creates creosote build-up on the interior surfaces of the chimney flue, reducing the chimney draft and creating a chimney fire hazard. There are three phases of wood combustion, mainly in reference to the temperature of the process: (i) drying; (ii) pyrolysis; and (iii) gasification and combustion.

- **Drying.** When wood is heated, water begins to evaporate from its surface. Evaporation typically starts below 100°C. Up to a temperature of 150–200°C wood loses the water it contains. As evaporation occurs, the temperature in the combustion chamber temporarily decreases, slowing the process of combustion and decreasing the thermal efficiency of the heating installation. This is the main reason for not using unseasoned wood. The wetter the wood, the more energy will be required to dry it and the lower the efficiency of wood combustion. High moisture content in wood leads to incomplete combustion, reduced thermal efficiency and increased emissions of air pollutants.
- **Pyrolysis.** At a temperature of around 200°C, wood starts to break down into volatile substances and solid carbon. The volatile fraction of wood – more than 75 per cent of the whole mass of wood – evaporates. At around 400°C, most of the volatile components have evaporated.
- **Gasification and combustion.** This phase, starting between 500°C and 600°C and continuing up to about 1,000°C, consists of complete oxidation of gases.

Combustion is completed when all wood components have completed their chemical reaction with oxygen. However, 100% complete combustion of wood is a purely theoretical concept due to limiting conditions, such as the right degree of mixture between air and fuel, which is quite difficult to achieve in a short time. When the conditions for complete combustion are not ideal, emissions of harmful substances increase. In reality, during combustion, the three above-mentioned phases overlap in a complex way, rather than occurring at distinct moments in time.

From the literature, it is clear that particle formation and emission is closely related not only to the fuel properties but also to the combustion conditions and processes of the furnace (Obaidullah et al., 2012). The effect of stove technology and combustion conditions on gas and particulate emissions from residential biomass combustion has been studied by (Bhattu et al., 2019). They have systematically examined the gas and particle phase emissions from seven wood combustion devices (Figure 18). Among total carbon mass emitted (excluding CO₂), CO emissions were dominant, together with nonmethane volatile organic compounds (NMVOCs) (10–40%). Automated devices emitted 1–3 orders of magnitude lower CH₄ (0.002–0.60 g kg⁻¹ of wood) and NMVOCs (0.01–1 g kg⁻¹ of wood) compared to batch-operated devices (CH₄: 0.25– 2.80 g kg⁻¹ of wood; NMVOCs: 2.5–19 g kg⁻¹ of wood). 60–90% of the total NMVOCs were emitted in the starting phase of batch-operated devices, except for the first load cycles.

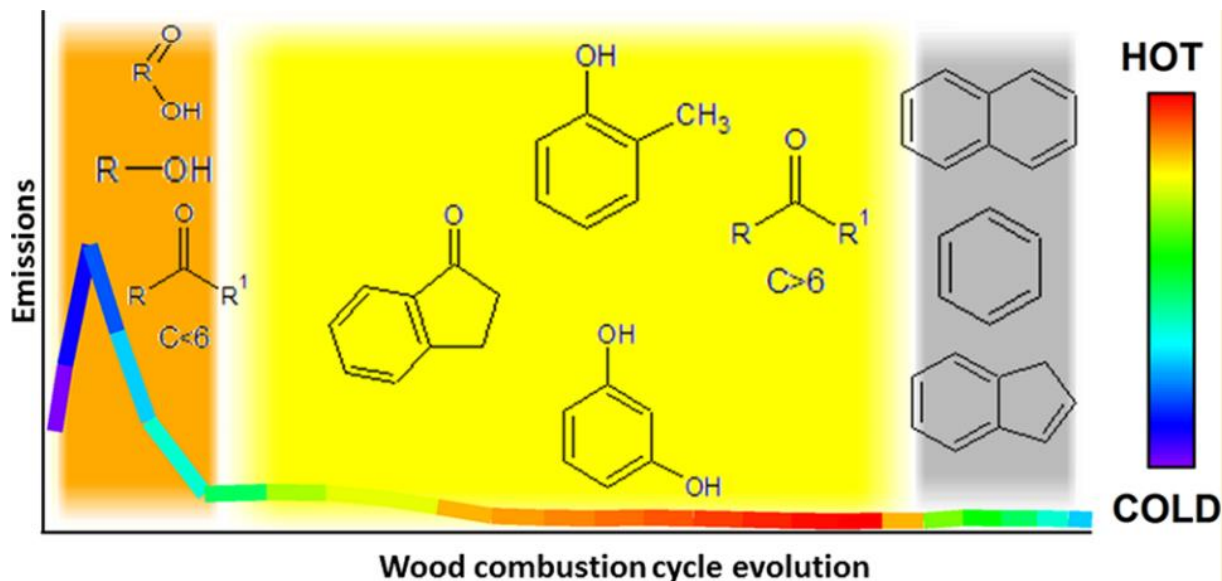


Figure 18: Visual summary of the effect of combustion on organic pollutant emissions (Bhattu et al., 2019)

Partial-load conditions or deviations from the normal recommended operating conditions, such as use of wet wood/wheat pellets, oxygen rich or deficit conditions, significantly enhanced the emissions. NMVOCs were largely dominated by small carboxylic acids and alcohols, and furans. Despite the large variability in NMVOCs emission strengths, the relative contribution of different classes showed large similarities among different devices and combustion phases (Figure 19).

The largest BC emissions are observed for logwood stove during the cold start. They show that specific improper operating conditions may even for advanced technology, do not result in the emission reduction of secondary organic aerosol (SOA) forming compounds and thus not reduce the impact of wood combustion on climate and health.

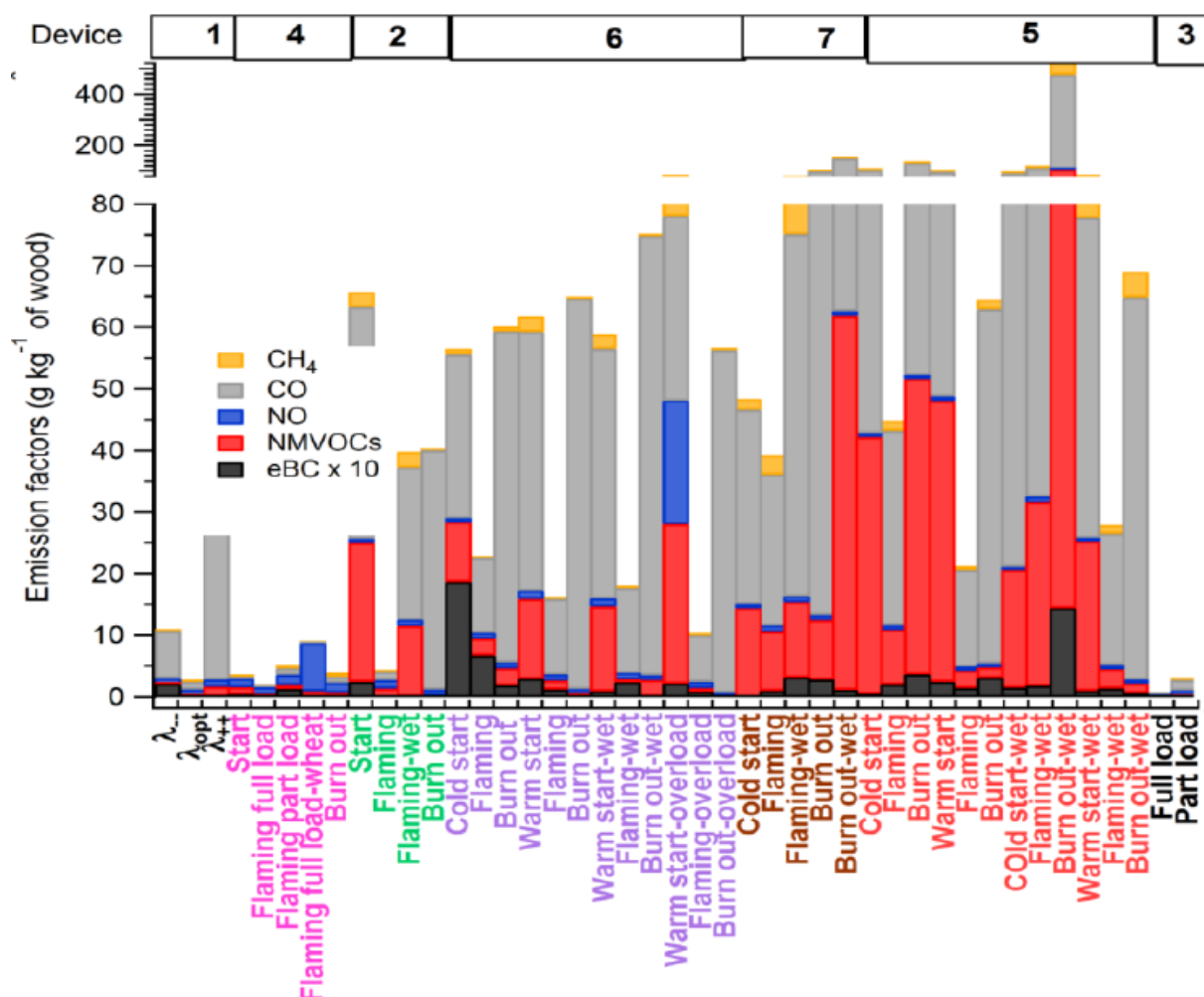


Figure 19: Combustion phase-specific “averaged EFs” (g kg⁻¹ of wood) of gas (CH₄, CO, NO and NMVOCs) and particle (eBC) phase compounds for device 1-7 of all investigated conditions (1: Pellet boiler, 2: Logwood Boiler, 3: Industrial Wood Chip Moving Grate Boiler, 4: Pellet stove, 5: Single-stage Combustion Logwood Stove, 6: Two-stage Combustion Logwood Stove, 7: Two-stage Combustion Logwood Stove) from (Bhattu et al., 2019)

It has been shown previously in the literature, that PAHs form in large quantities and may be emitted under high temperature air-starved wood combustion conditions. (Eriksson et al., 2014) illustrates that PAHs can also form during a few minutes following addition of fuel on glowing embers in a wood stove at lower temperatures (400– 500 °C), and that the fraction of PAHs with five rings or more increases with increasing temperature. It cannot be ruled out that this is because of gas/particulate partitioning differences, as the lower temperatures coincided with more concentrated organic emissions. In gasification research (the study of thermal degradation in the absence of oxygen) one typically distinguishes between primary tars that consist of primary pyrolysis products of cellulose and lignin such as monosaccharide anhydrides (*e.g.*, levoglucosan), and methoxyphenols formed at low temperatures. As the combustion temperature increases these are further broken down to phenols (600–700 °C) and methylated aromatics (>700 °C). At even higher temperatures, the yields of PAHs increase strongly. At such high temperatures, PAHs are also one of the few classes of organic compounds that are stable enough to survive. Based on this reasoning the strongly increasing can be understood as PAH/OA ratio and decreased concentration of OA for the intermediate phase of High Burn compared to the fuel addition phase. Gasification theory also predicts that EC formation and

emission increases as the temperature is further increased above the optimal temperature window for PAH formation Figure 20.

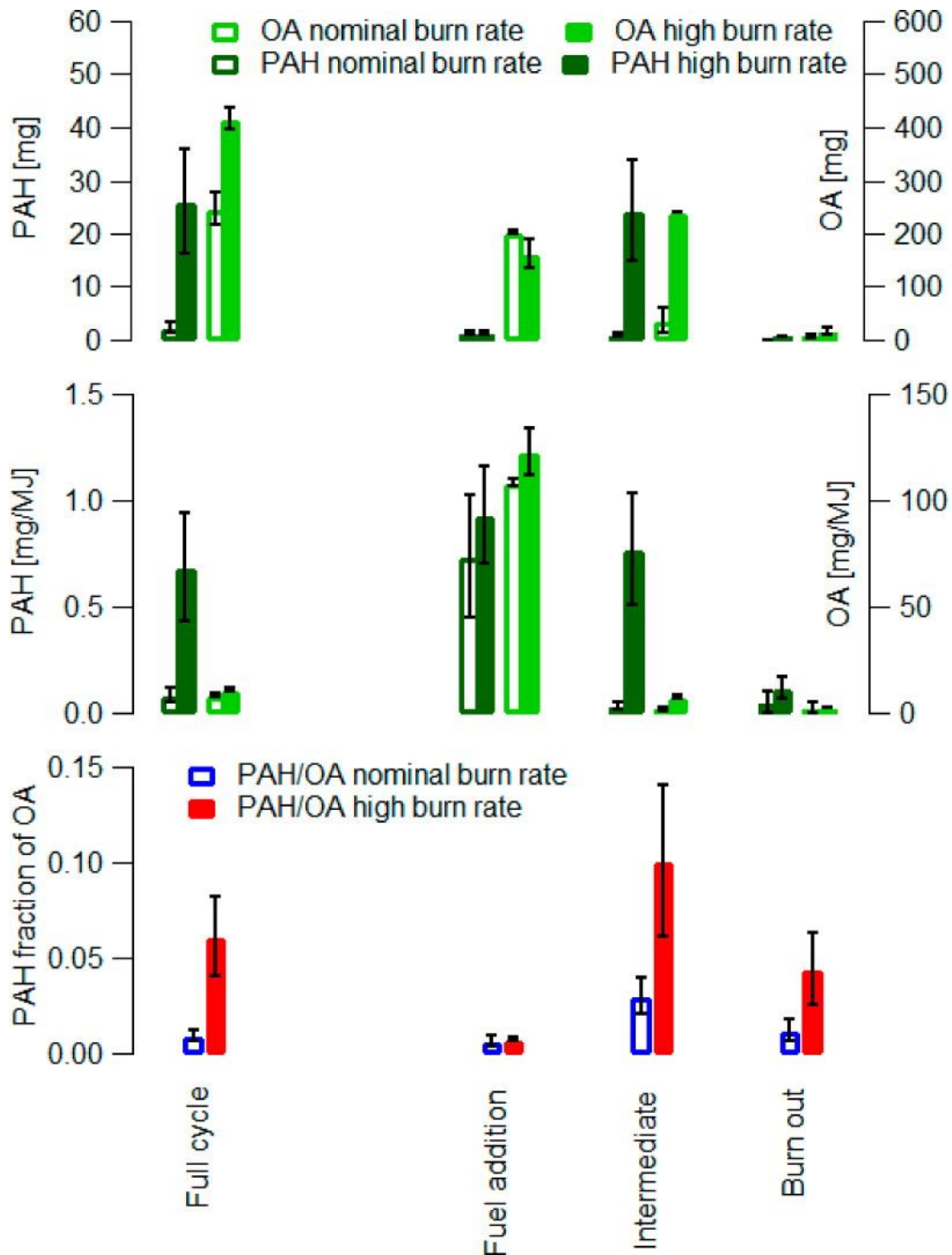


Figure 20: Average wood stove particulate emissions at nominal and high burn rates in mg and mg/MJ for the three combustion phases and the full cycle. Error bars represent range of observations (n = 2) (Eriksson et al., 2014)

In summary, previous data also support that PAH emissions from wood stoves can be strongly elevated at air starved combustion conditions at high heat release rates, even more so than found in (Eriksson et al., 2014). The most efficient way of reducing PAH emissions from wood stoves may therefore be to target combustion conditions with too high heat release rates that result in air deficits related to the functionality of the specific stove. In their study, fast burning conditions with less than 5% O₂ in the flue gases, corresponding to heat release rates of more

than 23 kW, were shown to coincide with increased PAH emissions. While the numbers are stove specific, this phenomenon is (qualitatively) likely not. Measures to avoid these situations may potentially reduce adverse effects on human health and possibly also have the co-benefit of **reducing black carbon emissions**. Furthermore, emissions of the potent greenhouse gas methane are also enhanced during this kind of intense incomplete combustion. The traditional recommendations to wood stove and boiler users and manufacturers are to avoid slow, low temperature combustion (*i.e.*, moist fuel and poor insulation). The (Eriksson et al., 2014) study illustrates how excessively high heat release rates are also undesirable, because of the emissions of particulate PAHs.

Time-resolved particle emissions from a conventional wood stove were investigated in (Nielsen et al., 2017) with aerosol mass spectrometry to provide links between combustion conditions, emission factors, mixing state of refractory black carbon and implications for organic tracer methods. The addition of a new batch of fuel results in low temperature pyrolysis as the fuel heats up, resulting in strong, short-lived, variable emission peaks of organic aerosol-containing markers of anhydrous sugars, such as levoglucosan (fragment at m/z 60). **Flaming combustion results in emissions dominated by refractory black carbon** coemitted with minor fractions of organic aerosol and markers of anhydrous sugars. Full cycle emissions are an external mixture of larger organic aerosol-dominated and smaller thinly coated refractory black carbon particles. PAHs are primarily associated with refractory black carbon-containing particles.

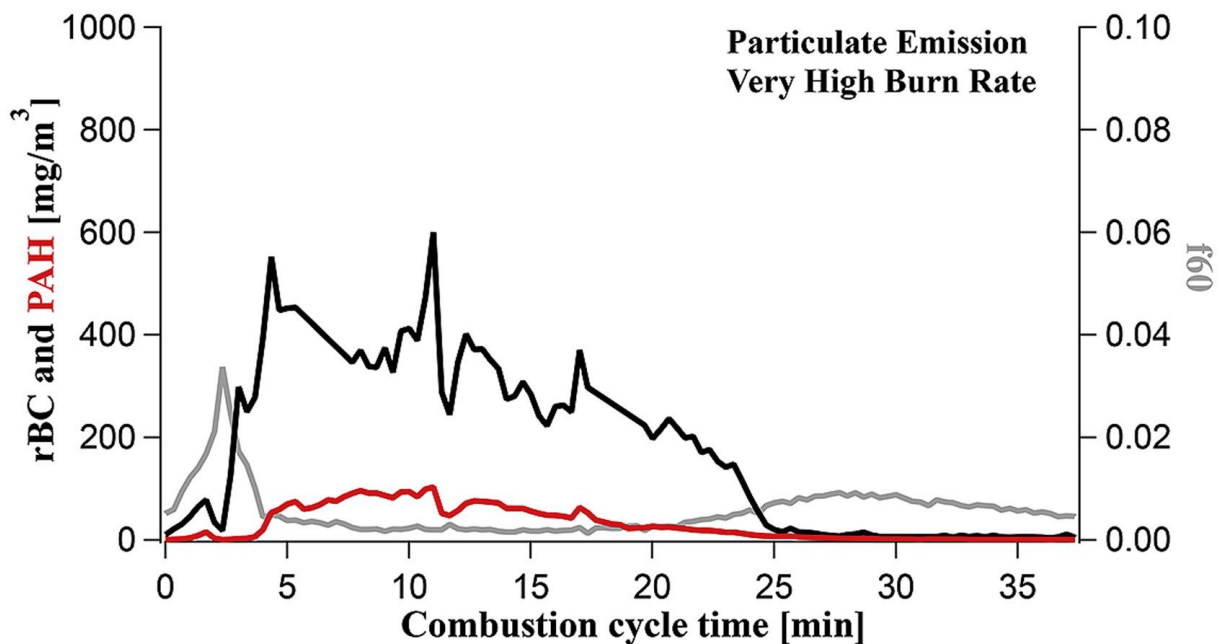


Figure 21: Evolution of refractory BC and PAH emissions during a combustion cycle from (Nielsen et al., 2017)

They hypothesise that at very high burn rates, the central parts of the combustion zone become air starved, leading to a locally reduced combustion temperature that reduces the conversion rates from polycyclic aromatic hydrocarbons to refractory black carbon. This facilitates a strong increase of polycyclic aromatic hydrocarbons emissions (Figure 21). A very high burn rate results in increased full cycle mass emission factors of 66, 2.7, 2.8 and 1.3 for particulate polycyclic aromatic hydrocarbons, refractory black carbon, total organic aerosol and m/z 60 (mass to charge ratio), respectively, compared to nominal burn rate (Figure 22). At nominal burn rates, full cycle emissions based on m/z 60 correlate well with organic aerosol, refractory

black carbon and particulate matter. However, at higher burn rates, m/z 60 does not correlate with increased emissions of polycyclic aromatic hydrocarbons, refractory black carbon and organic aerosol in the flaming phase. Their new findings can be used to advance source apportionment studies, reduce emissions of genotoxic compounds and model the climate impacts of refractory black carbon, such as absorption enhancement by lensing as defined in section 3.2.

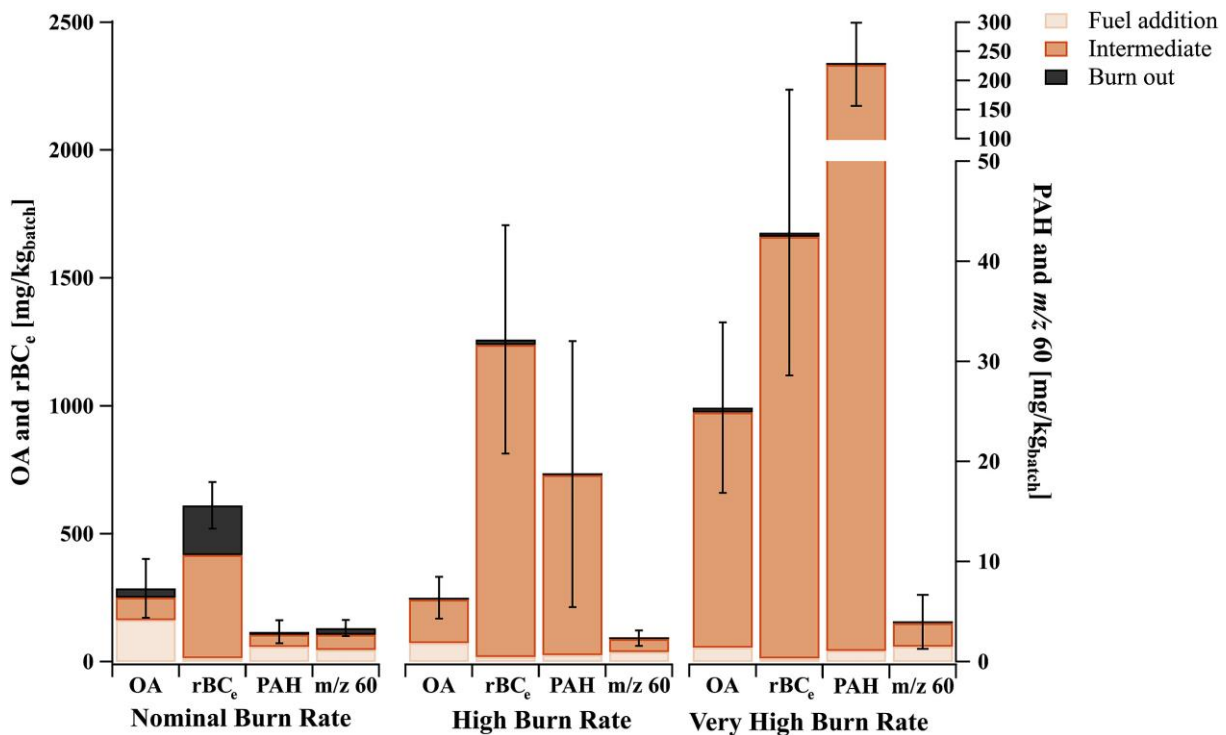


Figure 22: Full cycle emission factors of OA, rBC, PAH and m/z 60 for nominal (NB), high (HB), and very high (VHB) burn rate in $\text{mg}/\text{kg}_{\text{batch fuel}}$, where $\text{kg}_{\text{batch fuel}}$ refers to the dry weight of the whole batch. The results are based on 7, 6 and 3 cycles, respectively. The contributions to the full cycle emissions are given for the three phases: fuel addition, intermediate, and burn out. Error bars represent the variation of the full cycles and are given as the standard error of the mean (Nielsen et al., 2017)

In order to evaluate non-steady phase contribution to the total emissions of a pellet stove in real domestic operations, particulate matter and gaseous emissions (Venturini et al., 2015) determined separately for different operating conditions, *i.e.* ignition, partial load, increase in power and nominal load. TSP (Total suspended particulate) was sampled with a dilution system and characterized for TC (total carbon), PAHs (polycyclic aromatic hydrocarbons), the main soluble ions, Ni, As, Cd and Pb. Gas monitoring shows that CO and NO emission factors in ignition phase markedly differ from other operating conditions: NO emission factor is lower, while CO one is much higher, since it is a product of incomplete combustion. Start-up phase emission factors are also higher for TSP, Cd and other products of incomplete combustion, *i.e.* TC and PAHs. Despite being a non-steady phase, the increase in power phase emission factors appreciably differ from steady state ones only for PAHs. Moreover, the PAHs emitted in non-steady state phases have a higher toxicological burden. In conclusion, in order to evaluate the real impact of pellet stove on the environment, transient conditions should be taken into account. The ignition phase, even though it lasts only 20 min, can significantly contribute to pollutant emission.

(Horak et al., 2017) analysed different domestic heating boilers (automatic, over-fire, with down-draft combustion and gasification) and three types of fuel (lignite, wood and mixed fuel) were examined in 25 combustion tests and correlated with the emissions of particulate matter (PM), carbon monoxide (CO), total organic carbon (TOC) and 12 polycyclic aromatic hydrocarbons (PAHs with MW = 178-278 g mol⁻¹) focusing on particle phase. The highest emission factors of PAHs were measured for boilers of old construction, such as over-fire boiler (5.8-929 mg kg⁻¹) and boiler with down-draft combustion (3.1-54.1 mg/kg). Modern types of boilers produced much lower emissions of PAHs, in particular, automatic boiler (0.3 -3.3 mg kg⁻¹) and gasification boilers (0.2-6.7 mg kg⁻¹). In general, the inefficient combustion at reduced output of boilers generated 1.4-17.7 times more emissions of PAHs than the combustion at nominal output of boilers. They recommended to operate boilers at nominal output with sufficient air supply and to use the proper fuel to minimize PAHs emissions from domestic heating appliances.

(Toscano et al., 2014) has investigated the emission from realistic utilisation of wood pellet stove. Higher concentration of PM, up to 72% more than those measured in steady state condition, was shown in this study. A higher emission factor has been observed also for carbon monoxide (CO), total carbon (TC) and polycyclic aromatic hydrocarbons (PAHs) especially during unsteady combustion phases (*e.g.* ignition phase) which significantly affect the emission factor in particular when the pellet stove works for short time (less than 2 h). This shows that longer uses under steady combustion are encouraged to optimise the combustion.

Impacts on nanoparticles

A recent literature review identified combustion conditions that may result in increasing amounts of nanoparticles (NP) emissions (Trojanowski and Fthenakis, 2019). These are associated with the device type, its operation, and the fuel used. They often see an inverse relationship between the total PAH mass and its NP fraction. It is reported that PAH emissions could be up to 100 times higher if a stove were not operated properly, although NP production would be decreased. Also, it is reported that, if an advanced system's heating load is decreased, cordwood and automatic wood-fired boilers (pellet and chips) may have trouble modulating, causing them to cycle frequently and generate more mass PAH emissions, but lower NPs. It is a cause for concern that NPs may be undetected as by virtue of their large surface to volume ratio they adsorb larger amounts of reactive compounds and, therefore, may induce a more pronounced pro-inflammatory response than larger particles of the same compound.

A significant, and unexpected finding is that as conventional units are displaced by modern, more efficient, and “cleaner” systems, an increase in released NPs may follow. However, with more efficient boiler systems PAH levels are being decreased; causing one to argue what is more important NPs or PAHs? Particle distribution of batch-wise fired appliances (wood stoves) varied significantly during a burn cycle, while wood log and continuous fed boilers showed a fairly constant particle size distribution. These differences are likely to influence the biological effects induced by wood smoke particles and therefore it has been recommended to explore how combustion conditions influence the particle properties, their possible health risks, and reactivity within the environment.

Although a lot of work has been done to understand the health effects associated with RWC NPs, but little is known about the environmental fate of RWC NPs and their effect on climate. In addition, NP emission data from wood burning processes under real-world operating conditions are lacking. Several studies show results of size characterization, but morphology

and chemical composition data are limited. Predicting or studying the aggregation, agglomeration, dispersion, size, solubility, surface area, charge, and composition are all necessary parameters to better predict the environmental fate and any health concerns of biomass combustion NPs. While biomass is often considered and encouraged as a renewable energy source, it is important to not ignore consequences of poor combustion practices and NP production. Several articles have suggested pathways to reduce NPs such as emission control strategies or higher quality fuel sources. Emission control devices suggested for large biomass boilers include ESPs and condensing heat exchangers but their effectiveness in controlling NP has not been assessed.

This behaviour on fine particles is coherent with the study of (Wang et al., 2020). Both “cleaner” fuels and stoves that are designed to reduce PM_{2.5} emissions are found to be not necessarily effective in reducing ultrafine particle emissions, even increase their emissions in some cases. These findings indicate that the overlook of ultrafine particle emissions from residential solid fuel combustion can lead to potential health risk to household residents, especially to those vulnerable ones (*e.g.*, the elderly and children) who are more sensitive to indoor air pollution.

Based on experimental measurements, (Poláčik et al., 2021) formulate the following operational recommendations to reduce fine particles (FP between 17 nm and 544 nm). To reduce the production of fine particles during biomass combustion, the surface temperature of the combustion chamber walls must be above 300 °C. Also, during the ignition of fuel in a heated chamber, there is a significantly lower production of fine particles compared to a cold start. That leads to boiler power modulation being preferred to cyclic boiler switching-off and ignition. In general, automatic boilers produce a lower nominal emission of FP compared to manual stoves. The results achieved are summarized by the expression of the nominal FP emission presenting the number and mass emission corresponding to burning 1 kg of fuel. The tested automatic boiler fed by spruce pellets produced a nominal FP emission of 173 mg kg⁻¹ during the testing operation cycle. The tested manual stove, fed by beech logs, produced a nominal emission of 1043 mg kg⁻¹ in the same size range of particles during the similar testing cycle.

In (Ozgen et al., 2017), two common types of wood (beech and fir) were burned in commercial pellet (11.1 kW) and wood (8.2 kW) stoves following a combustion cycle simulating the behaviour of a real-world user (Figure 23). Ultrafine particulate matter (UFP, diameter < 100 nm) was sampled with three parallel multistage impactors and analysed for metals, main water-soluble ions, anhydrosugars, total carbon, and PAH content. The measurement of the number concentration and size distribution was also performed by a fourth multistage impactor. UFP mass emission factors averaged to 424 mg kg_{fuel}⁻¹ for all the tested stove and wood type (fir, beech) combinations except for beech log burning in the wood stove (838 mg kg_{fuel}⁻¹). Compositional differences were observed for pellets and wood UFP samples, where high TC levels characterize the wood log combustion and potassium salts are dominant in every pellet sample. Crucial aspects determining the UFP composition in the wood stove experiments are critical situations in terms of available oxygen (a lack or an excess of combustion air) and high temperatures. Whereas for the automatically controlled pellets stove local situations (*e.g.*, hindered air-fuel mixing due to heaps of pellets on the burner pot) determine the emission levels and composition. Wood samples contain more potentially carcinogenic PAHs with respect to pellets samples. Some diagnostic ratios related to PAH isomers and anhydrosugars compiled from experimental UFP data in the present study and compared to literature values proposed for the emission source discrimination for atmospheric aerosol, extend the evaluation usually limited to higher particle size fractions also to UFP.

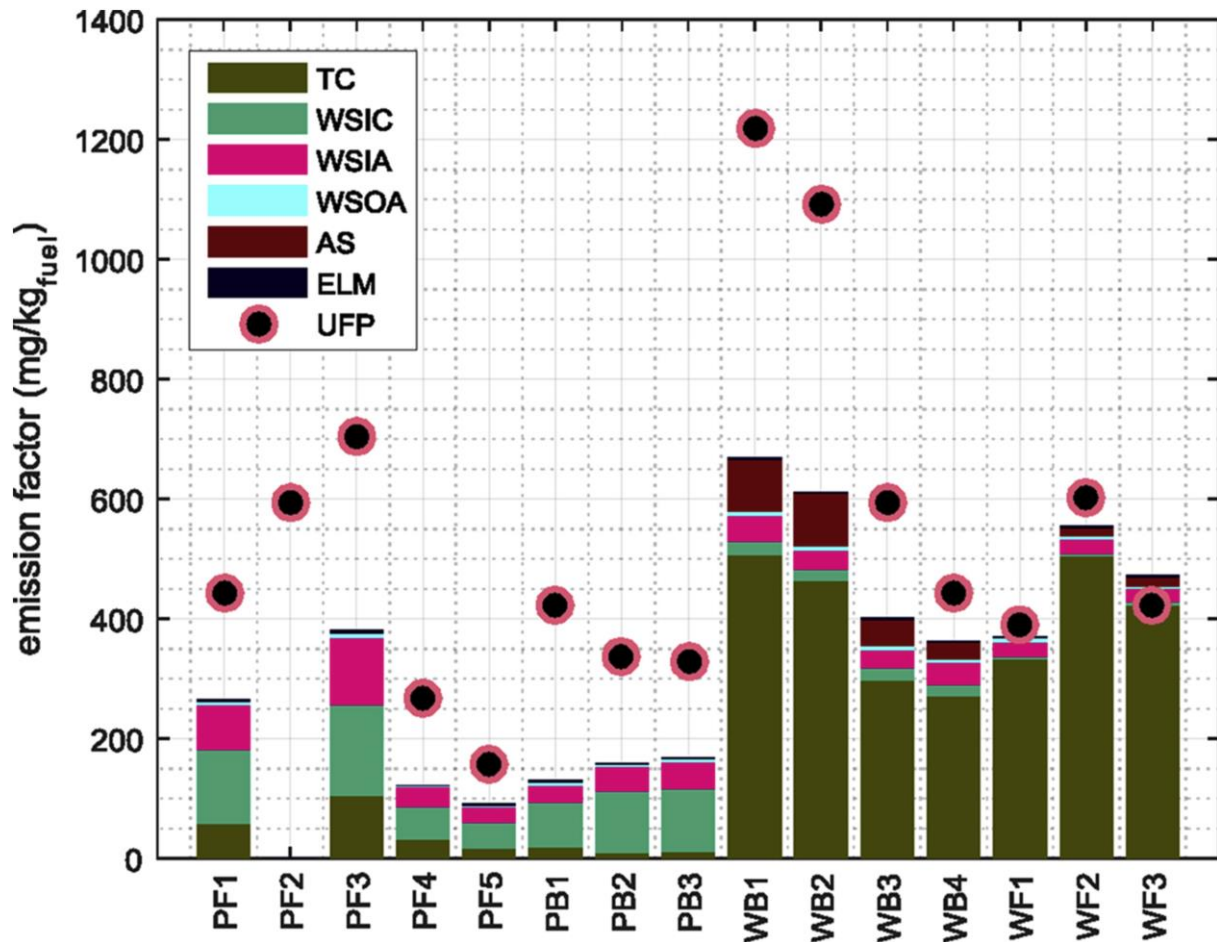


Figure 23: UFP species emission factors ($\text{mg kg}_{\text{fuel}}^{-1}$). (PF: pellet stove – fir pellets PB: pellet stove – beech pellets; WF: wood stove – fir firewood; WB: wood stove – beech firewood) (Ozgen et al., 2017)

The study of (Bertrand et al., 2017), using an atmospheric smog chamber, aimed at understanding the chemical nature and quantify the emission factors of the primary organic aerosols (POA) from three types of appliances for residential heating, and to assess the influence of aging thereon. Two, old and modern, logwood stoves and one pellet burner were operated under typical conditions. Emissions from an entire burning cycle (past the start-up operation) were injected, including the smoldering and flaming phases, resulting in highly variable emission factors. The stoves emitted a significant fraction of POA (up to 80%) and black carbon. After ageing, the total mass concentration of organic aerosol (OA) increased on average by a factor of 5. For the pellet stove, flaming conditions were maintained throughout the combustion. The aerosol was dominated by black carbon (over 90% of the primary emission) and amounted to the same quantity of primary aerosol emitted by the old logwood stove. However, after ageing, the OA mass was increased by a factor of 1.7 only, thus rendering OA emissions by the pellet stove almost negligible compared to the other two stoves tested. Therefore, the pellet stove was the most reliable and least polluting appliance out of the three stoves tested (Figure 24) in terms of total carbonaceous species.

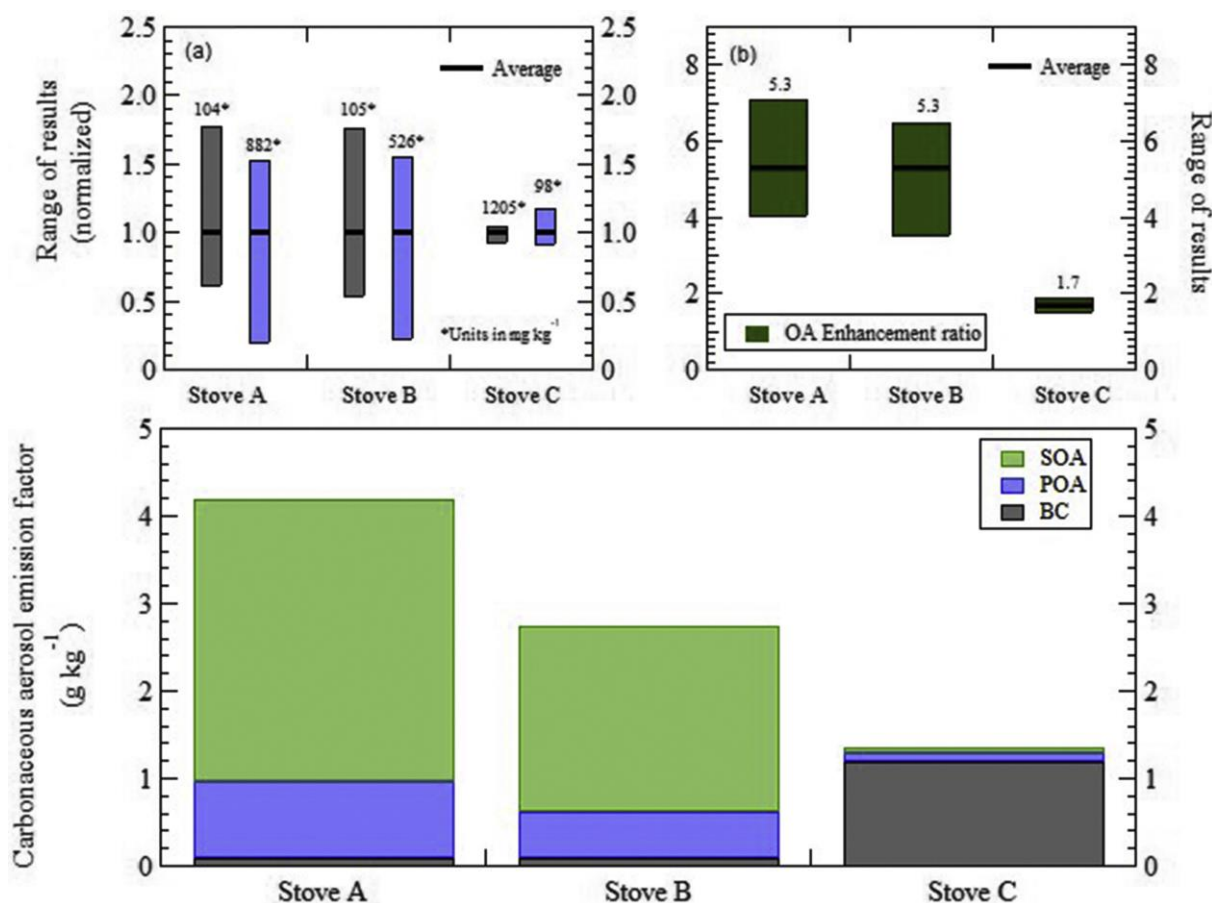


Figure 24: Primary and secondary aerosol emission factors of carbonaceous aerosol calculated for three types of stove (averaged over the replicates). The emission factors for the secondary emissions were determined at OH exposure = 5×10^6 molecules cm^{-3} hour. The top panels illustrate the variability within the results. On graph (a), the box encompasses the minimum and maximum values of POA and BC EF normalized to that of the average. The average value is indicated in the bolted line in the middle of the box. The actual value is noted on top. On graph (b) the box encompasses the minimum and maximum OA enhancement ratio (dark green). Stove A is a wood stove from before 2002, stove B is a wood stove from 2010, and stove C is an automated pellet stove from 2010 – from (Bertrand et al., 2017).

4.1.4 Innovative solutions to reduce PM

Laboratory studies of wood-burning cookstoves demonstrate that secondary air injection can greatly reduce the emission of harmful air pollution, but these experimental advancements are not easily translated into practical cookstove designs that can be widely adopted. (Caubel et al., 2020) use a modular cookstove platform to experimentally quantify the practical secondary air injection design requirements (*e.g.*, flow rate, pressure, and temperature) to reduce mass emissions of particulate matter (PM), carbon monoxide (CO), and black carbon (BC) by at least 90% relative to a traditional cooking fire (Caubel et al., 2018). Over the course of 111 experimental trials, they illuminate the physical mechanisms that drive emission reductions, and outline fundamental design principles to optimize existing cookstove performance.

Using the experimental data, they demonstrate that low-cost (<10\$) fans and blowers are available to drive the secondary flow and can be independently powered using an inexpensive thermoelectric generator mounted nearby. This system can be plugged on an existing installation. Furthermore, size-resolved PM measurements show that secondary air injection

inhibits particle growth, but the total number of particles generated remains relatively unaffected (not shown in the table).

Table 8: Mean performance and emissions metrics for a three stone fire (TSF) and the modular 431 stove (MOD), and the percent change of each metric from TSF to MOD from (Caubel et al., 2018)

	TSF	MOD	Change (%)
<i>Firepower (kW)</i>	5.3 ± 0.4	4.93 ± 0.06	-7 ± 8
<i>Thermal efficiency (%)</i>	23.3 ± 0.7	26.2 ± 0.4	12 ± 3
<i>CO (g kWd⁻¹)</i>	17 ± 3	2.1 ± 0.2	-88 ± 2
<i>PM2.5 (mg kWd⁻¹)</i>	1200 ± 200	130 ± 10	-89 ± 2
<i>BC (mg kWd⁻¹)</i>	530 ± 50	35 ± 3	-93 ± 1
<i>BC/PM2.5 (%)</i>	44 ± 8	27 ± 3	-40 ± 7

(Carvalho et al., 2018) studied the improvement of the performance of a wood stove (natural draft) traditionally used in Portugal (WSref) by the adoption of alternative combustion air retrofits (WSM). The reduction on the average OGCs emission factor from 241 mg Nm⁻³ (WSref.) to levels below 139 mg Nm⁻³, achieving values close (WSMC2) or even below (WSMC1) the Ecodesign requirement for organic gaseous compounds (120 mg Nm⁻³) after the retrofitting intervention (Figure 25).

- The reduction on the average CO emission factor from 4613 mg Nm⁻³ (WSref.) to 2808 mg Nm⁻³ (WSMC2), the latter value being in the same order of magnitude to that determined for marketed wood stoves used in Northern European countries, and a value closer to the Ecodesign requirement (1500 mg Nm⁻³) after the retrofitting intervention.
- The average PM2.5 emission factor was reduced from 8.9 g kg_{Fuel}⁻¹ (WSref.) to 6.9 kg_{Fuel}⁻¹ (WSMC1), being the latter value closer to the Ecodesign emission threshold (5 kg_{Fuel}⁻¹) than that determined in the reference test condition (WSref.).
- Significant reductions in the total annual emissions from residential wood combustion per retrofitted household associated with the 38% reduction of the wood fuel utilization in dwellings. Beyond the improvements described above, their research recommends that further efforts should be focused on reducing the CO and PM2.5 emission factors of wood stove installations already existing in Southern European dwellings, preferably to levels below the Ecodesign emission requirements for new stoves sold in the European market by 2022.

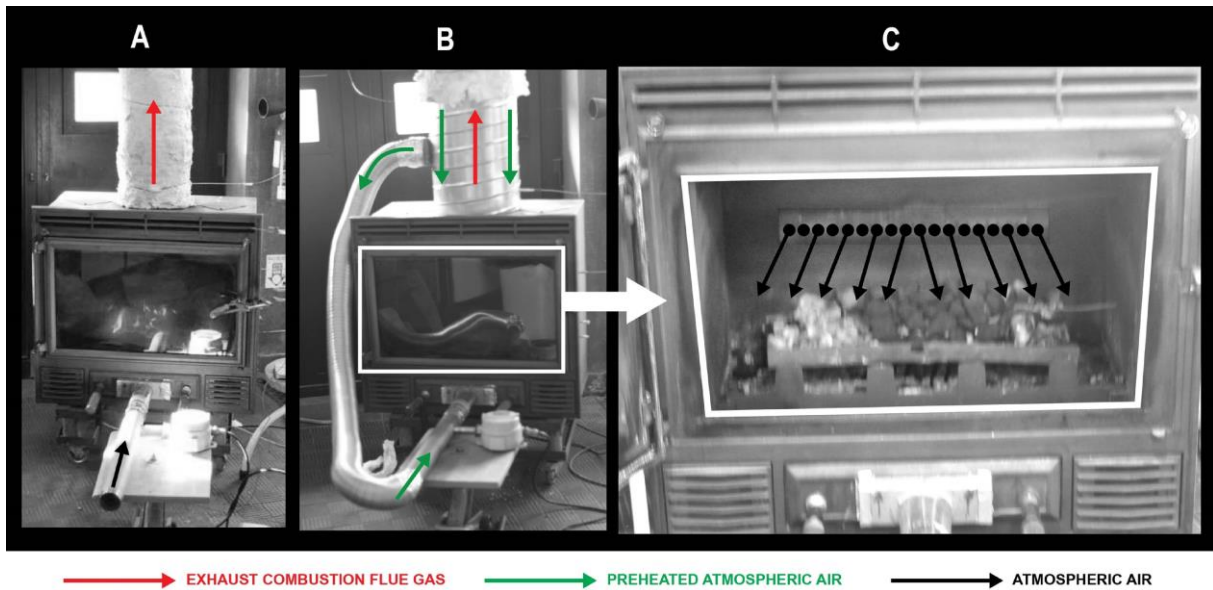


Figure 25: Wood stove and the retrofitting interventions: A – Wood stove as sold in the market (WSref); B – Wood stove with annular chimney (WSMC1); C – Combustion chamber of the wood stove with component of secondary air-inlets (18 nozzles) (WSMC2) (Carvalho et al., 2018)

The two retrofits enhanced a more stable heat release from the wood stove, which reached a thermal efficiency 11% lower than that achieved by the pellet stove. This research suggests that retrofitting stoves with chimney components that allow the admission of combustion air can substantially increase energy savings in dwellings. Further efforts should focus on improving the interplay between the outdoor air and secondary air admission to achieve higher emission reductions at low-cost.

BC emissions ranges from 28 to 134 mg Nm⁻³ in this study. When dry birch wood was used, average BC and EC concentrations were 72 and 73 mg Nm⁻³, respectively, with 3–6-fold differences between the lowest and highest emission stove. In the case where the secondary air is supplied and it takes part in the combustion process, the emissions are low. If the secondary air does not react, it cools the combustion process and increases emissions as seemed to be the case. This result on the effect on dryness must be modulated since it is commonly observed that above 25% humidity, the emission of TSP increase (PRIMEQUAL, 2018).

PAH concentrations and the PAH portion of PM1 have a clear connection and it seems that when PM1 is high, also PAH emission is high. In the range higher than 1000 mg Nm⁻³, the portion of PAH of PM1 is drastically increased.

The particle number concentration did not correspond with the completeness of combustion. On the contrary, the lowest number concentrations were found when the PM1, BC, and PAH concentrations were the highest. A possible explanation for this is that at high emission concentrations the prevailing high soot particle concentrations in the flue gas provide surface area for condensation of volatile ash species which in turn decreases nucleation of new ash particles in the cooling flue gas, which has been earlier suggested as the main mechanism responsible for the particle number emission (Sippula et al., 2007; Tissari et al., 2007).

4.1.5 Impact of wood type and quality on emissions

Next to purely technological reasons (*i.e.* type and age of appliance) and installation conditions (*i.e.* natural draft of chimney system), user behaviour which includes all influences caused by the user during operation has a considerable effect on the combustion performance of room heating appliances. User behaviour includes fuel related factors, different ways to ignite the fire, combustion air settings, as well as frequency and intensity of use. The objective of this work is to investigate user behaviour by means of a survey. The survey (Wöhler et al., 2016) aims to provide an overview as to how room heating appliances in European countries are used in real life. They performed a 28 question, multi-lingual online survey over a 14-week period. 1980 responses from 16 European countries (Figure 26 and Table 9) were received. Most respondents are from Italy (35%), Germany (34%), Austria (12%) and Sweden (11%).

Table 9: Used fuel types of one-fuel type users from (Wöhler et al., 2016)

Type of fuel	All countries	Italy (%)	Germany (%)	Sweden (%)	Austria (%)
Firewood from hardwood (HW)	90	88	89	97	90
Firewood from softwood (SW)	5	5	7	2	4
Wood briquette (WB)	2	0	2	0	4
Wood pellets (WP)	1	0	0	0	4
Waste wood (WW)	1	1	1	0	1
Other biomass (OB)	2	5	0	0	0

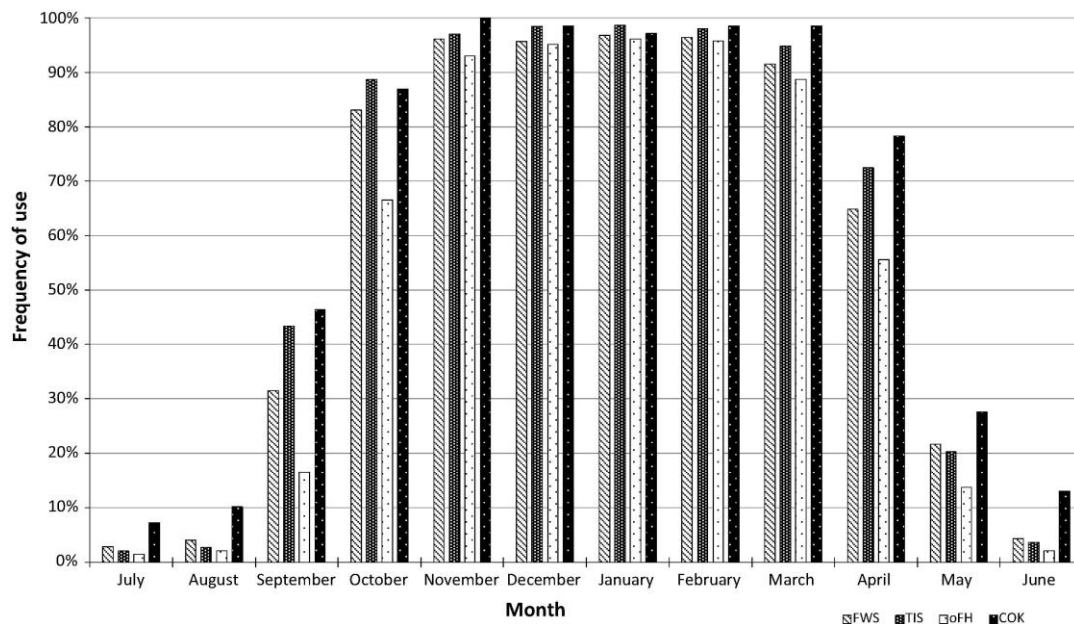


Figure 26: Monthly frequency of heater usage from (Wöhler et al., 2016)- : firewood stoves (FWS), tiled stoves (TIS), cookers (COK) and other firewood operated room heaters (oFH)

A literature review is proposed in the frame of the AIRUSE project (Querol et al., 2016) concerning the role wood types on PM and BC emissions. The EFs for the main particulate pollutants are reported in Table 10, Table 11 and Table 12. Maritime Pine exhibits the highest

EF of elemental carbon while the PM2.5 EF is not necessary the highest. Holm oaks usually produce the lowest EC emissions.

Table 10: Emission factors in mg MJ⁻¹ from traditional appliances (fireplace versus woodstove) from (Querol et al., 2016) with the following references: [1] (Gonçalves et al., 2011), [2] (Martins, 2012), [3] (Duarte, 2011), [4] (Vicente, 2013). Note: Calorific value 18.5 MJ kg⁻¹

	Fuel	PM2.5	PM10	OC	EC
Fireplace	Maritime Pine	372.97	-	156.76	33.51
	Golden Wattle	421.62	-	189.19	18.38
	Holm Oak	702.70	-	389.19	16.22
	[1] Eucalyptus	648.65	-	275.68	19.46
	Olive	1135.14	-	491.89	21.08
	Cork Oak	972.97	-	540.54	36.76
	Portuguese Oak	756.76	-	329.73	17.30
	Briquettes/Pellets	648.65	-	318.92	15.68
	European Beech	311.89	-	210.81	23.24
	[2] Pyrenean Oak	675.68	-	487.57	32.43
	Black Poplar	757.30	-	568.11	42.70
	Maritime Pine	-	722.42	431.88	81.86
	[3] Eucalyptus	-	1093.70	630.05	20.88
	Cork Oak	-	744.86	450.14	32.45
	Wood stove	Maritime Pine	281.08	-	135.14
Golden Wattle		427.03	-	221.62	15.68
Holm Oak		313.51	-	162.16	12.43
[1] Eucalyptus		540.54	-	281.08	20.00
Olive		470.27	-	248.65	24.86
Cork Oak		448.65	-	259.46	22.70
Portuguese Oak		702.70	-	335.14	17.30
Briquettes/Pellets		383.78	-	200.00	9.73
European Beech		149.73	-	86.49	23.24
[2] Pyrenean Oak		721.08	-	494.05	48.65
Black Poplar		236.76	-	154.59	47.57
Maritime Pine		-	256.09	107.00	89.80
[3] Eucalyptus		-	411.50	224.35	32.28
Cork Oak		-	300.73	160.53	26.80
[4] Maritime Pine		-	351.19	165.18	101.61
European Beech	-	338.19	142.95	67.29	

Table 11: Emission factors in mg MJ⁻¹ for ecolabelled wood stoves (Fernandes et al., 2011)

Fuel	PM10	OC	EC
<i>Maritime Pine</i>	60.54	15.68	23.78
<i>Golden wattle</i>	65.95	12.97	15.68
<i>Eucalyptus</i>	111.89	35.68	14.59
<i>Cork oak</i>	156.22	67.03	17.84

Table 12: Emission factors in mg MJ⁻¹ for pellet stoves (Querol et al., 2016)

Fuel	PM10	OC	EC
<i>Pellet – Type I</i>	24.55	6.82	3.61
<i>Pellet – Type II</i>	79.90	13.24	36.77
<i>Pellet – Type III</i>	94.05	7.73	7.67
<i>Pellet – Type IV</i>	69.01	14.05	20.46
<i>Olive Pit</i>	156.07	45.07	8.85
<i>Shell of Pine nuts</i>	108.28	17.29	38.13
<i>Almond Shell</i>	103.82	11.18	8.80

Results from several studies also reported in (Vicente and Alves, 2018), together with disaggregation of emissions factors by technology and fuel type, lead to quite large differences, especially between old-type residential appliances versus advanced residential energy conversion systems, such as modern woodstoves, and automatic pellet stoves and boilers with higher combustion efficiency. New technologies for biomass burning can perform far better than traditional systems, but their progress and application are advancing gradually. These systems are user-friendly presenting potential advantages, such as automatic control, and enabling a reduction in fuel consumption and emissions.

(Czech et al., 2018) have analysed emissions from a modern masonry heater fuelled with three types of common logwood (beech, birch and spruce) and a modern pellet boiler fuelled with commercial softwood pellets, which refer to representative combustion appliances in northern Europe. In particular, emphasis was put on the organic constituents of PM_{2.5}, including polycyclic aromatic hydrocarbons (PAHs), oxygenated PAHs (oPAHs) and phenolic species, by targeted and non-targeted mass spectrometric analysis techniques. As an extract in Table 13, clearly, pellets produce less carbonaceous emissions than Beech, Birch and Spruce. Slow ignition increases PAH emissions. EC emissions from spruce seems lower.

Table 13: Mean emission factors (EFs) and concentrations of some carbonaceous gaseous and particulate species from regular combustion experiments (modern masonry heater: beech, birch and spruce; pellet boiler: softwood pellets) and combustion experiments with slow ignition (modern masonry heater: spruce* and birch*). Entries of b.l.q. refer to EFs below the limit of quantification (Czech et al., 2018). IP: Indeno(1,2,3-cd)fluoranthene, BaP: Benzo(a)pyrene.

Species	Unit	Beech	Birch	Spruce	Pellet	Spruce*	Birch*
<i>OGC</i>		24	15.4	20.1	1.25	45	18.6
<i>OC</i>	$mg MJ^{-1}$	20	6.1	6.1	0.15	11	5.7
<i>EC</i>		27	47	13	0.27	17	34
<i>BaP</i>		0.88	0.55	0.97	0.02	5.81	7.77
<i>IP</i>	$\mu g MJ^{-1}$	0.33	0.18	0.48	b.l.q.	1.75	36
<i>Sum PAH</i>		35.3	32.4	22.2	0.9	65.8	139.3

According (Avagyan et al., 2016), pine burning in high burn rate had largest impact on particulate OH-PAH (hydroxy-PAH) emissions. OH-PAH nominal burn rate emissions correspond to 15% of high burn rate emissions. Emissions of OH-PAHs correspond on average to 32% of PAH emissions (Figure 27).

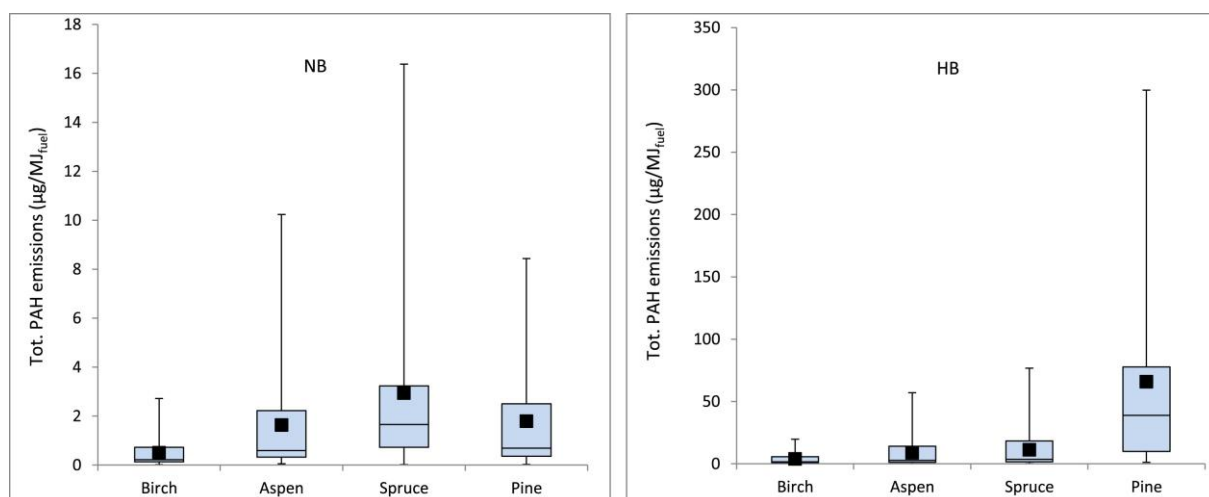


Figure 27: Box and whisker plots showing the total OH-PAH emissions ($\mu g/MJ_{fuel}$) from NB (Nominal Burn) and HB (High Burn) samples for different wood types (the bottom and the top of the box plot are the first and the third quartiles, the band is the second quartile (the median), the ends of the whisker are the minimum and maximum of all the data and the black square represent the average) (Avagyan et al., 2016)

The quality of wood pellet has been addressed in many studies. (Vicente et al., 2020) investigate the difference of emissions between the combustion of certified (type R and P) and uncertified pellets. The OC and EC emissions, in the range from 0.188 to 3.31 $mg MJ^{-1}$ and from 2.22 to 14.9 $mg MJ^{-1}$, respectively, were affected by both operating conditions of the stove and pellet type burned. The importance of fuel quality on carbonaceous emissions has been also highlighted in previous studies. (Vicente et al., 2015) reported OC EFs ranging from 7.40 ± 1.86 (wood pellets) to 48.7 ± 30.9 (agro fuels) $mg MJ^{-1}$, whereas the EC EFs ranged from 1.77 ± 0.44 (wood pellets) to 54.5 ± 23.5 (agro fuels) $mg MJ^{-1}$. More recently, the combustion of laboratory made acacia pellets under partial load conditions generated EFs of 22.9 ± 9.28 mg

MJ⁻¹ and 6.82 ± 2.47 mg MJ⁻¹ for OC and EC, respectively (Vicente et al., 2019). The carbonaceous emissions obtained in the present study for certified pellets are comparable with those reported by (Orasche et al., 2013, 2012) and (Schmidl et al., 2011) for the combustion of certified pellets in small scale stoves.

Generally, certified pellets P performed better than the other two pellet types. While the combustion of certified pellets R generated the highest CO and TOC emissions, noncertified pellets yielded the highest NO emissions and, under nominal load operation, NH₃ and carbonaceous compounds bound to PM. **In fact, both pellets generated PM emissions surpassing the thresholds set by the Ecodesign directive. Despite the high emissions, the highest power output and lowest excess of air were observed for the combustion of non-certified pellets.** On the other hand, the lowest temperatures in the combustion chamber were recorded for certified pellets R. Considering the distinct behaviour recorded for each fuel under different loads, it is not possible to point out the optimal operation condition. The pellet stove employed in this study, like most in-use stoves across Europe, was not equipped with a complete control system to measure the fuel supply into the combustion chamber, temperature or flue gas oxygen.

(Stewart et al., 2020) present new I/SVOCs emission factors from biomass burning (Figure 28) used by household in developing countries. This study found that phenolic and furanic species, two important classes of species for the SOA formation, were the most important gas-phase emissions by mass of I/SVOCs from biomass burning. New emission factors were developed for US EPA criteria PAHs present in gas and aerosol phases from a large range of fuel types. This suggested that many sources important to air quality in the developing world are larger sources of PAHs than conventional fuel wood burning (Stewart et al., 2020).

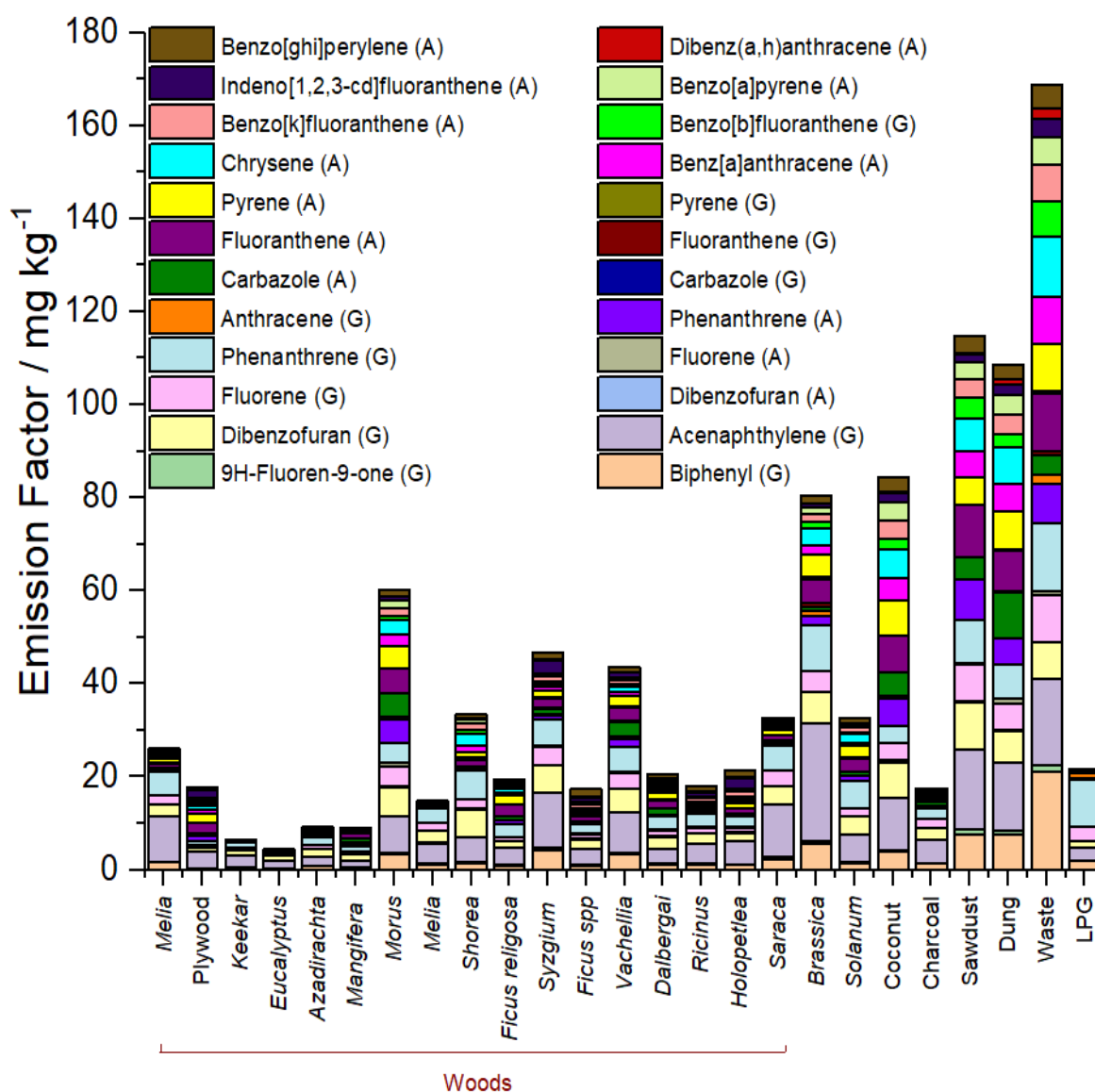


Figure 28: Emission factors of PAHs measured from SPE/PTFE (Teflon/Solid Phase Extraction) where (G) and (A) represent gas- and aerosol-phase samples, respectively, excluding naphthalene as well as naphthalenes with C1 and C2 substituents (Stewart et al., 2020)

The research from (Koniecznyński et al., 2017) was to assess the content and composition of the pollutants emitted by domestic central heating (CH) boilers equipped with an automatic underfeed fuel delivery system for the combustion chamber. It concerned fuel properties, flue gas parameters, contents of dust (fly ash) and gaseous substances polluting the air in the flue gases emitted from a domestic CH boiler burning bituminous coal, pellets from coniferous wood, cereal straw, miscanthus, and sunflower husks, coniferous tree bark, and oats and barley grain. The emission factors for dust and gaseous air pollutants were established as they are helpful to assess the contribution of such boilers in the atmospheric air pollution. When assessing the researched boiler, it was found out that despite the development in design and construction, flue gases contained fly ash with a significant EC content, which affected the air quality. The fly ash emitted from the domestic CH boiler contains large contents of the C carbon. The TC content in the fly ash from bituminous coal is approx. 460 mg/g with the dominant EC percentage (72% of the mass). High content of TC occurred also in the fly ash from the oats grain combustion (approx. 520 mg/g), with the dominant OC percentage (98% of

the mass). It was observed that the OC and EC percentage was similar in the fly ash from pellets made from straw, sunflower and miscanthus, coniferous tree bark and barley grains (Table 14).

Table 14: Contents and percentae of the C forms in the emitted fly ash from (Koniecznyński et al., 2017) – ND stands for “no data”. *CFB as for circulating fluidized bed boiler

Boiler	Fuel	OC		EC		TC
		mg g ⁻¹	%	mg g ⁻¹	%	mg g ⁻¹
Pulverised coal, 200 MW		47.83	66.81	23.35	33.19	71.17
Mechanical grate, water, 29MW		25.52	23.54	82.92	76.46	108.45
CFB*, 295 MW	Bituminous coal	22.76	69.30	10.08	30.70	32.85
Mechanical grate, steam, max. continuous rating: 9.7 kg/s		8.46	9.23	83.20	90.77	91.66
Tested domestic central heating boiler	Bituminous coal	124.18	27.90	334.14	72.10	458.32
	Pellets from coniferous wood	ND	79.36	ND	20.64	ND
	Pellets from cereal straw	43.94	48.55	46.57	51.45	90.51
	Pellets from miscanthus	112.80	51.15	107.73	48.85	220.53
	Pellets from sunflower hulls	28.04	46.01	32.90	53.99	60.93
	Coniferous tree bark	112.56	57.66	82.67	42.34	195.24
	Oats grains	509.32	98.35	8.53	1.65	517.84
	Barley grains	22.20	56.07	17.39	43.93	39.59

Case of sauna stoves

Sauna Stoves (SS) are simple wood combustion appliances used mainly in Nordic countries. They generate emissions that have an impact on air quality and climate. In (Tissari et al., 2019), a new measurement concept for comparing the operation, thermal efficiency, and real-life fine particle and gaseous emissions of SS was utilised. In addition, a novel, simple, and universal emission calculation procedure for the determination of nominal emission factors was developed for which the equations are presented for the first time. Fine particle and gaseous concentrations from 10 different types of SS were investigated. It was found that each SS model was an individual in relation to stove performance: stove heating time, air-to-fuel ratio, thermal efficiency, and emissions. Nine-fold differences in fine particle mass (PM1) concentrations, and about **90-fold differences in concentrations of polycyclic aromatic hydrocarbons (PAH) were found between the SS, when dry (11% moisture content) birch wood was used. By using moist (18%) wood, particle number and carbon monoxide concentrations increased, but interestingly, PM1, PAH, and black carbon (BC) concentrations clearly decreased**, when comparing to dry wood. *E.g.*, PAH concentrations were 5.5–9.6 times higher with dry wood than with moist wood. Between wood species, 2–3-fold maximum differences in the emissions were found, whereas about 1.5-fold differences were observed between bark-containing and debarked wood logs. On average, the emissions measured in this study were considerably lower than in previous studies and emission inventories. This suggests that overall, the designs of sauna stoves available on the market have improved during the 2010s. The

findings of this study were used to update the calculation scheme behind the inventories, causing the estimates for total PM emissions from SS in Finland to decrease.

4.1.6 Electrostatic precipitators (ESP)

An electrostatic precipitator (ESP) is an air pollution control device designed to trap and remove dust particles from the exhaust gas stream of an industrial process. ESPs operate by first electrostatically charging the dust particles in the incoming gas stream. The charged particles are then attracted to and deposited on plates or other collection devices. When enough dust has accumulated on to the collectors, they are shaken to dislodge the dust, causing the particulate matter to fall with the force of gravity to hoppers below the unit. The dust is then removed by a conveyor system for disposal or recycling (Cheremisinoff, 2016). Wood biomass burning systems equipped with ESP to generate district heat and power in communities have been investigated to study the efficiency of ESP (Ghafghazi et al., 2011). ESP efficiencies have slightly lower efficiencies compare to fabric filters but are more adapted to cyclone technologies more useful to tackle coarser particles (Figure 29).

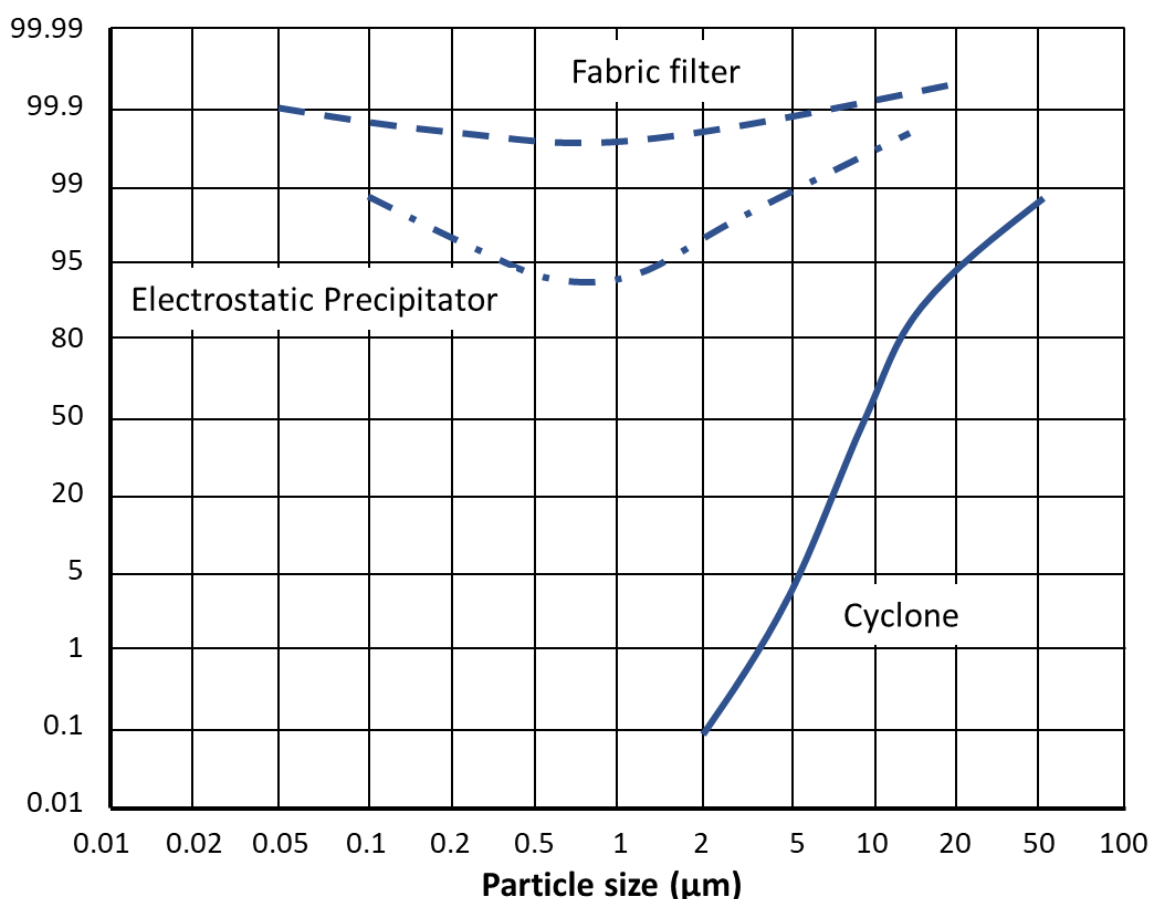


Figure 29: Efficiencies in % of ESP as a function of particle size compared to other secondary techniques inspired from (Ghafghazi et al., 2011)

These separators are often based on a design which is simplified compared to industrial applications for cost reasons. In some cases, high separation efficiencies of up to more than 90% were reported in (Nussbaumer, 2010a), while for other applications, moderate separation efficiencies in the order of only 50% are expected. In addition, the reduction potential in practice especially for soot and condensable organic compounds is uncertain for most applications and hence further experiences supposed to be improved.

(Bäfver et al., 2012) investigated the impact of an ESP on a small combustion wood pellet boiler emission (3-23 kW). In Figure 30, the masses sampled on filters are presented with the contents of organic carbon (OC) and elemental carbon (EC). At efficient (“Favourable”) combustion OC was 1-2 % and EC 13-15 % of the particles upstream of the ESP. Downstream of the ESP, OC constituted about 50 % of particulate mass, implying that the amount of particulate OC in the flue gas had increased over the ESP. This indicates formation of some particulate organic material (POM) in the ESP, possibly as a consequence of the falling gas temperature in the ESP from about 77°C to about 30°C. The temperature drop is caused by introduction of air into the ESP. The drop in temperature can cause condensation of semi volatile organic compounds. The removal efficiency for EC was found to be 89%. At poor combustion, carbonaceous compounds formed the major fraction of the particles both upstream and downstream of the ESP. In the poor combustion cases of this study, the removal efficiencies of OC were rather high: 92-96%. Simultaneously, the removal efficiencies of EC were 89% and 95%. The high removal efficiency for particulate organic compounds in poor combustion is likely due to a higher degree of condensation of organic vapours on particles upstream the ESP, caused by lower flue gas temperatures and higher concentrations of organic compounds compared to efficient combustion. These efficiencies on PM compounds are in line with results from (Omara et al., 2010) who found up to 98% efficiencies on particulate matter emissions.

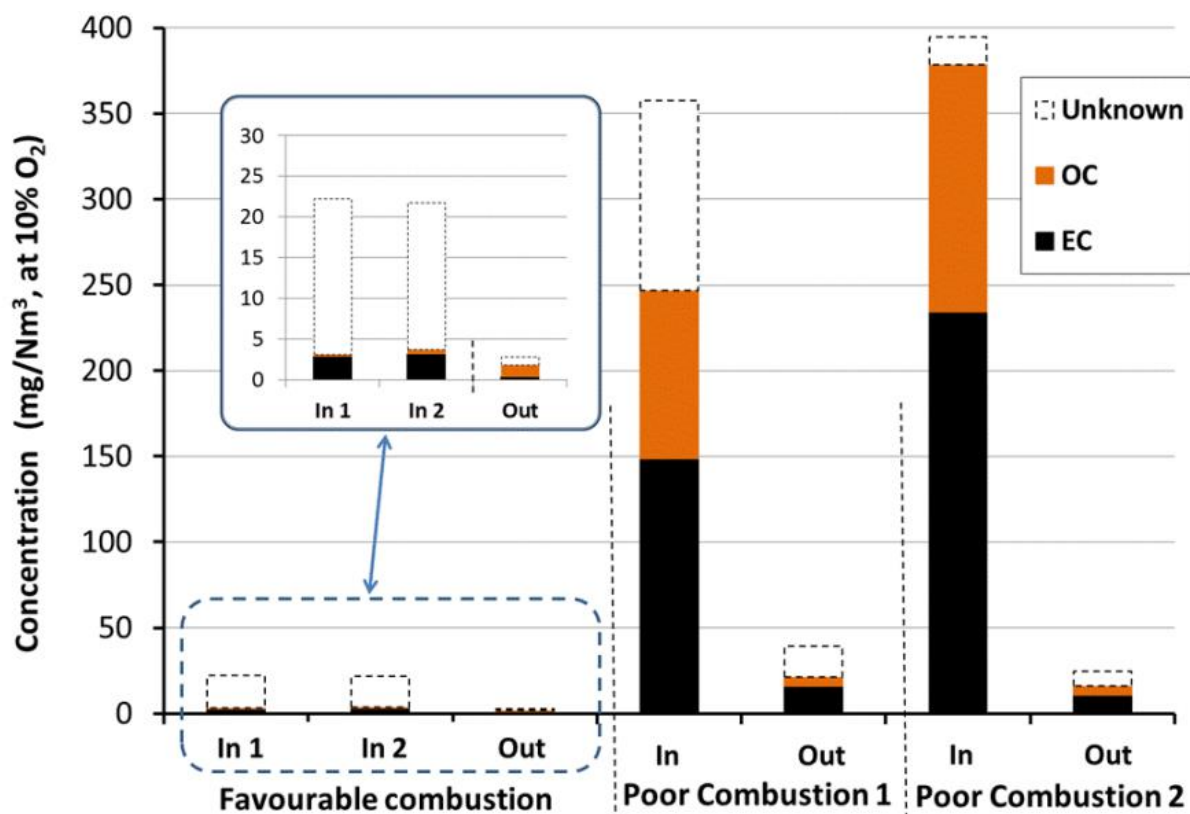


Figure 30: Concentration of particulate EC, OC, and unknown material. In. = Upstream ESP. Out. = Downstream ESP (Bäfver et al., 2012)

(Li et al., 2019) showed that the flue gas temperature upstream of the “low temperature”-ESP had significant effects on the removal of filterable and condensable PM. The removal efficiencies for filterable and condensable PM increased with decreasing inlet flue gas temperature.

(Mertens et al., 2020) for the first present the results of on-line measurements of residual nanoparticle numbers downstream of the flue gas treatment systems of a wide variety of medium- and large-scale industrial installations (Figure 31). EU's Best Available Technology documents (BAT) show removal efficiencies of Electrostatic Precipitator (ESP) and bag filter dedusting systems exceeding 99% when expressed in terms of weight. Their efficiency decreases slightly for particles smaller than 1 μm but when expressed in terms of weight, still exceeds 99% for bag filters and 96% for ESP. This study reveals that in terms of particle numbers, residual nanoparticles (NP) leaving the dedusting systems dominate by several orders of magnitude. In terms of weight, all installations respect their emission limit values and the contribution of NP to weight concentrations is negligible, despite their dominance in terms of numbers. Current World Health Organisation regulations are expressed in terms of PM_{2.5} wt concentrations and therefore do not reflect the presence or absence of a high number of NP. This study suggests that research is still needed on possible additional guidelines related to NP given their possible toxicity and high potential to easily enter the blood stream when inhaled by humans. This kind of results are in line and even better with previous work showing ESP efficiencies using a commercial 20kW wood pellet burner. The removal efficiency was measured to be 80% for submicron particles (Yan, 2009). Moreover, soot reveals high conductivity thus enabling high precipitation efficiency but severe re-entrainment of agglomerated particles according (Nussbaumer, 2016, 2010b). (IEA Bioenergy, 2011) analysed numerous ESP technologies and showed that efficiencies could range from 50 to 80% for dust removal.

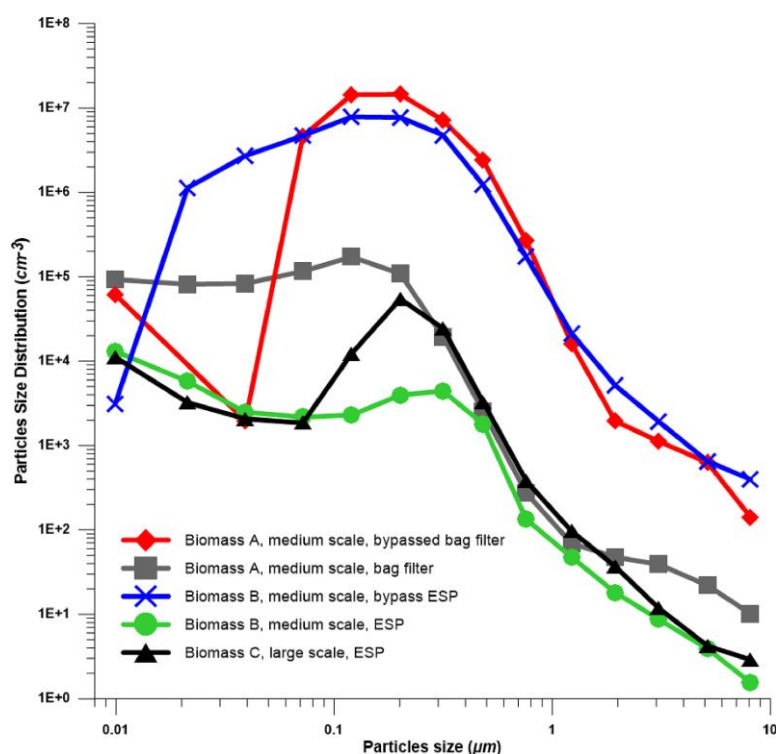


Figure 31: Comparison of the measured particle size distributions at all three biomass fired power plants equipped with ESP (ESP: ElectroStatic Precipitator) from (Mertens et al., 2020)

4.1.7 Catalyst combustors

The study carried out by (Wöhler et al., 2017) was to evaluate the performance of three emission control systems to be applied in firewood stoves which were a foam ceramic element, a catalytic active coated foam ceramic element, and a honeycomb catalyst (Figure 32). Combustion tests with these devices and dummies under real life operation conditions were conducted which

included starting phases and stove operation in nominal and partial load. Particulate and gaseous emissions were measured, and emission conversion rates were calculated. Results showed no significant emission reduction rates for the foam ceramic element. The catalytic active coated foam ceramic element reduced the emissions considerably in nominal and partial load operation up to 32% for carbon monoxide, 61% for organic gaseous carbon, and up to 41% for particulate matter. However, emission reduction rates were rather low in the starting phase. The honeycomb catalyst showed the highest emission reduction potential of all systems in the study. The reduction rates were significant in all combustion phases and were up to 73% for carbon monoxide, 58% for organic gaseous carbon, and up to 33% for particulate matter.

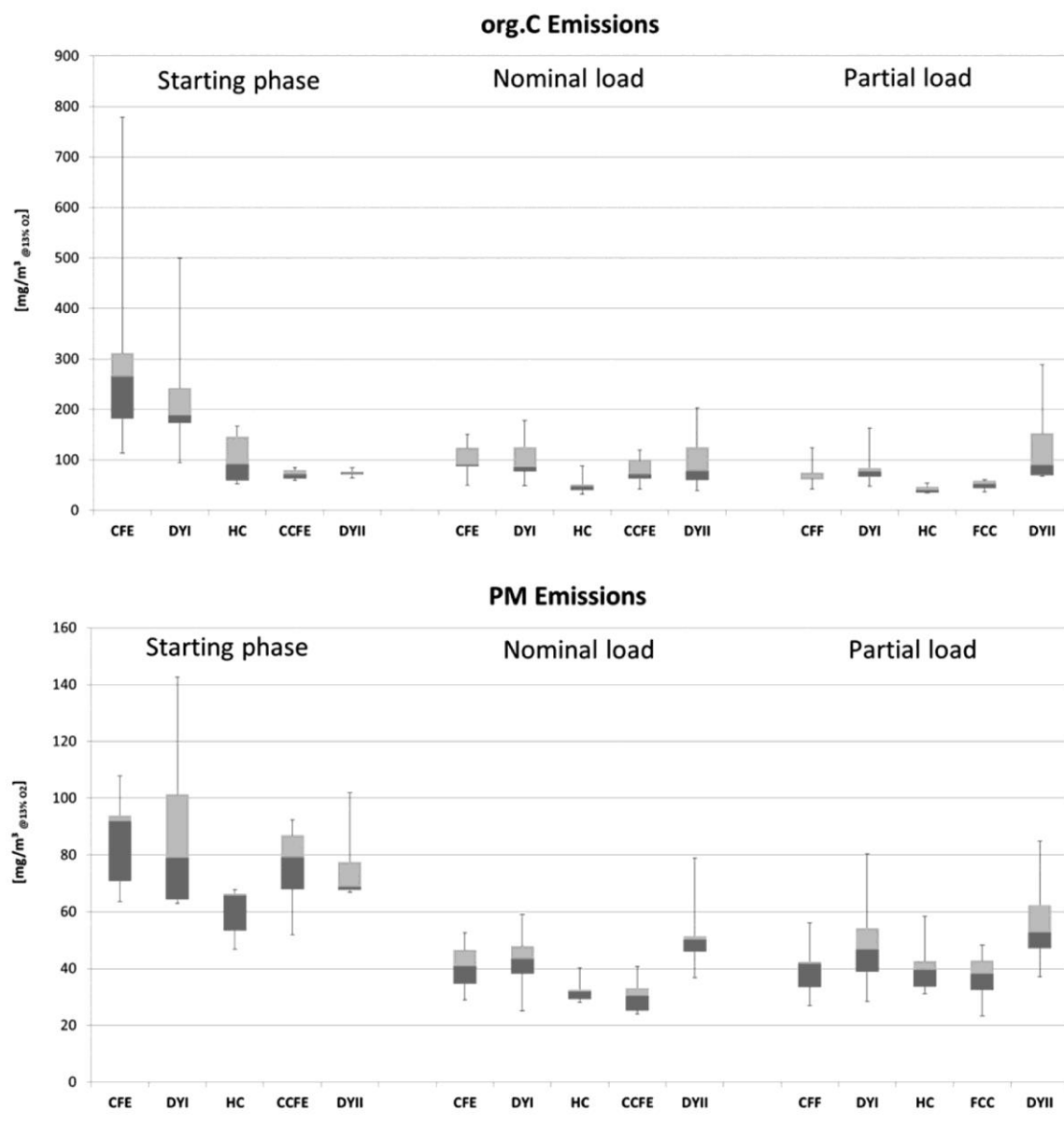


Figure 32: Result of combustion tests. Ceramic Foam Element (CFE), Catalytic Ceramic Foam Element (CCFE), Honeycomb Catalyst (HC), DYI and DYII are dummy devices (Wöhler et al., 2017)

In (Hukkanen et al., 2012), a catalytic combustor was used on a wood stove as a secondary emission reduction measure. An experimental comparison of emissions was done from combustion experiments with and without the catalyst. Samples were collected from

gasification and burn out phases and from the whole combustion cycle (from start-up to burn out). Concentrations of carbon monoxide (CO), carbon dioxide (CO₂), oxygen (O₂) and organic gaseous carbon (OGC), temperature and pressure were measured online directly from the flue gas stack. With the catalyst, the O₂ concentration in the flue gas was lower and the temperature higher than without the catalyst, due to the large amount of unburnt compounds which were oxidized by the catalyst. Reductions of 21% for CO and 14% for OGC were achieved during the whole combustion cycle. During the burn out phase, a reduction as high as 80% was achieved for CO. PM₁ (particle mass below aerodynamic size of 1 μm) was reduced by 30% during the whole combustion cycle. During gasification, a 44% reduction of PM₁ was achieved but there was no reduction during burn out. The organic and elemental carbon analysed from PM₁ had reduced also only during gasification by 56% and 37%, respectively. The particle emission reductions were notable, and it can be concluded that the catalyst affects the particles through oxidation of condensable organic vapours and oxidation of soot particles. This study shows catalyst has potential as a secondary emission reduction method but in order to achieve low emissions, also improved combustion technology for emission reduction needs to be developed.

Figure 33 shows the difference of average particle mass size distributions with and without catalyst. Clearly most of the mass is reduced between 200 nm and 1000 nm related to organic matter but the lower part of the distribution is less affected explaining why elemental carbon is less reduced than the organic matter.

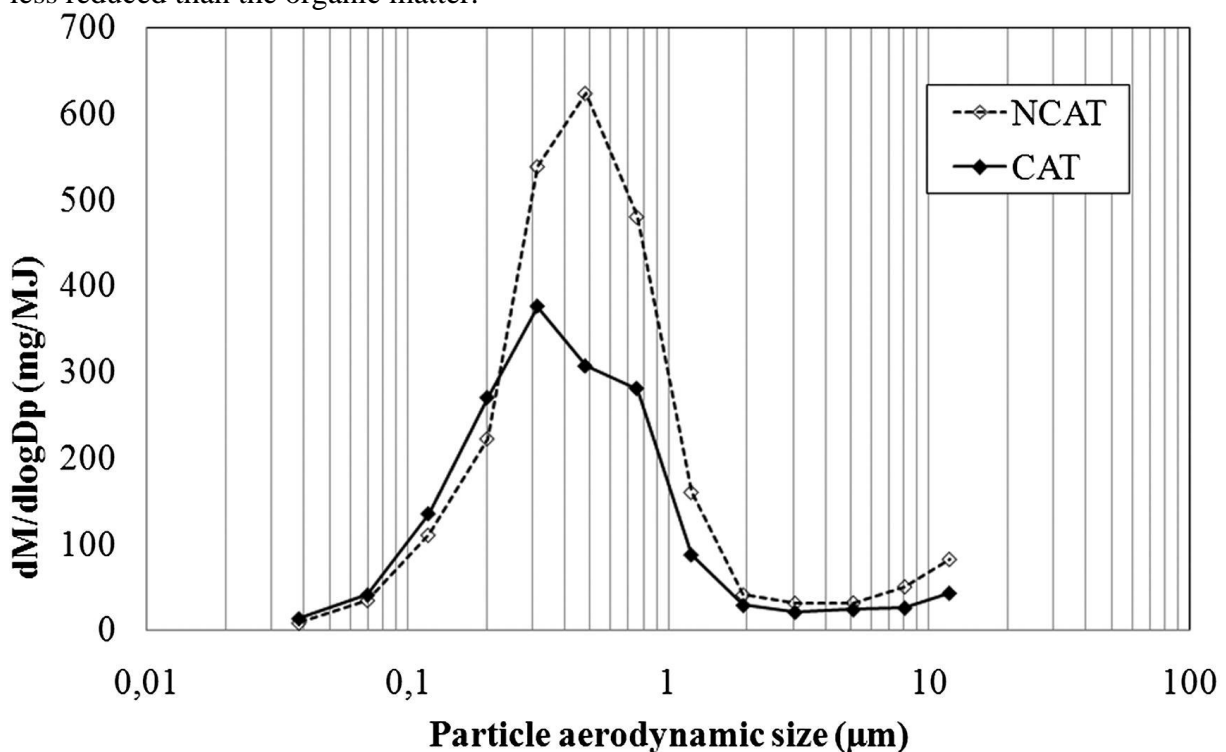


Figure 33: The average particle mass size distributions from combustions with (CAT) and without (NCAT) the catalytic combustor measured with a Dekati low pressure impactor (DLPI). Number of parallel samples in NCAT is four and in CAT is three (Hukkanen et al., 2012).

Another study pointed out the role of catalyst combustor (Figure 34) on pollutants (Kaivosoja et al., 2012). In this study birch logs were burned in a wood-fired stove (18 kW) with and without a catalytic converter with palladium and platinum as catalysts. PCDD/F, chlorophenol and PAH concentrations were analysed from three phases of combustion (ignition, pyrolysis and burnout) and from the whole combustion cycle. PCDD/F emissions without the catalytic converter were at a level previously measured for wood combustion (0.15–0.74 ng Nm⁻³). PAH

emissions without the catalytic converter were high (47–85 mg Nm⁻³) which is typical for batch combustion of wood logs. Total PAH concentrations were lower (on average 0.8-fold), and chlorophenol and PCDD/F levels were substantially higher (4.3-fold and 8.7-fold, respectively) when the catalytic converter was used. Increase in the chlorophenol and PCDD/F concentrations was most likely due to the catalytic effect of the platinum and palladium. Platinum and palladium may catalyse chlorination of PCDD/Fs via the Deacon reaction or an oxidation process.

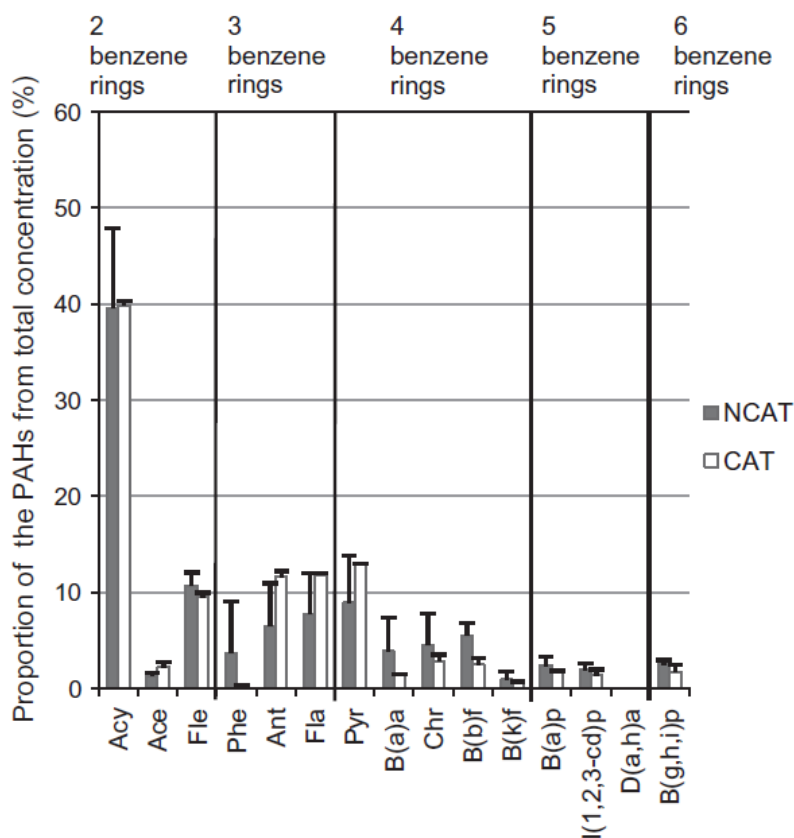


Figure 34: . Proportions of different PAH compounds in the total concentration of 14 PAHs (Kaivosoja et al., 2012)

4.1.8 Other techniques or operating conditions for larger combustion plants

Fabric filters

One of the most efficient secondary abatement emissions systems (SAES) for the particles consists of **fabric filter**. Nevertheless, this high trapping efficiency system is often bypassed due to condensation or burning issues. Small to medium-scale biomass combustion equipment are becoming an attractive non-fossil local and renewable energy means of production. Nevertheless, they remain poorly equipped with SAES because of their variable power output and subsequent condensation issues. (Brandelet et al., 2020) presents an optimization of the working temperature range for fabric filter in order to produce a cleaner energy. The present study clearly demonstrates that the dew point temperature of the smoke, for any combustion conditions and any fuels, is always higher than 70°C while the safety temperature of the fabric classically is 110 °C. Experimentations show condensation issues occur only during power change. The simulation of the optimization on the temperature range shows that the Total

Suspended Particles emissions can be reduced by 55% (mass fractions) for the same energy production (Figure 35).

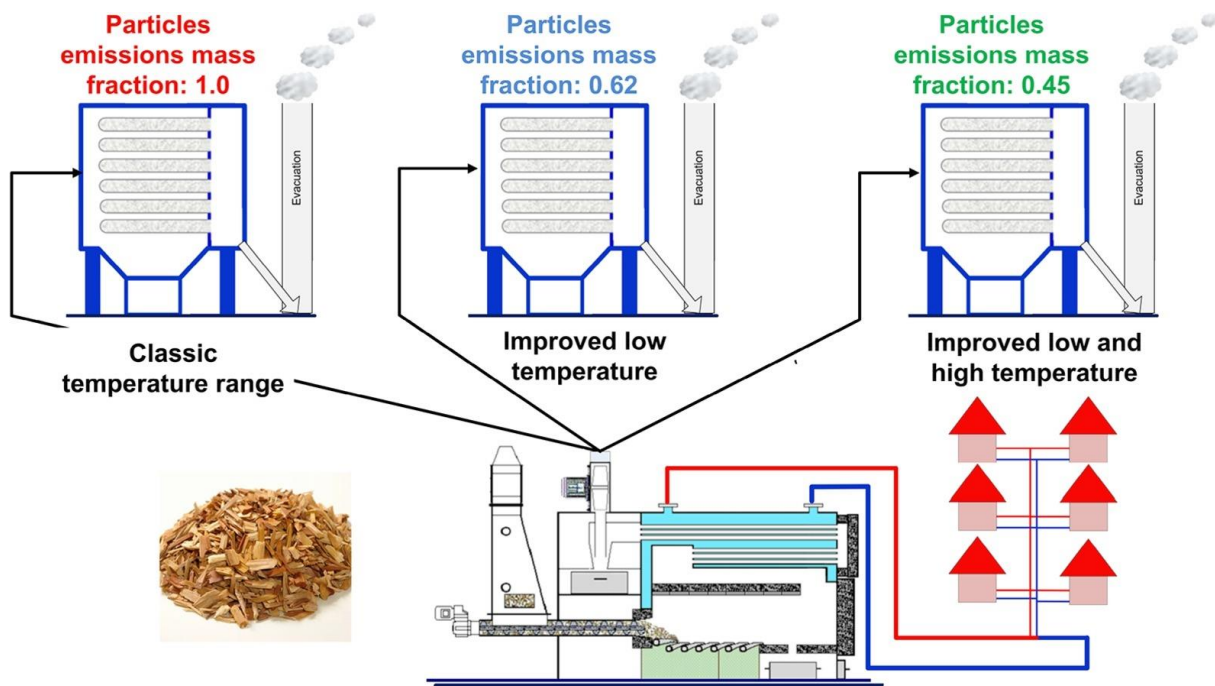


Figure 35: Fabric filter testing facility presented in (Brandelet et al., 2020)

Air staging

Gaseous and particulate emissions have been investigated with different **air staging strategies** over a wide range of secondary air flow rates for small scale appliances by (Khodaei et al., 2017). Laboratory scale wood pellet combustor, supplied by an underfeed fuel bed input, is used in this work. The air staging strategies have been employed to study burning rate, temperature in primary and post combustion zones, and NO, CO and PM emissions, taking into account the air to fuel stoichiometric ratio. 50% CO reduction and 9 times less particle mass concentration than non-staged combustion are achieved by deploying a uniform secondary air module in a higher position from the bed. The minimum NO (37% reduction than nonstaged) measured in the non-uniform air distribution module at the higher flow rate with lower distance from the fuel bed. The results demonstrate a trade-off between NO and CO, PM emissions but also significant potential for reducing particulate and gaseous emissions by deploying air staging in the pellet combustor. Overall, a higher secondary air flow rate in air staging strategies may contribute to NO_x reduction but result in less efficient combustion, which is not recommended due to several problem associated with PM, CO and thermal efficiency of combustion. The formation of solid particulate matters is highly sensitive to secondary air distance and uniformity of air distribution in the secondary air modules. Additional techniques such as flue gas recirculation (FGR), selective non-catalytic reduction (SNCR) and combined staging (CS) and application of deflector sheets in the post combustion zone should be investigated to reduce the formation of NO_x when biomass combustors are operating in the highest efficiencies.

Fuel reburning

Fuel reburning in a reburning zone usually serves in mitigating NO_x formation in stationary combustion sources (Figure 36). However, the use of biomass as reburning fuel could facilitate

the production of relatively more nitrogen-containing aromatic products of incomplete combustion. (Oluwoye et al., 2020) investigated the heterogeneous reaction between biomass and mixtures of NO/O₂ gases, employing isothermal high-temperature experiments in a vertically-entrained reactor, and in situ diffuse reflective infrared Fourier transform spectroscopy (DRIFTS) under a non-isothermal heating condition ranging from ambient temperature to 700 °C. The method enables sensitive evaluation of the surface species ensuing during the thermal reaction. Results from this study elucidate the formation of nitrated structures as active intermediate species of the heterogeneous reaction. The nitrogenated signatures persist on the surface of the residual ash, suggesting the production of N-aromatics such as nitro-PAH. The products suggest the formation of nitro-PAH, and other forms of brown carbons.

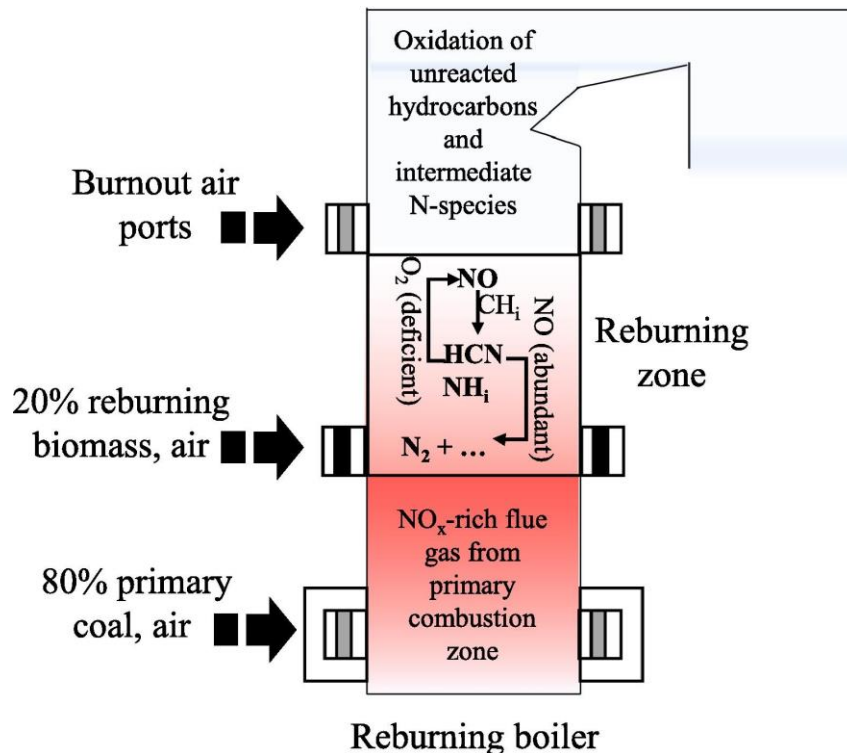


Figure 36: Schematic diagram of the three stages of the (biomass) reburning process by (Oluwoye et al., 2020)

Thermal Energy Storage

One approach to minimize emissions is to improve system efficiency and limit the number of boiler cycles that include start-up and shut down periods where emission rates are higher by utilizing thermal storage as part of the boiler system (Wang et al., 2019). In their study, emissions from two 25 kW European-designed, but U.S. manufactured wood pellet boilers (PB and WPB) with **thermal energy storage** (TES) as shown in Figure 37 were measured in actual home operation using the EPA CTM-039 stack sampling method including condensables. These measurements allowed the estimation of the emissions reductions due to the presence of TES. PB had much higher emissions than WPB because PB had frequent local oxygen deficit-induced non-uniform combustion, which highlights the significance of periodic onsite oxygen tuning after the boiler installation. Particulate emissions were dominated by PM_{2.5} and the particles mainly consisted of low melting point, alkali compounds such as K₂SO₄, KCl, Na₂SO₄, CaCl₂, etc. Both PM_{2.5} and polycyclic aromatic hydrocarbons (PAHs) emissions increased linearly with CO because they are products of incomplete combustion. Optimum boiler

operating conditions were found with 12% flue gas oxygen content for both systems to achieve minimum CO emissions, which is 2% higher than the manufacturer's set-point of 10%. The potential emissions reductions by using a system with TES instead of a non-TES system were estimated under three scenarios. The results showed **both significant gaseous and particulate matter emissions reductions that demonstrate that modern, high-efficiency wood pellet boilers with TES systems can produce heat with lower total emissions compared to non-TES systems.**

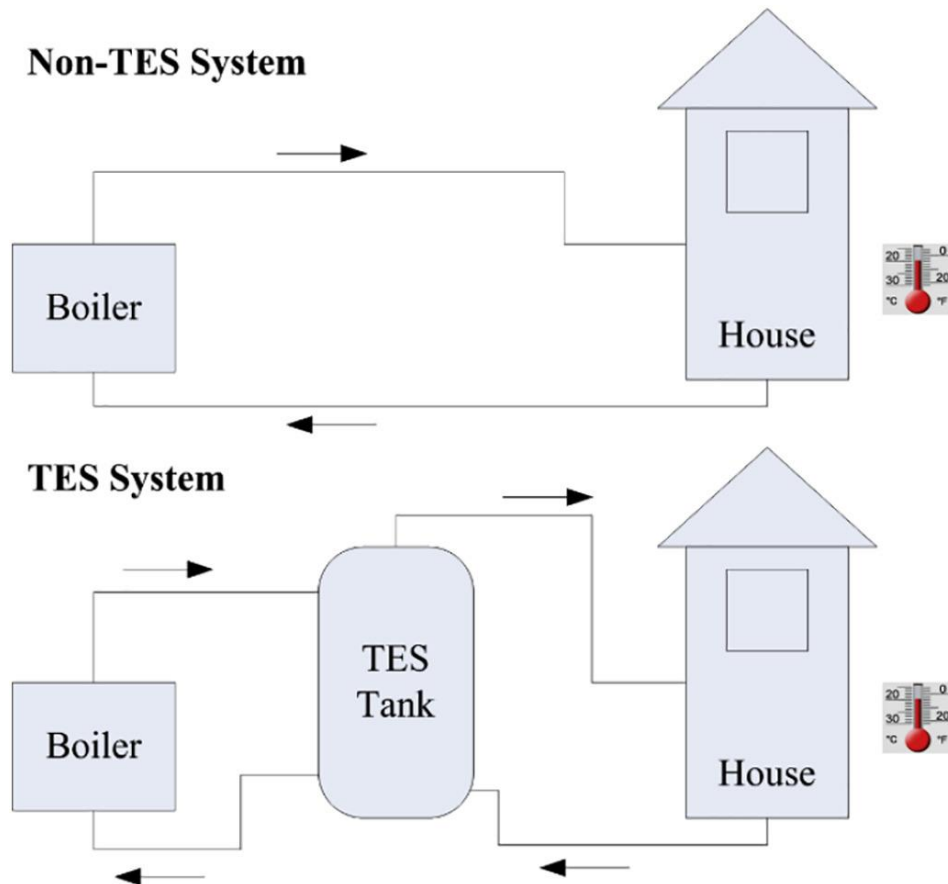


Figure 37: Schematic of non-TES (Thermal Energy Storage) and TES systems from (Wang et al., 2019)

Wood washing

In order to reduce pollutant emissions from biomass combustion, (Schmidt et al., 2018) investigated a wood washing method to reduce pollutant emissions. The wood logs were washed at room temperature in order to represent natural rain leaching before burning in a recent stove (2010s) of nominal output of 6.3 kW. Raw and washed woods were combusted for three different types of wood (oak, beech and fir) and the study focused on their particulate and gaseous emissions (Total Suspended Particles (TSP), Particulate Matter with diameter below 2.5 μm (PM_{2.5}), carbon monoxide (CO), nitrogen oxides (NO_x) and Total Volatile Organic Compounds (TVOC)). Polycyclic Aromatic Hydrocarbons (PAH), aldehydes and wood tracers as phenols compounds were also measured. In addition, considering the toxic equivalent factor, the human health impact of adsorbed and gaseous **PAH is considerably reduced (96%) in the case of washed fir combustion (Figure 38). Emission factors of CO and TSP for washed wood combustion also show a decrease up to 50%** depending on the type of wood used. Furthermore, phenolic compounds, Benzene, Toluene, Ethylbenzene, Xylenes and Trimethylbenzene (BTEXT) emissions can also be reduced by the washing of biomass. Washed

oak combustion leads to a clear decrease by 60% of the total of BTEXT. In the case of phenols emissions, phenol shows a significant decrease by 91% during the combustion of washed fir wood. These latter species are important precursors of SOA.

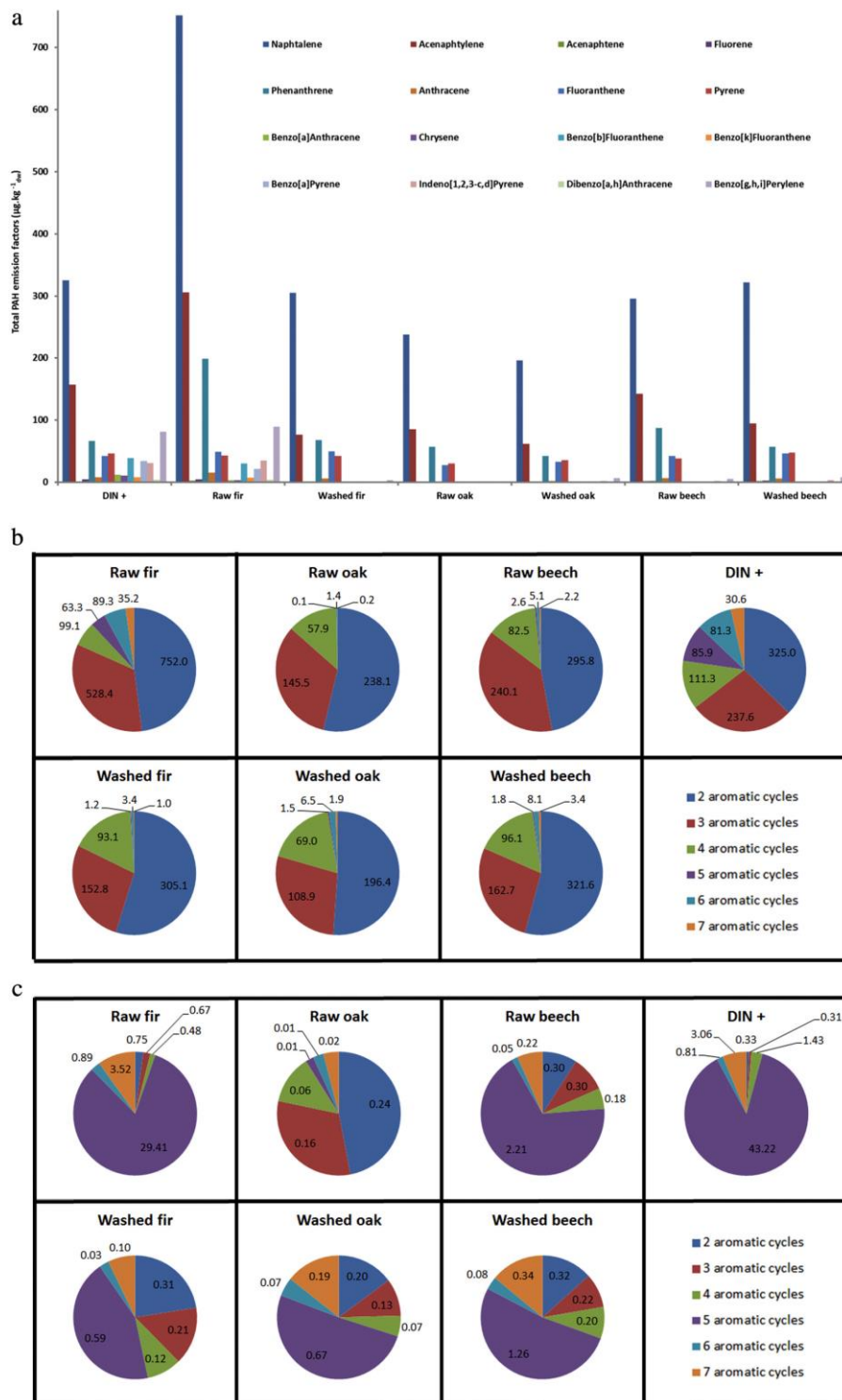


Figure 38: (a) Evolution of the individual PAH emission factors with the pre-treatment (total emission factors of the three phases (solid, condensed and gas); (b) number of cycle distributions of total PAH emissions (data expressed in $\mu\text{g}\cdot\text{kg}_{\text{dw}}^{-1}$); and (c) number of cycle distributions of total PAH emissions expressed into toxic equivalent (data expressed in $\mu\text{g eq. Benzo[a]Pyrene}\cdot\text{kg}_{\text{dw}}^{-1}$) – From (Schmidt et al., 2018)

4.1.9 Key conclusions

Biomass combustion can happen at different scales. While the basic principle is the same, technologies vary considerably depending on the size of the installation, from a wood stove commonly found in households to industrial-size boilers supplying hundreds of MW of electricity and/or heat to hundreds of thousands of citizens. Old wood appliances in Europe are characterized by low efficiency rates and incomplete combustion performance: at the lower end of the spectrum, open fires are the most polluting because the least efficient combustion method (efficiency below 30%). This is due to the fact that in an open fire, it is impossible to control the combustion process, which increases the chances of incomplete and therefore particularly polluting combustion. On the contrary, newly designed stoves are proven to be many times more energy efficient than the obsolete ones. From the literature review carried out, the following key conclusions would be:

- Exposure to outdoor and indoor air pollution is known to affect respiratory and cardiovascular health, and a recent study also shows its effects on cognitive function. Open fireplaces, traditional stoves and cookers as a source of indoor and outdoor air pollution, can be the origin of environmental inequities (gender, age) particularly in developing countries. There is a clear advantage to tackle residential wood combustion to both reduce health effects (and associated costs) and rapidly have a benefit on climate even if the impact is weak compare to other GHG.
- BC emissions from *residential combustion* is by far the largest contributor at the global scale. In EU27+UK, BC from *stationary combustion* emissions is 3 times higher than BC from the *passenger car* emissions in 2018. These emissions are mostly due to biomass burning and particularly wood burning.
- BC concentrations in waste gases are usually determined by thermo optical methods and certainly account for a fraction of organics. OM is usually derived from OC measurements issued from thermal methods.
- PM emitted by biomass burning from small combustion appliances are mainly composed of carbonaceous compounds (Elemental Carbon (EC) and Organic Matter (OM)). Most of particles are fine particles with diameter below 2.5 μm . A secondary production of particles is identified during the dilution of the plume and later in ambient conditions.
- Birch, Spruce and Pine often exhibit the highest emission factors of PM, BC and PAHs. Raw fir is a strong emitter of PAHs. Wood Oak emits the lowest BC. Burning wet wood is not recommended as presented in the Code of good practices for wood burning and small combustion installations (TFTEI, 2019), however some studies showed higher PM₁, PAH and BC emissions using very dry wood (11%) compared to wet wood (18%) while the particulate number (PN) is lower for dry wood.
- The use of modern stoves implementing advanced methods to limit the emission of pollutants like catalytic combustors, wood pellets and masonry stoves enables to reach the emission standards as defined in the EU by latest eco-design standards. The ban of not eco-labelled wood stove seems the most beneficial in some recent studies. However, the use of catalytic combustor can increase the emissions of PCDD/F due to the effect of the catalyst. Organic gases are also largely reduced with modern wood stoves which involve a potential positive effect to reduce the secondary organic aerosol (SOA) potential formation.
- Automatic fuel feeding and improvement of air staging combustion clearly improve the combustion efficiency. Low cost strategies of retrofit air injection on traditional stoves

can reduce PM and BC emissions. High burn rates should be avoided as they are associated to higher pollutant emissions.

- Wood pellet stoves have 2 to 3 times lower PM, EC and PAH emissions than wood logs in advanced wood stoves. However, their efficiency to reduce particle number is not as high as expected.
- Electrostatic Precipitator would be a good strategy to reduce particles. Efficiency exceeding more than 99% are commonly obtained in combustion plants, however in practice this technology is not suitable for residence appliances. The efficiency of ESPs to reduce nanoparticles is not clear yet. Under favourable combustion conditions, after the ESP during the cooling of the flue gas, organic matter can appear due to condensable species.
- Additional strategies like Thermal Energy Storage can help to optimize the heating cycle from the start-up and the shutdown. Start-up is a critical phase with high emissions of pollutants.
- The formation of solid particulate matters is highly sensitive to secondary air distance and uniformity of air distribution in the secondary air modules. Air staging can be optimized to reduce air pollutant emissions. However, air staging strategy in combination to reburning in order to reduce NO_x can produce nitro-PAH known to have a high carcinogenic potential.
- From (TFTEI, 2019), the following list of new technologies were identified and can be recommended. New advanced stoves equipped with improved air control, reflective materials and two combustion chambers; New smart stoves with automated control of air supply and combustion, thermostatic control, Wi-Fi-connected to collect and send combustion data to the manufacturer for better service; New advanced masonry stoves, operating at high efficiencies and low emissions; New advanced pellet boilers: fully automated boilers (electronic control of air supply, lambda sensors), condensing boilers, using standardised pellets; Wood carburettor boilers using log wood or chip wood; Heat accumulating equipment with heat accumulating reducing stop/start frequencies and operation at partial load, which generates higher emissions than operation at full load; Other: flue gas recirculation, reverse combustion, gasifier.
- Currently, test procedures for delivering labels are not able to characterise real conditions of use of domestic appliances. New normalised test procedures would be useful to better account for real utilisations of small-scale combustion appliances (starting phases, closing phases).
- Harmonized methods to determine the emission concentrations of PM and BC would be necessary. For PM, methods accounting for condensables like dilution tunnels are existing.
- Brown carbon (BrC) represents organic matter which can absorb solar radiation. BrC is mainly co-emitted by biomass burning or produced later during the plume dilution. So far, this species is not very well identified, and there are uncertainties in the radiative properties assigned to this species in climate models.

4.2 Road transport

4.2.1 Aftertreatment systems

Catalytic exhaust-gas aftertreatment with the aid of a three-way catalytic converter is currently the most effective form of emission control for gasoline engines (Frauhammer et al., 2015). The **three-way catalytic converter** (TWC) is an integral component of the exhaust-emission control systems of both manifold-injection engines and gasoline direct-injection engines. In the case of homogeneous mixture distribution with a stoichiometric air/fuel ratio ($\lambda = 1$), a three-way catalytic converter at normal operating temperature is able to convert the following pollutants virtually completely: carbon monoxide (CO), hydrocarbons (HCs) and nitrous oxides (NO_x). However, adhering exactly to a figure of $\lambda = 1$ requires mixture formation by means of electronically controlled gasoline injection; today, this system has completely replaced the carburetor, which was used primarily up until the introduction of the three-way catalytic converter. Precise lambda closed-loop control monitors the composition of the air/fuel mixture and regulates it at a value of $\lambda = 1$. Although these ideal conditions cannot always be maintained in all operating states, pollutant emissions can on average be reduced by more than 98 %. Because the three-way catalytic converter is unable to convert the nitrous oxides in lean mode ($\lambda > 1$), an additional NO_x accumulator-type catalytic converter is used in engines with a lean operating mode. Another means of reducing NO_x at $\lambda > 1$ is Selective Catalytic Reduction (SCR). The TWC is not directly involved in the suppression of direct PM emissions but can have an impact on secondary formation of PM.

The **selective catalytic reduction** (SCR) of NO_x with aqueous urea (“urea SCR”) is originally a steady-state technology used in stationary source NO_x control (Lambert, 2019). Catalysts for this application are usually quite large, and typically consist of lower cost materials such as vanadium/titanium or Fe/zeolite. The catalyst bed temperature may be controlled within an optimum NO_x conversion window, and the gas flow is fairly constant; therefore, the aqueous urea injection is also fairly constant. Vehicle operation, on the other hand, is highly transient in flow and temperature based on customer demanded vehicle speed, load, road conditions, weather, etc., and may not be predicted. A catalyst must work in the vast majority of conditions found in normal vehicle use, and the catalyst size is limited by space and weight considerations. Aqueous urea must be replenished for SCR to work, and the transient nature of the injection process makes it very different from stationary source NO_x control. The SCR catalyst must function and survive in a multi-component system that also controls hydrocarbons, carbon monoxide, and soot, and faces poisoning by sulphur, phosphorus, and a variety of other elements present in fuel, oil, and any upstream component including other catalysts. The SCR catalyst can experience temperatures below 200 °C and as high as 700 °C in typical vehicle operation, or even 900 °C when coated on a soot filter. The selection of functional materials, durability tests representing high mileage, and even more important, tests to failure, become critical decisions in the design of automotive urea SCR.

The **Diesel Oxidation Catalyst** (DOC) is a non-filter-based open monolith (flow-through) system resembling the conventional catalytic converters for gasoline and diesel engines with some significant variation of the catalyst composition so as to optimize the catalyst activity under lean conditions. The noble metals are impregnated into a highly porous alumina washcoat about 20-40 mm thick that is applied to the passageway walls. Most of the DOCs used in the international market contain platinum (Pt) and palladium (Pd) at a typical loading of 50-70 g/ft³. The current platinum group metal (PGM)-based DOCs play two primary functions in the commercial emission control systems:

- 1) Effectively promote the oxidation of unburned hydrocarbons (UHCs) and CO, as well as the SOF portion of PM as described by reactions (1) and (2), either to reduce emissions coming from the engine, or to oxidize diesel fuel to create exothermic heat used for the DPF active regeneration and lean NO_x trap (LNT) and desulphurisation (deSO_x);
- 2) Convert NO to NO₂ as in reaction (3), which is used to continuously oxidize soot on a DPF, *i.e.*, DPF passive regeneration in reaction (4), and/or for enhancing the SCR (selective catalytic reduction) NO_x removal (deNO_x) performance via the fast SCR reaction (5), particularly at low temperatures.

The **Diesel Particulate Filter (DPF)** is an extruded usually cylindrical ceramic structure with thousands of small parallel channels positioned in the longitudinal direction of the exhaust system. The porous surface wall-flow monoliths are made of ceramics with higher and more precisely controlled porosity, and the adjacent channels in the wall-flow filters are alternatively plugged at each end, thus forcing the diesel aerosol to flow through the porous substrate walls, which act as the filter medium. Particles that are too big to pass through the porous surface are physically collected and stored in the channels. The DPF walls are designed to have an optimum porosity enabling the exhaust gas to pass through the walls without much hindrance, and to be sufficiently impervious regarding collecting the particulate species. Extensive research has been conducted on the various particulate collection mechanisms including diffusion, interception, inertia, gravity, electrostatics, and thermophoretic. The main design criteria that can contribute to the successful performance of DPFs typically are high filter efficiency, low pressure drop, robust structural and thermal durability and reliability, and high capacity to resist high temperature excursions during a large number of regeneration events over their life cycles. The technological developments in DPF design include the advancements in cell shape and cell wall porosity optimization aimed at minimizing the engine backpressure and extending the interval between filter services as well as facilitating the catalyst coating.

The **Gasoline Particulate Filter (GPF)** technology is an adaptation of DPF to gasoline vehicles. With increasingly stringent emission regulations, research regarding the application of PM filters in GDI (Gasoline Direct Injection) engines will become an inevitable trend. The particulate filter must have high filtration efficiency and a long life and satisfy other requirements, and the flow resistance (pressure drop) must be small (Mu et al., 2019). To reduce the flow resistance of the GPF, technologies using a type of nested cylinder and diversion channel plug (NCDCP) GPF is tested. It is composed of nested foam metal cylinders and annular diversion channel plugs. The pressure drop and its influencing factors were theoretically studied. The results show that the structural parameters, such as the cylindrical layer spacing and the length-to-diameter ratio, and the pressure drop have trade-off relationships (Mu et al., 2019).

In a CDPF (Catalysed DPF), a catalytic material, mostly with low-level Platinum Group Metal, is coated onto the surface of the filter to lower the ignition temperature necessary for oxidizing accumulated PM in the 300-400 °C range, allowing the filter to self-regenerate during the periods of high exhaust gas temperature. CDPFs achieve over 90% reduction in PM and soot as well as in HC and CO. CDPFs exhibit excellent PM filtration efficiencies and are characterized by inherent relatively high pressure drop. It has been observed that the colder applications experience lowers the regeneration rates and cause higher pressure. DPFs are dynamic and complex systems, since the operating conditions vary over time, and different functionalities (catalysis and filtration) are usually assembled on the same monolithic support, which is a demanding requirement in terms of space and cost. Moreover, the feasibility of soot

combustion depends to a great extent on the catalyst–soot contact conditions, and it is therefore necessary to maximize the interaction between the soot particles and the catalyst, both of which are solid materials. A pioneering approach to maximize the soot–catalyst contact was implemented by *Peugeot-Citroën Société d’Automobiles (PSA)* in early 2000s, whose key component is a Ce-fuel additive that was reliably implemented in several million vehicles up to now. PSA vehicles have an active on-board additive system with its own tank-pump device that allows to dose the proper amount of Ce fuel additive to the Diesel fuel. This metal organic compound in fuel leads to the formation of CeO₂ particles well embedded in the structure of diesel particulate, and thus in very good contact with the soot particles (intimate soot–catalyst contact). Therefore, lower ignition temperatures can be reached by catalytic means, with the benefit of post-injected fuel savings (Fino et al., 2016).

These devices can be combined. Typically, there are two different conceptual architectures for combining the SCR and DPF technologies to achieve a desired level of emission reduction performance: either SCR is placed upstream of DPF, *i.e.*, DOC + SCR + DPF, or SCR is placed downstream of DPF, *i.e.*, DOC + DPF + SCR.

4.2.2 Carbonaceous composition of exhaust

Exhaust PM mainly consists of elemental carbon (EC), organic carbon (OC) and inorganic components including metallic ash and ions. Therefore, different literature values have been collected and average EC and OC values have been proposed by (Ntziachristos et al., 2007).

The variability of the data collected from tunnel, roadway and dynamometer studies, and the uncertainties in the measurement of, in particular, organic carbon (OC), indicate that exhaust PM speciation is bound to be highly uncertain. Because of this uncertainty, mean EC and black carbon (BC) values are considered practically equal (Battye et al., 2002; May et al., 2010). Although it is known that EC and BC definitions and determination methods differ, this is considered to be of inferior importance compared to the overall uncertainty in determining either of them per vehicle emission control technology.

Despite overall uncertainties, reliable BC/OC ratios can be developed, because there is a general agreement in the measurements from tunnel and laboratory studies with regard to the emission characteristics of diesel and petrol vehicles. The effect of different technologies (*e.g.* oxidation catalyst, diesel particle filter) on emissions is also rather predictable.

Table 15 from (Ntziachristos and Samarras, 2019) suggests ratios between organic material (OM) and black carbon (OM/BC) and BC/PM_{2.5} (both expressed as percentages) that can be applied to the exhaust PM emissions for different vehicle technologies. ‘Organic material’ is the mass of organic carbon corrected for the hydrogen and other atoms content of the compounds collected. The sources of these data, and the methodology followed to estimate these values, is given in (Ntziachristos et al., 2007). An uncertainty range is also proposed, based upon the values in the literature. The uncertainty is in percentage units, and is given as a range for both ratios proposed. For example, if the OM/EC ratio for a particular technology is 50 % and the uncertainty is 20 %, this would mean that the OM/EC ratio is expected to range from 40 % to 60 %. This is the uncertainty expected on fleet-average emissions, and not on an individual vehicle basis. Individual vehicles in a specific category may exceed this uncertainty range. The ratios also correspond to average driving conditions, with no distinction between driving modes or hot and cold-start operation.

The OM/BC ratio is larger for gasoline vehicles and decline from old to modern vehicles. For diesel HDV EURO VI, it is noteworthy to see the drop of BC/PM_{2.5} ratio with a surge of the

OM/BC ratio certainly due to soot mostly removed by the DPF and the dominance of OM formed during the cooling. They are associated to the lowest PM2.5 ELV.

Table 15: PM2.5 emission factors, split of PM in elemental (BC) and organic mass (OM) from (Ntziachristos and Samarras, 2019). Notes: The values originate from available data in the literature and engineering estimates of the effects of specific technologies (catalysts, DPFs, etc.) on emissions. The estimates are also based on the assumption that low-sulphur fuels (< 50 ppm t. S) are used. Hence, the contribution of sulphate to PM emissions is generally low. In cases where advanced aftertreatment is used (such as catalysed DPFs), then EC and OM does not add up to 100 %. The remaining fraction is assumed to be ash, nitrates, sulphates, water and ammonium salts. L-categories are Mopeds and Motorbikes**

Category	Euro Standard	PM2.5 EF (mg km ⁻¹)	BC/PM2.5 (%)	OM/BC (%)	Uncertainties (%)
<i>Petrol PC and LCV</i>	PRE-ECE	2.2-2.3	2	4900	50
	ECE 15 00/01	2.2-2.3	5	1900	50
	ECE 15 02/03	2.2-2.3	5	1900	50
	ECE 15 04	2.2-2.3	20	400	50
	Open loop	2.2-2.3	30	233	30
	Euro 1	2.2-2.3	25	250	30
	Euro 2	2.2-2.3	25	250	30
	Euro 3	1.1-2.2	15	300	30
	Euro 4	1.1	15	300	30
<i>Diesel PC and LCV</i>	Conventional	220.9-356	55	70	10
	Euro 1	84.2-117	70	40	10
	Euro 2	54.8-117	80	23	10
	Euro 3	39.1-78.3	85	15	5
	Euro 4	31.4-40.9	87	13	5
	Euro 3,4,5 equipped with DPF and fuel additive	-	10	500	50
	Euro 3,4,5 equipped with a catalyzed DPF	-	20	200	50
<i>Diesel HDV</i>	Conventional	333-491	50	80	20
	EURO I	129-358	65	40	20
	EURO II	61-194	65	40	20
	EURO III	56.5-151	70	30	20
	EURO IV	10.6-26.8	75	25	20
	EURO V	10.6-26.8	75	25	20
	EURO VI	0.5-1.3	15	300	30
<i>L-Categories**</i>	Conventional 2-stroke	176	10	900	50
	Euro 1 2-troke	45	20	400	50
	Euro 2 2-troke	26	20	400	50
	Conventional 4-stroke	14-176	15	560	50
	Euro 1 4 stroke	14-40	25	300	50
	Euro 2 4 stroke	3.5-7	25	300	50
	Euro 3 4 stroke	0.96-4	25	250	50

4.2.3 Impact of After-treatment systems on particulate matter emissions

In the last 30 years, diesel engines have made rapid progress to increased efficiency, environmental protection and comfort for both light- and heavy-duty applications (Fiebig et al., 2014). The technical developments include all issues from fuel to combustion process to exhaust gas aftertreatment. This paper provides a comprehensive summary of the available literature regarding technical developments and their impact on the reduction of pollutant emissions. This includes emission legislation, fuel quality, diesel engine- and exhaust gas aftertreatment technologies, as well as particulate composition, with a focus on the mass-related particulate emission of on-road vehicle applications. Diesel engine technologies representative of real-world on-road applications can be highlighted. Internal engine modifications now make it possible to minimize particulate and nitrogen oxide emissions with nearly no reduction in power. Among these modifications are cooled exhaust gas recirculation, optimized injections systems, adapted charging systems and optimized combustion processes with high turbulence. With introduction and optimization of exhaust gas aftertreatment systems, such as the diesel oxidation catalyst and the diesel particulate trap, as well as NO_x-reduction systems, pollutant emissions have been significantly decreased. Today, sulphur poisoning of diesel oxidation catalysts is no longer considered a problem due to the low-sulphur fuel used in Europe.

In the future, there will be an increased use of biofuels, which generally have a positive impact on the particulate emissions and do not increase the particle number emissions. Since the introduction of the EU emissions legislation, all emission limits have been reduced by over 90%. Further steps can be expected in the future. Retrospectively, the particulate emissions of modern diesel engines with respect to quality and quantity cannot be compared with those of older engines. Internal engine modifications lead to a clear reduction of the particulate emissions without a negative impact on the particulate-size distribution towards smaller particles. The residual particles can be trapped in a diesel particulate trap independent of their size or the engine operating mode. The usage of a wall-flow diesel particulate filter leads to an extreme reduction of the emitted particulate mass and number, approaching 100%. A reduced particulate mass emission is always connected to a reduced particle number emission.

Comparing the values of registered vehicles based on the exhaust type values published by the KBA (Federal Motor Transport Authority - Germany) in terms of the development from Euro 1 to Euro 6, it can be seen that the values of registered vehicles have been clearly below the limits in some cases, which is true especially for particulate emissions of vehicles with diesel particulate filters (DPF) in emission standard Euro 3 and Euro 4 (Figure 39). Starting with Euro 5, the lowest particulate levels have been universally achieved by using DPFs. Euro 6 certified passenger cars are now on the market. The Figure 39 (on the lower left) additionally shows that a fast market penetration of new emission standards has been reached by new registered vehicles after these standards were introduced. Euro VI certified commercial vehicles have only been available on the market for a short period of time (Emission standards for commercial vehicles highlighted by a roman numeral). The development of the emission limits and KBA registration numbers showed a similarly fast and significant reduction in all emissions for commercial vehicles (on the lower right), while the values were far below the limits in some cases. Euro IV and Euro V concepts have been used in series production both with (open symbols) as well as without DPF (closed symbols), since the majority of commercial vehicle manufacturers has pursued in-engine particle reduction and a reduction in NO_x emissions using the SCR technology for Euro V because of the associated fuel consumption benefits. Only a few manufacturers have used in-engine NO_x reduction and a DPF.

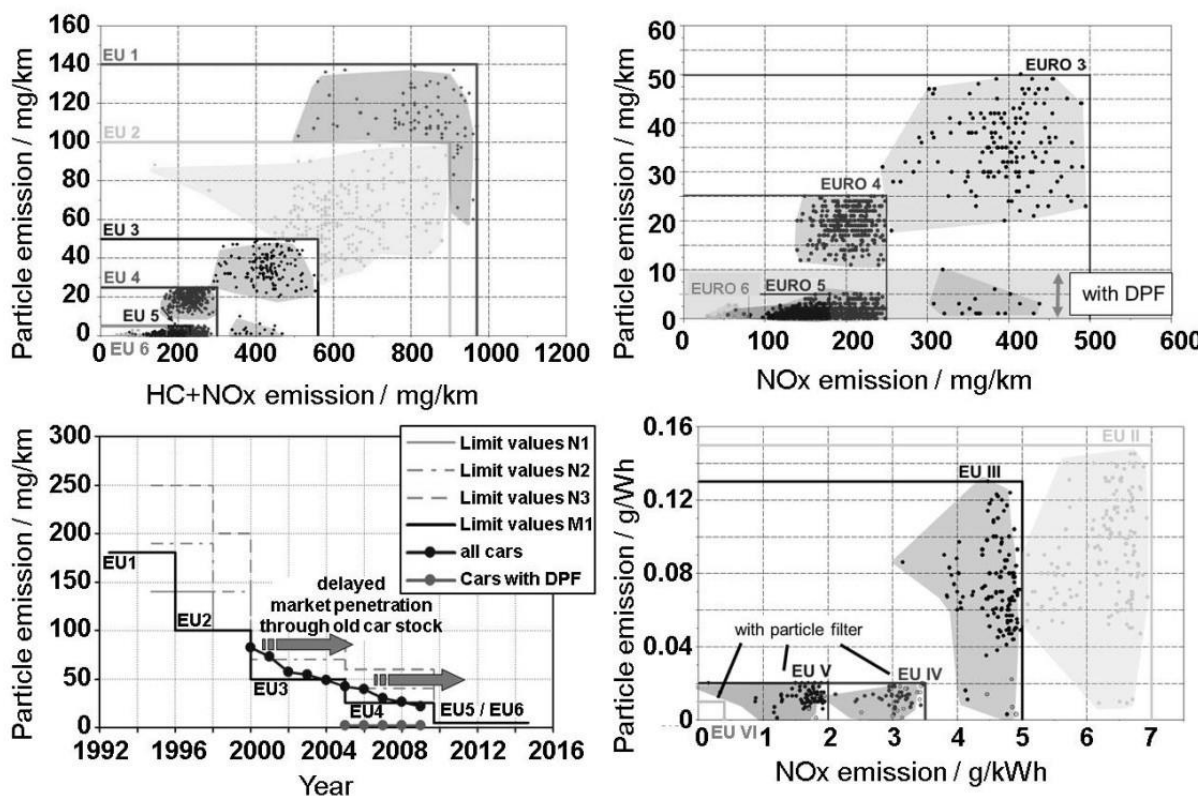


Figure 39: KBA emission limits values. Limit values for passenger cars (upper left). Detailed view of EURO 3 to 6 norm for passenger cars (upper right). Limit values for commercial vehicles (lower right). Market penetration of new emission limit levels for passenger cars (Fiebig et al., 2014)

The review (Guan et al., 2015) covers a comprehensive overview of the state-of-the-art DPF technologies, including the advanced filter substrate materials, the novel catalyst formulations, the highly sophisticated regeneration control strategies, the DPF uncontrolled regenerations and their control methodologies, the DPF soot loading prediction, and the soot sensor for the PM on-board diagnostics (OBD) legislations. Furthermore, the progress of the highly optimized hybrid approaches, which involves the integration of diesel oxidation catalyst (DOC) + (DPF, NOx reduction catalyst), the selective catalytic reduction (SCR) catalyst coated on DPF, as well as DPF in the high-pressure exhaust gas recirculation (EGR) loop systems, is well discussed. Besides, the impacts of the quality of fuel and lubricant on the DPF performance and the maintenance and retrofit of DPF are fully elaborated. Meanwhile, the high efficiency gasoline particulate filter (GPF) technology is being required to effectively reduce the PM and particulate number (PN) emissions from the gasoline direct injection (GDI) engines to comply with the future increasingly stricter emissions regulations (Figure 40).

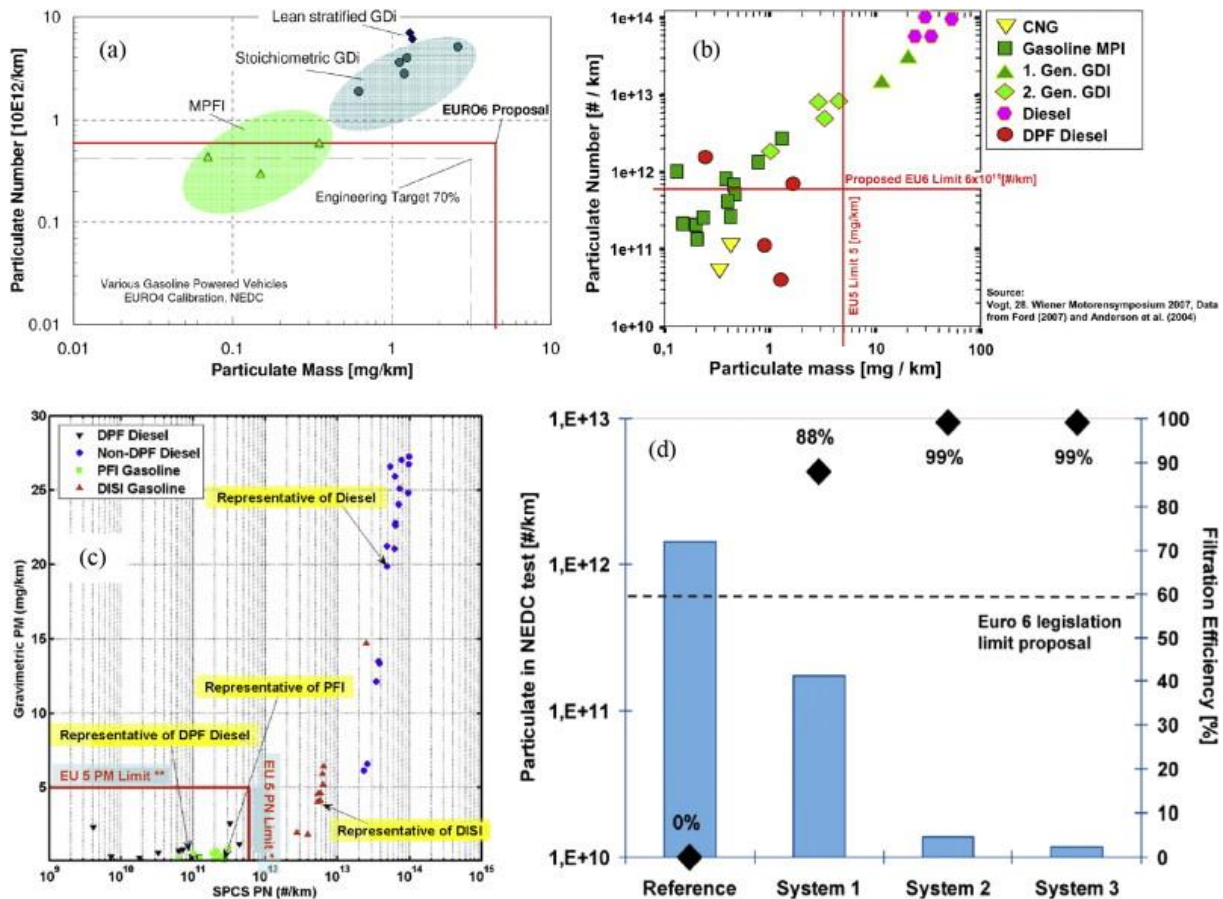


Figure 40: Schematic overview of DPF efficiency from (Guan et al., 2015). (a) Vehicle emission proposal for EURO 6 (Piock et al., 2011); (b) Comparison of particulate number and particulate mass emissions for gasoline and diesel engines (Whitaker et al., 2011); (c) Data set in PN-PM space for European light-duty vehicles (* Diesel only, ** Diesel and Direct Injection Spark Ignition only) (Braisher et al., 2010); and (d) NEDC PN emissions and filtration efficiency of GPF (Richter et al., 2012), Samples evaluated in NEDC on 2.0 L GTDI vehicle and high dynamic engine bench: reference) Reference system; systeme 1) test system with uncoated GPF in underbody position, systeme 2) test system with coated GPF in underbody position, system 3) test system with zoned close coupled TWC and coated GPF in underbody position.

The temperature of diesel exhaust gas has an important effect on reducing pollutant emissions. Besides catalyst type, space velocity of exhaust gas, and emission form are the other parameters affecting the efficiency. With the aftertreatment emission control systems, it is possible to reduce the damage of the pollutant emissions on air pollution, to meet emission standards and requirements, and to prevent the harmful effects of pollutant emissions on environment and human health (Reşitoğlu et al., 2015).

The study of (Louis et al., 2016b) focuses on (i) ultrafine particles, black carbon, BTEX, PAH, carbonyl compounds, and NO₂ emissions from Euro 4 and Euro 5 Diesel and gasoline passenger cars, (ii) the influence of driving conditions (*e.g.*, cold start, urban, rural and motorway conditions), and (iii) the impact of additive and catalysed DPF devices on vehicle emissions. Chassis dynamometer tests were conducted on four Euro 5 vehicles and two Euro 4 vehicles: gasoline vehicles with and without direct injection system and Diesel vehicles equipped with additive and catalysed particulate filters. The results showed that compared to hot-start cycles, cold-start urban cycles increased all pollutant emissions by a factor of two. The sole exception was NO₂, which was reduced by a factor of 1.3-6. Particulate and black carbon emissions from the gasoline engines were significantly higher than those from the Diesel engines equipped with

DPF. Moreover, the catalyzed DPF emitted about 3-10 times more carbonyl compounds and particles than additive DPF, respectively, during urban driving cycles, while the additive DPF vehicles emitted 2 and 5 times more BTEX and carbonyl compounds during motorway driving cycles. Regarding particle number distribution, the motorway driving cycle induced the emission of particles smaller in diameter (mode at 15 nm) than the urban cold-start cycle (mode at 80-100 nm). The results showed a clear positive correlation between particle, black carbon, and BTEX emissions, and a negative correlation between particles and NO₂. In Figure 41, we clearly see **the strong correlation between BC emissions and PN or PM10 emissions**.

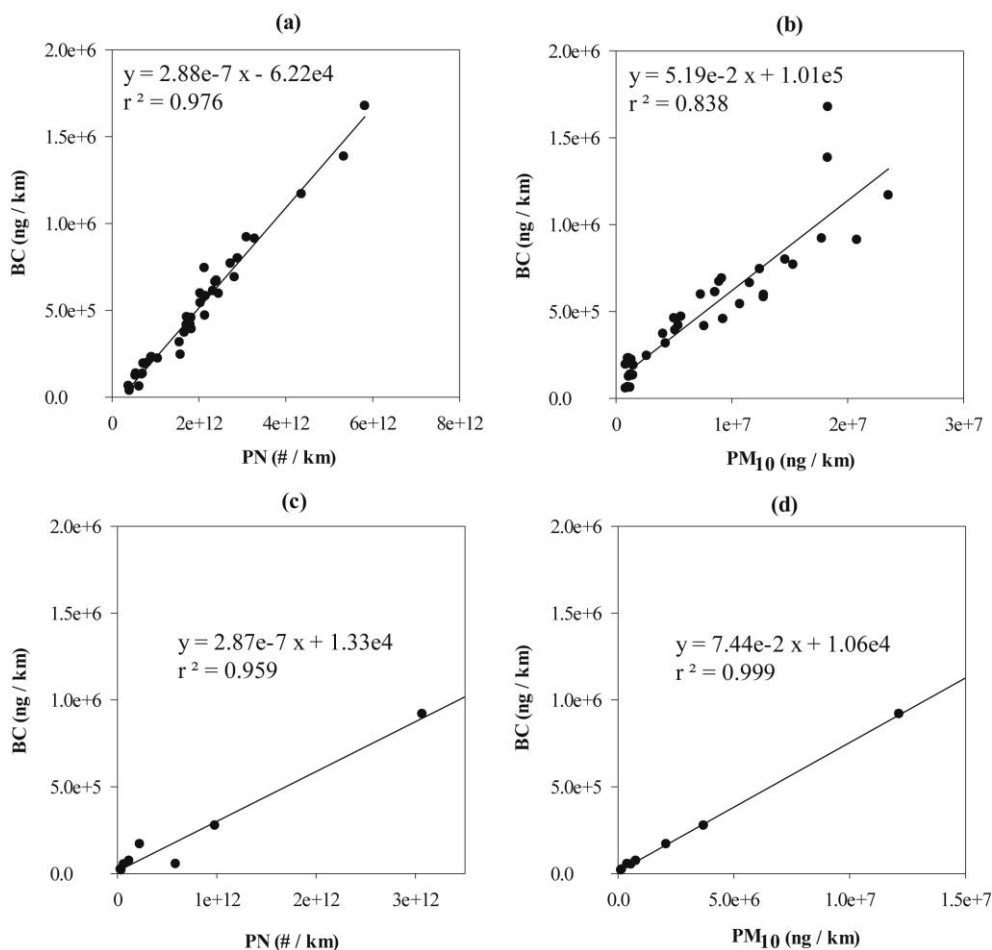


Figure 41: BC/PN and BC/PM10 correlations for gasoline (a and b) and Diesel vehicles (c and d). BC: black carbon; PN: particle number; PM10: particle mass with particle diameter below 10 μ m - From (Louis et al., 2016b)

Figure 42 shows PAH emissions for diesel and the aldehyde emission factors for the dynamometer tests conducted during the urban hot start driving cycle. (Louis et al., 2016b) observed a significant decrease in aldehyde emissions compared to (Caplain et al., 2006) and (Polo Rehn, 2013). The aldehyde emissions from the gasoline vehicles decreased from 12 mg km⁻¹ for the Euro 1 vehicles to 1 mg km⁻¹ for the Euro 4 vehicles. The aldehyde emissions from the Diesel vehicles decreased from 30 mg km⁻¹ for the pre-Euro vehicles to 0.5 mg km⁻¹ for the Euro 4 vehicles. A significant decrease in PAH emissions is observed compared to (Pillot et al., 2006) and (Polo Rehn, 2013). **PAH Diesel emissions decreased from 17 μ g km⁻¹ for pre-Euro vehicles to 1 μ g km⁻¹ for Euro 3 vehicles and remained below 0.2 μ g km⁻¹ for Euro 5 vehicles.** PAH gasoline emissions were quite low (below 8 ng km⁻¹) and close to the detection limit.

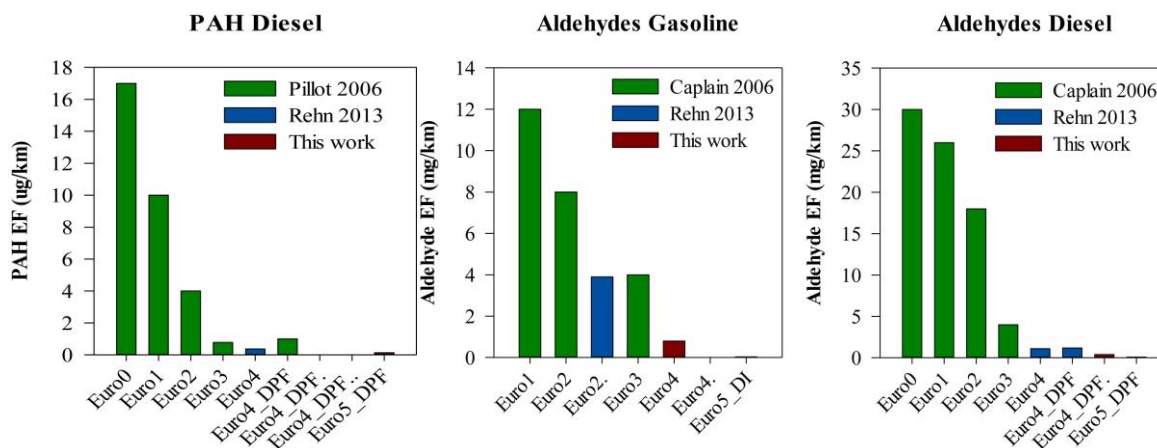


Figure 42: (Left) Comparison between the PAH emission factors (EF) for Diesel vehicles (red bar) and the findings of (Polo Rehn, 2013) (blue bar) and (Pilot et al., 2006) (green bar). Comparison between the aldehyde emission factors (EF) for gasoline vehicles (middle) and Diesel vehicles (right) (red bar) and the findings of (Polo Rehn, 2013) (blue bar) and (Caplain et al., 2006) (green bar). From (Louis et al., 2016b).

To investigate the effects of after-treatment systems on emission of pollutants, (Kostenidou et al., 2020) characterized the chemical composition of particles emitted from three diesel and four gasoline Euro 5 light duty vehicles on a chassis dynamometer facility (Figure 43). Black carbon (BC) was the dominant emitted species with emission factors (EFs) varying from 0.2 to 7.1 mg km⁻¹ for gasoline cars and 0.003 to 0.08 mg km⁻¹ for diesel cars. For gasoline cars, the organic matter (OM) EFs varied from 5 to 103 µg km⁻¹ for direct injection (GDI) vehicles, and from 1 to 8 µg km⁻¹ for port fuel injection (PFI) vehicles, while for the diesel cars it ranged between 0.15 and 65 µg km⁻¹. Twenty cold-start cycles and more specifically the first minutes of the cycle, contributed the largest fraction of the PM including BC, OM and Polycyclic Aromatic Hydrocarbons (PAHs). More than 40 PAHs, including methylated, nitro, oxygenated and amino PAHs were identified and quantified in both diesel and gasoline exhaust particles using an Aerodyne High Resolution Time-of-Flight Aerosol Mass Spectrometry (HR-ToF-AMS). The PAHs emissions from the GDI technology were a factor of 4 higher compared to the vehicles equipped with a PFI system during the cold start cycle, while the nitro-PAHs fraction was 25 much more appreciable in the GDI emissions. For two of the three diesel vehicles the PAHs emissions were close to the detection limit, but for one, which presented an after-treatment device failure, the average PAHs EF was 2.04 µg km⁻¹. Emissions of nanoparticles (below 30 nm), mainly composed by ammonium bisulphate, were measured during the passive regeneration of the catalyzed diesel particulate filter (CDPF) vehicle. Transmission Electronic Microscopy (TEM) images confirmed the presence of ubiquitous nanometric metal inclusions into soot particles emitted from the diesel vehicle equipped with a fuel borne catalyst - diesel 30 particulate filter (FBC-DPF). X-ray photoelectron spectroscopy (XPS) analysis of the particles emitted by the PFI car revealed both the presence of heavy elements (Ti, Zn, Ca, Si, P, Cl), and disordered soot surface with a significant concentration of carbon radical defects having possible consequences on both chemical reactivity and particle toxicity. Their findings show that different after-treatment technologies have an important effect on the level and the chemical composition of the emitted particles. In addition, this research highlights the importance of the particle filter devices condition and their regular checking.

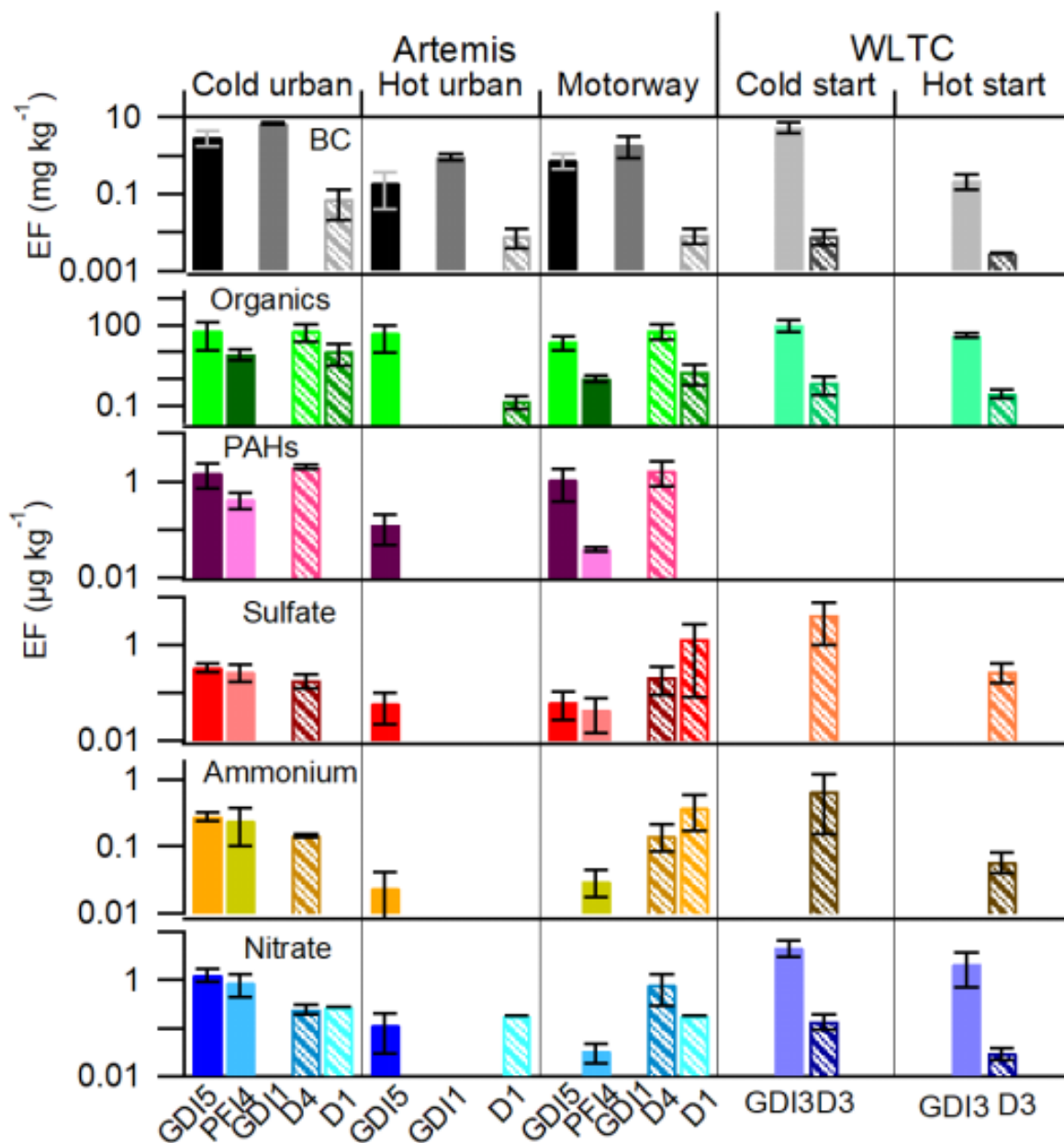


Figure 43: Emission factors for three diesel (D1, D3 and D4) and four gasoline (GDI1, GDI3, PFI4, GDI5) vehicles Euro5: BC EFs are expressed in mg km^{-1} , while for organics, PAHs, sulfate, ammonium and nitrate the values are expressed in $\mu\text{g km}^{-1}$. Two cycles ARTEMIS and WLTC are studied. Gasoline cars are shown with solid bars and diesel cars with pattern bars. The error bars correspond to $\pm 1\sigma$ standard deviation (Kostenidou et al., 2020)

As mentioned in section 3.4, IVOC can be an important precursor of SOA. (Drozd et al., 2019) comprehensively characterized intermediate volatility and semi volatile organic compound emissions using thermal desorption two-dimensional gas-chromatography–mass-spectrometry with electron impact ($\text{GC} \times \text{GC-EI-MS}$) and vacuum ultraviolet ($\text{GC} \times \text{GC-VUV-MS}$) ionization. Single-ring aromatic compounds with unsaturated C4 and C5 substituents contribute a large fraction of the intermediate volatility organic compound (IVOC) emissions in gasoline vehicle exhaust. The analyses of quartz filters used in $\text{GC} \times \text{GC-VUV-MS}$ show that primary organic aerosol emissions were dominated by motor oil. They combined new emissions data with published SOA yield parametrizations to estimate SOA formation potential. After 24 h of oxidation, IVOC emissions contributed 45% of SOA formation; BTEX compounds (benzene,

toluene, xylenes, and ethylbenzene), 40%; other VOC aromatics, 15%. The composition of IVOC emissions was consistent across the test fleet, suggesting that future reductions in vehicular emissions will continue to reduce SOA formation and ambient particulate mass levels (Figure 44).

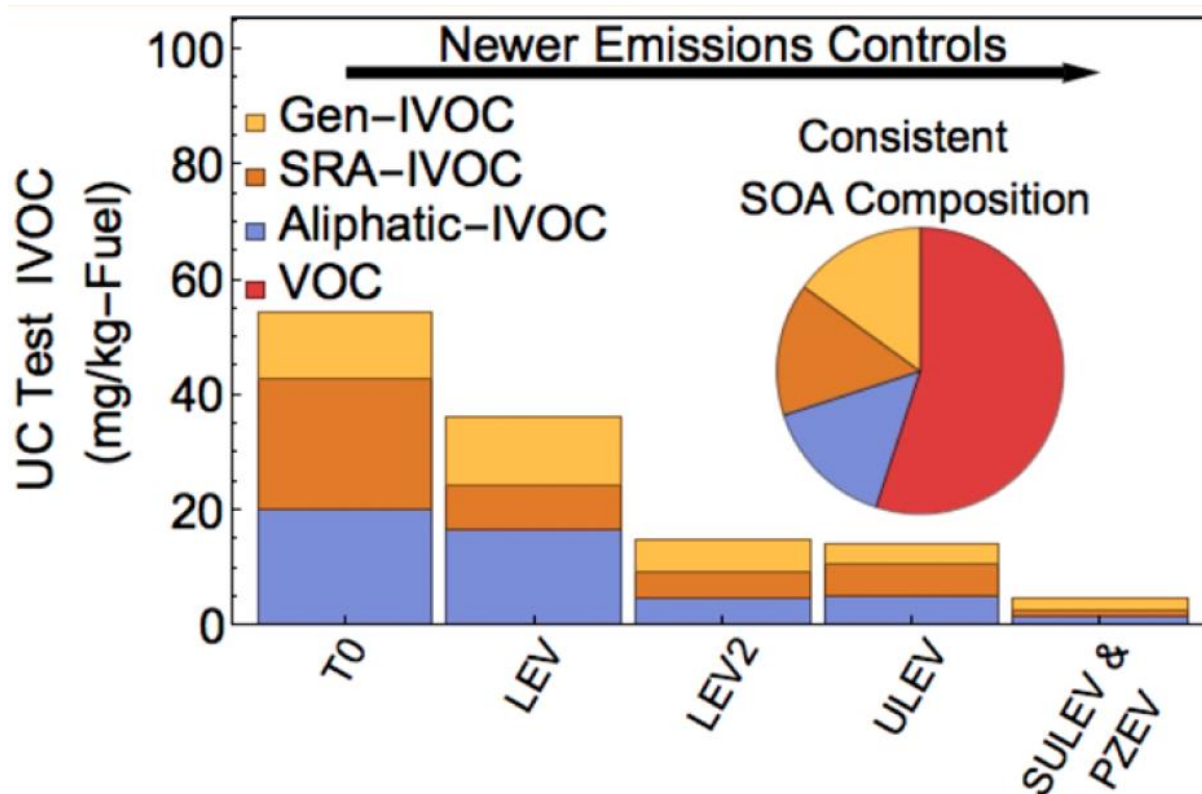


Figure 44: Impact of legislation on PM emissions including SOA formation from (Drozd et al., 2019). Vehicles are classified by their emissions certification standard. The test fleet included: one Tier 0 vehicle (T0), one low emission vehicle (LEV I), two Tier 2 low emission vehicles (LEV II) vehicles, five ultralow emission vehicles (ULEV), five superultra-low emission vehicles (SULEV), and six partial-zero emission vehicles (PZEV). Because the PZEV and SULEV vehicles have the same tailpipe emission standards, results from these are combined and termed SULEV.

(Chirico et al., 2010) present results from smog chamber investigations characterizing the primary organic aerosol (POA) and the corresponding SOA formation at atmospherically relevant concentrations for three in-use diesel vehicles with different exhaust aftertreatment systems. One vehicle lacked exhaust aftertreatment devices, one vehicle was equipped with a diesel oxidation catalyst (DOC) and the third vehicle used both a DOC and diesel particulate filter (DPF). The experiments presented here were obtained from the vehicles at conditions representative of idle mode, and for one car in addition at a speed of 60 km/h. An Aerodyne high-resolution time-of-flight aerosol mass spectrometer (HR-ToF-AMS) was used to measure the organic aerosol (OA) concentration and to obtain information on the chemical composition. For the conditions explored in this paper, primary aerosols from vehicles without a particulate filter consisted mainly of black carbon (BC) with a low fraction of organic matter (OM, OM/BC < 0.5), while the subsequent aging by photooxidation resulted in a consistent production of SOA only for the vehicles without a DOC and with a deactivated DOC. After 5 h of aging ~80% of the total organic aerosol was on average secondary and the estimated "emission factor" for SOA was 0.23–0.56 g/kg fuel burned. In presence of both a DOC and a DPF, only 0.01 g SOA per kg of fuel burned was produced within 5 h after lights on. The mass spectra indicate that POA was mostly a non-oxidized OA with an oxygen to carbon atomic ratio (O/C) ranging from 0.10 to 0.19. Five hours of oxidation led to a more oxidized OA with an O/C range of 0.21 to

0.37. The efficiency of the DOC+DPF is clearly highlighted either to reduce primary carbonaceous species and SOA (Figure 45) while when the DPF is not activated there are some differences on emissions according the regime studied.

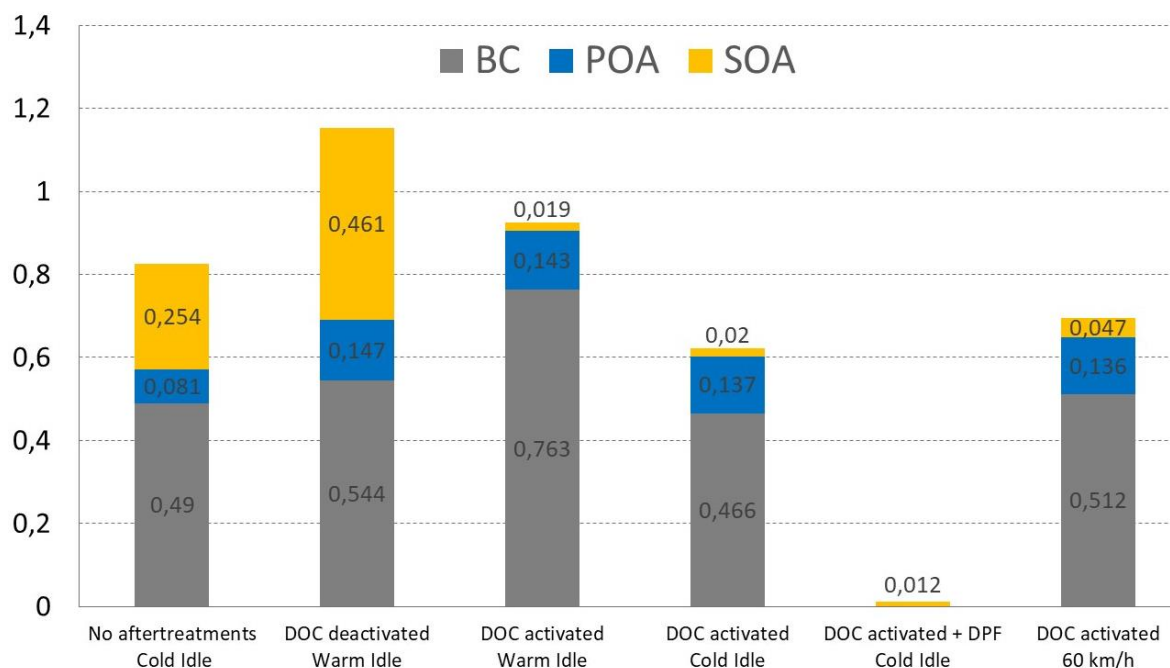


Figure 45: Emission factors from in-use vehicles of POA, SOA and BC in g kg_{fuel}⁻¹. SOA produced after 5hrs aging. After (Chirico et al., 2010).

4.2.4 The increasing role of gasoline vehicle on particle emissions (mass and number)

(Platt et al., 2017) provided a systematic examination of carbonaceous PM emissions and parameterisation of SOA formation from modern diesel and gasoline cars at different temperatures (22, -7°C) during controlled laboratory experiments. Carbonaceous PM emission and SOA formation is markedly higher from gasoline than diesel particle filter (DPF) and catalyst-equipped diesel cars, more so at -7°C, contrasting with nitrogen oxides (NO_x). Higher SOA formation from gasoline cars and primary emission reductions for diesels implies gasoline cars will increasingly dominate vehicular total carbonaceous PM, though older non-DPF-equipped diesels will continue to dominate the primary fraction for some time. Supported by state-of-the-art source apportionment of ambient fossil fuel derived PM, their results show that whether gasoline or diesel cars are more polluting depends on the pollutant in question, *i.e.* that diesel cars are not necessarily worse polluters than gasoline cars.

A recent study in China (Xing et al., 2020) aimed at evaluating the characteristics of individual particles emitted by a Euro 4 GDI vehicle and their ageing in a smog chamber under the Beijing urban environment, as part of the Atmospheric Pollution & Human Health (APHH) research programme. Using transmission electron microscopy, they identified the particles emitted from a commercial GDI-engine vehicle running under various conditions, namely cold-start, hot-start, hot stabilized running, idle, and acceleration states. The results showed that most of the particles were organic, soot, and Ca-rich ones, with small quantities of S-rich and metal-containing particles (Figure 46). In terms of particle size, the particles exhibited a bimodal distribution in number vs size, with one mode at 800–900 nm and the other at 140–240 nm. The numbers of organic particles emitted under hot-start and hot stabilized states were higher than

those emitted under other conditions. The number of soot particles was higher under cold-start and acceleration states. Under the idle state, the proportion of Ca-rich particles was highest, although their absolute number was low. In addition to quantifying the types of particles emitted by the engine, they studied the ageing of the particles during 3.5 h of photochemical oxidation in an environmental chamber under the Beijing urban environment. Ageing transformed soot particles into core-shell structures, coated by secondary organic species, while the content of sulphur in Ca-rich and organic particles increased. Overall, **the majority of particles from GDI-engine vehicles were organic and soot particles with submicron or nanometric size.** The particles were highly reactive; they reacted in the atmosphere and changed their morphology and composition within hours via catalyzed acidification that involved gaseous pollutants at high pollution levels in Beijing.

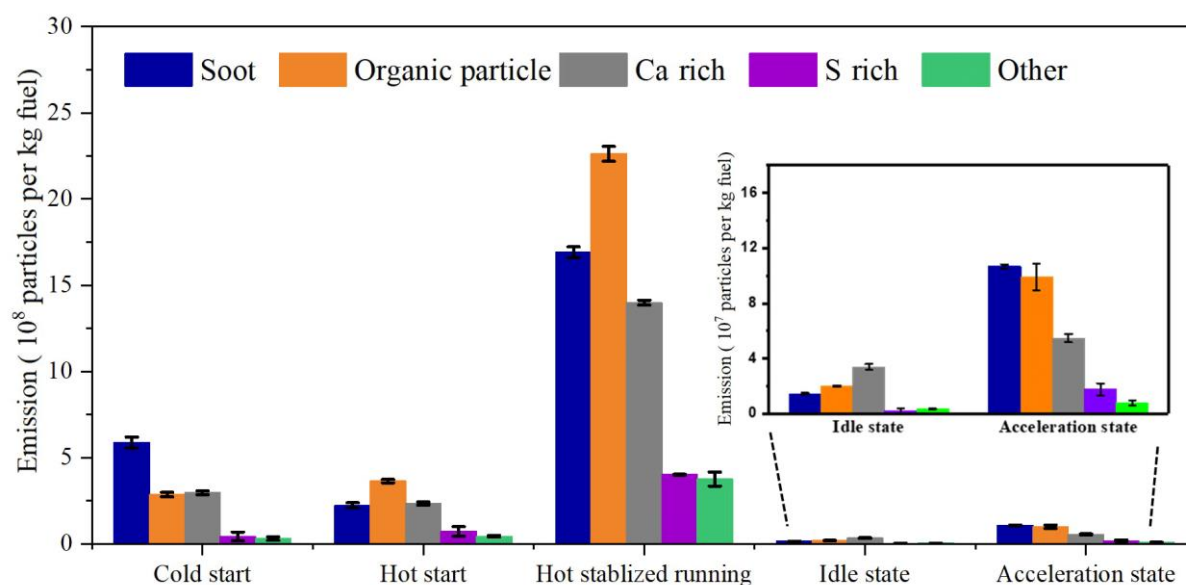


Figure 46: The number of different types of particles in the emissions from the GDI vehicle under the different running states by the burning per unit of fuel, including cold-start, hot-start, hot stabilized, idle, and acceleration states. Data presented as mean \pm standard deviation, N=3 from (Xing et al., 2020)

(Gentner et al., 2017) reviewed the SOA formation from gasoline and diesel vehicles. They proposed a picture of the composition of the OA emission as a function of carbon number. Fuel composition, engine design/technology (including computerized control), and exhaust aftertreatment technology are all determining factors in the composition of emissions. Gasoline engines use spark ignition of a lower molecular weight fuel with compounds in the C4–C10 range (premixed with air) compared to diesel engines with compression ignition of heavier fuels (C9–C25) at higher temperatures and fuel-lean conditions to achieve greater efficiencies (Figure 47). The organic composition of gasoline and diesel fuel has been intentionally controlled over the past 50 years in the U.S. and elsewhere via several regulated reformulations. They were modified to improve engine performance, fuel efficiency, and compatibility with catalytic converters, and also to reduce emissions (organic gases/aerosols, CO, NO_x, BC, SO₂, lead) and to minimize the ambient photochemical production of ozone (O₃) from emissions of reactive VOCs and NO_x. Reformulations have reduced volatility, reactivity, trace impurities, and/or propensity for forming NO_x, CO, or BC in the exhaust.

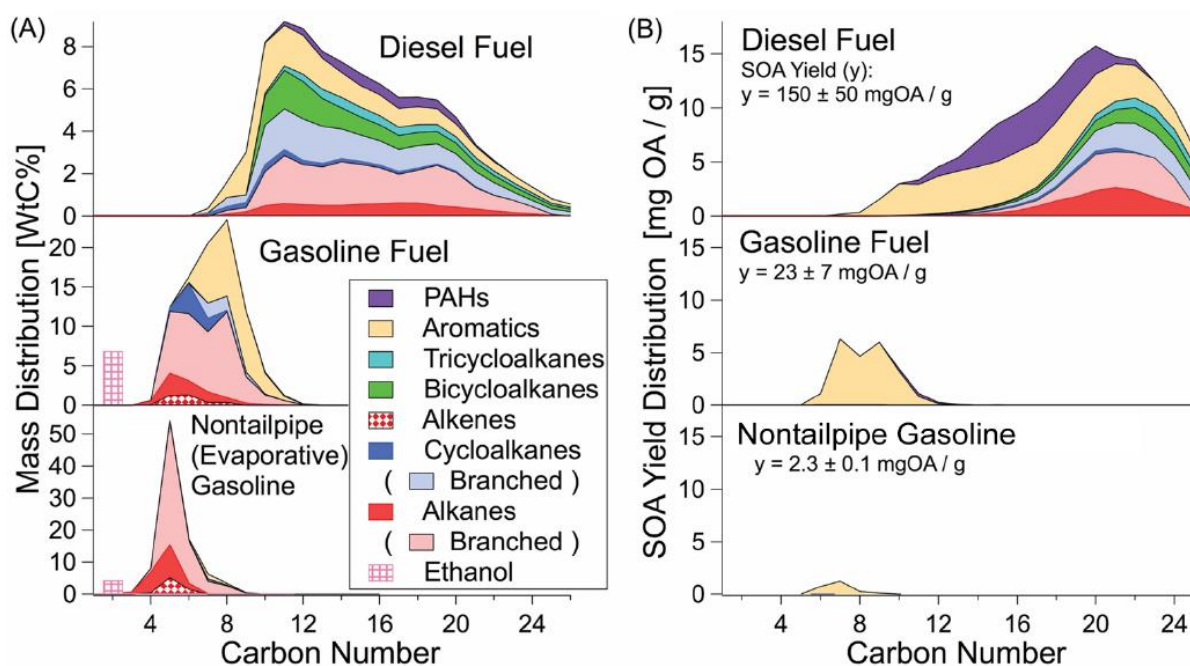


Figure 47: (A) Chemical composition of diesel fuel, gasoline, and evaporative gasoline emissions, with (B) SOA yield of each emission profile shown as a sum of SOA contributions; both are shown as a function of compound class and carbon number. Partitioning of oxidation products is calculated at an organic aerosol concentration of $10 \mu\text{g m}^{-3}$ after ~ 6 h of photochemical aging. Note: “branched cycloalkanes” refers to those with more than a single linear alkyl substituent (Gentner et al., 2017)

(Muñoz et al., 2018) investigated the co-formation and co-release of genotoxic PAHs, alkyl-PAHs and soot nanoparticles from gasoline direct injection vehicles. They hypothesized that particles are released together with polycyclic aromatic hydrocarbons (PAHs) formed under the same combustion conditions. Emission data of a fleet of 7 GDI vehicles (1.2–1.8 L) including Euro-3,-4,-5 and -6 technologies revealed substantial particle emissions on average of 2.5×10^{12} particles km^{-1} in the cold worldwide harmonized light vehicle test cycle (cWLTC), the future European legislative driving cycle. Particle emissions increased 2–3 orders of magnitude during acceleration like CO, indicating that transient driving produces fuel-rich conditions with intense particle formation. For comparison, an Euro-5 diesel vehicle (1.6 L) equipped with a particle filter released 3.9×10^{10} particles km^{-1} (cWLTC), clearly within the Euro-5/6 limit value of 6.0×10^{11} particles km^{-1} and 64-fold below the GDI fleet average. PAH and alkyl-PAH emissions of the GDI vehicles also exceeded those of the diesel vehicle. Mean GDI emissions of 2-, 3-, 4-, 5- and 6-ring PAHs in the cWLTC were 240, 44, 5.8, 0.5 and 0.4 $\mu\text{g km}^{-1}$, those of the diesel vehicle were only 8.8, 7.1, 8.6, 0.02 and 0.02 $\mu\text{g km}^{-1}$, respectively. Thus, mean PAH emissions of the GDI fleet were 2 orders of magnitude higher than the benchmark diesel vehicle. A comparison of the toxicity equivalent concentrations (TEQ) in the cWLTC of the GDI fleet and the diesel vehicle revealed that GDI vehicles released 200–1700 ng TEQ m^{-3} genotoxic PAHs, being 6–40 times higher than the diesel vehicle with 45 ng TEQ km^{-1} (Figure 48). The co-release of genotoxic PAHs adsorbed on numerous soot nanoparticles is critical due to the Trojan horse effect describing the property of sub-200 nm particles being deposited in the alveoli transporting genotoxic compounds into the lung. These nanoparticles are persistent and may eventually penetrate the alveolar membrane reaching the blood circulation system. They showed that **all GDI vehicles tested, released large numbers of nanoparticles carrying substantial loads of genotoxic PAHs**. If non-treated diesel exhaust is considered as class-1 carcinogen by the WHO inducing lung cancer in humans, these GDI vehicle exhausts may be

a major health risk too for those exposed to them, corroborating the progress achieved with current diesel vehicles, now equipped with efficient particle filters.

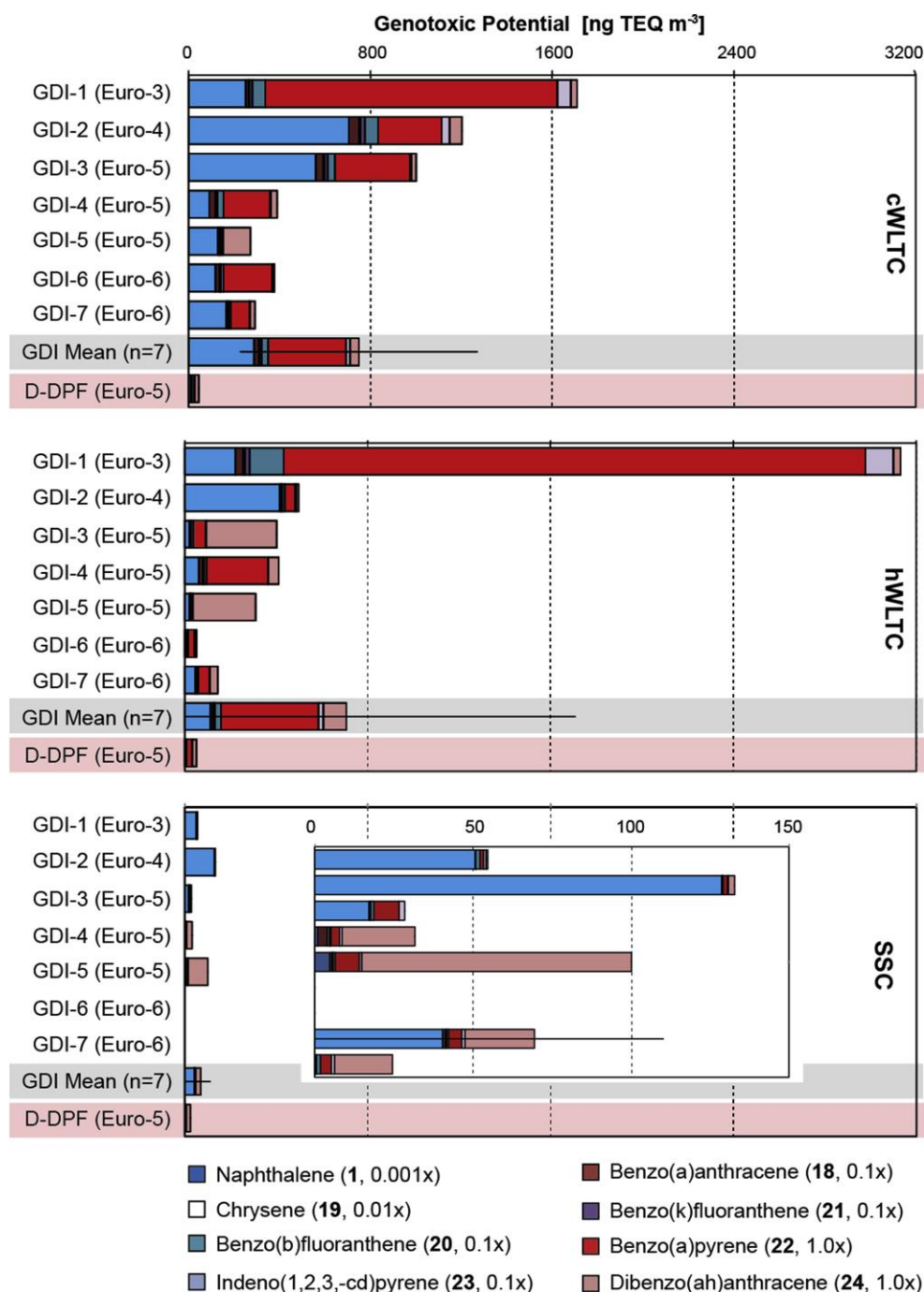


Figure 48: Cumulated and weighted genotoxic potential of GDI- and diesel vehicle exhausts (ng TEQ m⁻³) in the cold (upper), hot WLTC (middle) and the Start / Stop Coasting (SSC) (lower diagram). Mean values (\pm standard deviation) of the GDI fleet (n = 7) and the benchmark diesel vehicle with DPF are highlighted in grey and red. A zoom of the SSC data is also given (bottom) from (Muñoz et al., 2018)

In (Park et al., 2020), BC emissions from passenger cars using different fuels in South Korea were measured (Figure 49). The emissions were categorized according to fuel type and the vehicles were categorized by the engine technology used and the standards applied. Various vehicle speeds were also considered. In all types of vehicles, BC emission was reduced with driving speeds from low to high, but beyond a certain threshold (65.4 km h⁻¹ or 97.3 km h⁻¹), the emission increased again. In terms of fuel oil type, in NIER (National Institute of

Environmental Research) modes with preheating, the emission of GDI vehicles were $0.0032\text{--}0.27\text{ mg km}^{-1}$, and the highest value of 0.16 mg km^{-1} was observed in the regulation mode that included the cold start section. Diesel vehicles with DPF and LPG (Liquefied Petroleum Gas) vehicles showed low levels of emissions at 0.01 mg km^{-1} or less in NIER modes, and at 0.045 mg km^{-1} and 0.0009 mg km^{-1} in regulation modes, respectively. Among gasoline vehicles, GDI vehicles showed BC emissions of 2.8–5 times higher than that of MPI (Multi-Point Injection) vehicles. With the tightening of regulations, MPI vehicles showed reduced PM emissions other than BC. Among diesel vehicles, EURO 3 vehicles without DPF showed emissions of $6.21\text{--}66\text{ mg km}^{-1}$, which is estimated to be at least 1500 times higher than regulated vehicles with DPF. This confirms that DPF reduces BC emissions. **With the application and tightening of PM regulations, both gasoline and diesel vehicles exhibited reduced BC emissions as well as PM emissions.**

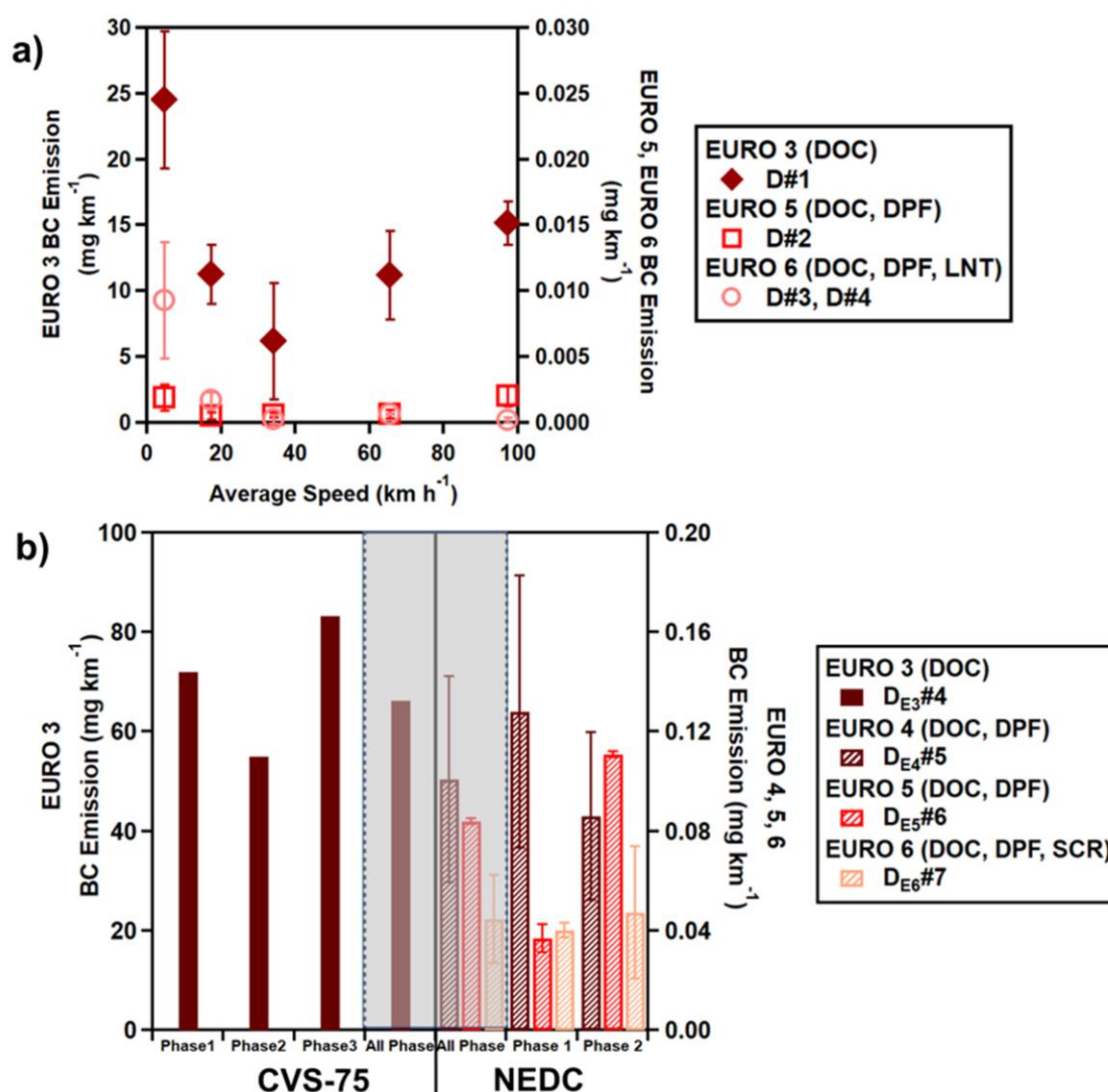


Figure 49: (a) Results of BC emission of EURO 3, 5, and 6 on five different NIER modes. (b) BC Emission from EURO 3 on CVS-75 mode, and EURO 4, 5, and 6 on NEDC mode as presented in (Park et al., 2020)

(Louis et al., 2016a) tested diesel and gasoline vehicles. Gasoline DI vehicle emitted 25% more CO₂ than Diesel vehicles for all ARTEMIS and NEDC driving conditions. The GDI emitted 2 to 200 times more PN and BC and 5 to 150 times less NO_x than Diesel vehicles. Comparing to Diesel catalysed DPF, additive DPF vehicles emitted 2 times more NO₂. No significant

differences were observed between additive and catalysed DPF for CO₂ and NO_x emissions. Moreover, a clear impact of cold start on emission was observed during their experiments. **Black carbon emissions were the highest by far for the GDI reaching $1531 \pm 207 \mu\text{g km}^{-1}$ and exhibited the highest PN emissions for the cold start ARTEMIS urban cycle.**

4.2.5 Impact of renewable fuels on emissions

(Pirjola et al., 2019) studied the potential of renewable fuel to reduce diesel exhaust particle emissions. Diesel exhaust emissions including particle number concentration and size distribution along with the particles' chemical composition and NO_x were investigated from a Euro 4 passenger car with a comprehensive set of high time-resolution instruments. The emissions were compared with three fuel standards – European diesel (EN590), Indian diesel (BS IV) and Finnish renewable diesel (Neste MY) – over the New European Driving Cycle (NEDC) and the Worldwide harmonized Light vehicles Test Cycle (WLTC). Fuel properties and driving conditions strongly affected exhaust emissions. The exhaust particulate mass emissions for all fuels consisted of BC (81–88%) with some contribution from organics (11–18%) and sulphate (0–3%). As aromatic-free fuel, the MY diesel produced around 20% lower black carbon (BC) emissions compared to the EN590 and 29–40% lower compared to the BS IV (Figure 50). High volatile nanoparticle concentrations at high WLTC speed conditions were observed with the BS IV and EN590 diesel, but not with the sulphur-free MY diesel. These nanoparticles were linked to sulphur-driven nucleation of new particles in cooling dilution of the exhaust. For all the fuels, non-volatile nanoparticles in sub-10 nm particle sizes were observed during engine braking, and they were most likely formed from lubricant-oil-originated compounds. With all the fuels, the measured particulate and NO_x emissions were significantly higher during the WLTC cycle compared to the NEDC cycle. **This recent study demonstrated that renewable diesel fuels enable mitigations of particulate and climate-warming BC emissions of traffic and would simultaneously help tackle urban air quality problems.**

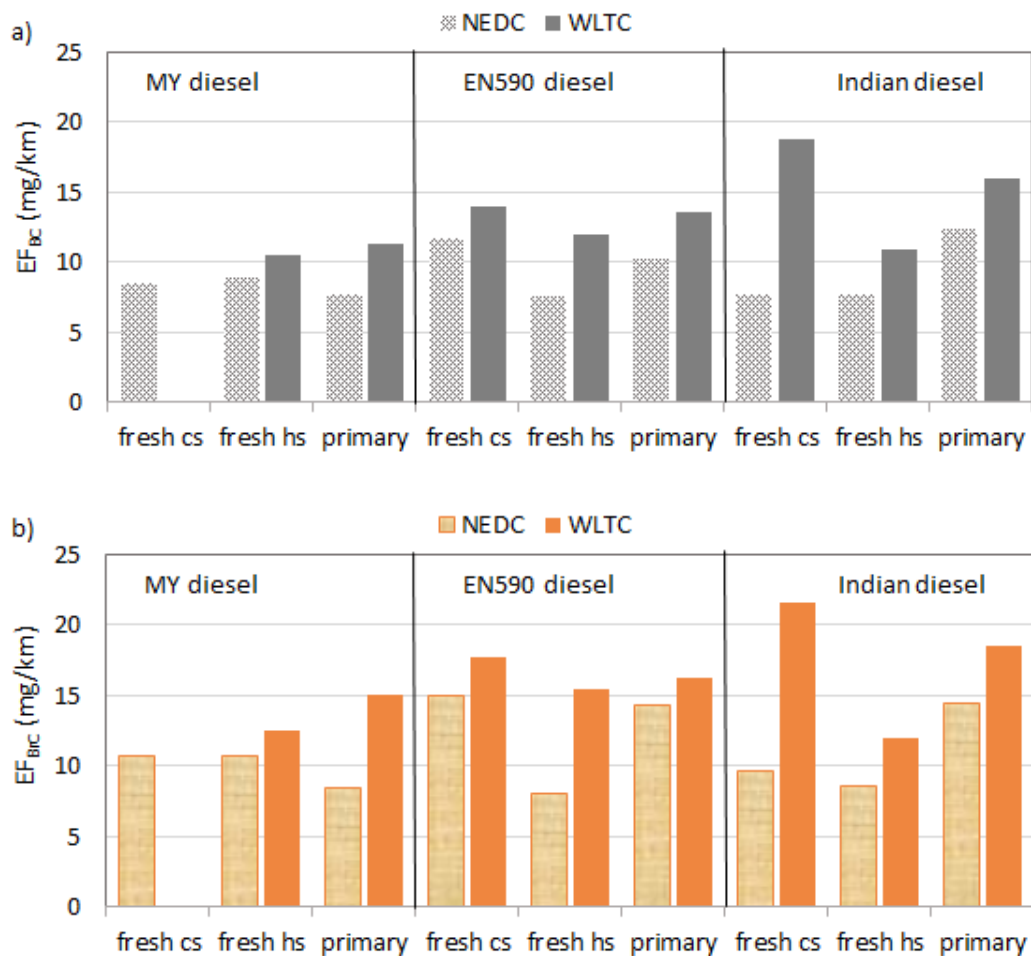


Figure 50: Primary and fresh exhaust emission factors (mg/km) for BC (a) and BrC (b) during the NEDC and WLTC with different fuels (MY diesel, EN950, Indian diesel). Emission factors were calculated from the AE33 data (880 nm for BC and 370 nm for BrC). Note that cs and hs refer to the cold start and hot start cycles, respectively from (Pirjola et al., 2019) in supplementary material.

Hydrotreated vegetable oil (HVO) diesel fuel was considered a promising biofuel candidate that could complement or substitute traditional diesel fuel in engines (Happonen et al., 2012; Hartikka et al., 2012). It has been already reported that by changing the fuel from conventional EN590 diesel to HVO (Hydrotreated Vegetables Oils) decreases exhaust emissions up to -30% for PM. However, as the fuels have certain chemical and physical differences, it is clear that the full advantage of HVO cannot be realized unless the engine is optimized for the new fuel. In this article, they studied how much exhaust emissions can be reduced by adjusting engine parameters for HVO. The results of (Happonen et al., 2012) indicate that, with all the studied loads (50%, 75%, and 100%), **particulate mass and NOx can both be reduced over 25% by engine parameter adjustments**. Further, the emission reduction was even higher when the target for adjusting engine parameters was to exclusively reduce either particulates or NOx.

The effect of biofuel use on the operation of Diesel Exhaust Aftertreatment System was investigated both numerically and experimentally by (Cordiner et al., 2016), by focusing on the contribution of three main factors: raw PM–NOx emissions trade-off, NO–NO₂ conversion efficiency of the Diesel Oxidation Catalyst (DOC) and PM reactivity toward oxidation. The possibility of limited interventions on assessed engine technologies is key toward the

deployment of the potential related to fuel-based greenhouse reduction policies, for both road and non-road markets. To verify its impact on the Aftertreatment System, a Diesel engine for non-road applications has been tested with Waste Cooking Oil (WCO) biodiesel blended with commercial fossil fuel at 6% and 30% v/v. Six engine operating modes have been selected as the most representative of the reference standard cycle (NRTC) for non-road Diesel engines and have been run to evaluate the biodiesel impact on engine emissions. Experimental results indicate a significant reduction of soot emissions, in line with literature trends, especially at high loads, as fuel oxygen enhances oxidation in the fuel rich regions of the combustion chamber. On the other side, only a slight increase in NO_x emissions has been observed, along with a similar trend of the equivalence ratio due to both the lower heating value and stoichiometric air/fuel ratio of biodiesel in comparison with fossil fuelling.

4.2.6 Impact of real driving conditions

(Simonen et al., 2019) present the characterization of real-drive emissions from three Euro 6 emission level passenger cars (two gasoline and one diesel) in terms of fresh particles and secondary aerosol formation. The gasoline vehicles were also characterized by chassis dynamometer studies. In the real-drive study, the particle number emissions during regular driving were 1.1-12.7 times greater than observed in the laboratory tests (4.8 times greater on average), which may be caused by more effective nucleation process when diluted by real polluted and humid ambient air. However, the emission factors measured in laboratory were still much higher than the regulatory value of 6×10^{11} particles km⁻¹. The higher emission factors measured here result probably from the fact that the regulatory limit considers only non-volatile particles larger than 23 nm, whereas here, all particles (also volatile) larger than 3 nm were measured. Secondary aerosol formation potential was the highest after a vehicle cold start when most of the secondary mass was organics. After the cold start, the relative contributions of ammonium, sulfate and nitrate increased. Using a novel approach to study secondary aerosol formation under real-drive conditions with the chase method resulted mostly in emission factors below detection limit, which was not in disagreement with the laboratory findings.

Regarding the emission of a EUROVI HDV real driving emissions (Grigoratos et al., 2019) found that solid PN emission levels of tested vehicles appear to be not of concern due to the effectiveness of the currently available DPF systems. Calculated emission factors are one order of magnitude lower than the current laboratory type approval limit and appear to be at the lower limit of the range given in the literature for older technology HDVs featuring a DPF system.

In a real world (Preble et al., 2019) has studied the evolution of BC concentrations in a tunnel in San Francisco. Compared to baseline measurements made in 2010 at the same location, the median truck model year observed in 2018 increased by 9 years, and DPF and SCR penetration increased from 15 to 91% and 2 to 59%, respectively. Over this period, fleet-average emission rates of BC and NO_x decreased by 79 and 57%, respectively. Fleet-average NO₂ emission rates remained about the same, despite the intentional oxidation of engine-out NO to NO₂ in DPF systems, due to the effectiveness of SCR systems in reducing NO_x emissions and mitigating the DPF-related increase in primary NO₂ emissions. Fleet-average emissions of NH₃ and N₂O increased from near-zero to levels that are comparable to NH₃ emissions from three-way catalyst-equipped light-duty cars, and to levels about equal to the N₂O emission limit for heavy-duty trucks. The NO_x emission reduction is about 150 times the increase in NH₃, which is a precursor to atmospheric formation of ammonium sulfate and ammonium nitrate.

4.2.7 Brake and tyre emissions

While the exhaust emissions decrease continuously due to improved exhaust aftertreatment and filter technologies, the non-exhaust share is increasing because of rising vehicle mileage. According to the recent results of the European Environment Agency (EEA), a significant fraction of 33.9% and 26.7% of the road transport-related PM is assigned to automobile tire and brake wear for PM10 and PM2.5, respectively. Further studies consider brake wear separately and report contributions of 21% to the traffic related PM10 in urban areas (Farwick zum Hagen et al., 2019).

(Ntziachristos and Boulter, 2019) chapter of the EEA guidebook covers the emissions of particulate matter (PM) including black carbon (BC) which are due to road vehicle tyre and brake wear (NFR code 1.A.3.b.vi), and road surface wear (NFR code 1.A.3.b.vii). PM emissions from vehicle exhaust are not included. The focus on primary particles — in other words, those particles emitted directly as a result of the wear of surfaces — and not those resulting from the resuspension of previously deposited material.

Table 16: Emission factors ranges for vehicles from two-wheeled to light heavy duty vehicles according to the Tier 2 methodology (Ntziachristos and Boulter, 2019)

	Tires	Brakes	Road wear
<i>TSP EF (mg km⁻¹)</i>	4.6 – 16.9	3.7 – 11.7	6 - 15
<i>Fraction (%)</i>			
<i>TSP</i>	100	100	100
<i>PM10</i>	60	98	50
<i>PM2.5</i>	42	39	27
<i>PM1</i>	6	10	-
<i>PM0.1</i>	4.8	8	-

The black carbon fraction is on average equal to 15.3% of TSP for tire and brake wear. (European Commission. Joint Research Centre. Institute for Energy and Transport., 2014; Grigoratos and Martini, 2015) proposed a review of brake wear emission factors. PM10 usually displays a unimodal mass size distribution with maxima between 2 and 6 μm with on average a PM10 EF of 6.7 $\text{mg km}^{-1} \text{ vehicle}^{-1}$. Particle number distributions of brake wear PM10 appear to be bimodal with both peaks lying within the fine mode. Most researchers report one peak of the distribution being among ultrafine particles (< 100 nm), while others find it at somewhat bigger sizes (approximately 300 nm) & The most important chemical constituents of brake wear are Fe, Cu, Ba and Pb. Organic carbon is also present in significantly higher concentrations compared to elemental carbon. On the other hand, there is very limited information regarding specific organic constituents of brake wear PM10. In addition (zum Hagen et al., 2019) found a particle number PN emission factor of approximately $4.9 \times 10^{10} \text{ km}^{-1} \text{ brake}^{-1}$ is estimated for realistic vehicle brake temperatures. The brake drag was estimated to contribute about 34% to the total airborne particle mass emission.

(Lyu and Olofsson, 2020) studied the content of BC in brake wear particles. This study used a pin-on-disc tribometer to simulate automotive disc brake system and investigate its black carbon emission. The results verified the existence of black carbon emission from disc brake system. Brake pad surface treatment and graphite content also have strong influence on black

carbon emission of disc brake contact. A scorched brake material features lower black carbon and particulate matter emissions than non-scorched brake materials. Meanwhile, high graphite content in the brake material tends to expedite black carbon emission. Black carbon emission shows a proportional correlation (Figure 51) with PM1 levels from disc brake system (about 20-30% of PM1). The fraction of black carbon in PM1 depends on the surface condition and graphite content of the brake materials.

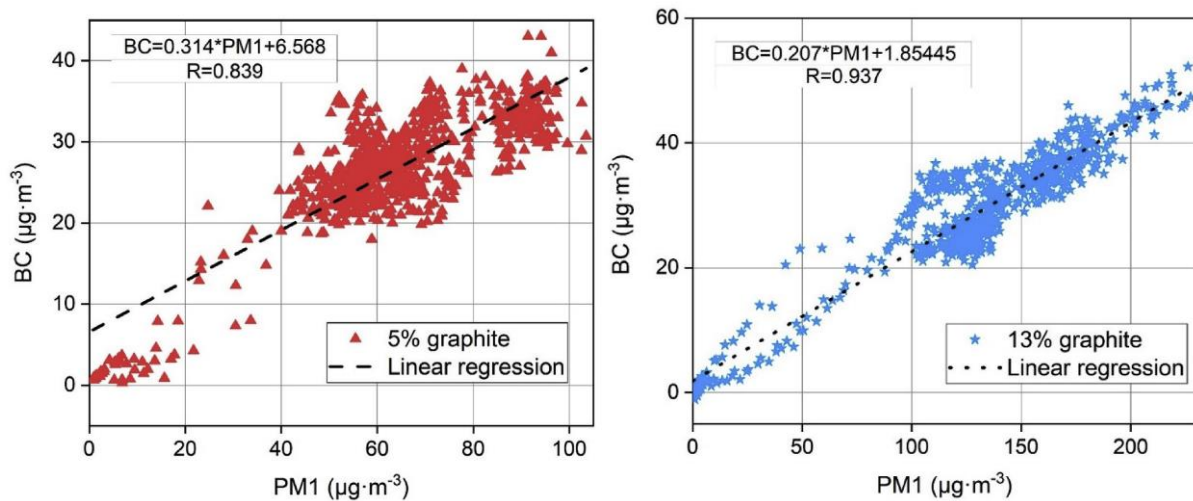


Figure 51: BC against simultaneous PM1 from 5 and 13% graphite brake material with correlated linear regression from (Lyu and Olofsson, 2020)

(Farwick zum Hagen et al., 2019) studied on-road vehicle measurements of brake wear particle emissions. For the conventional brake pad material, the TSP EF was in the range of 1.4–2.1 mg km⁻¹ brake⁻¹, while the use of a novel material composition showed about 18% lower PM10 emissions. Regarding particle numbers, the EF reached total numbers of 2×10¹²- 1.3×10¹³ km⁻¹ brake⁻¹, which was dominated by UFP emissions during high brake temperature sections and included volatile particles. The novel material produced about 60% less particles. However, the PN emissions were obtained during unrealistic high temperature sections and were not representative for realistic driving. For temperatures observed at the reference brake, the PN EF would not exceed 1×10¹⁰ km⁻¹ brake⁻¹. The critical brake temperature at which UF emission occurred, was found at 168 °C and 178 °C for the conventional and novel material, respectively. The temperature of the reference brake did not exceed 153 °C during the same test, thus UF brake emissions are not expected during normal driving.

(Mathissen et al., 2011) studied the potential generation of ultrafine particles from the tire road interface was investigated during real driving. An instrumented Sport Utility Vehicle equipped with summer tires was used to measure particle concentrations with high temporal resolution inside the wheel housing while driving on a regular asphalt road. Different driving conditions, *i.e.*, straight driving, acceleration, braking, and cornering were applied. For normal driving conditions no enhanced particle number concentration in the size range 6–562 nm was found. Unusual manoeuvres associated with significant tire slip resulted in measurable particle concentrations. The maximum of the size distribution was between 30 and 60 nm. An exponential increase of the particle concentration with velocity was measured directly at the disc brakes for full stop brakings.

A dilution tunnel was designed by (Mamakos et al., 2019) for the characterization of brake-wear particle emissions up to 10 µm on a brake dyno. The particulate matter emission levels from a single front brake were found to be 4.5 mg km⁻¹ (1.5 mg km⁻¹ being smaller than 2.5 µm) over a novel real-world brake cycle, for a commercial Economic Commission for Europe (ECE) pad. Particle Number (PN) emissions as defined in exhaust regulations were in the order

of 1.5 to 6×10^9 particles per km per brake ($\# \text{ km}^{-1} \text{ brake}^{-1}$). Concentration levels could exceed the linearity range of full-flow Condensation Particle Counters (CPCs) over specific braking events, but remained at background levels for 60% of the cycle. Similar concentrations measured with condensation and optical counters suggesting that the majority of emitted particles were larger than 300 nm. Application of higher braking pressures resulted in elevated PN emissions and the systematic formation of nano-sized particles that were thermally stable at 350 °C. Volatile particles were observed only during successive harsh braking events leading to elevated temperatures. The onset depended on the type of brakes and their prehistory, but always at relatively high disc temperatures (280 to 490 °C).

The Air Quality Expert Group elaborated mitigation strategies for ambient particle concentrations derived from non-exhaust emissions (NEE) include the following (AQEG, 2019):

- The most effective strategies to reduce NEE relate to traffic management: reduce the overall volume of traffic; lower the speed where traffic is free-flowing (such as trunk roads and motorways); and promote driving behaviour that reduces braking and high-speed cornering.
- Implement regenerative braking, where that does not lead to net disbenefit on road and tyre wear NEE because of increased vehicle mass.
- Establish particle mass (and/or number) and particle-associated metal emissions limits for brake pad and tyre technologies (including chemical formulation).
- Trap brake wear particles in the braking system before release into ambient air, although this technology is currently unproven.
- Reduce the material that is tracked onto public road surfaces as a result of vehicle movements in and out of construction sites, waste-management sites, quarries, farms, and similar.
- Wash and sweep streets and/or treat street surfaces for dust suppression; it is noted, however, that impacts on airborne PM from trials of these approaches have so far proven inconsistent and any benefits have been short-lived in nature.

To tackle brake emissions, the company Tallano has developed a brake particles collection system named TAMIC (Hascoët and Adamczak, 2020). TAMIC was designed to trap at least 80% of brake particles directly at the pad-disc interface without altering braking efficiency. It is composed of a brake calliper especially designed for the integration of grooved pads and of an aspiration system where brake particles are trapped. The aspiration system relies on pipes connected to a turbine equipped with a high efficiency filter. The whole system is driven by an embedded electric brushless motor. Several types of characterizations, like PIV (Particles Image Velocimetry) and simulations have been performed. Mass and number collection efficiencies have been assessed on brake rigs. A mass efficiency above 85% and a number efficiency up to 90% have been achieved. Performances on vehicle and impact on its behaviour have also been verified on test track and in real driving conditions with same level of collection performances.

4.2.8 Post Euro 6 regulations

The European Commission has started the regulatory work aimed at the next stage of emission standards (Rodríguez et al., 2019). Post-Euro 6 standards are expected to continue to improve the emissions performance of new road vehicles, addressing their contribution to the persistent

air quality issues across Europe. The objective of this paper is to highlight issues and limitations of the current standards, compare them to current and future regulations in other parts of the world, and offer policy recommendations. ICCT made the following recommendations, summarized in Table 17, on the different topics that should be considered for the light-duty post-Euro 6 standards.

These recommendations on PN and semi-volatile are supported by international researches like the recent works of (Xing et al., 2020) on gasoline vehicles GDI (Gasoline Direct Injection) in Beijing. Their results indicated that GDI-engine vehicles emitted a large amount of both primary and secondary organic aerosol. PM number emissions of organic particles from GDI-engine vehicle were 2.9×10^9 particles per kg fuel during the Beijing Driving Cycle. Secondary organic particles were predominant in the secondary aerosols, accounting for 80%–85 % of particles in the chamber. Their results also showed that POA emitted by GDI-engine vehicles could acquire OA and sulphate coatings rapidly, within a few hours, and increase a sizable fraction of total ambient aerosols existing as internal mixtures. In addition, the fast ageing further caused the increase in aged POA in the total OA; this consequently largely modified the properties of the particles such as their optical properties. The results of the experiments in the chamber showed that most of the aged POA had a core–shell structure, whereas most of the SOA produced by gas-phase reactions had a uniform structure. In terms of particle size, the particles exhibited a bimodal distribution in number vs size, with one mode at 800–900 nm and the other at 140–240 nm. The numbers of organic particles emitted under hot-start and hot stabilized states were higher than those emitted under other conditions. The number of soot particles was higher under cold-start and acceleration states. In addition to quantifying the types of particles emitted by the engine, they studied the ageing of the particles during 3.5 hours of photochemical oxidation in an environmental chamber under the Beijing urban environment. Ageing transformed soot particles into core–shell structures, coated by secondary organic species, while the content of sulphur in Ca-rich and organic particles increased. Overall, the majority of particles from GDI-engine vehicles were organic and soot particles with submicron or nanometric size. The particles were highly reactive; they reacted in the atmosphere and changed their morphology and composition within hours via catalysed acidification that involved gaseous pollutants at high pollution levels in Beijing.

In (Suarez-Bertoa et al., 2019), the measured PN from all recent diesel Euro 6 vehicles of the study also point to a very good performance of DPFs and DOCs during real-world operation. However, pollutant emissions that were not a matter of concern at the time the Euro 6 standards were developed, such as CO emissions from gasoline vehicles, or PN emissions from PFI (Port Fuel Injection) gasoline vehicles, were shown to be very high in some instances. Their results, although based on a limited sample, indicate that gasoline vehicles can - under certain conditions - exhibit substantial emissions of CO during RDE tests, and these can be up to eight times higher for Dynamic tests. Moreover, not only GDI vehicles exhibited high PN emissions: PN emissions, sometimes $> 6 \times 10^{11}$ # km⁻¹, were also recorded for PFI. The only GPF-equipped vehicle exhibited the lowest PN emissions of the gasoline vehicles by far (more than one order of magnitude below the PN limit).

Table 17: Summary of recommendations for post-Euro 6 standards by (Rodríguez et al., 2019). Bold characters highlight relevant statements for particulate matter emissions.

<i>Limits</i>	-Introduce fuel- and technology-neutral emission limits -Tighten the emission limits to harmonize with other markets -Introduce application-neutral emission limits
<i>Ultrafine particles</i>	-Lower the size cut-off for particle counting from 23 nm to at least 10 nm -Develop a methodology to measure volatile and semi-volatile particles -Include emissions that occur during filter regeneration -Make particulate number (PN) standards fuel- and technology-neutral -Investigate the feasibility of PN tailpipe measurements
<i>Unregulated pollutants</i>	-Set limits for ammonia emissions -Set limits for CH ₄ and N ₂ O emissions and account for them in the CO ₂ standards -Set limits for aldehyde emissions -Regulate all VOCs and not just HC -Set emission limits for brake wear particles -Consider limits for NO ₂ emissions

These recommendations are in line with some options planned by the European Commission in its roadmap to revise the Euro6/VI standards by setting stringent threshold of ELV and address new pollutants and sources (EC, 2020) with a possible Euro 7/VII regulation entering in force in 2025.

4.2.9 Key conclusions

Diesel particulate filters (DPFs) have been widely used in the motor vehicle industry for decades and found to be cost-effective, including in their reduction of pre-mature deaths and other health problems. In parallel, as PM and BC emissions have decreased with very efficient aftertreatment systems, the PM emissions portion from tires and brakes is continuously increasing. From the recent literature review the following statements can be drawn.

- PM produced by combustion emitted at the exhaust pipe are mostly fine particles below 2.5 µm and are mainly composed of carbonaceous species.
- PM, BC, PN (particle number), and PAH emissions are effectively reduced using tailpipe aftertreatment systems as Diesel Particulate Matter (DPF) or Gasoline Particulate Matter (GPF). Decreases from 90 to 100% are commonly observed for most particulate pollutants.
- As an order of magnitude of PM_{2.5} emission factors, changes from Conventional to Euro VI for Heavy Duty Vehicles (HDV) from 333-491 to 0.5-1.3 mg km⁻¹ can be observed. The fraction of BC in PM ranges from 10 to 20% in Euro VI HDV vehicles.
- Since emission factors of solid particles have decreased by at least 2 orders of magnitude, the counter part is an increase of the part of the OM due to the dilution and cooling effects producing mainly organic condensable species.
- However, the cooling and dilution effects in the exhaust plumes produce less and less absolute emissions of condensables with the implementation of successive Euro legislations. Aftertreatment systems reduce the intermediate volatility organic compounds (IVOC) emissions but there are still several gaps in the knowledge of these compounds and their chemical transformation after emissions and in ambient conditions.

- With the decrease of PM emissions, gasoline vehicles even recent, can now produce more particles. The use of GPF for gasoline is a key technology to reduce PN and PM emissions. However, a study has reported larger genotoxic PAH emissions from gasoline vehicles (mainly Gasoline Direct Injection vehicles) even equipped with DPF compared to diesel equipped with DPF (2 orders of magnitude higher).
- Recent research findings show that different after-treatment technologies have an important effect on the level and the chemical composition of the emitted particles, and highlight the importance of the particle filter device conditions and their regular checking to maintain the best performances.
- For non-equipped diesel vehicles, the use of biofuels can reduce BC emissions by 30% and could be an option to achieve sooner the legal air quality thresholds.
- Even if brake, tire and road wear emit mainly coarse particles, a non-negligible fine fraction of PM is emitted. The TSP emissions per km are larger than current Euro 6/VI emissions and a similar fraction of BC is observed either in exhaust and not-exhaust PM emissions. Brakes also produce ultrafine particles, metals and PAHs, the temperature greatly affect the PM emissions. BC emissions from brakes are very correlated to PM1 emissions.
- There is no widely used after-treatment system to control brake, tire and road wear emissions. The type of materials, and the behaviour of the driver is often cited as a key to reduce emissions. Some companies have developed brake particles collection system that would reduce by 80% to 90 % respectively the brake mass and number emissions.
- PM resuspension from the road are also significant. This emission is responsible for a large fraction of total road traffic emissions. It depends on meteorology (wind, temperature, humidity, precipitation) and the site climatology (land use in the vicinity).

4.3 Gas Flaring

4.3.1 Definition and use of Gas Flaring

A relief, vent, or disposal system is an emergency system for discharging gas during abnormal conditions, by manual or controlled means or by an automatic pressure relief valve from a pressurized vessel or piping system, to the atmosphere to relieve pressure in excess of the maximum allowable working pressure or design pressure. The **relief system** may include the relief device, the collection piping, flashback protection, and a gas outlet. A scrubbing vessel should be provided for liquid separation if liquid hydrocarbons are anticipated. The relief-system outlet may be either vented or flared. If designed properly, vent or flare emergency-relief systems from pressure vessels may be combined (Stewart, 2016).

The definition of **gas flaring** is by Canadian Association of Petroleum Producers as the controlled burning of natural gas that cannot be processed for sale or use because of technical or economic reasons (Emam, 2015). Gas flaring can also be defined by the combustion devices designed to safely and efficiently destroy waste gases generated in a plant during normal operation. It is coming from different sources such as associated gas, gas plants, well-tests and other places.

It is collected in piping headers and delivered to a flare system for safe disposal. A flare system has multiple flares to treat the various sources for waste gases. Most flaring processes usually take place at the top of stack by burning of gases with the visible flame. Height of the flame depends upon the volume of released gas, while brightness and color depend upon composition.

Gas flaring systems are installed on onshore and offshore platforms production fields, on transport ships and in port facilities, at storage tank farms and along distribution pipelines. A complete flare system consists of the flare stack or boom and pipes which collect the gases to be flared (Figure 52). The flare tip at the end of the stack or boom is designed to assist entrainment of air into the flare to improve burn efficiency. Seals installed in the stack prevent flashback of the flame, and a vessel at the base of the stack removes and conserves any liquids from the gas passing to the flare. Depending on the design, one or more flares may be required at a process location.

Industrial sites may use gas flaring as an Associated Petroleum Gas (APG) removal process either continuously or intermittently. **Continuous flaring** occurs primarily as a result of a complete, or partial, lack of a utilization route for APG. It is often referred to as routine flaring, although any precise and universally accepted definition of this term does not exist. Globally, the majority of continuous flaring is caused by a lack of market outlets, shortage of local demand or unsuitable geology for reinjection, and is accentuated by the physical, technical, and economic constraints of gas utilization. Flare reduction efforts primarily focus on this type of continuous flaring. A second category of continuous flaring has operational causes related to use of pilot flames, purge gas, and degassing of produced water and glycol regeneration.

Intermittent flaring is undertaken for short periods of time for a variety of operational causes. Intermittent flaring can be further subdivided into:

- (i) **Exploration flaring**, which occurs when large volumes of gas are combusted for short periods of time during a gas oil potential test that is used to determine the production capacity of a well. While the volumes of APG flared can be considered significant, it is only temporary,
- (ii) **Process flaring**, which typically occurs at lower rates during routine gas processing (e.g. when some waste gases are removed from the production stream), is generally considered less significant, however, its frequency can vary during normal operations and plant failures.

- (iii) **Emergency flaring**, which can occur as a result of pressure surges, fires, or other disruptions in infrastructure (e.g. valve, compressor, or pipe failures), may result in the burning of large volumes of gas at high rates over a short duration of time.

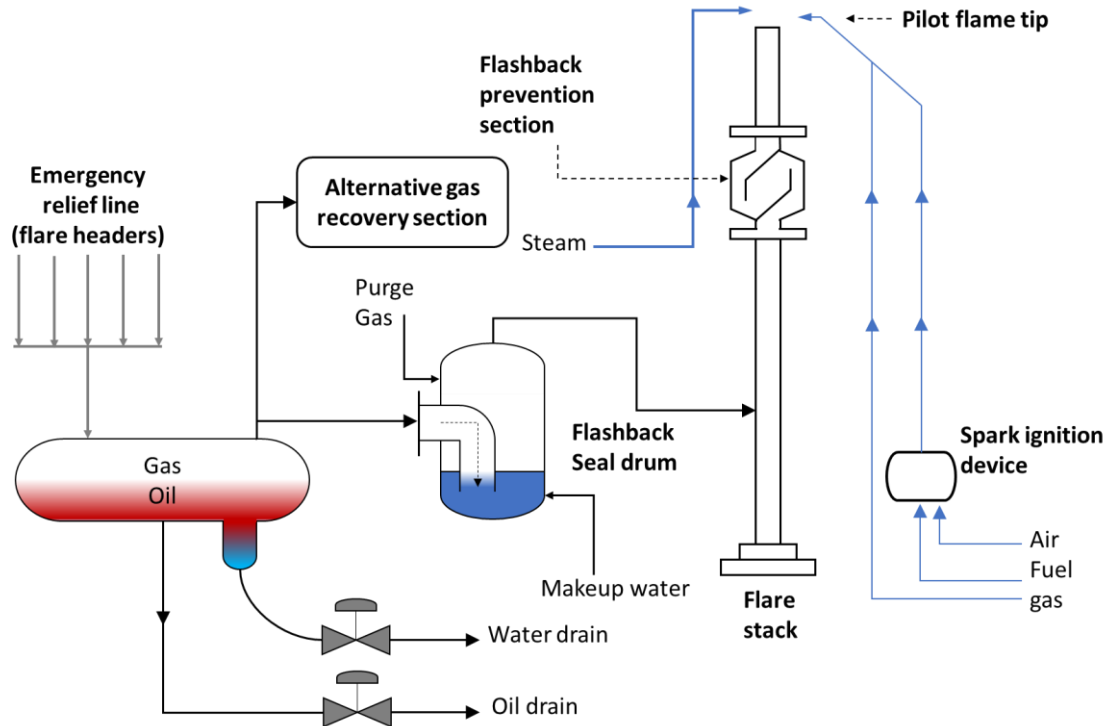


Figure 52: Schematic flow diagram of an overall elevated flare stack system in an industrial plant

4.3.2 Emissions flaring activities

As discussed by (Calel and Mahdavi, 2020), flaring and venting waste 8% of global natural gas production annually, contribute 6% of global greenhouse gas emissions, and disperse a range of pollutants that harm human health and local environments. Capturing and using this gas would be a pro-development, cost-effective means of reducing greenhouse gas emissions, yet current efforts to curtail the problem are struggling to make headway.

In 2015 the World Bank’s Global Gas Flaring Reduction Partnership (GGFR) launched the “Zero Routine Flaring by 2030” initiative (GGFR, 2016), which promotes regulations on flaring and, to a lesser degree, the financing of new gas infrastructure. (Calel and Mahdavi, 2020) in their “Opinion” publication present evidence that both of these approaches are seriously flawed so far. The authors pointed out that while the World Bank and its partners are working to eliminate flaring, they should be mindful of the risk that regulatory solutions might unintentionally drive up venting. To the extent that they pursue gas infrastructure development instead, they would do well to prioritize the adoption of new production taxes as the primary means of financing to mitigate the risk of increasing downstream emissions. Ending the practices of flaring and venting provides an opportunity for rapid low-cost emissions reductions, thus slowing the near-term accumulation of greenhouse gases and reducing the risk of crossing climatic tipping points. Development of remote sensing technologies, production taxes, and investments in infrastructure are essential to this project, but only as a waypoint on the road to a zero-carbon future.

Figure 53 and Figure 54 show the distribution of the volume of gas flaring throughout the world and the evolution from 2014 to 2019. Clearly, close to the Arctic region, Russia and USA could have a large impact on BC impact over Arctic.

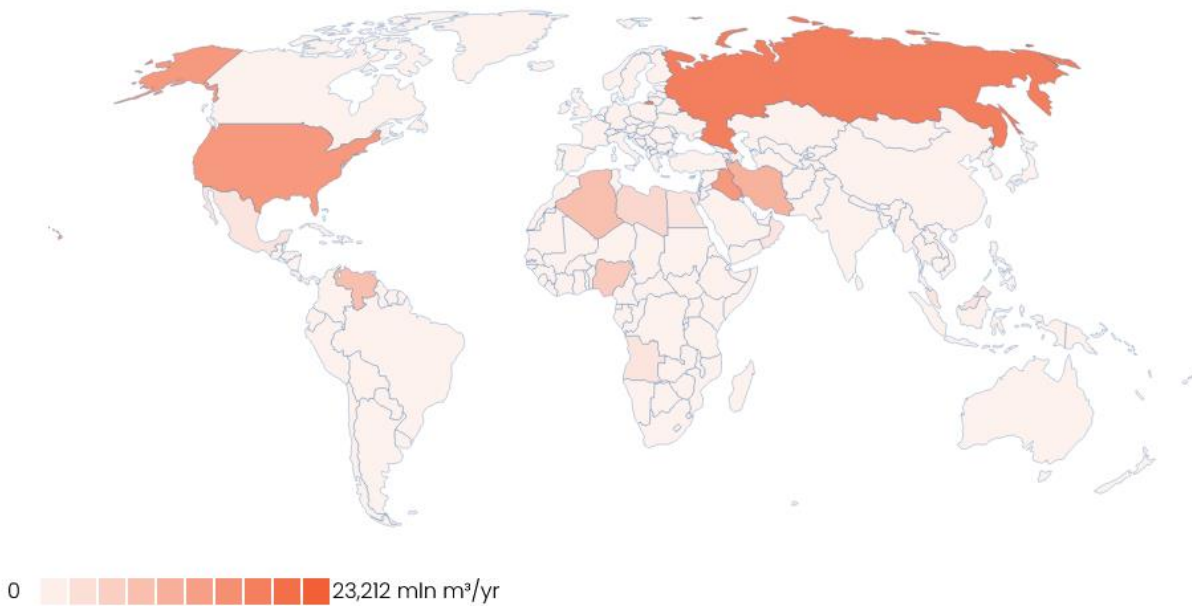


Figure 53: Upstream Gas Flaring 2019 - million cubic meters for flaring - mln m³ yr⁻¹ (GGFR, 2016)

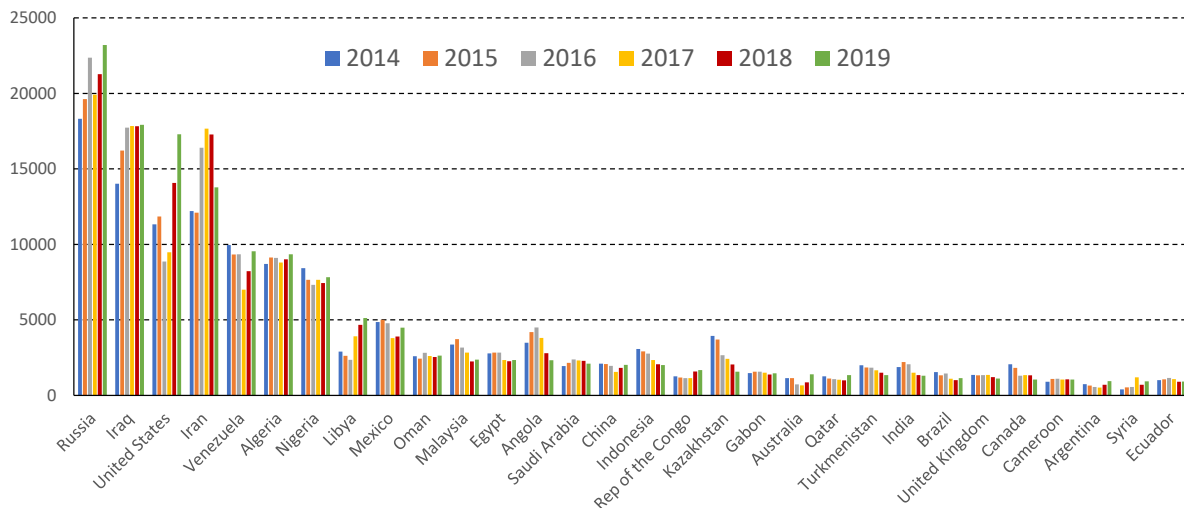


Figure 54: Top 30 Flaring countries by the World Bank (GGFR, 2016)

Satellite observations are commonly used to assess or evaluate emissions from Flaring. (Faruolo et al., 2020) examined the literature pertaining to the analysis of Gas Flaring (GF) with satellite-based observations from the 1970s through July 2019. They classified the methodologies into three main categories: those devoted to identifying gas flares, those aimed at their characterization (temperature, area, and radiant power), and those that assess the environmental impacts of GF by estimating gas-flared volumes as well as air pollutants and GHG emissions. Satellite data have proven to be a useful tool for analysing gas flares, thus improving the knowledge of their spatiotemporal distribution and evolution, which is incomplete if limited to only in situ measurements and publicly available data. RS methodologies utilizing long-term time series acquired by multiple optical and Specific Absorption Rate (SAR) sensors spanning several decades have been developed to fulfil the requirement of comprehensive and accurate information on Offshore platforms, which effectively support the conventional surveys. The

availability of global observations from multiple sensors guaranteed by current and future satellite missions makes it possible to extend and further improve the consistency and reliability of gas flare monitoring. Further, substantial efforts also have to be made for using daytime images. To date, using satellite-based approaches allows for locating flaring sites and computing their temperature, area, and radiant power.

Reasonable estimations of flared volumes and GF emissions can then be inferred from the aforementioned parameters with empirical calibrations over regions that are well observed on the ground. The main issues affecting the quantitative accuracy of satellite estimates arise from the lack of reference data and the great variability in the chemical process, both of which introduce discrepancies with current inventories. Relatively recent satellite launches of more sophisticated sensors (*e.g.*, the SLSTR/Sentinel 3, VIIRS/NPP and NOAA-20, OLI/Landsat-8, and TROPOMI/Sentinel-5P) provide optimism for continued and lasting advances related to the study of GF. These newer sensors, featuring higher spatial and spectral resolution, have greater capabilities for remotely studying GF, which may improve the scientific understanding of these systems and minimize the need for extensive field measurements. Data derived from satellite imagery have provided interesting results on this phenomenon, both regionally and globally, since the 1990s.

As an example, recent estimates from (Caseiro et al., 2020) propose emission of BC to the atmosphere by gas flaring in 2017 at 73 Gg with a confidence interval of [20-239] Gg, with Iraq, Iran, Russia, and Algeria being responsible for roughly one-half of those emissions. The most active flaring location, which is also the one with the highest emissions, is estimated to have yearly emissions of 0.35 Gg of BC in 2017. This study shows that the SLSTR instruments on-board the Copernicus Sentinel-3 satellites are well suited for the quantitative characterisation of the gas flares in terms of flame temperature, size, and radiative power, as well as BC emissions. This will allow to increase the detection opportunity for gas flares in an observation system that comprises SLSTR and VIIRS instruments.

For Russia, (Evans et al., 2017) estimated BC emissions at 688 Gg and OC emissions at 9224 Gg in 2014. They found that Arctic forcing from Russia's BC and OC emissions is 39% lower than was previously estimated by (Sand et al., 2016), to a large extent because of policy interventions that have reduced emissions from flaring and transportation.

Large discrepancies are usually observed for GF emissions likely due to either differences in the methodologies used to estimate the emissions, in the values of the emission factors considered, or in the definition of flaring sector. Estimations from (Doumbia et al., 2019) suggest that BC flaring emissions in Africa account for 1–15% (on average 7% of African total anthropogenic emissions (Table 18).

Table 18: Comparison of flaring emissions in Africa by (Doumbia et al., 2019), ECLIPSEv5a, EDGARv4.2 in 2005. For (Doumbia et al., 2019), a range of emissions using lowest and highest EFs is provided. The unit is in kiloton (kt yr⁻¹).

Species	Source	Africa
OC	(Doumbia et al., 2019)	6.6
	ECLIPSEv5a (Stohl et al., 2015)	16.1
	EDGAR4.3 (Janssens-Maenhout et al., 2012)	0.04
BC	(Doumbia et al., 2019)	6.2-141.2
	ECLIPSEv5a (Stohl et al., 2015)	80.6
	EDGAR4.3 (Janssens-Maenhout et al., 2012)	0.46

4.3.3 BC Gas Flaring emissions factors

Gas flaring is an important source of VOCs, CO, CO₂, SO₂, PAH, NO_x and soot (black carbon), all of which are important pollutants which interact, directly and indirectly, in the Earth's climatic processes. Globally, over 130 billion cubic metres of gas are flared annually. We review the contribution of gas flaring to air pollution on local, regional and global scales, with special emphasis on black carbon (BC as “soot”). The temporal and spatial characteristics of gas flaring distinguishes it from mobile combustion sources (transport), while the open-flame nature of gas flaring distinguishes it from industrial point-sources; the high temperature, flame control, and spatial compactness distinguishes gas flaring from both biomass burning and domestic fuel-use. All of these distinguishing factors influence the quantity and characteristics of BC production from gas flaring, so that it is important to consider this source separately in emissions inventories and environmental field studies. Estimate of the yield of pollutants from gas flaring have, to date, paid little or no attention to the emission of BC with the assumption often being made that flaring produces a smokeless flame. In gas flares, soot yield is known to depend on a number of factors, and there is a need to develop emission estimates and modelling frameworks that take these factors into consideration. Hence, emission inventories, especially of the soot yield from gas flaring should give adequate consideration to the variation of fuel gas composition, and to combustion characteristics, which are strong determinants of the nature and quantity of pollutants emitted. The buoyant nature of gas flaring plume, often at temperatures in the range of 2000 K, coupled with the height of the stack enables some of the pollutants to escape further into the free troposphere aiding their long-range transport, which is often not well-captured by model studies (Fawole et al., 2016).

According (Conrad and Johnson, 2019), **flare-generated carbon was found to be primarily elemental in composition (typically >92%)**, and most probably externally-mixed based on detailed analysis of attenuation vs. evolved carbon data and consideration of flare-specific mechanisms for organic carbon emissions. Single-particle analysis revealed the dominance of elemental carbon vs. oxidized and metal-contaminated particles for a small scale gas Flaring (Popovicheva et al., 2019), and infrared spectroscopy showed the presence of alkanes and aromatics with oxygenated compounds. Intercomparing the microstructure and the composition, shows the vast majority of particles are hydrophobic. This high level of BC has also been identified by (Fortner et al., 2012) who also provide particle number distributions for different Flare operating conditions (Figure 55). The figure shows the change in propene flare particle size distributions with Destruction Removal Efficiencies (DRE). At high DREs the steam assist size mode mobility diameter (D_m) peaks around 90 nm and the air assist size mode D_m appears close to 70 nm. As DRE is reduced particle size mode shifts to smaller sizes as seen. Figure 55 shows the size modes for various DREs going as low as 60%, where size distribution peaks have shifted to 30 and 20 nm for propene mix with steam- and air-assist, respectively. Considering that the BC particles measured are fractal in nature and the SMPS determines a mobility diameter rather than a geometric diameter, the possibility that changes in mobility diameter may actually be due to changes in the shape of the BC particle rather than a change in the geometric diameter of the particle cannot be ruled out.

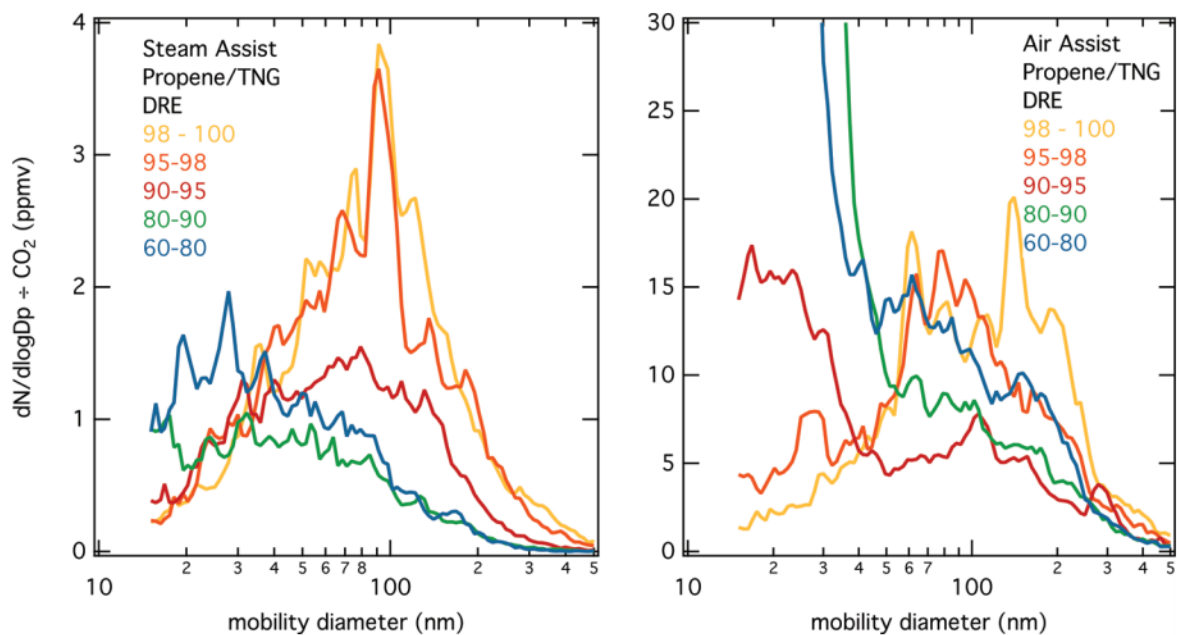


Figure 55: Size modes of PM as determined by SMPS (scanning mobility particle sizer) are depicted as a function of DRE (Destruction Removal Efficiency from 60 to 100%) for steam and air assisted flares. Propene/TNG is 80% propene 20% Tulsa Natural Gas, and Propane/TNG is 80% propane 20% Tulsa Natural Gas. SMPS scanned from 15 to 500 nm mobility diameters in all cases.

Field-measured BC yields in Ecuador (Conrad and Johnson, 2017) are shown in Figure 56 as a function of volumetric Higher Heating Value (HHV) with 95% confidence intervals. A potential range of BC yields from the measurements of (Weyant et al., 2016) in the Bakken region is shown as a shaded area on the graph, where data have been converted from a mass of hydrocarbons basis to a volume of flare gas basis using the cited range of flare gas compositions of seven flares in the Bakken and are plotted spanning the range of heating values in these same samples. The measured BC yields in Ecuador spanned more than 2 orders of magnitude from 0.03 to 3.85 g m⁻³ with **an average of 1.83 g m⁻³**. The heaviest-sooting flare was ~27 times greater than the estimated average for the Bakken region, while only the lightest-sooting flare was within the range of those same measurements.

(Fawole et al., 2016) state that emission factors used for BC emission from gas flaring are inadequate to estimate emission from a typical real-world gas flare as most of the fuels used in the studies for such emission factors are not representative of fuel gas from most Flow Stations around the world. (Dombia et al., 2019) report a large variation of BC emission factors from 0.14 to 3.9 g kg⁻¹ for industrial fires with **1.29 g kg⁻¹** as an average value.

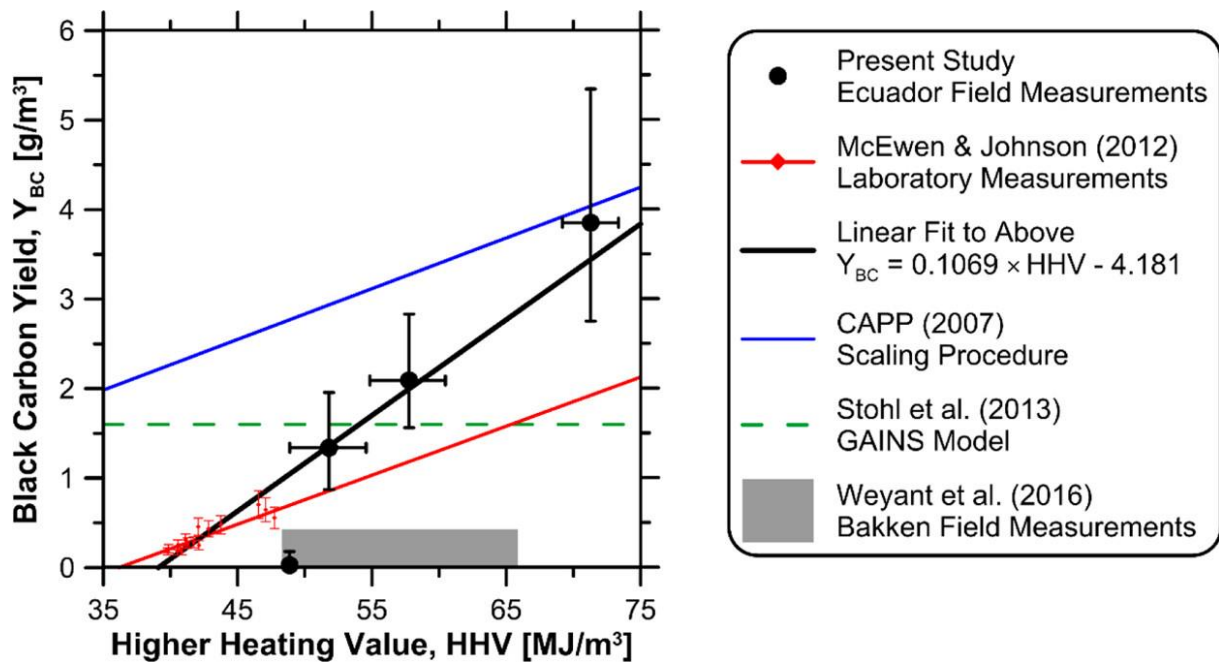


Figure 56: Mean and 95% confidence interval of measured BC yields on a mass-per-volume basis shown as a function of volumetric higher heating value (Conrad and Johnson, 2017)

The EEA guidebook (Plejdstrup et al., 2019) propose official emission factors to elaborate emission inventories for particulate criteria pollutants, Table 19 summarizes some species EF for criteria particulate matter compounds.

Table 19: Emission factors for source category “1.B.2.c Venting and Flaring” (Plejdstrup et al., 2019). * Tier2 and **Tier1

Pollutant	Value	Unit	95% confidence interval		Reference
			Lower	Upper	
TSP*	0.89	g GJ ⁻¹	0.3	3	(CONCAWE, 2015)
PM10*	0.89	g GJ ⁻¹	0.3	3	(CONCAWE, 2015)
PM2.5*	0.89	g GJ ⁻¹	0.3	3	(CONCAWE, 2015)
Benzo(a)pyrene*	0.67	µg GJ ⁻¹	0.134	3.35	(CONCAWE, 2015)
Benzo(b)fluoranthene*	1.14	µg GJ ⁻¹	0.228	5.70	(CONCAWE, 2015)
Benzo(k)fluoranthene*	0.63	µg GJ ⁻¹	0.126	3.15	(CONCAWE, 2015)
Indeno(1,2,3-cd)pyrene*	0.63	µg GJ ⁻¹	0.126	3.15	(CONCAWE, 2015)
BC** as 24% of PM2.5	0.624	g kg ⁻¹ throughput	-	-	(McEwen and Johnson, 2012; Villasenor, 2003)

Figure 57 from (Huang and Fu, 2016) presents a global map of the mean values of $EF_{flare,BC}$ for gas flaring regions identified by the NOAA DMSP nighttime light products (see flaring regions in the following section). The histogram of $EF_{flare,BC}$ (inner plot in the bottom left corner of Figure 57) indicates that $EF_{flare,BC}$ varies across a wide range, from a minimum of almost zero to a maximum of 2.27 g m⁻³ (Russia). Around 37% of the regions have $EF_{flare,BC}$ of 0.2–0.5 g m⁻³, and around 56% of the regions have $EF_{flare,BC}$ higher than 0.6 g m⁻³.

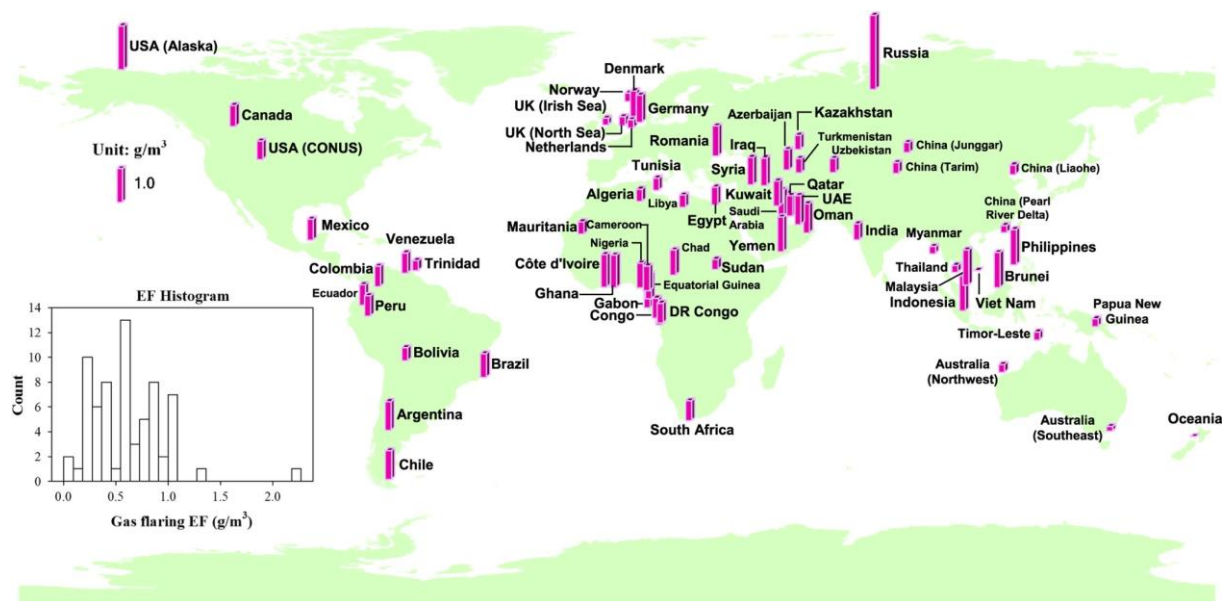


Figure 57: The global map of the mean values of $EF_{\text{flare,BC}}$ for various gas flaring regions by (Huang and Fu, 2016). A histogram of $EF_{\text{flare,BC}}$ is shown inside the bottom left corner of the figure. Abbreviations of some regions are defined as: USA—United States of America; CONUS—Conterminous United States; UK—United Kingdom of Great Britain and Northern Ireland; DR Congo—Congo (Democratic Republic of the); UAE—United Arab Emirates.

4.3.4 Measures to reduce flare emissions

To address black carbon emission reduction over the Arctic regions, Canada, Denmark, Norway, and the Russian Federation have endorsed the Zero Routine Flaring by 2030 initiative (GGFR, 2016). If the target of the initiative is met, black carbon emissions will be significantly reduced. Countries and companies who have signed on to ZRF 2030 are obliged to publicly report their flaring and progress towards the Initiative on an annual basis. Data on flare volumes have been submitted to the World Bank, which manages ZRF 2030.

According (Shapovalova, 2016), the adoption of an Arctic gas flaring treaty could be facilitated by using Offshore Guidelines and the Framework Document on BC as the basis for the future document. Moreover, the working gas flaring policy model is already present and just needs to be modified to address national peculiarities. As India and China, large emitters, are now observers to the Arctic Council, they are influenced by the Council processes and could potentially participate in future agreements. There is still undoubtedly a question on whether certain Arctic States would agree to a binding treaty, especially between States currently experiencing political and diplomatic tensions. It is important to note here that amidst the resent conflicts between the US and Russia over the situation in Ukraine and annexation of Crimea, the Arctic Council activities have not been disrupted. Substantial reductions of BC emissions in the Arctic could have an immediate effect and provide the international community with so much needed time to negotiate a strong climate treaty under the UNFCCC framework. Routine gas flaring, the largest source of BC, is not only an unnecessary waist of a valuable resource but also an obsolete practice that needs to be eliminated. The effectiveness of current gas flaring policies and practices vary across the Arctic and the only way to stop routine flaring is to adopt the best preventative practices across the region. Even though the Arctic Council is a soft law institution, it has a capacity to make the first step in imposing the best environmental standards on the Arctic oil industry.

The report (Arctic Council, 2019) provides a full list of measures taken by the countries of the Arctic zone to reduce their Flaring emissions. Canada, Russia and Norway all have regulations in place that limit the amount of flaring that is permitted. For instance, in Norway flaring of natural gas is only permitted when necessary for safety reasons. The Russian Federation has scaled up its flare reduction efforts with higher economic penalties for flaring above allowed norms. A special multiplier for the pollution charges for flaring was introduced in 2013 (equal to 12) and was increased twofold the following year. Flare volumes have dropped by some 42% from 2012 to 2015 according to national statistics, but satellite data suggest an increase of flaring in Russia from 2013 until 2016, with a reduction after 2017. The national goal is to achieve a 95% utilization rate for all associated petroleum gas (set in 2012). As reported by the Federal State Statistics Service, 88% of associated petroleum gas was utilized in 2016. Russia is also in the process of implementing best available technology (BAT) standards which will help reduce black carbon emissions from flares. Four specific BAT documents for the oil and gas industry have been published. They consider the EU Best Available Technologies Reference document (BREF) as well as local conditions of the Russian oil and gas sector. Black carbon emissions from flaring can in broad terms be addressed in three ways:

- i. By reducing volume of gas going to flare stacks,
- ii. By use of flaring technology and practices which minimize emissions of particulates,
- iii. By separating the heavier components of associated gas prior to flaring.

From a policy and regulatory perspective, the main focus has been on controlling total flare volumes. All oil and gas producing Arctic States have explicit regulations for flaring of associated gas, with emphasis on routine flaring. Approaches being applied vary between the Arctic States. In the Russian Federation, pollution charges on emissions from flare quantities above permissible levels are a key policy instrument, although it remains to be seen how effective the pollution charges have been at changing behaviour.

4.3.5 Gas flaring reduction technologies

Flare gas recovery (FGR) reduces noise and thermal radiation, operating and maintenance costs, air pollution and gas emission and reduces fuel gas and steam consumption. Various proven gas utilization technologies for different applications are addressed in World Bank Report (Bank, 2004). These FGR technologies are summarized here below after (Soltanieh et al., 2016) and references therein. Plans for new oil field development should incorporate such methodologies to eliminate routine flaring since emissions and venting from oil and gas facilities are poorly detected, measured, and monitored (Masnadi et al., 2018).

Re-injection is a commonly used method to preserve gas for future use or to increase the efficiency of the oil production process. The technology involves the installation of a gas compressor to re-pressurize areas of low-pressure formation gas, enhancing oil production. As an alternative to gas compressors, multiphase pump systems – in which oil and gas can flow together – have a smaller equipment size and allow determination of the flow characteristics without the need to separate oil and gas. Re-injection or recycle is often applied offshore in order to boost oil recovery by maintaining reservoir pressure and simultaneously reduce or eliminate the need for gas transportation facilities.

Power Generation is an option for meeting the nearby electricity demand or export the electricity to the grid. In Argentina, aeroderivative gas turbine burns 0.45 million cubic meters

per day of previously flared low Btu gas to generate about 40 MW of power. Gas turbines are more sensitive to the fuel gas in comparison with the other type of turbines. These systems are designed such that their construction consists of an ignition chamber and a turbine. A hot gas will enter and collide with the turbine blades, and this will cause them to rotate. The turbine is coupled with a turbo generator and will produce electricity that can be reserved.

Pipeline natural gas (PNG) is the principal and most convenient method of transporting gas; either from an offshore location to onshore for processing or to interface with existing distribution grids. It is also used for transportation of export gas. Nevertheless, for offshore transport of natural gas, pipelines become challenging as the water depth and the transporting distance increase. Gas to pipelines are not flexible as the gas will leave the source and arrive at its destination. Once the pipeline diameter is decided the quantities of gas that can be delivered is fixed by the pressures, although an increase in the maximum quantity can be achieved by adding compressors along the line, extra pipe in the form of loops or by increasing the average pipeline pressure.

Liquefied petroleum gas (LPG) is an alternative way of utilizing associated gas because of its easy storage and transport to local markets, and due to the higher percentage of propane and butane in associated gas compression compared to non-associated gas. Before extracting the liquefied petroleum gases, associated gas must first be treated for removal of impurities including water vapor, CO₂, mercury vapor and H₂S. Conventional LPG processes treat the whole gas stream before extracting the LPG content. These processes are not economical and practical for associated gas produced in much lower volumes and have a lower pressure than non-associated gas from gas wells.

Liquefied natural gas (LNG) uses a straightforward refrigeration process. The gas is pre-treated for impurities such as sulphur, CO₂, water, and other contaminants, transformed into liquid by being cooled to -162 °C, and stored until it is shipped onboard LNG tankers. LNG has a volume ~1/600 that of gas at room temperature. After transport to a receiving terminal, the liquefied gas is re-gasified for use in gas markets. A new LNG technology concept that has yet to be developed and proven commercially is called floating LNG (FLNG). This process is a combination of conventional LNG and floating deep water offshore production technologies. The combined FLNG vessels will contain liquefaction facilities onboard and can be moved to small and remote oil fields easily, without having the need to build large, new facilities at each location.

Natural gas hydrates (NGH) are crystallized natural gas, a solid material in an ice state and chemically stable at -20 °C. The stabilizing temperature is considerably higher than that the LNG temperature of -162 °C, which leads to lower capital, transportation, and storage costs. However, NGH is far less dense than LNG and quantity of gas transportable in hydrate form is correspondingly lower than LNG technology.

Gas-to-liquid (GTL) technology is a chemical process that converts methane gas into transportation fuels, such as gasoline or diesel fuels. GTL technology is still in development since it has not been economically feasible and has involved more technical risks. A world scale GTL plant can convert 8.5 MMscmd (Million Metric Standard Cubic Meter Per Day) of gas into 30,000 bpd of diesel or gasoline. Over the last few years, mini GTL technologies have been developed to monetize smaller volumes of gas (less than 0.7 MMscmd) and thereby offer opportunities to extinguish flares. The direct conversion of flare gas to “drop-in” fuels at the oil wellhead results in the production of an economically valuable product from the associated gas

resource that is currently wasted according (Tan et al., 2018) with an additional benefit on PM emissions reduction when this synthetic fuel is used as blended fuel.

Methanol and ammonia production. Methane in natural gas and associated gas can also be converted to methanol. Methanol is further used to produce dimethyl ether (DME) and olefins such as ethylene and propylene in simple reactor systems, conventional operating conditions and commercial catalysts. Lurgi's Mega Methanol, MTP, and Mega Syn technologies and Topsoe's DME process provide cost-effective and large economy-of-scale solutions to gas conversion. Methane in associated gas can also be converted to ammonia via the Haber process to produce nitrogen fertilizers. This method is quite common in the Persian Gulf oil-producing countries.

Some of these Flare gas recovery (FGR) have been evaluated by (Hajizadeh et al., 2018). The major concerns about environmental impacts of GHG emission lead refineries to deploy different FGR methods, most of which requiring new equipment and high cost of design and construction. The feasibility of three methods for FGR has been evaluated by (Hajizadeh et al., 2018) in a giant gas refinery in Iran. The first two methods considered liquefaction and LPG production by implementing flare gases as feed for existing LPG unit. Different parameters were studied in feed liquefaction and LPG production. The third studied option is using a three-stage compression unit to compress the flare gases. Finally, an economic evaluation was performed to find the most profitable method. Based on simulation results, the 0.75-barg pressure of flash drum leads to maximum LPG production. The economic evaluation shows that rate of return (ROR) for liquefaction unit and LPG production unit are more than 200% for different scenarios and are higher than compression.

In (Zolfaghari et al., 2017), three methods including gas to liquid (GTL), gas turbines generation (GTG) and gas to ethylene (GTE) are introduced and compared with the best method from economic point of view being identified. For this purpose, a natural gas sample was taken from Asalloyeh Refinery Plant and the process has been simulated using Aspen HYSYS model. Meanwhile, estimation of the capital and operating costs and evaluation of the processes involved were made using Aspen Capital Cost Estimator. According to the results obtained, production of the electric power from flaring gases is one of the most economical methods. GTG method has a greater ROR percent.

Among the available technologies, the **liquid ring compressor** (LRC) is a promising FGR option as it can compress and treat the flare gas simultaneously. However, there are several fundamental questions regarding the best operating conditions as well as the appropriate integration of such devices into a flare gas recovery system. The study of (Yazdani et al., 2020) deals with the design of a flare gas recovery system consisting of liquid ring compressors and an aqueous amine solvent for the abatement of acid gases, mainly hydrogen sulfide. Three different system configurations were investigated to find the optimal system layout for the efficient and continuous recovery of flare gas in a refinery complex.

4.3.6 Steam assisted flares

Based on the design and operating condition of the system, flares can be categorized as air-assisted, steam-assisted, non-assisted and pressure-assisted (Fawole et al., 2016). Flares are assisted primarily to enhance the turbulence and mixing of the fuel gas and air in the combustion zone, to suppress smoking of the resulting flame. A summary of these techniques is displayed in Table 20.

Table 20: Summary of the properties of flare types by (Fawole et al., 2016)

	Steam-assisted	Air-assisted	Pressure-assisted	Non-assisted
<i>Method</i>	Steam is introduced into the combustion zone to enhance mixing.	Air is introduced from a blower to enhance the mixing and turbulence of the fuel gas in the combustion zone	The vent pressure of the gas flow is used to enhance mixing at the tip of the flare burner	No assistance is given to the combustion process
<i>Efficiency</i>	Most efficient in terms of suppressing soot formation. Some of the CO formed can be oxidized to CO ₂	Less efficient than the steam assisted flare but relatively efficient than the other two types	Not as efficient as steam and air-assisted but can equally suppress sooting.	Only efficient for non-sooting combustion especially in light hydrocarbons
<i>Benefits</i>	Fuel with high heat value, and hence, high sooting propensity can be disposed of with relatively less soot	Prolongs the life span of the flare tip. Less expensive than steam-assisted and easy to maintain, hence, it is the most commonly used.	Enhance combustion efficiency when the gas flux pressure is sufficiently high enough without the additional cost of steam and air generation	Can be used for occasional emergency flaring of near smokeless gas
<i>Relative size</i>	They are often large flares as they include the steam generator and are usually employed in large gas facilities.	Not as large as the steam assisted.	May be of same size as air-assisted flare depending on the flow capacity of the facility	Often smaller in size compared to the other types
<i>Shortcoming</i>	Over-steaming can result in reduced efficiency of flare. It is also expensive to maintain on a large-scale	Over-aeration can also result in less efficiency. A limit of air assist to gas ratio must be maintained for effectiveness of the flare.	The fluctuation of gas flow pressure has a bearing consequence on the efficiency of the combustion. Requires large space in a remote area.	Cannot be used for dense fuels with high sooting propensity which are typical gas in oil and gas processing facilities

Steam undergoes thermal dissociation in a flare flame to give H and OH free radicals that react with carbon to give CH₂– and –CHO radical moieties. The steam induced free radicals enhance the formation of C=O bonds rather than C–C bonds, **promoting completeness of combustion**. The steam can also react with intermediate products like CO, oxidizing it further to CO₂. For a steam assisted flare, combustion efficiency starts to decrease when the steam-to-fuel gas ratio goes beyond a threshold which depends on the heat content of the fuel gas and the location at which the steam is injected into the combustion zone in the flare.

According to (Kumar et al., 2020) **steam injection is the most efficient way to reduce the smoke produced while flaring**, but due to non-availability of steam, the air assisted flare can be used. The quantity of air required is approximately 1.2 times that of steam and the system is also expensive as per installations point of view. High pressure flare technology can also suppress the smoke generation but it should be incorporated only when the calorific value of flare gas is very high. It can be used where steam is not available, and the system needs low-cost design. High pressure flares can greatly reduce the flare flame radiation and also increase the combustion efficiency exceeding 98%.

To better understand the effect of air- and steam-assist on flaring operations on carbon conversion efficiency and pollutant emissions, a lab-scale coflow burner constructed of two concentric circular tubes has been developed by (Ahsan et al., 2019). Natural gas at 20 standard

litre per minute flowed through the annular space and increasing amounts of air or steam were added through the inner tube until flame extinction was invoked. The combustion products were captured by an exhaust hood and analysed using a gas chromatograph to measure the concentrations of CH₄, C₂H₆, C₃H₈, C₄H₁₀, CO and CO₂. A photoacoustic extincitometer and a NO_x analyser were used to measure BC and NO_x concentrations, respectively. A challenge associated with the experiments was to accurately resolve stark transitions in conversion efficiency and orders of magnitude change in key emissions. Results indicated that the addition of air or steam to a natural gas jet diffusion flame caused a sudden collapse in carbon conversion efficiency, occurring at a coflow-fuel gas mass flow ratio of 1.8 for steam and 5.0 for air. As was expected, the CO₂ emission indices for both air and steam coflow followed their respective carbon conversion efficiency trends. Conversely, the total unburned hydrocarbon emission indices increased with the reduction in carbon conversion efficiency. NO_x emission indices for air and steam coflow were shown to decrease by an order of magnitude compared to the unassisted flame. For air coflow this occurred before the collapse in carbon conversion efficiency, while for steam coflow this occurred concurrently. **Black carbon emission indices decreased rapidly by three orders of magnitude** for both air and steam coflow (Figure 58). For both these lab-scale air and steam assisted flares there was a range of mass flow rates of the assist fluid that resulted in high combustion efficiency and low pollutant emissions.

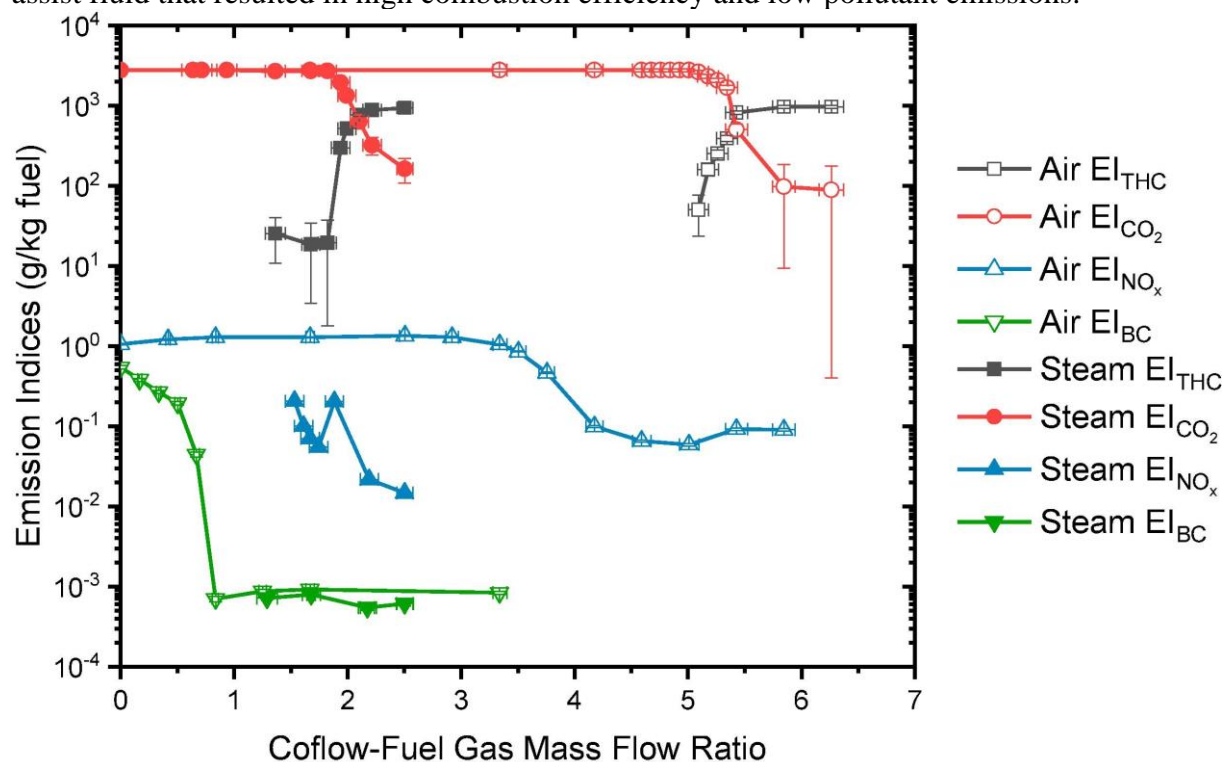


Figure 58: Emission indices of a natural gas flame with air or steam coflow. Data includes error bars for the propagation of measurement uncertainties in calculating emission indices and mass flow rates for the methodologies described in (Ahsan et al., 2019).

4.3.7 Other Optimized Combustion systems – Advanced Flare Design

Associated gas is recovered from the conventional flare stack and sent to an appropriately-sized and well-maintained knockout drum to remove heavier hydrocarbons from the flare stream before being directed to an improved flare stack where it is combusted using advanced flare tip and flare ignition technology. A full list of Best Available Techniques are reported in (EU Action on Black Carbon in the Arctic, 2019).

Diffusion Flame

In most flares, combustion occurs by means of a diffusion flame. In this set-up, air diffuses across the boundary of the combustion product stream towards the center of the fuel flow, forming an envelope of combusting gas around a fuel gas core. On ignition, this mixture creates a stable flame zone above the tip of the burner. Smoking can occur due to a deficiency of oxygen (O₂) or cooling of the carbon particles below their ignition temperature. In larger diffusion flames, a vortex can form around the burning portion of the gas which cuts the O₂ supply and causes localized instability or flickering of the flame that can be accompanied by BC formation. Ensuring adequate air supplies and mixing are therefore essential for minimizing smoke and maximizing combustion. The various flare designs differ primarily in their accomplishment of mixing.

Flare System Controls

Flare system control can be completely automated or completely manual. Components of a flare system that can be controlled automatically include the auxiliary gas, the ignition system, and steam injection (if steam is used). Fuel gas consumption can be minimized by continuously measuring the vent gas rate and heat content, and automatically adjusting the amount of auxiliary fuel to maintain the required minimum total gas. Automatic ignition panels sense the presence of a flame with visual temperature measurements or thermal sensors, and reignite pilots when flameouts occur. Fuel consumption by the pilot flame should be minimized to the extent possible without compromising the ability to ignite the flare under all conditions.

(Srinivasarao and Muralikrishna, 2014) show an example of automatic control system to minimize soot and unburnt hydrocarbons from flares. To achieve quick action of S/C ratio control system with reliable ultrasonic flow measurement and feed forward signal introduced by calculated hydrocarbon number. The study results depict that soot minimization can be achievable within 5 minutes by adopting feed forward control system

Knockout Drum Design

The design and maintenance of a knockout drum can also impact BC emissions from flaring. A knockout drum is a separator used to remove any liquids from the gas stream prior to being flared. If it is not sized or maintained properly, some liquid droplets may be entrained by a waste gas stream, leading to smoke formation. Micro-condensation units to aid in recovering liquids, could be considered as a BC emission reduction option. The economics of vessel design dictates the choice between a horizontal or vertical drum. When a large liquid storage vessel is required and the vapor flow is high, a horizontal drum is typically more economical. Vertical drum separation is used when there is small liquid load, limited plot space, or where ease of level control is desired. It is assumed here that the drum is not sized for emergency releases and that liquid flow is minimal. Properly sizing and operating knockout drums can also have an immediate effect on BC emissions, and must be considered.

Currently, simple guidelines for flare operations to maintain high combustion efficiency (CE) remain elusive. The publication of (Chen and Alphones, 2019) fills the gap by investigating the characteristics of the incipient smoke point (ISP), which is widely recognized as the condition for good combustion. The incipient smoke point of a flare is the point of operation immediately before the flare begins to smoke. It is also a point (but not the only point) at which combustion

efficiency is at a maximum. The incipient smoke “point” is not really a point. It will shift based on vent gas composition, flare flow rate and exit velocity, and of course steam or air assist rate. This study characterizes the ISP in terms of 100-% combustion inefficiency (CE), percent opacity, absorbance, air assist, steam assist, air equivalence ratio, steam equivalence ratio, exit velocity, vent gas net heating value, and combustion zone net heating value. Flame lengths were calculated for buoyant and momentum-dominated plumes under calm and windy conditions at stable and neutral atmosphere. Opacity was calculated using the Beer–Lambert law based on soot concentration, flame diameter, and mass specific extinction cross section of soot. The calculated opacity and absorbance were found to be lognormally distributed. Linear relations were established for soot yield versus absorptivity with $R^2 > 0.99$ and power-law relations for opacity versus soot emission rate with $R^2 \geq 0.97$ for steam assisted, air-assisted, and non-assisted flares. The characterized steam/air assists, combustion zone/ vent gas heating values, exit velocity, steam, and air equivalence ratios for the incipient smoke point serve as a useful guideline for efficient flare operations.

4.3.8 Multiple tips for soot reduction

Splitting flare tip into multiple branches is an idea that is thought to reduce soot formation by increasing the contact surface and providing better mixing. In this study of (Mostafayi and Rashidi, 2020), changing a single tip of an industrial flare into multiple tips (Figure 59) was investigated by Computational Fluid Dynamic software Ansys Fluent 18. Reynolds Average Navier–Stokes approach was used to model the fluid flow, and its turbulence was modelled by realizable $k-\epsilon$ model. The steady laminar flamelet model was chosen as the combustion model. Soot formation was modelled using Moss–Brookes approach, and validated by comparing the simulation results with available experimental data. Effects of tip diameter, number of branches, and distance between branches on soot and NO_x yields, and flame stability were studied. According to the results, increasing the number of branches having larger diameters by taking flame stability limitations into consideration, and choosing optimum distances between branches caused **significant soot reduction without noticeable changes in the NO_x formation** (Figure 60).

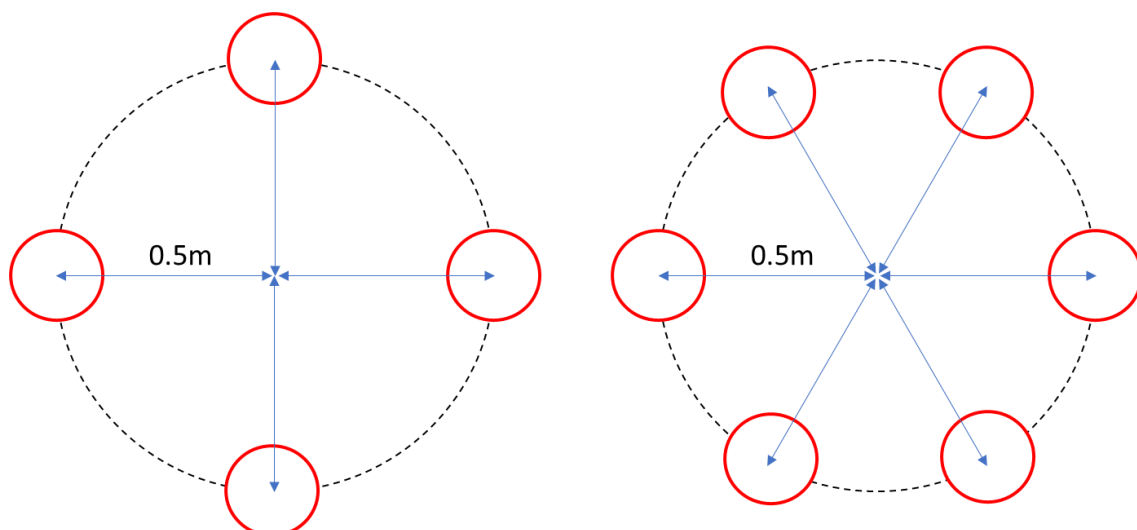


Figure 59: Upper view of the flare with multiple tips (left: $n=4$ left, right: $n=6$)

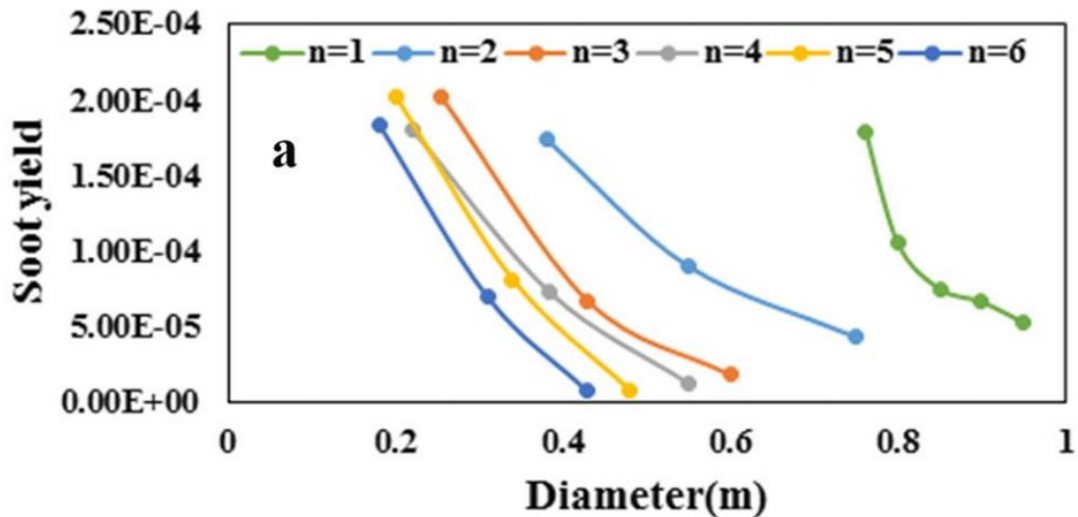


Figure 60: Soot yield at different branches and diameters from (Mostafayi and Rashidi, 2020)

4.3.9 Modelling approaches

Computational fluid dynamic (CFD) analysis has been used by (Castiñeira and Edgar, 2006) to simulate the effect of steam and air addition in turbulent combustion flames in order to understand industrial flare behaviour. They analysed the effect of steam and air addition on the resulting combustion efficiency of the flames. The simulations show that incomplete combustion of hydrocarbons may occur at high steam/fuel and air/fuel ratios up to the point where the flame becomes extinguished. For the steam addition case, our results show that inefficient combustion can be predicted based on the global heating value of the fuel gas. In fact, inefficient combustion occurs at heating values below 7.45 MJ m^{-3} , which has also been observed in industrial flares. Hence, based on our simulation models, potential control strategies could be developed to compensate for the Lower heating values (LHV) of the gases below the recommended lower limits and to reduce hydrocarbon emissions for flares.

Based on the numerical results, (Patki et al., 2014) concluded that, among three different soot models, the Moss-Brooke model provides more reasonable results for methane mixture flame. The study also indicates that when more air is supplied, the soot yield is higher. As expected, results with different fuel mixture advocate that soot yield increases as carbon percentage in fuel increases. Furthermore, it can be inferred that, the equilibrium model provided in fluent produces significantly lower soot yield than LU 1.0 mechanism steady flamelet model. By using a radiation model it is seen that the radiation effect is negligible on methane mixture soot yield and flame temperature. Finally, soot yield results with different jet velocities propose that **soot yield increases as jet velocity increases**. In the meantime, the flame maximum temperature also increases slightly when the jet velocity becomes higher.

How to simultaneously achieve high combustion efficiency (CE) and low soot emission is an important issue. Soot emissions are influenced by many factors. Flare operators tend to over-steam or over-air to suppress smoke, which results in low CE. How to achieve optimal flare performance remains a question to the industry and the regulatory agencies. (Wang et al., 2016) reviewed regulations in the US regarding flaring. In order to determine the optimal operating window for the flare, different combustion mechanisms related to soot emissions were summarized in this study. A new combustion mechanism (**Vsoot**) for predicting soot emissions was developed and validated against experimental data. Computational fluid dynamic (CFD) models combined with Vsoot combustion mechanism were developed to simulate the flaring

events. It was observed that simulation results agree well with experimental data. Vsoot combustion mechanism can handle C1–C4 hydrocarbons combustion and predict soot emissions, since Vsoot combustion mechanism contains important soot precursor species including acetylene, ethylene and benzene. From comparison with reference experimental data, Vsoot combustion mechanism performs well in computing laminar flame speed, ignition delay time and adiabatic flame temperature, the simulation results are in good agreement with experimental data (Table 21). With Vsoot combustion mechanism, CFD simulation of air assist flare cases in ANSYS Fluent are performed with a turbulence and turbulence-chemistry interaction models, the non-premixed Probability Density Function (PDF) model. It is shown that CFD simulation with PDF model can predict good soot yields and CE results.

Table 21: Comparison of soot emissions after (Wang et al., 2016)

Air assisted Case N°	Experimental results / (lb MMBTU ⁻¹)	Vsoot simulation results / (lb MMBTU ⁻¹)	Error /%
1	3.05	4.16	1.36
2	4.6	6.15	1.41
3	3.95	2.84	1.39
4	2.68	2.13	1.26
5	3.45	2.54	1.36
6	8.05	6.78	1.18
Avg.			1.33

As depicted by (Gai et al., 2020), it is difficult to measure flare combustion efficiency (CE), destruction and removal efficiency (DRE), and soot emission directly. **Vsoot combustion** mechanism was developed and validated in computational fluid dynamic (CFD) flare combustion models to calculate CE, DRE, and soot yields. It was found that **soot yields increase with carbon percentage in fuel** and flare gas jet velocity. However, it is difficult to implement CFD simulation for online control of flare because CFD simulation takes long time to converge. Therefore, with the development of optical measurement and modeling, some innovative technologies were developed for online application. Sky-LOSA (line-of-sight attenuation using skylight) is an imaging technique that enables the quantification of instantaneous BC emission rate through an artificial control surface within the image plane of a scientific camera. Sky-LOSA optimal measurement technique (Conrad and Johnson, 2017) combined with Monte Carlo-based uncertainty analysis was developed to measure flare gas volume-specific soot yields. It was reported that **soot yields were strongly correlated with flare gas heating value**.

(Damodara et al., 2020) developed Neural Network (NN) models that can be robustly used in the industry to achieve the desired combustion efficiency (CE) without visible emissions (smoke). Steam-/air-assist rates, exit velocity, and the vent gas composition, which can be either controlled or measured in flare operations, are used as independent variables in the models. NN models were developed for the air-assisted, steam-assisted, and non-assisted flares using various types of fuels like propylene, propane, natural gas, methane, and ethylene. The flare performance models such as CE and opacity were developed using neural network toolbox in MATLAB. NN models for steam and air-assisted flare tests are in good agreement with experimental data

and have been demonstrated by the average correlation coefficient of 0.95 and 0.97 for air-assisted and steam-assisted flare data, respectively. The very low mean absolute errors of 1.1% and 1.4% for air-assisted and steam-assisted flare data, respectively, also indicate the robustness of the NN models. 2-D and 3-D contour plots are presented to show the effect of key operating parameters. The set points (amount of steam/air/make-up fuel required) at the Incipient Smoke Point (ISP) and for Smokeless Flaring (SLF) have been developed based on the neural network models.

4.3.10 Key conclusions

Based on the recent literature review, the following key conclusions regarding Gas Flare can be summarized as follow:

- Black carbon emissions from the oil & gas industry by Gas Flares is an important source and particularly in areas surrounding the Arctic zone as they affect the radiative budget and enhance snow melting. Russia, USA, Africa and some Middle East countries are among the largest emitting countries.
- Usually, at least 90% of carbonaceous species in the Gas Flare flue gas is made of Black Carbon.
- Emission factors from GF are uncertain since the combustion conditions can vary and can be not monitored enough. The emission factors (EF) can vary over several order of magnitude generally in the range 0.2 to 2.27 g m⁻³.
- Emission inventories deriving from these EF are therefore uncertain and often gap filled or assessed by Satellite observations.
- Routine flaring from a lack of gas utilisation sources is the most important and largest source of BC emissions from flaring, however, intermittent flaring and continuous flaring for operational reasons can also be significant sources.

An overview of the potential routes to reduce BC emissions from gas flaring can be broken down into several type of options.

- Using associated gas for on-site application or export (Power, heat, gas generation) is a natural solution to reduce BC and other flaring emissions by avoiding the flue gas emission. Associated gas utilization virtually eliminates BC emissions, however, flaring and low gas utilization rates are often common during the first years of production in new fields because decisions on gas infrastructure construction are often made only after production starts. In addition, even when it is economically interesting to utilize Associated Petroleum Gas (APG), there will typically be some degree of flaring for safety or other operational reasons. Finally, in some cases, no gas recovery solution will be available or considered feasible.
- Under these conditions, other options to minimize BC emissions exist: extraction of heavy components from the flared gas stream.
- A flare with multiple tips seems a good example showing good performances on BC emission reductions.
- Steam-assist flares are clearly the most efficient in terms of suppressing soot formation. However high pressure-assisted flares can be an efficient technique if water is not available on site. Steams assisted flares show less emission of very small particles (below 50 nm) compared to air steam assisted flares.

- The optimization of flare design and combustion conditions is an option thanks to the use of Computational Fluid Dynamic (CFD) model. Model and control systems can be used to monitor the flue gas characteristics and control the input data.
- New models based on Artificial Intelligence techniques can be used to set optimized input parameters to lower emission flaring and therefore reduce BC emissions.

5 Conclusions

This report provides an overview of black carbon (BC), Polycyclic Aromatic Hydrocarbons (PAH) and Ultrafine Particles emissions and the effect PM emission reduction strategies on these species emissions. Three target sectors have been identified, two of them, small combustion sources, and road transport because they are the major sources of BC, and Gas Flaring (GF) because this source is an important source for both air quality and climate impact in the Arctic regions.

Residential wood burning remains a major issue, and many efforts still need to be made to reduce emissions. The use of advanced or eco-labelled stoves and boilers can be promoted. The quality and the type of wood is also important and dry wood is usually recommended. However, if BC emissions is likely to be reduced, particle number is questioning during the dilution of emissions. The decrease of available mass for condensation and lower temperature can increase nucleation processes and then increase the number of particles.

The determination of Emission Factors with more reliable standards is a critical issue. Methods must inform on the filterable and condensable fractions of particles to develop emission inventories more relevant for the modelling community who use these data to help the development strategies for policy makers to both curb air pollution and adverse climate impacts.

With the shift to more stringent regulations applied to vehicles, PM emissions and all particulate species at the exhaust pipe are likely to decrease. Therefore, tyre and brake emissions are turning dominant sources and they are also a source of BC even if these particles are mainly in the coarse mode (diameter > 2.5 μm). Ultrafine particles can also be emitted by brake uses. The choice of pad material is the main technical way to decrease emissions even if? some suction devices could be used to remove most particles from brakes.

At least 90% of carbonaceous species in the Gas Flare flue gas is made of Black Carbon. Steam-assist Flares are clearly the most efficient in terms soot emission reductions. However high pressure-assisted Flares can be an efficient technique if water is not available on site. New model based on neural networks could help to better assist the Flaring operations to better control soot formation.

To better tackle Climate Change and Air Quality through the BC emission reduction, it would be also important to address the emission of Brown Carbon (BrC). BrC is a light-absorbing particulate matter mainly co-emitted by biomass burning or produced later during the plume dilution. So far, this species is not yet very well identified, and the radiative properties assigned to this species in climate models are still associated to uncertainties. Improve the knowledge to obtain the most appropriate responses to emission changes would be useful.

6 Bibliography

- ACAP, 2015. Recommended Actions of the ACAP Report on the Reduction of Black Carbon Emissions from Residential Wood Combustion.
- ACAP, 2014. Reduction of Black Carbon Emissions from Residential Wood Combustion in the Arctic – Black Carbon Inventory, Abatement Instruments and Measures. Arctic Contaminants Action Program.
- Ahsan, A., Ahsan, H., Olfert, J.S., Kostiuk, L.W., 2019. Quantifying the carbon conversion efficiency and emission indices of a lab-scale natural gas flare with internal coflows of air or steam. *Exp. Therm. Fluid Sci.* 103, 133–142. <https://doi.org/10.1016/j.expthermflusci.2019.01.013>
- Akherati, A., He, Y., Coggon, M.M., Koss, A.R., Hodshire, A.L., Sekimoto, K., Warneke, C., de Gouw, J., Yee, L., Seinfeld, J.H., Onasch, T.B., Herndon, S.C., Knighton, W.B., Cappa, C.D., Kleeman, M.J., Lim, C.Y., Kroll, J.H., Pierce, J.R., Jathar, S.H., 2020. Oxygenated Aromatic Compounds are Important Precursors of Secondary Organic Aerosol in Biomass-Burning Emissions. *Environ. Sci. Technol.* 54, 8568–8579. <https://doi.org/10.1021/acs.est.0c01345>
- Ali, M.U., Siyi, L., Yousaf, B., Abbas, Q., Hameed, R., Zheng, C., Kuang, X., Wong, M.H., 2020. Emission sources and full spectrum of health impacts of black carbon associated polycyclic aromatic hydrocarbons (PAHs) in urban environment: A review. *Crit. Rev. Environ. Sci. Technol.* 1–40. <https://doi.org/10.1080/10643389.2020.1738854>
- ALPINE SPACE, 2019. Deliverable D.T1.4.1 - A report about the different regulations about BB regarding both appliances and fuels.
- Alves, C., Gonçalves, C., Fernandes, A.P., Tarelho, L., Pio, C., 2011. Fireplace and woodstove fine particle emissions from combustion of western Mediterranean wood types. *Atmospheric Res.* 101, 692–700. <https://doi.org/10.1016/j.atmosres.2011.04.015>
- Amann, M., Cofala, J., Klimont, Z., Nagl, C., Schieder, W., 2018. Measures to address air pollution from small combustion sources (Contract ENV.C.3/FRA/2013/00131 of DG-Environment of the European Commission). IIASA, Vienna, Austria.
- Amann, M., Kiesewetter, G., Schöpp, W., Klimont, Z., Winiwarter, W., Cofala, J., Rafaj, P., Höglund-Isaksson, L., Gomez-Sabriana, A., Heyes, C., Purohit, P., Borken-Kleefeld, J., Wagner, F., Sander, R., Fagerli, H., Nyiri, A., Cozzi, L., Pavarini, C., 2020. Reducing global air pollution: the scope for further policy interventions. *Philos. Trans. R. Soc. Math. Phys. Eng. Sci.* 378, 20190331. <https://doi.org/10.1098/rsta.2019.0331>
- AQEG, 2019. Non-Exhaust Emissions from Road Traffic. Air Quality Expert Group for the Department for Environment, Food and Rural Affairs, Scottish Government, Welsh Government and Department of the Environment in Northern Ireland, London, UK.
- Archer, G., 2016. Dieselgate: Who? What? How? | Transport & Environment [WWW Document]. URL <https://www.transportenvironment.org/publications/dieselgate-who-what-how> (accessed 11.4.20).
- Arctic Council, 2019. Expert Group on Black Carbon and Methane - Summary of Progress and Recommendations.
- Avagyan, R., Nyström, R., Lindgren, R., Boman, C., Westerholm, R., 2016. Particulate hydroxy-PAH emissions from a residential wood log stove using different fuels and burning conditions. *Atmos. Environ.* 140, 1–9. <https://doi.org/10.1016/j.atmosenv.2016.05.041>

- Bäfver, L., Yngvesson, Y., Niklasson, F., 2012. Residential Electrostatic Precipitator - Performance at efficient and poor combustion conditions (SP Rapport :2012:42). SP Technical Research Institute of Sweden, Borås, Sweden.
- Bank, 2004. Flared gas utilization strategy opportunities for small-scale uses of gas (No. 5). The International Bank for Reconstruction and Development - The World Bank Group, Washington DC, USA.
- Battye, W., Boyer, K., Pace, T.G., 2002. Methods for Improving Global Inventories of Black Carbon and Organic Carbon Particulates. EC/R Incorporated and US EPA.
- Bergström, R., Denier van der Gon, H.A.C., Prévôt, A.S.H., Yttri, K.E., Simpson, D., 2012. Modelling of organic aerosols over Europe (2002–2007) using a volatility basis set (VBS) framework: application of different assumptions regarding the formation of secondary organic aerosol. *Atmospheric Chem. Phys.* 12, 8499–8527. <https://doi.org/10.5194/acp-12-8499-2012>
- Bertrand, A., Stefenelli, G., Bruns, E.A., Pieber, S.M., Temime-Roussel, B., Slowik, J.G., Prévôt, A.S.H., Wortham, H., El Haddad, I., Marchand, N., 2017. Primary emissions and secondary aerosol production potential from woodstoves for residential heating: Influence of the stove technology and combustion efficiency. *Atmos. Environ.* 169, 65–79. <https://doi.org/10.1016/j.atmosenv.2017.09.005>
- Bertrand, A., Stefenelli, G., Jen, C.N., Pieber, S.M., Bruns, E.A., Ni, H., Temime-Roussel, B., Slowik, J.G., Goldstein, A.H., El Haddad, I., Baltensperger, U., Prévôt, A.S.H., Wortham, H., Marchand, N., 2018. Evolution of the chemical fingerprint of biomass burning organic aerosol during aging. *Atmospheric Chem. Phys.* 18, 7607–7624. <https://doi.org/10.5194/acp-18-7607-2018>
- Bessagnet, B., Rosset, R., 2001. Fractal modelling of carbonaceous aerosols-application to car exhaust plumes. *Atmos. Environ.* 35, 4751–4762.
- Bhattu, D., Zotter, P., Zhou, J., Stefenelli, G., Klein, F., Bertrand, A., Temime-Roussel, B., Marchand, N., Slowik, J.G., Baltensperger, U., Prévôt, A.S.H., Nussbaumer, T., El Haddad, I., Dommen, J., 2019. Effect of Stove Technology and Combustion Conditions on Gas and Particulate Emissions from Residential Biomass Combustion. *Environ. Sci. Technol.* 53, 2209–2219. <https://doi.org/10.1021/acs.est.8b05020>
- Bjørner, T.B., Brandt, J., Gårn Hansen, L., Källström, M.N., 2019. Regulation of air pollution from wood-burning stoves. *J. Environ. Plan. Manag.* 62, 1287–1305. <https://doi.org/10.1080/09640568.2018.1495065>
- Braisher, M., Stone, R., Price, P., 2010. Particle Number Emissions from a Range of European Vehicles. Presented at the SAE 2010 World Congress & Exhibition, pp. 2010-01–0786. <https://doi.org/10.4271/2010-01-0786>
- Brandelet, B., Pascual, C., Debal, M., Rogaume, Y., 2020. A cleaner biomass energy production by optimization of the operational range of a fabric filter. *J. Clean. Prod.* 253, 119906. <https://doi.org/10.1016/j.jclepro.2019.119906>
- Brewer, T.L., 2019. Black carbon emissions and regulatory policies in transportation. *Energy Policy* 129, 1047–1055. <https://doi.org/10.1016/j.enpol.2019.02.073>
- Calel, R., Mahdavi, P., 2020. Opinion: The unintended consequences of anti-flaring policies—and measures for mitigation. *Proc. Natl. Acad. Sci.* 117, 12503–12507. <https://doi.org/10.1073/pnas.2006774117>
- Caplain, I., Cazier, F., Nouali, H., Mercier, A., Déchaux, J.-C., Nollet, V., Joumard, R., André, J.-M., Vidon, R., 2006. Emissions of unregulated pollutants from European gasoline

- and diesel passenger cars. *Atmos. Environ.* 40, 5954–5966. <https://doi.org/10.1016/j.atmosenv.2005.12.049>
- Cappa, C.D., Lim, C.Y., Hagan, D.H., Coggon, M., Koss, A., Sekimoto, K., de Gouw, J., Onasch, T.B., Warneke, C., Kroll, J.H., 2020. Biomass-burning-derived particles from a wide variety of fuels – Part 2: Effects of photochemical aging on particle optical and chemical properties. *Atmospheric Chem. Phys.* 20, 8511–8532. <https://doi.org/10.5194/acp-20-8511-2020>
- Carvalho, R.L., Vicente, E.D., Tarelho, L.A.C., Jensen, O.M., 2018. Wood stove combustion air retrofits: A low cost way to increase energy savings in dwellings. *Energy Build.* 164, 140–152. <https://doi.org/10.1016/j.enbuild.2018.01.002>
- Caseiro, A., Gehrke, B., Rücker, G., Leimbach, D., Kaiser, J.W., 2020. Gas flaring activity and black carbon emissions in 2017 derived from the Sentinel-3A Sea and Land Surface Temperature Radiometer. *Earth Syst. Sci. Data* 12, 2137–2155. <https://doi.org/10.5194/essd-12-2137-2020>
- Castiñeira, D., Edgar, T.F., 2006. CFD for Simulation of Steam-Assisted and Air-Assisted Flare Combustion Systems. *Energy Fuels* 20, 1044–1056. <https://doi.org/10.1021/ef050332v>
- Caubel, J.J., Rapp, V.H., Chen, S.S., Gadgil, A.J., 2020. Practical design considerations for secondary air injection in wood-burning cookstoves: An experimental study. *Dev. Eng.* 5, 100049. <https://doi.org/10.1016/j.deveng.2020.100049>
- Caubel, J.J., Rapp, V.H., Chen, S.S., Gadgil, A.J., 2018. Optimization of Secondary Air Injection in a Wood-Burning Cookstove: An Experimental Study. *Environ. Sci. Technol.* 52, 4449–4456. <https://doi.org/10.1021/acs.est.7b05277>
- Chen, D.H., Alphones, A., 2019. Characterization of the incipient smoke point for steam-/air-assisted and nonassisted flares. *J. Air Waste Manag. Assoc.* 69, 119–130. <https://doi.org/10.1080/10962247.2018.1525443>
- Chen, X., Yang, W., Wang, Zifa, Li, J., Hu, M., An, J., Wu, Q., Wang, Zhe, Chen, H., Wei, Y., Du, H., Wang, D., 2019. Improving new particle formation simulation by coupling a volatility-basis set (VBS) organic aerosol module in NAQPMS+APM. *Atmos. Environ.* 204, 1–11. <https://doi.org/10.1016/j.atmosenv.2019.01.053>
- Chen, Y., Borken-Kleefeld, J., 2014. Real-driving emissions from cars and light commercial vehicles – Results from 13 years remote sensing at Zurich/CH. *Atmos. Environ.* 88, 157–164. <https://doi.org/10.1016/j.atmosenv.2014.01.040>
- Cheremisinoff, N.P. (Ed.), 2016. Electrostatic Precipitators, in: *Pollution Control Handbook for Oil and Gas Engineering*. John Wiley & Sons, Inc., Hoboken, NJ, USA, pp. 375–407. <https://doi.org/10.1002/9781119117896.ch29>
- Chirico, R., DeCarlo, P.F., Heringa, M.F., Tritscher, T., Richter, R., Prévôt, A.S.H., Dommen, J., Weingartner, E., Wehrle, G., Gysel, M., Laborde, M., Baltensperger, U., 2010. Impact of aftertreatment devices on primary emissions and secondary organic aerosol formation potential from in-use diesel vehicles: results from smog chamber experiments. *Atmospheric Chem. Phys.* 10, 11545–11563. <https://doi.org/10.5194/acp-10-11545-2010>
- Cho, M.-H., Park, R.J., Yoon, J., Choi, Y., Jeong, J.I., Labzovskii, L., Fu, J.S., Huang, K., Jeong, S.-J., Kim, B.-M., 2019. A missing component of Arctic warming: black carbon from gas flaring. *Environ. Res. Lett.* 14, 094011. <https://doi.org/10.1088/1748-9326/ab374d>

- Chow, J.C., Watson, J.G., Green, M.C., Wang, X., Chen, L.-W.A., Trimble, D.L., Cropper, P.M., Kohl, S.D., Gronstal, S.B., 2018. Separation of brown carbon from black carbon for IMPROVE and Chemical Speciation Network PM_{2.5} samples. *J. Air Waste Manag. Assoc.* 68, 494–510. <https://doi.org/10.1080/10962247.2018.1426653>
- Commodo, M., Kaiser, K., De Falco, G., Minutolo, P., Schulz, F., D'Anna, A., Gross, L., 2019. On the early stages of soot formation: Molecular structure elucidation by high-resolution atomic force microscopy. *Combust. Flame* 205, 154–164. <https://doi.org/10.1016/j.combustflame.2019.03.042>
- CONCAWE, 2015. Air pollutant emission estimation methods for E-PRTR reporting by refineries, 2015 edition. CONCAWE, Brussels, Belgium.
- Conrad, B.M., Johnson, M.R., 2019. Mass absorption cross-section of flare-generated black carbon: Variability, predictive model, and implications. *Carbon* 149, 760–771. <https://doi.org/10.1016/j.carbon.2019.04.086>
- Conrad, B.M., Johnson, M.R., 2017. Field Measurements of Black Carbon Yields from Gas Flaring. *Environ. Sci. Technol.* 51, 1893–1900. <https://doi.org/10.1021/acs.est.6b03690>
- Cordiner, S., Mulone, V., Nobile, M., Rocco, V., 2016. Impact of biodiesel fuel on engine emissions and Aftertreatment System operation. *Appl. Energy* 164, 972–983. <https://doi.org/10.1016/j.apenergy.2015.07.001>
- Cornelissen, G., Gustafsson, Ö., Bucheli, T.D., Jonker, M.T.O., Koelmans, A.A., van Noort, P.C.M., 2005. Extensive Sorption of Organic Compounds to Black Carbon, Coal, and Kerogen in Sediments and Soils: Mechanisms and Consequences for Distribution, Bioaccumulation, and Biodegradation. *Environ. Sci. Technol.* 39, 6881–6895. <https://doi.org/10.1021/es050191b>
- Corsini, E., Marinovich, M., Vecchi, R., 2019. Ultrafine Particles from Residential Biomass Combustion: A Review on Experimental Data and Toxicological Response. *Int. J. Mol. Sci.* 20, 4992. <https://doi.org/10.3390/ijms20204992>
- Couvidat, F., Bessagnet, B., Garcia-Vivanco, M., Real, E., Menut, L., Colette, A., 2018a. Development of an inorganic and organic aerosol model (CHIMERE 2017? v1.0): seasonal and spatial evaluation over Europe. *Geosci. Model Dev.* 11, 165–194.
- Couvidat, F., Vivanco, M.G., Bessagnet, B., 2018b. Simulating secondary organic aerosol from anthropogenic and biogenic precursors: Comparison to outdoor chamber experiments, effect of oligomerization on SOA formation and reactive uptake of aldehydes. *Atmospheric Chem. Phys.* 18, 15743–15766.
- Czech, H., Miersch, T., Orasche, J., Abbaszade, G., Sippula, O., Tissari, J., Michalke, B., Schnelle-Kreis, J., Streibel, T., Jokiniemi, J., Zimmermann, R., 2018. Chemical composition and speciation of particulate organic matter from modern residential small-scale wood combustion appliances. *Sci. Total Environ.* 612, 636–648. <https://doi.org/10.1016/j.scitotenv.2017.08.263>
- Daellenbach, K.R., Uzu, G., Jiang, J., Cassagnes, L.-E., Leni, Z., Vlachou, A., Stefanelli, G., Canonaco, F., Weber, S., Segers, A., Kuenen, J.J.P., Schaap, M., Favez, O., Albinet, A., Aksoyoglu, S., Dommen, J., Baltensperger, U., Geiser, M., El Haddad, I., Jaffrezo, J.-L., Prévôt, A.S.H., 2020. Sources of particulate-matter air pollution and its oxidative potential in Europe. *Nature* 587, 414–419. <https://doi.org/10.1038/s41586-020-2902-8>
- Damodara, V.D., Alphones, A., Chen, D.H., Lou, H.H., Martin, C., Li, X., 2020. Flare performance modeling and set point determination using artificial neural networks. *Int. J. Energy Environ. Eng.* 11, 91–109. <https://doi.org/10.1007/s40095-019-00314-3>

- Denier van der Gon, H.A.C., Bergström, R., Fountoukis, C., Johansson, C., Pandis, S.N., Simpson, D., Visschedijk, A.J.H., 2015. Particulate emissions from residential wood combustion in Europe – revised estimates and an evaluation. *Atmospheric Chem. Phys.* 15, 6503–6519. <https://doi.org/10.5194/acp-15-6503-2015>
- Donahue, N.M., Kroll, J.H., Pandis, S.N., Robinson, A.L., 2012. A two-dimensional volatility basis set – Part 2: Diagnostics of organic-aerosol evolution. *Atmospheric Chem. Phys.* 12, 615–634. <https://doi.org/10.5194/acp-12-615-2012>
- Donahue, N.M., Robinson, A.L., Pandis, S.N., 2009. Atmospheric organic particulate matter: From smoke to secondary organic aerosol. *Atmos. Environ.* 43, 94–106. <https://doi.org/10.1016/j.atmosenv.2008.09.055>
- Doumbia, E.H.T., Lioussé, C., Keita, S., Granier, L., Granier, C., Elvidge, C.D., Elguindi, N., Law, K., 2019. Flaring emissions in Africa: Distribution, evolution and comparison with current inventories. *Atmos. Environ.* 199, 423–434. <https://doi.org/10.1016/j.atmosenv.2018.11.006>
- Drozd, G.T., Zhao, Y., Saliba, G., Frodin, B., Maddox, C., Oliver Chang, M.-C., Maldonado, H., Sardar, S., Weber, R.J., Robinson, A.L., Goldstein, A.H., 2019. Detailed Speciation of Intermediate Volatility and Semivolatile Organic Compound Emissions from Gasoline Vehicles: Effects of Cold-Starts and Implications for Secondary Organic Aerosol Formation. *Environ. Sci. Technol.* 53, 1706–1714. <https://doi.org/10.1021/acs.est.8b05600>
- Duarte, M.A.C., 2011. Emissões de compostos carbonosos pela queima doméstica de biomassa (Master Thesis). Universidad de León, León, Portugal.
- Eastwood, P., 2008. Particulate emissions from vehicles, Wiley-Professional engineering publishing series. Wiley, Chichester.
- EC, 2020. Combined evaluation roadmap / Inception impact assesment (Ares(2020)1800668). EU, Brussels, EU.
- EC, 2015a. Commission Regulation (EU) 2015/1185 of 24 April 2015 implementing Directive 2009/125/EC of the European Parliament and of the Council with regard to ecodesign requirements for solid fuel local space heaters.
- EC, 2015b. Commission Regulation (EU) 2015/1189 of 28 April 2015 implementing Directive 2009/125/EC of the European Parliament and of the Council with regard to ecodesign requirements for solid fuel boilers.
- EC, 2009. Directive 2009/125/EC of the European Parliament and of the Council of 21 October 2009 establishing a framework for the setting of ecodesign requirements for energy-related products (recast).
- EC, 2007. REGULATION (EC) No 715/2007 OF THE EUROPEAN PARLIAMENT AND OF THE COUNCIL of 20 June 2007 on type approval of motor vehicles with respect to emissions from light passenger and commercial vehicles (Euro 5 and Euro 6) and on access to vehicle repair and maintenance information. European Commission, EU.
- ECE, 2020. Draft guidance document on prioritizing reductions of particulate matter so to also achieve reduction of black carbon.
- ECE, 2019. Executive Body for the Convention on Long-range Transboundary Air Pollution - Report of the Executive Body on its thirty-eighth session (Report No. ECE/EB.AIR/142). UNECE, UN.

- ECE, 2018a. Revised mandate of the Task Force on Techno-economic Issues (Decision No. 7). UNECE, UN.
- ECE, 2018b. Long-term strategy for the Convention on Long-range Transboundary Air Pollution for 2020–2030 and beyond (Decision No. ECE/EB.AIR/114). UNECE, UN.
- ECE, 2013. 1999 Protocol to Abate Acidification, Eutrophication and Ground-level Ozone to the Convention on Longrange Transboundary Air Pollution, as amended on 4 May 2012 (Protocol No. ECE/EB.AIR/114). UNECE, UN.
- ECE, 2010. The 1998 Protocol on Persistent Organic Pollutants, Including the Amendments Adopted by the Parties on 18 December 2009 (No. ECE/EB.AIR/104). United Nations, Geneva, Switzerland.
- Emam, E.A., 2015. Gas flaring in industry : An overview. *Pet. Coal* 57, 532–555.
- EMEP/CEIP, 2020. Present state of emission data [WWW Document]. Emiss. Database. URL <https://www.ceip.at/status-of-reporting-and-review-results/2020-submissions> (accessed 11.3.20).
- Eriksson, A.C., Nordin, E.Z., Nyström, R., Pettersson, E., Swietlicki, E., Bergvall, C., Westerholm, R., Boman, C., Pagels, J.H., 2014. Particulate PAH Emissions from Residential Biomass Combustion: Time-Resolved Analysis with Aerosol Mass Spectrometry. *Environ. Sci. Technol.* 48, 7143–7150. <https://doi.org/10.1021/es500486j>
- ETC/ACM, 2016. Contribution of residential combustion to ambient air pollution and greenhouse gas emissions (Technical Paper 2015/1). European Topic Centre on Air Pollution and Climate Change Mitigation.
- EU, 2016. Directive (EU) 2016/2284 of the european parliament and of the council of 14 december 2016 on the reduction of national emissions of certain atmospheric pollutants, amending directive 2003/35/EC and repealing directive 2001/81/EC. EU.
- EU Action on Black Carbon in the Arctic, 2019. Best Available Techniques Economically Achievable to Address Black Carbon from Gas Flaring: EU Action on Black Carbon in the Arctic (Technical report No. 3).
- European Commission. Joint Research Centre. Institute for Energy and Transport., 2014. Non-exhaust traffic related emissions - Brake and tyre wear PM: literature review. Publications Office, LU.
- Evans, M., Kholod, N., Kuklinski, T., Denysenko, A., Smith, S.J., Staniszewski, A., Hao, W.M., Liu, L., Bond, T.C., 2017. Black carbon emissions in Russia: A critical review. *Atmos. Environ.* 163, 9–21. <https://doi.org/10.1016/j.atmosenv.2017.05.026>
- Evans, S., 2019. EPA-Rethink OTM-37 for Condensable Particulate. *Worldw. Pollut. Control Assoc. WPCA Summer 2019*, 15–17.
- Faruolo, M., Lacava, T., Caseiro, A., Kaiser, J.W., 2020. Gas Flaring: A review focused on its analysis from space. *IEEE Geosci. Remote Sens. Mag.* 0–0. <https://doi.org/10.1109/MGRS.2020.3007232>
- Farwick zum Hagen, F.H., Mathissen, M., Grabiec, T., Hennicke, T., Rettig, M., Grochowicz, J., Vogt, R., Benter, T., 2019. On-road vehicle measurements of brake wear particle emissions. *Atmos. Environ.* 217, 116943. <https://doi.org/10.1016/j.atmosenv.2019.116943>

- Fawole, O.G., Cai, X.-M., MacKenzie, A.R., 2016. Gas flaring and resultant air pollution: A review focusing on black carbon. *Environ. Pollut.* 216, 182–197. <https://doi.org/10.1016/j.envpol.2016.05.075>
- Feng, Y., Li, Y., Cui, L., 2018. Critical review of condensable particulate matter. *Fuel* 224, 801–813. <https://doi.org/10.1016/j.fuel.2018.03.118>
- Fernandes, A.P., Alves, C.A., Gonçalves, C., Tarelho, L., Pio, C., Schimdl, C., Bauer, H., 2011. Emission factors from residential combustion appliances burning Portuguese biomass fuels. *J. Environ. Monit.* 13, 3196. <https://doi.org/10.1039/c1em10500k>
- Fiebig, M., Wiartalla, A., Holderbaum, B., Kiesow, S., 2014. Particulate emissions from diesel engines: correlation between engine technology and emissions. *J. Occup. Med. Toxicol.* 9, 6. <https://doi.org/10.1186/1745-6673-9-6>
- Fino, D., Bensaid, S., Piumetti, M., Russo, N., 2016. A review on the catalytic combustion of soot in Diesel particulate filters for automotive applications: From powder catalysts to structured reactors. *Appl. Catal. Gen.* 509, 75–96. <https://doi.org/10.1016/j.apcata.2015.10.016>
- Fortner, E., Onasch, T., Canagaratna, M., Williams, L.R., Lee, T., Jayne, J., Worsnop, D., 2018. Examining the chemical composition of black carbon particles from biomass burning with SP-AMS. *J. Aerosol Sci.* 120, 12–21. <https://doi.org/10.1016/j.jaerosci.2018.03.001>
- Fortner, E.C., Brooks, W.A., Onasch, T.B., Canagaratna, M.R., Massoli, P., Jayne, J.T., Franklin, J.P., Knighton, W.B., Wormhoudt, J., Worsnop, D.R., Kolb, C.E., Herndon, S.C., 2012. Particulate Emissions Measured During the TCEQ Comprehensive Flare Emission Study. *Ind. Eng. Chem. Res.* 51, 12586–12592. <https://doi.org/10.1021/ie202692y>
- Frauhammer, J., Schenck zu Schweinsberg, A., Winkler, K., 2015. Catalytic emission control, in: Reif, K. (Ed.), *Gasoline Engine Management*. Springer Fachmedien Wiesbaden, Wiesbaden, pp. 268–283. https://doi.org/10.1007/978-3-658-03964-6_18
- Frenklach, M., Wang, H., 1991. Detailed modeling of soot particle nucleation and growth. *Symp. Int. Combust.* 23, 1559–1566. [https://doi.org/10.1016/S0082-0784\(06\)80426-1](https://doi.org/10.1016/S0082-0784(06)80426-1)
- Gai, H., Wang, A., Fang, J., Lou, H.H., Chen, D., Li, X., Martin, C., 2020. Clean combustion and flare minimization to reduce emissions from process industry. *Curr. Opin. Green Sustain. Chem.* 23, 38–45. <https://doi.org/10.1016/j.cogsc.2020.04.006>
- Gentner, D.R., Jathar, S.H., Gordon, T.D., Bahreini, R., Day, D.A., El Haddad, I., Hayes, P.L., Pieber, S.M., Platt, S.M., de Gouw, J., Goldstein, A.H., Harley, R.A., Jimenez, J.L., Prévôt, A.S.H., Robinson, A.L., 2017. Review of Urban Secondary Organic Aerosol Formation from Gasoline and Diesel Motor Vehicle Emissions. *Environ. Sci. Technol.* 51, 1074–1093. <https://doi.org/10.1021/acs.est.6b04509>
- GGFR, 2016. *Global Gas Flaring Reduction Partnership [WWW Document]*. URL <https://www.worldbank.org/en/programs/gasflaringreduction> (accessed 11.25.20).
- Ghafghazi, S., Sowlati, T., Sokhansanj, S., Bi, X., Melin, S., 2011. Particulate matter emissions from combustion of wood in district heating applications. *Renew. Sustain. Energy Rev.* 15, 3019–3028. <https://doi.org/10.1016/j.rser.2011.04.001>
- Giechaskiel, B., 2020. Gaseous and Particulate Emissions of a Euro 4 Motorcycle and Effect of Driving Style and Open or Closed Sampling Configuration. *Sustainability* 12, 9122. <https://doi.org/10.3390/su12219122>

- Gonçalves, C., Alves, C., Fernandes, A.P., Monteiro, C., Tarelho, L., Evtyugina, M., Pio, C., 2011. Organic compounds in PM_{2.5} emitted from fireplace and woodstove combustion of typical Portuguese wood species. *Atmos. Environ.* 45, 4533–4545. <https://doi.org/10.1016/j.atmosenv.2011.05.071>
- Grigoratos, T., Fontaras, G., Giechaskiel, B., Zacharof, N., 2019. Real world emissions performance of heavy-duty Euro VI diesel vehicles. *Atmos. Environ.* 201, 348–359. <https://doi.org/10.1016/j.atmosenv.2018.12.042>
- Grigoratos, T., Martini, G., 2015. Brake wear particle emissions: a review. *Environ. Sci. Pollut. Res.* 22, 2491–2504. <https://doi.org/10.1007/s11356-014-3696-8>
- Guan, B., Zhan, R., Lin, H., Huang, Z., 2015. Review of the state-of-the-art of exhaust particulate filter technology in internal combustion engines. *J. Environ. Manage.* 154, 225–258. <https://doi.org/10.1016/j.jenvman.2015.02.027>
- Habib, G., Kumar, S., 2016. Evaluation of portable dilution system for aerosol measurement from stationary and mobile combustion sources. *Aerosol Sci. Technol.* 50, 717–731. <https://doi.org/10.1080/02786826.2016.1178502>
- Hajizadeh, A., Mohamadi-Baghmolaei, M., Azin, R., Osfouri, S., Heydari, I., 2018. Technical and economic evaluation of flare gas recovery in a giant gas refinery. *Chem. Eng. Res. Des.* 131, 506–519. <https://doi.org/10.1016/j.cherd.2017.11.026>
- Happonen, M., Heikkilä, J., Murtonen, T., Lehto, K., Sarjoavaara, T., Larmi, M., Keskinen, J., Virtanen, A., 2012. Reductions in Particulate and NO_x Emissions by Diesel Engine Parameter Adjustments with HVO Fuel. *Environ. Sci. Technol.* 46, 6198–6204. <https://doi.org/10.1021/es300447t>
- Harmsen, M.J.H.M., van Dorst, P., van Vuuren, D.P., van den Berg, M., Van Dingenen, R., Klimont, Z., 2020. Co-benefits of black carbon mitigation for climate and air quality. *Clim. Change.* <https://doi.org/10.1007/s10584-020-02800-8>
- Harrison, R.M., 2020. Airborne particulate matter. *Philos. Trans. R. Soc. Math. Phys. Eng. Sci.* 378, 20190319. <https://doi.org/10.1098/rsta.2019.0319>
- Hartikka, T., Kuronen, M., Kiiski, U., 2012. Technical Performance of HVO (Hydrotreated Vegetable Oil) in Diesel Engines. Presented at the SAE 2012 International Powertrains, Fuels & Lubricants Meeting, pp. 2012-01–1585. <https://doi.org/10.4271/2012-01-1585>
- Hascoët, M., Adamczak, L., 2020. At source brake dust collection system. *Results Eng.* 5, 100083. <https://doi.org/10.1016/j.rineng.2019.100083>
- Hodzic, A., Jimenez, J.L., Madronich, S., Canagaratna, M.R., DeCarlo, P.F., Kleinman, L., Fast, J., 2010. Modeling organic aerosols in a megacity: potential contribution of semi-volatile and intermediate volatility primary organic compounds to secondary organic aerosol formation. *Atmospheric Chem. Phys.* 10, 5491–5514. <https://doi.org/10.5194/acp-10-5491-2010>
- Horak, J., Kubonova, L., Krpec, K., Hopan, F., Kubesa, P., Motyka, O., Laciok, V., Dej, M., Ochodek, T., Placha, D., 2017. PAH emissions from old and new types of domestic hot water boilers. *Environ. Pollut.* 225, 31–39. <https://doi.org/10.1016/j.envpol.2017.03.034>
- Huang, K., Fu, J.S., 2016. A global gas flaring black carbon emission rate dataset from 1994 to 2012. *Sci. Data* 3, 160104. <https://doi.org/10.1038/sdata.2016.104>
- Hukkanen, A., Kaivosoja, T., Sippula, O., Nuutinen, K., Jokiniemi, J., Tissari, J., 2012. Reduction of gaseous and particulate emissions from small-scale wood combustion with

- a catalytic combustor. *Atmos. Environ.* 50, 16–23.
<https://doi.org/10.1016/j.atmosenv.2012.01.016>
- IEA Bioenergy, 2011. Particle precipitation devices for residential biomass combustion (Final report No. Task 3.2). Institute for Process and Particle Engineering, Graz, Austria.
- Janssens-Maenhout, G., Pagliari, V., Guizzardi, D., Muntean, M., 2012. Global emission inventories in the Emission Database for Global Atmospheric Research (EDGAR): manual (I) - gridding: EDGAR emissions distribution on global gridmaps. Publications Office, Luxembourg.
- Kaivosoja, T., Virén, A., Tissari, J., Ruuskanen, J., Tarhanen, J., Sippula, O., Jokiniemi, J., 2012. Effects of a catalytic converter on PCDD/F, chlorophenol and PAH emissions in residential wood combustion. *Chemosphere* 88, 278–285.
<https://doi.org/10.1016/j.chemosphere.2012.02.027>
- Kampf, C.J., Filippi, A., Zuth, C., Hoffmann, T., Opatz, T., 2016. Secondary brown carbon formation via the dicarbonyl imine pathway: nitrogen heterocycle formation and synergistic effects. *Phys. Chem. Chem. Phys.* 18, 18353–18364.
<https://doi.org/10.1039/C6CP03029G>
- Kausch, F., Seljeskog, M., Østnor, A., 2020. New European particulate emission test method for small scale appliances fired by solid fuel - EN-PME+EN16510-1 PM emission test method vs NS 3058/3059:1994 (RISE report 20012-72). RISE, Trondheim, Norway.
- Khodaei, H., Guzzomi, F., Patiño, D., Rashidian, B., Yeoh, G.H., 2017. Air staging strategies in biomass combustion-gaseous and particulate emission reduction potentials. *Fuel Process. Technol.* 157, 29–41. <https://doi.org/10.1016/j.fuproc.2016.11.007>
- Kim, Y., Sartelet, K., Seigneur, C., Charron, A., Besombes, J.-L., Jaffrezo, J.-L., Marchand, N., Polo, L., 2016. Effect of measurement protocol on organic aerosol measurements of exhaust emissions from gasoline and diesel vehicles. *Atmos. Environ.* 140, 176–187.
<https://doi.org/10.1016/j.atmosenv.2016.05.045>
- Kinsey, J.S., 2009. Characterization of emissions from commercial aircraft engines during the aircraft particle emissions experiment (APEX) 1–3 (Technical report No. EPA/600/R-09/130). US Environmental Protection Agency Office of Research and Development National Risk Management Research Laboratory, Washington DC, USA.
- Klimont, Z., Kupiainen, K., Heyes, C., Purohit, P., Cofala, J., Rafaj, P., Borken-Kleefeld, J., Schöpp, W., 2017. Global anthropogenic emissions of particulate matter including black carbon. *Atmospheric Chem. Phys.* 17, 8681–8723. <https://doi.org/10.5194/acp-17-8681-2017>
- Kodros, J.K., Papanastasiou, D.K., Paglione, M., Masiol, M., Squizzato, S., Florou, K., Skyllakou, K., Kaltsonoudis, C., Nenes, A., Pandis, S.N., 2020. Rapid dark aging of biomass burning as an overlooked source of oxidized organic aerosol. *Proc. Natl. Acad. Sci.* <https://doi.org/10.1073/pnas.2010365117>
- Koniecznyński, J., Komosiński, B., Cieślik, E., Konieczny, T., Mathews, B., Rachwał, T., Rzońca, G., 2017. Research into properties of dust from domestic central heating boiler fired with coal and solid biofuels. *Arch. Environ. Prot.* 43, 20–27.
<https://doi.org/10.1515/aep-2017-0019>
- Koo, B., Knipping, E., Yarwood, G., 2014. 1.5-Dimensional volatility basis set approach for modeling organic aerosol in CAMx and CMAQ. *Atmos. Environ.* 95, 158–164.
<https://doi.org/10.1016/j.atmosenv.2014.06.031>

- Kostenidou, E., Martinez-Valiente, A., R'Mili, B., Marques, B., Temime-Roussel, B., André, M., Liu, Y., Louis, C., Vansevenant, B., Ferry, D., Laffon, C., Parent, P., D'Anna, B., 2020. Technical note: Emission factors, chemical composition and morphology of particles emitted from Euro 5 diesel and gasoline light duty vehicles during transient cycles (preprint). *Aerosols/Laboratory Studies/Troposphere/Chemistry (chemical composition and reactions)*. <https://doi.org/10.5194/acp-2020-842>
- Kubica, K., Paradiz, B., Dilara, P., 2007. *Small combustion installations :techniques, emissions and measures for emission reduction*. Publications Office, LU.
- Kuenen, J., Trozi, C., 2019. *EMEP/EEA air pollutant emission inventory guidebook 2019 - Small Combustion*. Environment European Agency, Copenhagen, DK.
- Kulmala, M., Petäjä, T., Ehn, M., Thornton, J., Sipilä, M., Worsnop, D.R., Kerminen, V.-M., 2014. Chemistry of Atmospheric Nucleation: On the Recent Advances on Precursor Characterization and Atmospheric Cluster Composition in Connection with Atmospheric New Particle Formation. *Annu. Rev. Phys. Chem.* 65, 21–37. <https://doi.org/10.1146/annurev-physchem-040412-110014>
- Kumar, A., Phadatare, S., Deore, P., 2020. A GUIDE ON SMOKELESS FLARING: AIR/STEAM ASSISTED AND HIGH PRESSURE FLARING. *Int. J. Eng. Appl. Sci. Technol.* 04, 517–520. <https://doi.org/10.33564/IJEAST.2020.v04i12.092>
- Kupiainen, K.J., Aamaas, B., Savolahti, M., Karvosenoja, N., Paunu, V.-V., 2019. Climate impact of Finnish air pollutants and greenhouse gases using multiple emission metrics. *Atmospheric Chem. Phys.* 19, 7743–7757. <https://doi.org/10.5194/acp-19-7743-2019>
- Kwon, H.-S., Ryu, M.H., Carlsten, C., 2020. Ultrafine particles: unique physicochemical properties relevant to health and disease. *Exp. Mol. Med.* 52, 318–328. <https://doi.org/10.1038/s12276-020-0405-1>
- Lack, D.A., Moosmüller, H., McMeeking, G.R., Chakrabarty, R.K., Baumgardner, D., 2014. Characterizing elemental, equivalent black, and refractory black carbon aerosol particles: a review of techniques, their limitations and uncertainties. *Anal. Bioanal. Chem.* 406, 99–122. <https://doi.org/10.1007/s00216-013-7402-3>
- Lai, A., Shan, M., Deng, M., Carter, E., Yang, X., Baumgartner, J., Schauer, J., 2019. Differences in chemical composition of PM_{2.5} emissions from traditional versus advanced combustion (semi-gasifier) solid fuel stoves. *Chemosphere* 233, 852–861. <https://doi.org/10.1016/j.chemosphere.2019.06.013>
- Lamarque, J.-F., Bond, T.C., Eyring, V., Granier, C., Heil, A., Klimont, Z., Lee, D., Liousse, C., Mieville, A., Owen, B., Schultz, M.G., Shindell, D., Smith, S.J., Stehfest, E., Van Aardenne, J., Cooper, O.R., Kainuma, M., Mahowald, N., McConnell, J.R., Naik, V., Riahi, K., van Vuuren, D.P., 2010. Historical (1850–2000) gridded anthropogenic and biomass burning emissions of reactive gases and aerosols: methodology and application. *Atmospheric Chem. Phys.* 10, 7017–7039. <https://doi.org/10.5194/acp-10-7017-2010>
- Lambert, C.K., 2019. Perspective on SCR NO_x control for diesel vehicles. *React. Chem. Eng.* 4, 969–974. <https://doi.org/10.1039/C8RE00284C>
- Laskin, A., Laskin, J., Nizkorodov, S.A., 2015. Chemistry of Atmospheric Brown Carbon. *Chem. Rev.* 115, 4335–4382. <https://doi.org/10.1021/cr5006167>
- Lelieveld, J., Pozzer, A., Pöschl, U., Fnais, M., Haines, A., Münzel, T., 2020. Loss of life expectancy from air pollution compared to other risk factors: a worldwide perspective. *Cardiovasc. Res.* 116, 1910–1917. <https://doi.org/10.1093/cvr/cvaa025>

- Li, X., Zhou, C., Li, J., Lu, S., Yan, J., 2019. Distribution and emission characteristics of filterable and condensable particulate matter before and after a low-low temperature electrostatic precipitator. *Environ. Sci. Pollut. Res.* 26, 12798–12806. <https://doi.org/10.1007/s11356-019-04570-y>
- Long, C.M., Nascarella, M.A., Valberg, P.A., 2013. Carbon black vs. black carbon and other airborne materials containing elemental carbon: Physical and chemical distinctions. *Environ. Pollut.* 181, 271–286. <https://doi.org/10.1016/j.envpol.2013.06.009>
- Louis, C., Goriaux, M., Tassel, P., Perret, P., André, M., Liu, Y., 2016a. Impact of Aftertreatment Device and Driving Conditions on Black Carbon, Ultrafine Particle and NOx Emissions for Euro 5 Diesel and Gasoline Vehicles. *Transp. Res. Procedia* 14, 3079–3088. <https://doi.org/10.1016/j.trpro.2016.05.454>
- Louis, C., Liu, Y., Tassel, P., Perret, P., Chaumond, A., André, M., 2016b. PAH, BTEX, carbonyl compound, black-carbon, NO2 and ultrafine particle dynamometer bench emissions for Euro 4 and Euro 5 diesel and gasoline passenger cars. *Atmos. Environ.* 141, 80–95. <https://doi.org/10.1016/j.atmosenv.2016.06.055>
- Lyu, Y., Olofsson, U., 2020. On black carbon emission from automotive disc brakes. *J. Aerosol Sci.* 148, 105610. <https://doi.org/10.1016/j.jaerosci.2020.105610>
- Maher, B.A., O’Sullivan, V., Feeney, J., Gonet, T., Anne Kenny, R., 2021. Indoor particulate air pollution from open fires and the cognitive function of older people. *Environ. Res.* 192, 110298. <https://doi.org/10.1016/j.envres.2020.110298>
- Mamakos, A., Arndt, M., Hesse, D., Augsburg, K., 2019. Physical Characterization of Brake-Wear Particles in a PM10 Dilution Tunnel. *Atmosphere* 10, 639. <https://doi.org/10.3390/atmos10110639>
- Martins, V.I.F., 2012. Emissões de carbono particulado durante a queima doméstica de biomassa (Thesis). Universidade de Aveiro, Aveiro.
- Masnadi, M.S., El-Houjeiri, H.M., Schunack, D., Li, Y., Englander, J.G., Badahdah, A., Monfort, J.-C., Anderson, J.E., Wallington, T.J., Bergerson, J.A., Gordon, D., Koomey, J., Przesmitzki, S., Azevedo, I.L., Bi, X.T., Duffy, J.E., Heath, G.A., Keoleian, G.A., McGlade, C., Meehan, D.N., Yeh, S., You, F., Wang, M., Brandt, A.R., 2018. Global carbon intensity of crude oil production. *Science* 361, 851–853. <https://doi.org/10.1126/science.aar6859>
- Mathissen, M., Scheer, V., Vogt, R., Benter, T., 2011. Investigation on the potential generation of ultrafine particles from the tire–road interface. *Atmos. Environ.* 45, 6172–6179. <https://doi.org/10.1016/j.atmosenv.2011.08.032>
- May, J., Bosteels, D., Favre, C., 2010. Emissions Control Systems and Climate Change Emissions. Association for Emissions Control by Catalyst (AECC), Brussels, Belgium.
- McEwen, J.D.N., Johnson, M.R., 2012. Black carbon particulate matter emission factors for buoyancy-driven associated gas flares. *J. Air Waste Manag. Assoc.* 62, 307–321. <https://doi.org/10.1080/10473289.2011.650040>
- McNeill, V.F., 2017. Atmospheric Aerosols: Clouds, Chemistry, and Climate. *Annu. Rev. Chem. Biomol. Eng.* 8, 427–444. <https://doi.org/10.1146/annurev-chembioeng-060816-101538>
- Mertens, J., Lepaumier, H., Rogiers, P., Desagher, D., Goossens, L., Duterque, A., Le Cadre, E., Zarea, M., Blondeau, J., Webber, M., 2020. Fine and ultrafine particle number and size measurements from industrial combustion processes: Primary emissions field data. *Atmospheric Pollut. Res.* 11, 803–814. <https://doi.org/10.1016/j.apr.2020.01.008>

- Miller, J., Jin, L., 2019. Global progress towards soot-free diesel vehicles in 2019 (Report). International Council on Clean Transportation (ICTT), Washington DC, USA.
- Monks, P.S., Williams, M.L., 2020. What does success look like for air quality policy? A perspective. *Philos. Trans. R. Soc. Math. Phys. Eng. Sci.* 378, 20190326. <https://doi.org/10.1098/rsta.2019.0326>
- Mostafayi, S.S., Rashidi, F., 2020. Effect of dividing single flare tip into multiple tips on soot reduction. *Clean Technol. Environ. Policy* 22, 1097–1108. <https://doi.org/10.1007/s10098-020-01852-9>
- Mu, M., Li, X., Qiu, Y., Shi, Y., 2019. Study on a New Gasoline Particulate Filter Structure Based on the Nested Cylinder and Diversion Channel Plug. *Energies* 12, 2045. <https://doi.org/10.3390/en12112045>
- Muñoz, M., Haag, R., Honegger, P., Zeyer, K., Mohn, J., Comte, P., Czerwinski, J., Heeb, N.V., 2018. Co-formation and co-release of genotoxic PAHs, alkyl-PAHs and soot nanoparticles from gasoline direct injection vehicles. *Atmos. Environ.* 178, 242–254. <https://doi.org/10.1016/j.atmosenv.2018.01.050>
- Murphy, B.N., Donahue, N.M., Robinson, A.L., Pandis, S.N., 2014. A naming convention for atmospheric organic aerosol. *Atmospheric Chem. Phys.* 14, 5825–5839. <https://doi.org/10.5194/acp-14-5825-2014>
- Nielsen, I.E., Eriksson, A.C., Lindgren, R., Martinsson, J., Nyström, R., Nordin, E.Z., Sadiktsis, I., Boman, C., Nøjgaard, J.K., Pagels, J., 2017. Time-resolved analysis of particle emissions from residential biomass combustion – Emissions of refractory black carbon, PAHs and organic tracers. *Atmos. Environ.* 165, 179–190. <https://doi.org/10.1016/j.atmosenv.2017.06.033>
- Ntziachristos, L., Boulter, P., 2019. EMEP/EEA air pollutant emission inventory guidebook 2019 - 1.A.3.b.vi Road transport: Automobile tyre and brake wear - 1.A.3.b.vii Road transport: Automobile road abrasion. European Environment Agency.
- Ntziachristos, L., Mellios, G., Fontaras, G., Gkeivanidis, S., Kousoulidou, M., Gkatzoflias, D., Papageorgiou, Th., Kouridis, C., 2007. Updates of the Guidebook Chapter on Road Transport (LAT report No. 0706).
- Ntziachristos, L., Samarras, Z., 2019. EMEP/EEA air pollutant emission inventory guidebook 2019 - 1.A.3.b.i, 1.A.3.b.ii, 1.A.3.b.iii, 1.A.3.b.iv Passenger cars, light commercial trucks, heavy-duty vehicles including buses and motor cycles. Environment European Agency, Copenhagen, DK.
- Nussbaumer, T., 2016. Particulate Matter (PM) from biomass combustion - An overview of measures to reduce particle emissions.
- Nussbaumer, T., 2010a. Overview on Technologies for Biomass Combustion and Emission Levels of Particulate Matter. Swiss Federal Office for the Environment (FOEN) as a contribution to the Expert Group on Techno-Economic Issues (EGTEI) under the Convention on Long-Range Transboundary Air Pollution (CLRTAP), Zürich, Switzerland.
- Nussbaumer, T. (Ed.), 2010b. Potenzial und Technik zur Holzenergie-Nutzung: 11. Holzenergie-Symposium ; 17. September 2010, ETH Zürich. TEMAS AG [u.a.], Arbon.
- Obaidullah, O., Bram, S., Verma, V.K., De Ruyck, J., 2012. A Review on Particle Emissions from Small Scale Biomass Combustion. *Int. J. Renew. Energy Res.* 2, 147–159.

- Obernberger, I., Brunner, T., Mandl, C., Kerschbaum, M., Svetlik, T., 2017. Strategies and technologies towards zero emission biomass combustion by primary measures. *Energy Procedia* 120, 681–688. <https://doi.org/10.1016/j.egypro.2017.07.184>
- Oluwoye, I., Altarawneh, M., Gore, J., Dlugogorski, B.Z., 2020. Products of incomplete combustion from biomass reburning. *Fuel* 274, 117805. <https://doi.org/10.1016/j.fuel.2020.117805>
- Omara, M., Hopke, P.K., Raja, S., Holsen, T.M., 2010. Performance Evaluation of a Model Electrostatic Precipitator for an Advanced Wood Combustion System. *Energy Fuels* 24, 6301–6306. <https://doi.org/10.1021/ef101031u>
- Omidvarborna, H., Kumar, A., Kim, D.-S., 2015. Recent studies on soot modeling for diesel combustion. *Renew. Sustain. Energy Rev.* 48, 635–647. <https://doi.org/10.1016/j.rser.2015.04.019>
- Orasche, J., Schnelle-Kreis, J., Schön, C., Hartmann, H., Ruppert, H., Arteaga-Salas, J.M., Zimmermann, R., 2013. Comparison of Emissions from Wood Combustion. Part 2: Impact of Combustion Conditions on Emission Factors and Characteristics of Particle-Bound Organic Species and Polycyclic Aromatic Hydrocarbon (PAH)-Related Toxicological Potential. *Energy Fuels* 27, 1482–1491. <https://doi.org/10.1021/ef301506h>
- Orasche, J., Seidel, T., Hartmann, H., Schnelle-Kreis, J., Chow, J.C., Ruppert, H., Zimmermann, R., 2012. Comparison of Emissions from Wood Combustion. Part 1: Emission Factors and Characteristics from Different Small-Scale Residential Heating Appliances Considering Particulate Matter and Polycyclic Aromatic Hydrocarbon (PAH)-Related Toxicological Potential of Particle-Bound Organic Species. *Energy Fuels* 26, 6695–6704. <https://doi.org/10.1021/ef301295k>
- Ots, R., Young, D.E., Vieno, M., Xu, L., Dunmore, R.E., Allan, J.D., Coe, H., Williams, L.R., Herndon, S.C., Ng, N.L., Hamilton, J.F., Bergström, R., Di Marco, C., Nemitz, E., Mackenzie, I.A., Kuenen, J.J.P., Green, D.C., Reis, S., Heal, M.R., 2016. Simulating secondary organic aerosol from missing diesel-related intermediate-volatility organic compound emissions during the Clean Air for London (ClearfLo) campaign. *Atmospheric Chem. Phys.* 16, 6453–6473. <https://doi.org/10.5194/acp-16-6453-2016>
- Ozgen, S., Becagli, S., Bernardoni, V., Caserini, S., Caruso, D., Corbella, L., Dell'Acqua, M., Fermo, P., Gonzalez, R., Lonati, G., Signorini, S., Tardivo, R., Tosi, E., Valli, G., Vecchi, R., Marinovich, M., 2017. Analysis of the chemical composition of ultrafine particles from two domestic solid biomass fired room heaters under simulated real-world use. *Atmos. Environ.* 150, 87–97. <https://doi.org/10.1016/j.atmosenv.2016.11.048>
- Pang, B., Xie, M.-Z., Jia, M., Liu, Y.-D., 2013. Development of a Phenomenological Soot Model Coupled with a Skeletal PAH Mechanism for Practical Engine Simulation. *Energy Fuels* 27, 1699–1711. <https://doi.org/10.1021/ef400033f>
- Park, G., Kim, K., Park, T., Kang, S., Ban, J., Choi, S., Yu, D.-G., Lee, S., Lim, Y., Kim, S., Lee, J., Woo, J.-H., Lee, T., 2020. Characterizing Black Carbon Emissions from Gasoline, LPG, and Diesel Vehicles via Transient Chassis-Dynamometer Tests. *Appl. Sci.* 10, 5856. <https://doi.org/10.3390/app10175856>
- Patki, A., Li, X., Chen, D., Lou, H., Richmond, P., Damodara, V., Liu, L., Rasel, K., Alphones, A., Zhou, J., 2014. On Numerical Simulation of Black Carbon (Soot) Emissions from Non-Premixed Flames. *J. Geosci. Environ. Prot.* 02, 15–24. <https://doi.org/10.4236/gep.2014.24003>

- Petzold, A., Ogren, J.A., Fiebig, M., Laj, P., Li, S.-M., Baltensperger, U., Holzer-Popp, T., Kinne, S., Pappalardo, G., Sugimoto, N., Wehrli, C., Wiedensohler, A., Zhang, X.-Y., 2013. Recommendations for reporting “black carbon” measurements. *Atmospheric Chem. Phys.* 13, 8365–8379. <https://doi.org/10.5194/acp-13-8365-2013>
- Pillot, D., Guegan, H., Paturel, L., Cazier, F., Déchaux, J.C., Combet, E., André, J.-M., Vidon, R., Tassel, P., Mercier, A., Perret, P., Nouali, H., 2006. Emissions unitaires de métaux et de polluants non réglementés des voitures particulières équipées ou non de filtre à particules (No. Rapport LTE n° 0624). INRETS for ADEME n°0366 C0040, Paris, France.
- Piock, W., Hoffmann, G., Berndorfer, A., Salemi, P., Fusshoeller, B., 2011. Strategies Towards Meeting Future Particulate Matter Emission Requirements in Homogeneous Gasoline Direct Injection Engines. *SAE Int. J. Engines* 4, 1455–1468. <https://doi.org/10.4271/2011-01-1212>
- Pirjola, L., Kuuluvainen, H., Timonen, H., Saarikoski, S., Teinilä, K., Salo, L., Datta, A., Simonen, P., Karjalainen, P., Kulmala, K., Rönkkö, T., 2019. Potential of renewable fuel to reduce diesel exhaust particle emissions. *Appl. Energy* 254, 113636. <https://doi.org/10.1016/j.apenergy.2019.113636>
- Platt, S.M., El Haddad, I., Pieber, S.M., Zardini, A.A., Suarez-Bertoa, R., Clairotte, M., Daellenbach, K.R., Huang, R.-J., Slowik, J.G., Hellebust, S., Temime-Roussel, B., Marchand, N., de Gouw, J., Jimenez, J.L., Hayes, P.L., Robinson, A.L., Baltensperger, U., Astorga, C., Prévôt, A.S.H., 2017. Gasoline cars produce more carbonaceous particulate matter than modern filter-equipped diesel cars. *Sci. Rep.* 7, 4926. <https://doi.org/10.1038/s41598-017-03714-9>
- Plejdrup, M., Deslauriers, M., Kuenen, J., Rypdal, K., Woodfield, M., 2019. EMEP/EEA air pollutant emission inventory guidebook 2019 - 1.B.2.c Venting and flaring (Guidebook). European Environmental Agency, Copenhagen, DK.
- Poláčik, J., Sitek, T., Pospíšil, J., Šnajdárek, L., Lisý, M., 2021. Emission of fine particles from residential combustion of wood: Comparison of automatic boiler, manual log feed stove and thermo-gravimetric analysis. *J. Clean. Prod.* 279, 123664. <https://doi.org/10.1016/j.jclepro.2020.123664>
- Polo Rehn, L., 2013. Caractérisation et impacts des émissions de polluants du transport routier : Apports méthodologiques et cas d'études en Rhône Alpes (Thesis). Grenoble University, Grenoble, France.
- Popovicheva, O., Timofeev, M., Persiantseva, N., Jefferson, M.A., Johnson, M., Rogak, S.N., Baldelli, A., 2019. Microstructure and Chemical Composition of Particles from Small-scale Gas Flaring. *Aerosol Air Qual. Res.* 19, 2205–2221. <https://doi.org/10.4209/aaqr.2019.04.0177>
- Pöschl, U., 2005. Atmospheric Aerosols: Composition, Transformation, Climate and Health Effects. *Angew. Chem. Int. Ed.* 44, 7520–7540. <https://doi.org/10.1002/anie.200501122>
- Preble, C.V., Harley, R.A., Kirchstetter, T.W., 2019. Measuring real-world emissions from the on-road heavy-duty truck fleet (CARB No. 12–315). Department of Civil and Environmental Engineering University of California, Berkeley, CA, USA.
- PRIMEQUAL, 2018. Le chauffage individuel au bois : des atouts à valoriser, des pratiques et appareils à améliorer. Presented at the Colloque de valorisation, MTES-ADEME, Lyon, France.

- Querol, X., Karanasiou, A., de Vasconcelos, C., 2016. Emission factor for biomass burning - Deliverable 4.1: AIRUSE LIFE 11 ENV/ES/584.
- Randerson, J.T., Ven Der Werf, G.R., Giglio, L., Collatz, G.J., Kasibhatla, P.S., 2017. Global Fire Emissions Database, Version 4.1 (GFEDv4) 1925.7122549999906 MB. <https://doi.org/10.3334/ORNLDAAAC/1293>
- Raventos, C., INERIS, 2018. Caractérisation au rejet d'installations, des émissions atmosphériques de Black Carbon -Facteurs d'émissions de sources de combustion - Synthèse. ADEME.
- Reşitoğlu, İ.A., Altinişik, K., Keskin, A., 2015. The pollutant emissions from diesel-engine vehicles and exhaust aftertreatment systems. *Clean Technol. Environ. Policy* 17, 15–27. <https://doi.org/10.1007/s10098-014-0793-9>
- Richter, J.M., Klingmann, R., Spiess, S., Wong, K.-F., 2012. Application of Catalyzed Gasoline Particulate Filters to GDI Vehicles. *SAE Int. J. Engines* 5, 1361–1370. <https://doi.org/10.4271/2012-01-1244>
- Robinson, A.L., Donahue, N.M., Shrivastava, M.K., Weitkamp, E.A., Sage, A.M., Grieshop, A.P., Lane, T.E., Pierce, J.R., Pandis, S.N., 2007. Rethinking Organic Aerosols: Semivolatile Emissions and Photochemical Aging. *Science* 315, 1259–1262. <https://doi.org/10.1126/science.1133061>
- Rodríguez, F., Bernard, Y., Dornoff, J., Mock, P., 2019. Recommendations for post-Euro 6 standards for light-duty vehicles in the european union. International Council on Clean Transportation, Berlin, Germany.
- Samburova, V., Connolly, J., Gyawali, M., Yatavelli, R.L.N., Watts, A.C., Chakrabarty, R.K., Zielinska, B., Moosmüller, H., Khlystov, A., 2016. Polycyclic aromatic hydrocarbons in biomass-burning emissions and their contribution to light absorption and aerosol toxicity. *Sci. Total Environ.* 568, 391–401. <https://doi.org/10.1016/j.scitotenv.2016.06.026>
- Samset, B.H., Fuglestedt, J.S., Lund, M.T., 2020. Delayed emergence of a global temperature response after emission mitigation. *Nat. Commun.* 11, 3261. <https://doi.org/10.1038/s41467-020-17001-1>
- Sand, M., Berntsen, T.K., von Salzen, K., Flanner, M.G., Langner, J., Victor, D.G., 2016. Response of Arctic temperature to changes in emissions of short-lived climate forcers. *Nat. Clim. Change* 6, 286–289. <https://doi.org/10.1038/nclimate2880>
- Savolahti, M., Karvosenoja, N., Kupiainen, K., 2014. Ecodesign directive for residential wood combustion appliances: impacts and emission reduction potential in Finland. Presented at the SUSTAINABLE CITY 2014, Siena, Italy, pp. 1493–1504. <https://doi.org/10.2495/SC141262>
- Schauer, J.J., Kleeman, M.J., Cass, G.R., Simoneit, B.R.T., 2002. Measurement of Emissions from Air Pollution Sources. 5. C₁–C₃₂ Organic Compounds from Gasoline-Powered Motor Vehicles. *Environ. Sci. Technol.* 36, 1169–1180. <https://doi.org/10.1021/es0108077>
- Schauer, J.J., Kleeman, M.J., Cass, G.R., Simoneit, B.R.T., 1999. Measurement of Emissions from Air Pollution Sources. 2. C₁ through C₃₀ Organic Compounds from Medium Duty Diesel Trucks. *Environ. Sci. Technol.* 33, 1578–1587. <https://doi.org/10.1021/es980081n>
- Schmidl, C., Luisser, M., Padouvas, E., Lasselsberger, L., Rzaca, M., Ramirez-Santa Cruz, C., Handler, M., Peng, G., Bauer, H., Puxbaum, H., 2011. Particulate and gaseous emissions

- from manually and automatically fired small scale combustion systems. *Atmos. Environ.* 45, 7443–7454. <https://doi.org/10.1016/j.atmosenv.2011.05.006>
- Schmidt, G., Trouvé, G., Leysens, G., Schönnenbeck, C., Genevray, P., Cazier, F., Dewaele, D., Vandenbilcke, C., Faivre, E., Denance, Y., Le Dreff-Lorimier, C., 2018. Wood washing: Influence on gaseous and particulate emissions during wood combustion in a domestic pellet stove. *Fuel Process. Technol.* 174, 104–117. <https://doi.org/10.1016/j.fuproc.2018.02.020>
- Segersson, D., Eneroth, K., Gidhagen, L., Johansson, C., Omstedt, G., Nylén, A.E., Forsberg, B., 2017. Health Impact of PM₁₀, PM_{2.5} and Black Carbon Exposure Due to Different Source Sectors in Stockholm, Gothenburg and Umea, Sweden. *Int. J. Environ. Res. Public Health* 14. <https://doi.org/10.3390/ijerph14070742>
- Shapovalova, D., 2016. The Effectiveness of the Regulatory Regime for Black Carbon Mitigation in the Arctic. *Arct. Rev. Law Polit.* 7. <https://doi.org/10.17585/arctic.v7.427>
- Shindell, D., Borgford-Parnell, N., Brauer, M., Haines, A., Kuylenstierna, J.C.I., Leonard, S.A., Ramanathan, V., Ravishankara, A., Amann, M., Srivastava, L., 2017. A climate policy pathway for near- and long-term benefits. *Science* 356, 493–494. <https://doi.org/10.1126/science.aak9521>
- Simonen, P., Kalliokoski, J., Karjalainen, P., Rönkkö, T., Timonen, H., Saarikoski, S., Aurela, M., Bloss, M., Triantafyllopoulos, G., Kontses, A., Amanatidis, S., Dimaratos, A., Samaras, Z., Keskinen, J., Dal Maso, M., Ntziachristos, L., 2019. Characterization of laboratory and real driving emissions of individual Euro 6 light-duty vehicles – Fresh particles and secondary aerosol formation. *Environ. Pollut.* 255, 113175. <https://doi.org/10.1016/j.envpol.2019.113175>
- Simpson, D., 2020. Condensable organics - Summary of issues and NMR workshop.
- Sippula, O., Hytönen, K., Tissari, J., Raunemaa, T., Jokiniemi, J., 2007. Effect of Wood Fuel on the Emissions from a Top-Feed Pellet Stove. *Energy Fuels* 21, 1151–1160. <https://doi.org/10.1021/ef060286e>
- Soltanieh, M., Zohrabian, A., Gholipour, M.J., Kalnay, E., 2016. A review of global gas flaring and venting and impact on the environment: Case study of Iran. *Int. J. Greenh. Gas Control* 49, 488–509. <https://doi.org/10.1016/j.ijggc.2016.02.010>
- Srinivasarao, R., Muralikrishna, K., 2014. Simulation Study to Minimize Soot and Unburnt Hydro Carbons from Steam Assisted Flares and Health Effects of Soot. *Int. J. Sci. Res. IJSR*.
- Stettler, M.E.J., Boies, A.M., Petzold, A., Barrett, S.R.H., 2013. Global Civil Aviation Black Carbon Emissions. *Environ. Sci. Technol.* 130823150610008. <https://doi.org/10.1021/es401356v>
- Stewart, G.J., Nelson, B.S., Acton, W.J.F., Vaughan, A.R., Farren, N.J., Hopkins, J.R., Ward, M.W., Swift, S.J., Arya, R., Mondal, A., Jangirh, R., Ahlawat, S., Yadav, L., Sharma, S.K., Yunus, S.S.M., Hewitt, C.N., Nemitz, E., Mullinger, N., Gadi, R., Sahu, L.K., Tripathi, N., Rickard, A.R., Lee, J.D., Mandal, T.K., Hamilton, J.F., 2020. Emissions of intermediate-volatility and semi-volatile organic compounds from domestic fuels used in Delhi, India (preprint). *Aerosols/Laboratory Studies/Troposphere/Chemistry (chemical composition and reactions)*. <https://doi.org/10.5194/acp-2020-860>
- Stewart, M., 2016. Relief, vent and flare disposal systems, in: *Surface Production Operations*. Elsevier, pp. 549–638. <https://doi.org/10.1016/B978-1-85617-808-2.00008-0>

- Stohl, A., Aamaas, B., Amann, M., Baker, L.H., Bellouin, N., Berntsen, T.K., Boucher, O., Cherian, R., Collins, W., Daskalakis, N., Dusinska, M., Eckhardt, S., Fuglestvedt, J.S., Harju, M., Heyes, C., Hodnebrog, Ø., Hao, J., Im, U., Kanakidou, M., Klimont, Z., Kupiainen, K., Law, K.S., Lund, M.T., Maas, R., MacIntosh, C.R., Myhre, G., Myriokefalitakis, S., Olivie, D., Quaas, J., Quennehen, B., Raut, J.-C., Rumbold, S.T., Samset, B.H., Schulz, M., Seland, Ø., Shine, K.P., Skeie, R.B., Wang, S., Yttri, K.E., Zhu, T., 2015. Evaluating the climate and air quality impacts of short-lived pollutants. *Atmospheric Chem. Phys.* 15, 10529–10566. <https://doi.org/10.5194/acp-15-10529-2015>
- Stohl, A., Klimont, Z., Eckhardt, S., Kupiainen, K., Shevchenko, V.P., Kopeikin, V.M., Novigatsky, A.N., 2013. Black carbon in the Arctic: the underestimated role of gas flaring and residential combustion emissions. *Atmospheric Chem. Phys.* 13, 8833–8855. <https://doi.org/10.5194/acp-13-8833-2013>
- Suarez-Bertoa, R., Valverde, V., Clairotte, M., Pavlovic, J., Giechaskiel, B., Franco, V., Kregar, Z., Astorga, C., 2019. On-road emissions of passenger cars beyond the boundary conditions of the real-driving emissions test. *Environ. Res.* 176, 108572. <https://doi.org/10.1016/j.envres.2019.108572>
- Sumlin, B.J., Pandey, A., Walker, M.J., Pattison, R.S., Williams, B.J., Chakrabarty, R.K., 2017. Atmospheric Photooxidation Diminishes Light Absorption by Primary Brown Carbon Aerosol from Biomass Burning. *Environ. Sci. Technol. Lett.* 4, 540–545. <https://doi.org/10.1021/acs.estlett.7b00393>
- Sun, J., Zhi, G., Hitznerberger, R., Chen, Y., Tian, C., 2020. Brown carbon's emission factors and optical characteristics in household biomass burning: Developing a novel algorithm for estimating the contribution of brown carbon (preprint). *Aerosols/Laboratory Studies/Troposphere/Physics (physical properties and processes)*. <https://doi.org/10.5194/acp-2020-548>
- Takemura, T., Suzuki, K., 2019. Weak global warming mitigation by reducing black carbon emissions. *Sci. Rep.* 9, 4419. <https://doi.org/10.1038/s41598-019-41181-6>
- Tan, E.C.D., Schuetzle, D., Zhang, Y., Hanbury, O., Schuetzle, R., 2018. Reduction of greenhouse gas and criteria pollutant emissions by direct conversion of associated flare gas to synthetic fuels at oil wellheads. *Int. J. Energy Environ. Eng.* 9, 305–321. <https://doi.org/10.1007/s40095-018-0273-9>
- TFTEI, 2019. Code of good practice for wood-burning and small combustion installations (Thirty-ninth session Geneva, 9–13 December 2019 Item 5 (b) of the provisional agenda Review of implementation of the 2018–2019 workplan: policy). Task Force on Techno-economic Issues, Geneva, Switzerland.
- Timonen, H., Karjalainen, P., Aalto, P., Saarikoski, S., Mylläri, F., Karvosenoja, N., Jalava, P., Asmi, E., Aakko-Saksa, P., Saukkonen, N., Laine, T., Saarnio, K., Niemelä, N., Enroth, J., Väkevä, M., Oyola, P., Pagels, J., Ntziachristos, L., Cordero, R., Kuittinen, N., Niemi, J.V., Rönkkö, T., 2019. Adaptation of Black Carbon Footprint Concept Would Accelerate Mitigation of Global Warming. *Environ. Sci. Technol.* 53, 12153–12155. <https://doi.org/10.1021/acs.est.9b05586>
- Tissari, J., Hytönen, K., Lyyränen, J., Jokiniemi, J., 2007. A novel field measurement method for determining fine particle and gas emissions from residential wood combustion. *Atmos. Environ.* 41, 8330–8344. <https://doi.org/10.1016/j.atmosenv.2007.06.018>
- Tissari, J., Väätäinen, S., Leskinen, J., Savolahti, M., Lamberg, H., Kortelainen, M., Karvosenoja, N., Sippula, O., 2019. Fine Particle Emissions from Sauna Stoves: Effects

- of Combustion Appliance and Fuel, and Implications for the Finnish Emission Inventory. *Atmosphere* 10, 775. <https://doi.org/10.3390/atmos10120775>
- Toscano, G., Duca, D., Amato, A., Pizzi, A., 2014. Emission from realistic utilization of wood pellet stove. *Energy* 68, 644–650. <https://doi.org/10.1016/j.energy.2014.01.108>
- Trojanowski, R., Fthenakis, V., 2019. Nanoparticle emissions from residential wood combustion: A critical literature review, characterization, and recommendations. *Renew. Sustain. Energy Rev.* 103, 515–528. <https://doi.org/10.1016/j.rser.2019.01.007>
- Tsimpidi, A.P., Karydis, V.A., Zavala, M., Lei, W., Molina, L., Ulbrich, I.M., Jimenez, J.L., Pandis, S.N., 2010. Evaluation of the volatility basis-set approach for the simulation of organic aerosol formation in the Mexico City metropolitan area. *Atmospheric Chem. Phys.* 10, 525–546. <https://doi.org/10.5194/acp-10-525-2010>
- Turpin, B.J., Saxena, P., Andrews, E., 2000. Measuring and simulating particulate organics in the atmosphere: problems and prospects. *Atmos. Environ.* 34, 2983–3013. [https://doi.org/10.1016/S1352-2310\(99\)00501-4](https://doi.org/10.1016/S1352-2310(99)00501-4)
- Tytgat, T., Walpot, G., Cools, J., Lenaerts, S., 2017. Literature review of emissions of modern wood combustion devices and emissions reducing technologies, under real-life conditions. FLANDERS ENVIRONMENT AGENCY, University of Antwerp.
- Venturini, E., Vassura, I., Zanetti, C., Pizzi, A., Toscano, G., Passarini, F., 2015. Evaluation of non-steady state condition contribution to the total emissions of residential wood pellet stove. *Energy* 88, 650–657. <https://doi.org/10.1016/j.energy.2015.05.105>
- Vicente, E.A.D., 2013. Medidas para mitigar as emissões da combustão doméstica de biomassa. (Thesis). Universidade de Aveiro, Aveiro, Portugal.
- Vicente, E.D., Alves, C.A., 2018. An overview of particulate emissions from residential biomass combustion. *Atmospheric Res.* 199, 159–185. <https://doi.org/10.1016/j.atmosres.2017.08.027>
- Vicente, E.D., Duarte, M.A., Tarelho, L.A.C., Nunes, T.F., Amato, F., Querol, X., Colombi, C., Gianelle, V., Alves, C.A., 2015. Particulate and gaseous emissions from the combustion of different biofuels in a pellet stove. *Atmos. Environ.* 120, 15–27. <https://doi.org/10.1016/j.atmosenv.2015.08.067>
- Vicente, E.D., Vicente, A.M., Evtyugina, M., Carvalho, R., Tarelho, L.A.C., Paniagua, S., Nunes, T., Otero, M., Calvo, L.F., Alves, C., 2019. Emissions from residential pellet combustion of an invasive acacia species. *Renew. Energy* 140, 319–329. <https://doi.org/10.1016/j.renene.2019.03.057>
- Vicente, E.D., Vicente, A.M., Evtyugina, M., Tarelho, L.A.C., Almeida, S.M., Alves, C., 2020. Emissions from residential combustion of certified and uncertified pellets. *Renew. Energy* 161, 1059–1071. <https://doi.org/10.1016/j.renene.2020.07.118>
- Villasenor, R., 2003. An air quality emission inventory of offshore operations for the exploration and production of petroleum by the Mexican oil industry. *Atmos. Environ.* 37, 3713–3729. [https://doi.org/10.1016/S1352-2310\(03\)00445-X](https://doi.org/10.1016/S1352-2310(03)00445-X)
- Wang, A., Lou, H.H., Chen, D., Yu, A., Dang, W., Li, X., Martin, C., Damodara, V., Patki, A., 2016. Combustion mechanism development and CFD simulation for the prediction of soot emission during flaring. *Front. Chem. Sci. Eng.* 10, 459–471. <https://doi.org/10.1007/s11705-016-1594-y>

- Wang, D., Li, Q., Shen, G., Deng, J., Zhou, W., Hao, J., Jiang, J., 2020. Significant ultrafine particle emissions from residential solid fuel combustion. *Sci. Total Environ.* 715, 136992. <https://doi.org/10.1016/j.scitotenv.2020.136992>
- Wang, K., Nakao, S., Thimmaiah, D., Hopke, P.K., 2019. Emissions from in-use residential wood pellet boilers and potential emissions savings using thermal storage. *Sci. Total Environ.* 676, 564–576. <https://doi.org/10.1016/j.scitotenv.2019.04.325>
- Washenfelder, R.A., Attwood, A.R., Brock, C.A., Guo, H., Xu, L., Weber, R.J., Ng, N.L., Allen, H.M., Ayres, B.R., Baumann, K., Cohen, R.C., Draper, D.C., Duffey, K.C., Edgerton, E., Fry, J.L., Hu, W.W., Jimenez, J.L., Palm, B.B., Romer, P., Stone, E.A., Wooldridge, P.J., Brown, S.S., 2015. Biomass burning dominates brown carbon absorption in the rural southeastern United States: Biomass burning dominates brown carbon. *Geophys. Res. Lett.* 42, 653–664. <https://doi.org/10.1002/2014GL062444>
- Weyant, C.L., Shepson, P.B., Subramanian, R., Cambaliza, M.O.L., Heimbürger, A., McCabe, D., Baum, E., Stirm, B.H., Bond, T.C., 2016. Black Carbon Emissions from Associated Natural Gas Flaring. *Environ. Sci. Technol.* 50, 2075–2081. <https://doi.org/10.1021/acs.est.5b04712>
- Whitaker, P., Kapus, P., Ogris, M., Hollerer, P., 2011. Measures to Reduce Particulate Emissions from Gasoline DI engines. *SAE Int. J. Engines* 4, 1498–1512. <https://doi.org/10.4271/2011-01-1219>
- Wöhler, M., Andersen, J.S., Becker, G., Persson, H., Reichert, G., Schön, C., Schmidl, C., Jaeger, D., Pelz, S.K., 2016. Investigation of real life operation of biomass room heating appliances – Results of a European survey. *Appl. Energy* 169, 240–249. <https://doi.org/10.1016/j.apenergy.2016.01.119>
- Wöhler, M., Jaeger, D., Pelz, S.K., Thorwarth, H., 2017. Potential of Integrated Emissions Reduction Systems in a Firewood Stove under Real Life Operation Conditions. *Energy Fuels* 31, 7562–7571. <https://doi.org/10.1021/acs.energyfuels.7b00803>
- Wong, J.P.S., Nenes, A., Weber, R.J., 2017. Changes in Light Absorptivity of Molecular Weight Separated Brown Carbon Due to Photolytic Aging. *Environ. Sci. Technol.* 51, 8414–8421. <https://doi.org/10.1021/acs.est.7b01739>
- Xie, M., Hays, M.D., Holder, A.L., 2017. Light-absorbing organic carbon from prescribed and laboratory biomass burning and gasoline vehicle emissions. *Sci. Rep.* 7, 7318. <https://doi.org/10.1038/s41598-017-06981-8>
- Xing, J., Shao, L., Zhang, W., Peng, J., Wang, W., Shuai, S., Hu, M., Zhang, D., 2020. Morphology and size of the particles emitted from a gasoline-direct-injection-engine vehicle and their ageing in an environmental chamber. *Atmospheric Chem. Phys.* 20, 2781–2794. <https://doi.org/10.5194/acp-20-2781-2020>
- Yamineva, Y., Romppanen, S., 2017. Is law failing to address air pollution? Reflections on international and EU developments. *Rev. Eur. Comp. Int. Environ. Law* 26, 189–200. <https://doi.org/10.1111/reel.12223>
- Yan, J., Wang, X., Gong, P., Wang, C., Cong, Z., 2018. Review of brown carbon aerosols: Recent progress and perspectives. *Sci. Total Environ.* 634, 1475–1485. <https://doi.org/10.1016/j.scitotenv.2018.04.083>
- Yan, K. (Ed.), 2009. *Electrostatic Precipitation*. Springer Berlin Heidelberg, Berlin, Heidelberg. <https://doi.org/10.1007/978-3-540-89251-9>
- Yang, H.-H., Arafath, S.Md., Wang, Y.-F., Wu, J.-Y., Lee, K.-T., Hsieh, Y.-S., 2018. Comparison of Coal- and Oil-Fired Boilers through the Investigation of Filterable and

- Condensable PM_{2.5} Sample Analysis. *Energy Fuels* 32, 2993–3002. <https://doi.org/10.1021/acs.energyfuels.7b03541>
- Yang, H.-H., Lee, K.-T., Hsieh, Y.-S., Luo, S.-W., Huang, R.-J., 2015. Emission Characteristics and Chemical Compositions of both Filterable and Condensable Fine Particulate from Steel Plants. *Aerosol Air Qual. Res.* 15, 1672–1680. <https://doi.org/10.4209/aaqr.2015.06.0398>
- Yang, H.-H., Lee, K.-T., Hsieh, Y.-S., Luo, S.-W., Li, M.-S., 2014. Filterable and Condensable Fine Particulate Emissions from Stationary Sources. *Aerosol Air Qual. Res.* 14, 2010–2016. <https://doi.org/10.4209/aaqr.2014.08.0178>
- Yazdani, E., Asadi, J., Dehaghani, Y.H., Kazempoor, P., 2020. Flare gas recovery by liquid ring compressors-system design and simulation. *J. Nat. Gas Sci. Eng.* 84, 103627. <https://doi.org/10.1016/j.jngse.2020.103627>
- Yim, S.H.L., Lee, G.L., Lee, I.H., Allroggen, F., Ashok, A., Caiazzo, F., Eastham, S.D., Malina, R., Barrett, S.R.H., 2015. Global, regional and local health impacts of civil aviation emissions. *Environ. Res. Lett.* 10, 034001. <https://doi.org/10.1088/1748-9326/10/3/034001>
- Zhang, A., Wang, Y., Zhang, Y., Weber, R.J., Song, Y., Ke, Z., Zou, Y., 2020. Modeling the global radiative effect of brown carbon: a potentially larger heating source in the tropical free troposphere than black carbon. *Atmospheric Chem. Phys.* 20, 1901–1920. <https://doi.org/10.5194/acp-20-1901-2020>
- Zhang, Q.J., Beekmann, M., Drewnick, F., Freutel, F., Schneider, J., Crippa, M., Prevot, A.S.H., Baltensperger, U., Poulain, L., Wiedensohler, A., Sciare, J., Gros, V., Borbon, A., Colomb, A., Michoud, V., Doussin, J.-F., Denier van der Gon, H.A.C., Haefelin, M., Dupont, J.-C., Siour, G., Petetin, H., Bessagnet, B., Pandis, S.N., Hodzic, A., Sanchez, O., Honoré, C., Perrussel, O., 2013. Formation of organic aerosol in the Paris region during the MEGAPOLI summer campaign: evaluation of the volatility-basis-set approach within the CHIMERE model. *Atmospheric Chem. Phys.* 13, 5767–5790. <https://doi.org/10.5194/acp-13-5767-2013>
- Zhang, Y., Albinet, A., Petit, J.-E., Jacob, V., Chevrier, F., Gille, G., Pontet, S., Chrétien, E., Dominik-Sègue, M., Levigoureux, G., Močnik, G., Gros, V., Jaffrezo, J.-L., Favez, O., 2020. Substantial brown carbon emissions from wintertime residential wood burning over France. *Sci. Total Environ.* 743, 140752. <https://doi.org/10.1016/j.scitotenv.2020.140752>
- Zhao, R., Lee, A.K.Y., Huang, L., Li, X., Yang, F., Abbatt, J.P.D., 2015. Photochemical processing of aqueous atmospheric brown carbon. *Atmospheric Chem. Phys.* 15, 6087–6100. <https://doi.org/10.5194/acp-15-6087-2015>
- Zhou, J., Zotter, P., Bruns, E.A., Stefenelli, G., Bhattu, D., Brown, S., Bertrand, A., Marchand, N., Lamkaddam, H., Slowik, J.G., Prévôt, A.S.H., Baltensperger, U., Nussbaumer, T., El-Haddad, I., Dommen, J., 2018. Particle-bound reactive oxygen species (PB-ROS) emissions and formation pathways in residential wood smoke under different combustion and aging conditions. *Atmospheric Chem. Phys.* 18, 6985–7000. <https://doi.org/10.5194/acp-18-6985-2018>
- Zolfaghari, M., Pirouzfard, V., Sakhaeinia, H., 2017. Technical characterization and economic evaluation of recovery of flare gas in various gas-processing plants. *Energy* 124, 481–491. <https://doi.org/10.1016/j.energy.2017.02.084>

zum Hagen, F.H.F., Mathissen, M., Grabiec, T., Hennicke, T., Rettig, M., Grochowicz, J., Vogt, R., Benter, T., 2019. Study of Brake Wear Particle Emissions: Impact of Braking and Cruising Conditions. *Environ. Sci. Technol.* 53, 5143–5150. <https://doi.org/10.1021/acs.est.8b07142>